EXPRESSION, FUNCTIONAL AND GENOMIC STUDY OF HEPARAN SULFATE 6-O-SULFOTRANSFERASE 3 IN BREAST CANCER

OMID IRAVANI

(MD)

A THESIS SUBMITTED FOR THE

DEGREE OF DOCTOR OF PHILOSOPHY

DEPARTMENT OF ANATOMY

FACULTY OF MEDICINE

NATIONAL UNIVERSITY OF SINGAPORE

2011

ACKNOWLEDGEMENTS

First and foremost, I would like to express my sincerest gratitude to my supervisor, Associate Professor Yip Wai Cheong, George, who has excellently supported me throughout my graduate studies with his patience, knowledge and guidance whilst allowing me the room to work in my own way. I attribute my PhD degree to his encouragement and effort and without him this work, too, would not have been accomplished or written. One simply could not wish for a better or friendlier supervisor.

I am heartily thankful to my co-supervisor, Professor Bay Boon Huat, the Head of Department of Anatomy, whose encouragement, guidance and support from the initial to the final level enabled me to work confidently on my research project. His valuable and timely guidance provided a golden opportunity for me to earn a lot of teaching experiences besides my research project. I owe my deepest gratitude to him for all of the support and advices which he has done me.

I gratefully acknowledge Professor Ling Eng Ang, the ex-head of Department of Anatomy for providing the opportunity to pursue my graduate studies in the Department of Anatomy.

It is my pleasure to pay tribute also to the collaborators of my research projects, Associate Professor Tan Puay Hoon, Head of Department of Pathology, Singapore General Hospital (SGH) and Dr. Aye Aye Thike for providing clinical samples of breast

cancer and helping me to learn and practice on immunohistochemical aspect of my project.

I would like to thank Mrs. Yong Eng Siang, Mrs. Ng Geok Lan, Mrs.Wu Ya Jun and Mr. Poon Zhung Wei for their helpful technical supports. I would like to acknowledge Mr. Yick Tuck Yong for his timely multimedia assistance.

I would like to express my great appreciation to the previous and current fellow students who has shared their knowledge and experiences with me under a very friendly atmosphere. Particularly, I would like to appreciate Dr. Koo Chuay Yeng, Dr. Yvonne Teng, Ms. Sen Yin Ping and Ms. Leong Shu Xian, Grace for their great helps and support.

I offer my regards and blessings to the entire student and staffs who supported me during the completion of the project in the Department of Anatomy.

I would like to sincerely thank my family members, especially my lovely wife, Somayeh Keshani, and my daughter Ava Iravani for supporting and encouraging me to pursue my studies. Without my wife's encouragement, I would not have finished my degree. In addition, my deepest gratitude goes to my parents for their unflagging love and support throughout my life.

I would like to appreciate A*STAR and National University of Singapore (NUS) for granting me excellent competitive research scholarships to complete my post-graduate studies in Singapore.

Last but not the least, I am very much thankful to the one above all of us, the omnipresent God, for answering my prayers for giving me the health, strength and emotion to stand against all of the difficulties despite my constitution wanting to give up, thank you so much Dear Lord.

TABLE OF CONTENTS

CHAPTER 2

CHAPTER 3

CHAPTER 4

Summary

Breast carcinoma is the most commonly diagnosed malignancy in females, accounting for 23% of all of new cancer cases worldwide. It is currently the leading cause of cancer death among women and accouns for 14% of all cancer death worldwide in 2008. Ductal breast carcinoma is one of the most common types of breast malignancies and is categorized into two subtypes, ductal carcinoma *in situ* (DCIS) and invasive ductal carcinoma (IDC). DCIS is the most frequent type of non-infiltrating breast carcinoma accounting for 10-20% of all breast malignancies. IDC is the most frequent type of breast carcinoma, accounting for 60-80% of all breast malignancies.

Heparan sulfate is a linear-structured polysaccharide that is covalently attached to various core proteins, and is expressed ubiquitously in human cells, and is found at the cell surface and in the extracellular matrix. It has interactions with several proteins and mediates a variety of cellular and biological processes. These interactions, which are critically dependent on the O-sulfation patterns within heparan sulfate chains could define binding sites for proteins and regulate key events in embryonic development and in homeostasis, including the regulation of growth factor signaling, proliferation, cell adhesion, coagulation and mobility. Sulfation pattern of heparan sulfate chains is a significant factor that critically determines the interactions between heparan sulfate and several ligands such as growth factors and cytokines.

One of the most important sulfation modifiers of heparan sulfate is 6-O-sulfotransferase (HS6ST) that specifically transfers sulfate groups from 3'-phosphoadenosine 5'-phosphosulfate (PAPS) to the C6 position of N-acetylglucosamine (GlcNAc) residues of heparan sulfate. Three 6-O-sulfotransferase isoforms have been described in humans. Several studies have demonstrated that HS6ST isoforms are involved in important cellular and biological processes such as embryonic organogenesis, postnatal growth and development.

Endosulfatases (SULFs) are other sulfation modifying enzymes which specifically edit 6-O-sulfation on the cell membrane and extracellular matrix by removing the sulfate group from the C6 position of N-acetylglucosamine in heparan sulfate chains, thereby modulating the biological activity of heparan sulfate. SULF1 and SULF2 are two isoforms of endosulfatases which have been identified in humans. Recently, a growing body of research has focused on expression patterns of SULF1 and SULF2 in several malignancies, and it was identified that the expression of these enzymes are deregulated in a number of human malignancies including breast cancer. Although some studies proposed that alteration of the expression of 6-O-sulfation editing enzymes may be involved in the carcinogenesis process, there is limited information on the function of HS6ST(s) and SULF(s) in the tumorigenesis process.

The aim of this study is to elucidate the functional roles of HS6ST3 in breast cancer cell lines. *HS6ST3* was silenced using siRNA and then functional and genomics studies were

performed. The immunohistochemical expression of HS6ST3 and SULF1 were examined on clinical samples of ductal breast carcinoma by using immunohistostaining techniques.

Our study found that *HS6ST3* could modulate the growth and progression of breast cancer by directly regulating the expression of critical genes, as well as influencing the interactions between heparan sulfate and several growth factors on the cell surface. In addition, it was shown that *HS6ST3* has an important regulatory role in biosynthesis of heparan sulfate on the cell surface of the tumor cells. *HS6ST3* was also found to modulate cellular response to the cytotoxic effects of Cisplatin and 5-Fluorouracil in breast cancer. On the other hand, the immunohistochemical findings on heparan sulfate editing enzymes using HS6ST3 and SULF1 antibodies in breast cancer showed that the expression of SULF1 and HS6ST3 were dysregulated in breast cancer. Besides, the analysis showed that HS6ST3 could be used as a novel diagnostic and prognostic tool for breast cancer, while SULF1 could be used as a prognostic factor in breast carcinoma.

These finding are of considerable significance in implicating HS6ST3 in breast cancer. The significance of the current study is not limited to the regulatory role of HS6ST3 in cellular processes because it could also be used as a novel prognostic and diagnostic biomarker in breast cancer. In addition, HS6ST3 might be a possible therapeutic target for treating breast cancer as well as other oncogenic malignancies.

LIST OF FIGURES

LIST OF TABLES

LIST OF ABBREVIATIONS

ATCC	American type culture collection
BRCA	Breast cancer gene
5-fu	5-flouracil
Ab	Antibody
AC	Doxorubicin, cyclophosphamide
AC-T	AC followed by paclitaxel
bp	Base pair
BSA	Bovine serum albumin
cDNA	complementary DNA
CMF	Cyclophosphamide, methotrexate and 5-flurouacil
CMF	Cyclophosphamide, methotrexate, 5-fluorouracil
CS	Chondroitin sulfate
DAVID	Data for annotation, visualization and integrated discovery
DCIS	Ductal carcinoma in situ
DEPC	Diethylpyrocarbonate
DFS	Disease free survival
DMEM	Delbeco's modified Eagle's medium
DMSO	Dimethyl sulphoxide
DNA	Deoxyribonucleic acid
dNTP	Deoxyribonucleotide triphosphate
DS	Dermatan sulfate
DTT	Dithiothretol
EC	Epirubicin, cyclophosphamide
ECM	Extracellular matrix
EC-T	EC followed by paclitaxel
ER	Estrogen receptor
EXT	Gycosyltransferases
FBS	Fetal bovine serum
GAG	Glycosaminoglycans
GalIT, GalIIT	Galactose transferase I, II
GalNAc	N-acetylgalactosamine
GalT-I	Galactosyltransferase II
GlcAT-I	Glucuronyltransferase I
GlcAT-II	Glucuronyltransferase II
GlcNAc	N-acetylglucosamine
GlcNAcT-I	GlcNAc transferase I

GlcNAcT-II	GlcNAc transferase II
HA	Hyaluronan
HER2	Human epithelial growth factor 2
HexA	Hexuronic acid
HRP	Horse radish peroxidase
HS	Heparan sulfate
HS6ST	Heparan sulfate 6-O sulftransferase
HS6ST2	Heparan sulfate 6-O sulftransferase 2
HS6ST3	Heparan sulfate 6-O sulftransferase 3
ICC	Immunocytochemistary
IGF1R	Insulin-like growth factor I receptor
IgG	Immunoglobulin G
IgM	Immunoglobulin M
IHC	Immunohistochemistary
IRS	Immunoreactivity score
iterPLIER	Iterative PLIER
KS	Keratan sulfate
LD50	Lethal dose of 50%
L-IdoA	L-iduronic acid
MM	Mismatch
MRI	Magnetic resonance imaging
mRNA	Messenger RNA
OD	Optical density
OS	Overal survival
PAPS	3'-phsphoadenyl 5'-phosphosulfate
PBS	Phosphate buffer saline
PCR	Polymerase chain reaction
PGs	Proteoglycans
PI	Propidium iodide
PLIER	Probe Logarithmic Intensity Error Estimation
PM	Perfect match
PR	Progestrone receptor
PSPG	Heparan sulfate proteoglycan
PVDF	Polyvinyl difluride
qRT-PCR	Quantitative real polymerase chain reaction
RIN	RNA integrity number
RMA	Robust multi-array analysis
RNA	Ribonucleic acid
SAR	Survival after recurrence

SDS	Sodium dodecyl sulfate
SE	Standard error
shRNA	Short hairpin RNAs
siRNA	small interfering RNA
SULF	Sulfatase
SULF1	Sulfatase 1
SULF2	Sulfatase 2
TBST	Tris buffered salin in 1% Tween-20
TC	Docetaxel, cyclophosphamide
TCH	Docetaxel, carboplatin, trastuzumab
TEM	Transmission electron microscopy
TEMED	N,N,N',N'-Tetramethylethylenediamine
TMA	Tissue microarray
TNM	Tumor-node-metastasis
TS	Tumor size
WAI	Weighted average intensity
WB	Western blotting
XAF1	X chromosome-linked inhibitor of apoptosis protein (XIAP)-associated factor 1
XylT	Xylosyltransferase

LIST OF PUBLICATION AND PRESENTATION

Journals

1. Omid Iravani, George W Yip, Boon-Huat Bay. Submitting “Clinical significance of differentially expressed SULF1 in breast cancer to “American journal of Modern pathology”.

Abstarcts

1. Omid Iravani, George W Yip, Boon-Huat Bay. “RNA knock down of *HS6ST3* in breast cancer modulates cellular response to cisplatin and 5- fluorouracil”. Presented at the International Anatomical Sciences and Cell Biology Conference, Singapore, 2010.

2. Omid Iravani, George W Yip, Boon-Huat Bay. “RNA knock down of *HS6ST3* in breast cancer modulates cellular behavior *in vitro*”. Presented at the Singapore Microscopy Society, 2010.

3. Omid Iravani, George W Yip, Boon-Huat Bay. “Functional roles of *HS6ST3* in human breast cancer *in vitro*”. Presented at the 102nd Annual meeting of American Association of Cancer Research, Orlando, 2011.

CHAPTER 1

INTRODUCTION

1.1 Introduction to breast cancer

Breast is a common location for development of benign and malignant pathologies in females. However, in a rare condition, less than 1% of males may develop breast cancer. (Mouna et al. 2011) Breast cancer is a term used for a variety of malignant pathologies arising in breast. This cancer may develop from several tissues of breast, thus having a basic knowledge about anatomy and developmental process of a normal breast is essential to have a better understanding about its pathologies such as malignancies. The malignancies of breast are classified into different groups which will be discussed in next sections. Although the etiology of breast cancer is considered multifactorial, there are several known risk factors which may increase the chance of developing a breast cancer during a woman's life such as genetic predisposition, age, family history, diet and medication (American, Cancer Society, Breast Cancer Facts and Figures, 2009-2010).

Innovative improvement in medicine brought many advantages for breast cancer as well as other cancers. One of these innovations is the early screening methods that enable the clinicians to make an early diagnosis. For example, mammography is a common method that is wildly used all over the world for screening purposes. Surgical therapies, chemotherapy, radiotherapy and hormonal treatments have been other important improvements that improve the lifespan of breast cancer patients in a considerable extent.

1.1.1Anatomy of normal breast

Breast is a circular organ located in front of pectoralis major muscle of the chest wall in a fertile woman. Superioinferiorly, it extends from second to fifth rib and laterally, extends from the external border of sternum to anterior auxiliary line. Breast consists of ducts and lobular system which are surrounded by connective tissues.

Each breast is composed of about 15-20 structural units, called lobes which radiate out from nipple. Lobes are separated out from each other by fibrous septa which function as suspensory ligaments. Lobes are embedded in connective tissue and divided into several lobules by fibrous connective tissue. Each lobule is further divided into several alveoli which considered as milk secreting units in breast. The milk secreted from alveoli of the lobules flows into the ducts which are collecting tubes. All ducts of each lobe connect to each others to form a major duct of the lobe. Then, the ducts dilate at their terminating location where they connect to the nipple, called ampulla or lactiferous duct. Finally, the milk flows from 15-20 opening in the nipple. The nipple is surrounded by a pigmented area, called areola which contains a lot of sebaceous glands (Figure.1.1).

Clinically breast is divided to four quadrants: upper lateral, upper medial, lower lateral and lower medial. The lymph drainage of the breast has of great importance since they are the common routs for development and spreading of a variety of breast malignancies. The lymph of lateral quadrants of breast drains into anterior auxiliary and pectoral lymph

nodes. The medial quadrants drain their lymph into internal and posterior thoracic lymph nodes (Figure 1.2).

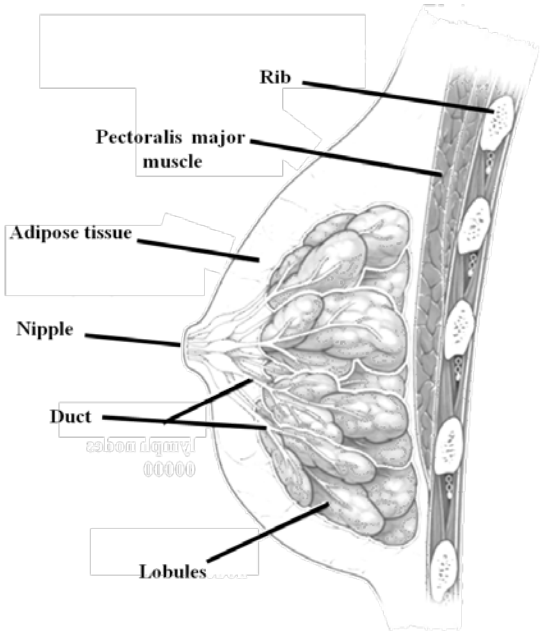

Figure 1.1. Gross structural anatomy of the breast.

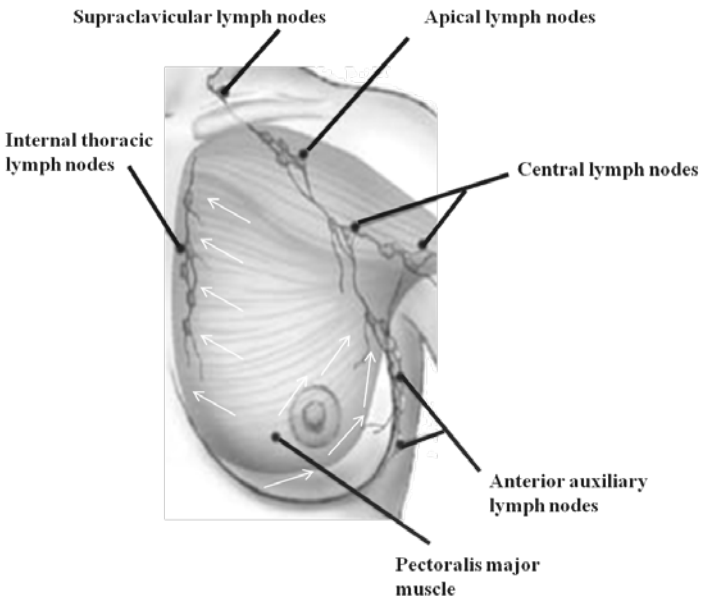

Figure 1.2. Lymphatic drainage of the breast.

1.1.2 Development of the breast

Breast is a dynamic specialized glandular organ that produces and secretes the milk. They present in a pair in both male and female; however, in male it is immature, while in female they develop during puberty and adulthood. In fetus, maternal and placental hormones ignite the proliferation of the ducts and connective tissues. Therefore, breast bud could be seen in both sexes in newborns (Howard and Gusterson 2000).

During puberty, ovarian hormones influence the breasts to form a circular enlargement. In this process, the ductal system elongates and the margins of breast extend; however, this enlargement is mainly due to the deposition of adipose tissue than elongation of ducts. In a fertile woman, breast has more enlargements and tends to protrude forward. Thus, during each menstrual cycle the size of the breast may vary under the influence of estrogen and progesterone level of secretion (Knight and Sorensen 2001).

During the early pregnancy, ductal system starts branching while they elongate. The secreting alveoli which are located at the end of small ducts expand and filled a major volume in breast. The vascularity of connective tissue of breast considerably increases in this period. The nipple enlarges and the areola expands and darkens due to more pigmentation of this area. In late pregnancy, although enlargement of the breast continue due to the distention of secretory alveoli, the speed of growth process decrease. During

lactation period, secretory alveoli are very active to produce the milk (Russo and Russo 2008; Howard and Gusterson 2000).

After lactation period, the breasts tend to turn back to their inactive condition. Therefore, the secretory alveoli start shrinking and then disappearing and the space between the lobes fill with a thick connective tissue. The nipples also shrink into their original size and the pigmentation of the areola diminishes. During the menopause state, the secreting alveoli start vanishing and the breasts shrink and become more pendulous due to the absence of ovarian secreting hormones (Estrogen and progesterone), a process which is called breast atrophy (Jose Russu, 2011(Russo and Russo 2004).

1.1.3 Epidemiology of breast cancer

Breast carcinoma is the most commonly diagnosed malignancy in females accounting for 23% of all of new cancer cases. In males, lung cancer is the most frequently diagnosed malignancy which has been the first top-ranked cause of cancer death. In the United state, 12% of females experience invasive type of breast cancer during their life (American Cancer Society, 2011a).

The incidence rate of breast cancer rate is generally higher in developed countries compared to developing country; however, the mortality rates remains nearly similar. Thus, the incidence rate of breast cancer was estimated to be the highest among females

living in West and North of the Europe as well as in North of the US and also Australia, while the lowest incidence rate was reported from Sub Saharan district of Africa and Asia. The incidence rates of other countries were ranked as intermediate. This variation might be firstly attributable to the different physical and hormonal factors of a variety of people living in different conditions, and secondly due to the availability of the screening methods such as mammography. In fact, the high incidence rate of breast cancer in Western countries has been mainly due to the intensive screening programs, hormone therapy during menopausal period and the increased awareness of their people (Althuis et al. 2005; Ravdin et al. 2007; Cronin, Ravdin and Edwards 2009; Edwards et al. 2010; Parkin 2009; Séradour et al. 2009; Canfell et al. 2008). On the other hand, in countries such as US, UK, Australia and France the incidence rates were diminished which was relatively because of limited usage of combinational hormone therapy during the menopausal period (Figure 1.3: A). Although the incidence rate of breast cancer was generally increased, the death rate was remarkably decreased in many European countries as well as North America.

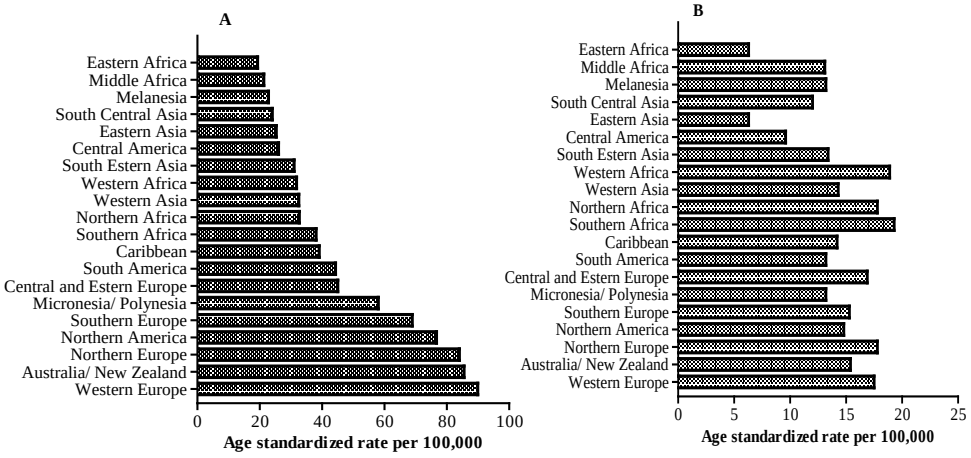

Figure 1.3. Incidence rate of breast cancer after age-adjustment (A) mortality rate of breast cancer after age-adjustment (B) (Jemal et al. 2011).

Breast cancer is currently the top cause of cancer mortality among females specifically in developing societies accounting for 14% of cancer death in 2008, while cancer of cervix was the leading cause of cancer death during the 1990s. Nearly, half of breast cancers happen in developing societies, but sixty percent of breast cancer mortalities were reported in these societies. The breast cancer mortality had a decreasing trend in the North of US and also many European countries over the last decades (Jemal et al. 2010). On the other hand, this trend has been increasing in several African and some Asian countries such as India and Uganda mainly due to their lifestyle changes (Parkin et al. 2010; Ito et al. 2009; Jemal et al. 2011; Colditz, Sellers and Trapido 2006) (Figure 1.3: B). The decreasing trend of death rate in developed countries was mainly because of early screening for cancer detection as well as newly improved treatment. Overall, the five year survival of the breast carcinoma has increased from fifty percent to more than seventy five percent (Jemal et al. 2011; Autier et al. 2010).

In Singapore, breast carcinoma has been the most frequent malignancy affecting females and accounting for 29.2% of all cancers among females of various ethnic groups (Chinese, Malay and Indian) during 2005-2009 (Figure 1.4). Similar to many other countries, breast cancer has been the top cause of cancer death in Singapore accounting for 17.8% of all cancer mortalities (National Registry of Diseases Office, 2011).

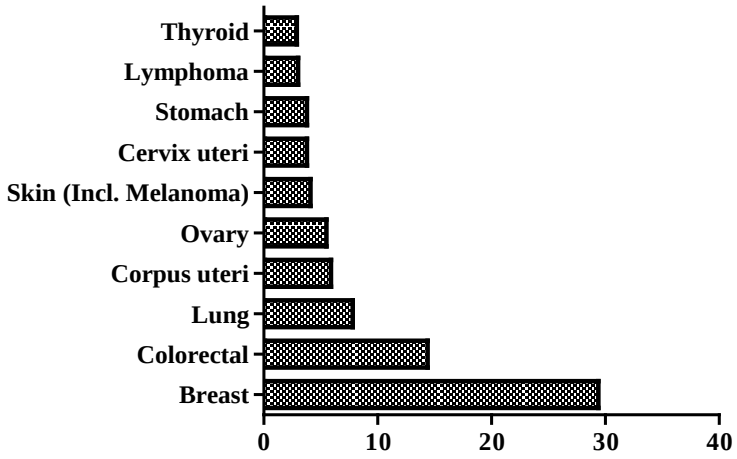

Figure 1.4. Percentage of the most frequent malignancies in Singapore women during 2005 – 2009. (Singapore National Registry of Diseases Office, 2011).

1.1.4 Risk factors of Breast Cancer

Many factors were identified as risk factor for breast cancer. Although the main cause of breast cancer is still unknown, exposing to at least one of risk factors could increase the chance of developing breast cancer during a female's life. Thus, increasing awareness of females about risk factors and the importance of timely screening may lead to reducing the incidence as well as mortality of breast cancer. These risk factors may be classified as genetic and environmental; however, many of them seem to be not separable. In the next sections, the established risk factors of breast cancer will be explained (American Cancer Society, 2011b).

1.1.4.1 Age and Ethnicity

The chance of developing breast cancer increases by aging in females. The median age of the breast cancer cases at the time of diagnosis was estimated at 61. About 95 percent of new breast cancer cases and also 97 percent of breast cancer mortalities happened in females who were below 40 years old during 2002 to 2006. Although developing breast cancer is not a rare phenomenon in female below 40 years old, its risk is considerably lower than higher ages. The lowest rate was reported for the age of 20 to 24, while women between 75 to 79 years old had the highest incidence rate for developing this carcinoma. However, the decrease in the incidence trend of breast cancer over 80 years old might be due to imperfect screening. White females who are more than 40 years old are at higher risk of breast carcinoma compared to African American at the similar ages. On the other hand, African American females who are under 40 years old are in a higher risk for developing and dying of breast cancer than American white women of the same ages. Breast carcinoma is also ranked on the top of the causes of cancer mortalities in the females between 35 to 54 years old (American Cancer Society, 2011a; Horner et al. 2009).

1.1.4.2 Family history of breast cancer

Females whose first-degree family such as mother, sister and/ or daughter had a history of breast cancer are at a higher risk for developing breast carcinoma. This risk will be increase in females when more than one of their first degree family are affected or when disease occurs in a member of their close relatives at young ages (Collaborative Group on

Hormonal Factors in Breast Cancer 2001). In specific syndromes, having a history of ovarian carcinoma in close family could increase the chance of developing breast cancer. Genetic inheritance is said to be responsible for about nearly five to ten percent of breast cancer's occurrence (National Cancer Institute 2009). This genetic predisposition was reported when mutations happen in BRACA1 and BRACA2 genes. These mutations are rare (1 %) (Ford et al. 1998); however, when they occur, the chance of developing breast carcinoma before the age of seventy is 57% and 49% in BRACA1 and BRACA2 respectively (Chen and Parmigiani 2007; Bonaïti-Pellié et al. 2009). However, scientist believed that lifestyle is a determining factor which could influence the inheritance (Lichtenstein et al. 2000).

1.1.4.3 Hormonal factors

Endogenous sex hormones such as Estrogen and Progesterone always influence the growth and development of the breast. They are specifically adjusting the stimulation of cell proliferation and inducing the cell death, apoptosis. Thus, they play a critical role in predisposing a female to develop a breast cancer. Early menarche or late menopause are two important condition that increase the exposure time of a female to sex hormones, and therefore could predispose a female to breast carcinoma (Hulka and Moorman 2008; Hulka and Moorman 2001). Multiparous women and those who were pregnant below 30 years old are at lower risk for breast cancer. However, pregnancies at older ages have been associated with slight rise in risk of the disease (Lambe et al. 1994; Albrektsen et al. 2005). In addition, breast feeding showed to remarkably decreased the risk of developing this cancer (Collaborative Group on Hormonal Factors in Breast Cancer 2002).

Exogenous sex hormones which are used in contraceptives or combined in hormone replacement therapy (post-menopausal prescriptions) have been reported to increase the risk of developing breast cancer (Johnson and Millard 1996; Bjelic-Radisic and Petru 2010). Thus, the longer time a women used these exogenous hormones, the higher is the risk of breast cancer occurrence; however, stop using of these hormones was showed to decrease the risk after five years (Breast cancer and hormone replacement therapy 1997 (Calle et al. 2009; Heiss et al. 2008).

1.1.4.4 Obesity, physical activity and Diet

Body weight is a significant adjustable risk factor for breast carcinoma. Gaining weight which might be due to unhealthy diet, hormone replacement therapy and/ or physical inactivity could enhance the chance of developing breast cancer after the menopause. Production of endogenous estrogen occurs in adipose tissue after the menopausal period; thus gaining more fat in this period enhance the level of this estrogen in circulation and predispose the female to breast cancer. Although body mass and weight gain are generally associated with each other, weight gain seems to be an important determining factor that positively increase the risk of the breast cancer (Feigelson et al. 2004; Morimoto et al. 2002; Eliassen et al. 2006).

Several studies have focused on the role of physical exercise on breast cancer. It was shown that those females who do physical exercise regularly are at lower risk physical of breast cancer. This effect was well observed in females with normal body mass index

(BMI) after the menopause; however, the mechanism of this effect is still unclear (Ballard-Barbash et al. 2009; Neilson et al. 2009; Friedenreich and Cust 2008; Peters et al. 2009; Schmidt et al. 2009).

Alcohol intake is an important dietary risk factor that positively increases the risk of breast cancer. This risk was enhanced the risk rate up to 21% in those who had more than 24 g of ethanol consumption per day. Other studies showed that even when the daily alcohol intake is below this level, the risk of breast cancer may slightly increase. One possible reason might be the effect of ethanol on generating of endogenous sex hormones such as estrogen and androgen (Allen et al. 2009; Singletary and Gapstur 2001; Lew et al. 2009). Overall, it seems that adjusting the body mass by having a balance between energy intake and physical exercise could be beneficial to prevent breast cancer.

1.1.4.5 Other risk factors of breast cancer

Many studies have reported the association between tobacco smoking and breast cancer. Active and passive smoker both may be at higher risk for breast cancer than none smokers. However, apart from breast cancer smokers are at higher risk of developing other cancers; therefore, non-smokers could benefit from a healthier physical condition (Kasim et al. 2005; Lee and Hamling 2006; Miller et al. 2007; Takezaki et al. 1996).

Exposure to a high dose radiation is also suggested to be a potential risk factor specifically in adulthood. This event was reported mainly in those survivors who were experienced the atomic bomb in Japan. Exposure to low-dose radiation during diagnostic

and therapeutic procedures has been also associated with breast cancer; therefore, risk assessment before performing these procedures seems to be necessary for physicians (Boice et al. 1979; Nekolla, Griebel and Brix 2008; Ma et al. 2008).

1.1.5 Symptoms of breast cancer

When the tumor is big enough, it would be palpable in physical examination or self examination, but generally there is no pain unless inflammation or space occupying mass develops. Lymph node metastasis may leads to lymphadenopathy in some cases, while the local tumor is still small and/ or painless. Although not frequent but some other times a carcinoma of breast give a feeling of heaviness to the breast. Other signs and symptoms include pain, asymmetry in breast's bulk, nipple discharge or bleeding, skin retraction, redness and/ or thickening. Once a female found any of these signs or symptoms, she should seek for consulting with a physician. In some cases, breast carcinomas are asymptomatic specifically when the tumor is not big enogh to be palpable. Thus, awareness of timely screening systems would be very significant to detect the breast cancer in earlier stages (American Cancer society, Breast Cancer Facts and Figures 2011a).

1.1.6 Classification of breast cancer

Breast cancer classification is critical for physician to decide on treatment as well as determine the prognosis of the patients. For this purpose two important system was developed, grading and staging. Grading classification is performed on the basis of

tumoral cellular structures compared to the normal differentiated cells by a pathologist. Thus, the tumors classify into three grades (Grade I, Grade II and Grade III) based on the microscopic structure of the tumor cells and cellular growth.

Staging is another important classification for breast cancer. Staging defines how much the tumor extended from its original location into other parts of the body. By staging, physician could estimate the survival of the breast cancer patients and therefore decide on the optimal treatment that the patients may needs. The American Joint Committee on Cancer (AJCC) introduced a standardized staging strategy for clinical physicians, called TNM system. T is state tumor size ranging from 0 to 4, N state the number of lymph node(s) which are involved and ranging from 0 to 3 and M stands for the existence of metastasis to other organs which is 0 or 1 (Escobar et al. 2007; Arnone et al. 2010). The details of TNM staging system are as following:

Stage 0: Carcinoma in-situ, the cancer cells are limited to the original location without invasion.

Stage I: Tumor size ≤ 2cm with no lymph node involvement.

Stage II: Tumor size ≤ 2cm with metastasis to the adjacent lymph nodes OR tumor size is between 2-5 cm with OR without metastasis to the lymph nodes OR tumor size ≥ 5 cm without cancer spread.

Stage III: Tumor is any size with metastasis to the auxiliary lymph nodes (stage IIIA) OR the tumor is any size with spread to the breast's skin or the chest wall (stage IIIB) OR the tumor is any size with metastasis to the chest wall, breast's skin and spread into the infraclavicular nodes (stage IIIC).

Stage IV: Tumor is at any size and the cancer spreads beyond of the breast into the other organs such as lung, liver or brain (American Cancer Society, 2011c).

Histologically, breast cancer is categorized into several types. This classification includes Ductal carcinoma (Invasive or In-Situ), Lobular carcinoma (Invasive or In-Situ), Medullary breast carcinoma, Tubular carcinoma, Mucinous carcinoma (colloid), Inflammatory breast carcinoma, Scirrhous carcinoma, Papillary carcinoma, Paget disease and Undifferentiated carcinomas. Other tumors such as Phyllodes, Angiosarcoma and Primary lymphoma may occur in breast but they are not histologically classified as sub-types of the breast cancer (Edge SB et al. 2010; Carter and Page 2004; Yeatman et al. 1995; Chaney et al. 2000; Piñero-Madrona et al. 2008). In this classification, some types are common such as ductal and lobular carcinoma, while some others are rare such as Paget disease. Since ductal carcinoma was used in this study, it will be discussed in the next section (American Cancer Society, 2011c; Egyed, Járay and Péntek 2006).

1.1.6.1 Ductal breast carcinoma

Ductal breast carcinoma is one of the most common types of breast malignancies. In this carcinoma, the tumor cells originate from epithelial cells lining the inner layer of the milk ducts. Ductal breast carcinomas are categorized into two subtypes based on the location and invasion of the tumor cells into basement membrane of the ducts.

Invasive or infiltrating ductal carcinoma (IDC) is the most frequent subtype of breast carcinoma and accounting for 60- 80% of all breast malignancies. Thus, IDC develops in ducts and then invades the basement membrane of the ducts and finally may spread to the

adjacent lymph nodes and tissues as well as other organs (American Cancer Society, 2011c; Lee et al. 2010; Harris et al. 1984; Wasif et al. 2010). If the tumor cells are limited to the basement membrane of the ducts it is called ductal carcinoma In-Situ (DCIS) which is the most frequent types of non-infiltrating breast carcinoma accounting for 10-20% of all breast malignancies. DCIS by itself is not fatal, but it may increase the chance of developing IDC in a female Thus, the probability of recurring after 5 to 10 years is about 30% specifically if the breast cancer patient was not undergone the radiotherapy. However, if radiotherapy performs in combination with other optimal therapies, the risk of recurring drops to nearly half (Moriya and Silverberg 1994; Farese and Aebi 2009; Jansen 2011; Betsill et al. 1978; Kerlikowske 2010; Barth et al. 1995; Leonard and Swain 2004).

1.1.7 Diagnosis of breast cancer

As noted breast cancer may or may not have an apparent signs or symptoms. However, in some cases lumps may be detected by patient in self-examination or by physician. Other symptoms such as skin redness, rash, retraction or nipple discharges should be taken as a serious matter until prove otherwise by examining physician. However, once a female seek a physician there could be several diagnostic steps for detecting a breast cancer that will be discussed in next sections.

1.1.7.1 Physical examination

The clinical physician may find some potential abnormalities in breast examination. These findings may include asymmetry of breasts, skin inflammation, discharge or

retraction of the nipple, lumps or bump in breast, lymphadenopathy in auxiliary, infra or supra clavicular lymph nodes. Although normal clinical examination is promising, it could not completely rule out the existence of any malignancy in the breast specifically in females more than 40 years old. Thus, a regular screening system is recommended to perform on females older than 40 years old.

1.1.7.2 Mammography

Mammography is a medical procedure in which the breast image is taken by x-ray. American National Cancer Institute recommends females to do mammography every 1-2 years in those who are above 40 as a screening method. However, if a clinical physician is suspicious to any abnormality in the breast's breast, it is recommended to perform mammography as a first diagnostic step for females at any ages. In fact, the exposure time of the x-ray and its precision is higher in diagnostic mammography than screening mammography. Sometimes mammography could detect abnormalities which are not palpable for patient or physician. In addition, micro calcifications are easily detected in mammography which could be an important sign of malignant cancer. However, mammography has some false negative or false positive results which should be considered by examining physician for further evaluation (Golinger et al. 1979; Borràs, Espinàs and Castells 2003; Vidal and Cozzi 1970; Ostapenko et al. 2004; Shetty 2011).

1.1.7.3 Ultrasonography

Ultrasonography is a non invasive imaging method could scan internal parts of breast as well as other soft tissues by using high frequency sound waves. Therefore, this method

enables the physicians to have a real time image of internal parts of breast. Solid and cystic masses could be detected and discriminated in the breast by ultrasonography. Following this step, the clinical physician could decide about the next diagnostic step. However, the interpretation of ultrasound in some cases is difficult or even unreliable specifically in dense breasts. Some time the real time ultrasonography is used as a good guide for taking biopsy from the breast (Guarneri et al. 2011; Le-Petross and Shetty 2011; Shin et al. 2011; Garcia-Ortega et al. 2011).

1.1.7.4 Magnetic Resonance Imaging (MRI)

MRI is another non-invasive screening test which is more sensitive than mammography ultrasound as it could detect the abnormalities even in dense breasts; however, it is nat sensitive for detecting micro calcifications. In this method, cross sectional images of the internal organs could be taken by using magnet and radio waves. MRI could be used for different purposes such as screening for those who are at high risk of breast cancer, reevaluating the suspicious area of the breast and also used for following up of the breast cancer patients after treatment (McLaughlin and Hylton 2011; Jansen 2011; Monticciolo 2011; Miller, Abbott and Tuttle 2011; Postma et al. 2011; Fakkert et al. 2011; Guarneri et al. 2011; Le-Petross and Shetty 2011).

1.1.7.5 Positron emission tomography (PET-scan)

PET scan is generally used for evaluating breast cancer patient in stage II, IIIA, IIIB and IV in order to detect any potential metastasis specifically after treatment. Thus, radiopharmaceutical [18F] 2-deoxyglucose is intravenously injected to the patient and

then patient will be scanned for 90 minutes. Changing of the metabolism of glucose by tumor cell could be indicative of metastasis. On the other hand, this method is expensive and has a higher rate of false positive results compared to other methods (Park et al. 2011; Champion et al. 2011; Clapp, Peller and Subramaniam 2011; Warning et al. 2011; Choi et al. 2011; Niikura et al. 2011).

1.1.7.6 Fine needle aspiration (FNA) and breast biopsy

FNA is an easy and rapid test which is done on breast lumps by using a fine needle. FNA is a less invasive diagnostic method that enables a physician to discriminate a cystic mass from a solid mass found in the breast after screening. In addition, FNA provides a small sample of breast's lumps for further laboratory evaluations.

Biopsy is basically a definite gold standard way for diagnosis of the breast abnormality. Thus, the breast's abnormality will be partially or totally removed by a surgeon. However, based on the surgeon's decision, obtaining the sample may be performed by using different less invasive or invasive procedures. In some cases, biopsy will be done under a guide of ultrasound. Then, the obtained sample would be microscopically evaluated by a pathologist to make a diagnosis based on histopathology and cytological features of the specimen(Hong et al. 2011; Miyake et al. 2011; Lianidou and Markou 2011; Canavese et al. 2011; Simsir, Rapkiewicz and Cangiarella 2009; Zhao, 2009 Michelow, Dezube and Pantanowitz 2010).

1.1.8 Treatment of breast cancer

1.1.8.1 Surgery

Surgery is a common therapeutic method for breast cancer that may be used in combination with other treatments. For example, in ductal carcinoma in-situ the combination of surgery and radiotherapy are recommended. Most of the time, surgery is considered as a diagnostic and prognostic procedure. There are different types of surgery depending on the tumor grading and staging as well as the patient general health condition. The type of surgery ranges from local lumpectomy and partial (segmental) mastectomy to radical mastectomy depending on above conditions. In the latter, in addition to the breast, auxiliary or surrounding lymph nodes and sometimes the underlying muscles are also removed by surgeon (American Cancer Society, 2011c).

1.1.8.2 Radiation therapy

Radiotherapy is a therapeutic method used for breast cancer by using high energy x-ray. This method induces the apoptosis and also inhibits uncontrolled proliferation in cancer cells. Depending on the type and stage of the breast cancer external or internal therapy may be hired. External radiotherapy emit x-ray on the external surface of the cancer region, while in internal method, radioactive chemicals are directly guided into the cancer location via a needle or catheter. This method is usually used in combination with other methods such as surgery or chemotherapy. Thus, radiotherapy may apply pre or post-operatively in breast cancer patients. Performing radiation therapy together with surgery was associated with a less recurrence rate as well as a better survival for breast cancer

patients (Ragaz 1990; Ragaz, Spinelli and Coldman 2000; Woodward et al. 2010; Clarke et al. 1985; Clarke et al. 2005; Early Breast Cancer Trialists' Collaborative Group (EBCTCG) et al. 2010; Miyake et al. 2011; Lianidou and Markou 2011).

Systemic treatment is referred to using a wide variety of the chemical (chemotherapy), hormonal (hormonal therapy) or targeted-agent (biological therapy) medication on breast cancer patients via systemic circulation. These medications are generally used in combination with surgical operations; thus they are used before surgery (called neo-adjutant) to kill the tumor cells and reduce the tumor size or used after surgery (adjutant) to decrease the recurrence rate. Using either of these methods depends on the cancer stage, patient's condition and the presence of specific biomarkers. In addition, based on the clinical status of the patients different protocols may be used for combining several of these systemic medications. Although these therapeutic medications were associated with improved survival of the patients, they might exhibit undesired side effects due to their influence on the normal cells (Sakr and Dizon 2011; Bantema-Joppe et al. 2011; Glasziou and Houssami 2011; Hall et al. 2011).

1.1.8.3 Systemic therapy

1.1.8.3.1 Chemotherapy

Chemotherapeutic drugs generally inhibit the growth and/ or induce cell death in cancer. A combination of these drugs was shown to be more effective than single chemotherapy; and thus they routinely used in a 2 or 3 combinational protocols. Their frequent successful combinations are shown in Table 1.1. Although using these drugs are basically

shown to be beneficial for decreasing the relapse rate and also increasing the patient's survival, several undesired side effects may appear such as nausea, vomiting, constipation, diarrhea, hair loss and fatigue (Kimmick 2011; Yin et al. 2011; Horio et al. 2011; Yagata, Kajiura and Yamauchi 2011; Choi, Craft and Geraci 2011; Fitzal et al. 2011; Müller et al. 2011; Vera-Ramirez et al. 2011).

Table 1.1. Common chemotherapeutic combinations used for breast cancer.

Abbreviation	Combinational chemotherapy
AC	Doxorubicin, cyclophosphamide
AC-T	AC followed by paclitaxel
EC	Epirubicin, cyclophosphamide
EC-T	EC followed by paclitaxel
CMF	Cyclophosphamide, methotrexate, 5-fluorouracil
TC	Docetaxel, cyclophosphamide
TCH	Docetaxel, carboplatin, trastuzumab

1.1.8.3.2 Hormonal therapy

The proliferation of the tumor cells in some of the breast carcinomas is closely rely on the existence of estrogen or progesterone. The hormonal therapy mainly blocks or inhibits the influence of the estrogen or progesterone on their corresponding receptors. Therefore, the hormonal therapy may be useful on cancer cells that exhibit estrogen or progesterone receptors. Before the menopause, patients may benefit from estrogen receptor blockers such as Tamoxifen. In addition, estrogen receptor blockers may be used in combination with ovarian suppressor drugs such as Leuperolide or Goserlin, Aromidex, Aromasin. Aromatase inhibitors are shown to be beneficial after menopause. They inhibit the endogenous production of estrogen in the body. The well known members of this group are Anastrazol, Letrozole and Exemestane. Fulvestrant is a member of estrogen receptor

blockers which is recommended to be used after menopause. On the other hand, using hormonal therapy may cause some undesired side effects such as hot flash feeling, infertility and irregular menses (Mouridsen et al. 2003; Poole and Paridaens 2007; von Minckwitz et al. 2001; Eiermann et al. 2001; de Haes and Olschewski 1998; Barker 2003; Bohnet and Bertram 1989; Spinelli et al. 2008; Vrbanec et al. 1998).

1.1.8.3.3 Targeted therapy (Biological therapy)

In biological therapy, the drugs target certain critical molecules which are responsible for growth and progression of the tumor cells. For instance, over expression of HER2/neu gene in some breast cancer may lead to rapid proliferation as well as progression of the tumor cells in the body. Trastuzumab is a monoclonal antibody that is able to bind into HER2 protein on the cell membrane of cancer cells and thus, inhibits the cell signaling which cause cellular proliferation as well as invasion. Biological therapy is usually given in combination with other anti tumor treatments. Bevacizumab is another monoclonal antibody which is able to inhibit angiogenesis in tumor tissues and therefore, limits the cancer growth and progression. Undesired side effects may happen during the biological therapy such as rash, fever, chill, diarrhea, hypertension, heart, liver or kidney dysfunction (Ferreira et al. 2011; Munagala, Aqil and Gupta 2011; Syrigos et al. 2011; Kümler and Nielsen 2011; Polyzos et al. 2011; Petrelli et al. 2011; Pivot et al. 2011; Burris 2011; Spano et al. 2011; Fang et al. 2011; Rack et al. 2011; Denkert et al. 2011; Alonso Gordoa et al. 2011).

1.2 Introduction to glycosaminoglycans (GAGs)

Glycosaminoglycans (GAGs) are long unbranched polysaccharides macromolecules comprising of an alternating disaccharide subunit of uronic acid isoforms such as L-iduronic acid or D-glucuronic acid and an N-acetyl-hexosamine such as N-acetylglucosamine (GlcNAc) or N-acetylgalactosamine (GalNAc). They range from sulfated macromolecules with a highly negative charge (heparin) to unsulfated molecules (Hyaluronan). GAGs could not only be found on the cell surface but they are forming the important components of extracellular matrix of a variety of the human tissues. The main members of GAGs super family are heparan sulfate, dermatan sulfate, chondroitin sulfate, keratan sulfate and hyluronan (Figure 1.5). Except hyluronan, other glycosaminoglycans chains might be bounded to a variety of the core protein by covalent links to form proteoglycan (PGs) (Figure 1.6).

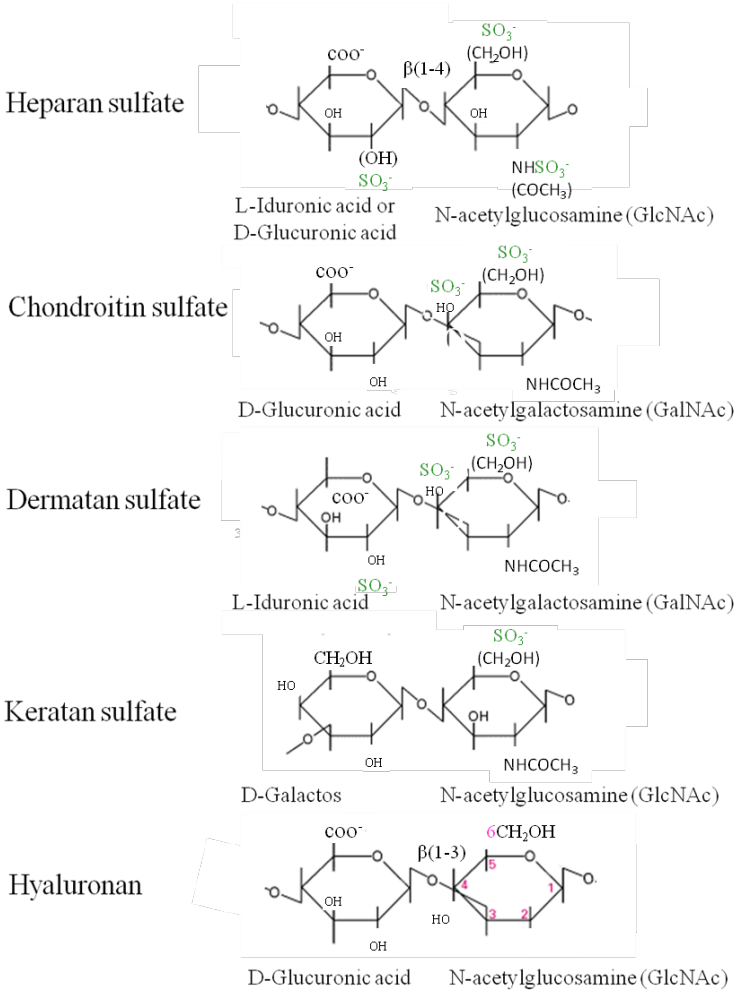

Figure 1.5. The structure of disaccharides of different glycosaminoglycans (GAGs). Except hyluronan, other GAGs could be sulfated in a diverse manner.

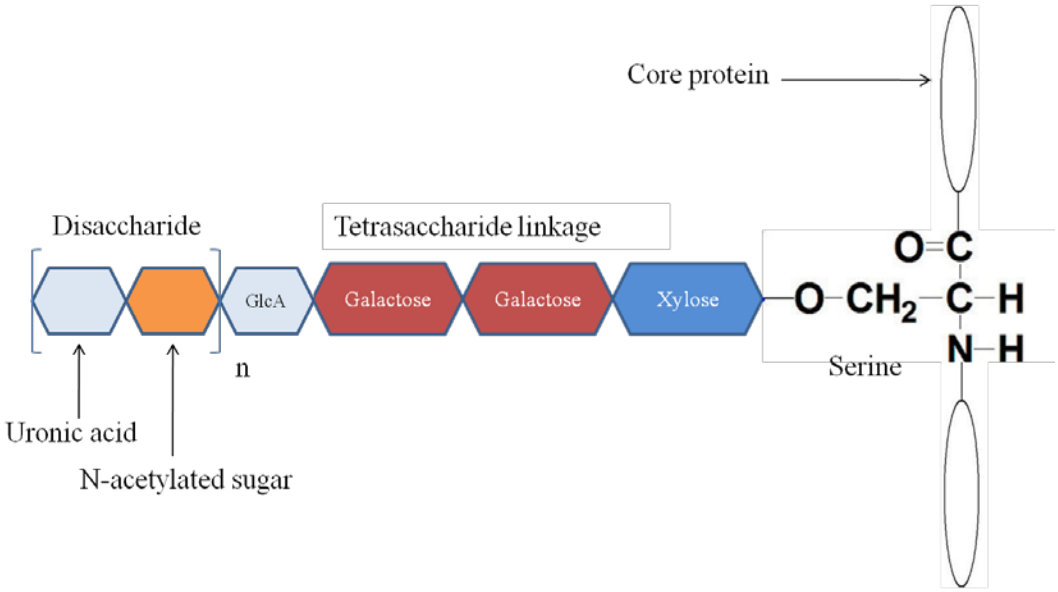

Figure 1.6. The backbone structure of Proteoglycans (PGs). Glycosaminoglycans covalently attach to core proteins via a serine residue.

Heparan sulfate (HS) is a long sulfated negatively charged GAG that composed of alternating subunit of D-glucuronic acid and N-acetylglucosamine disaccharides or L-iduronic acid and N-acetylglucosamine. Heparan sulfate is an unbranched macromolecule that could be abundantly found on the cell surfaces as well as in extracellular matrix. Heparin, a well known highly sulfated type of heparan sulfate is recognized as the most negatively charged molecule in the nature which abundantly found in mast cell granules and has an anticoagulant function in human body. HS molecules are involved in a variety of cellular and physiological mechanisms in living organism from invertebrate to human. It is of great importance since it has critical role in many biological and pathological conditions in human such as growth development and carcinogenesis (Whitelock and Melrose 2011; Rabenstein 2002). In the next sections, the types and functions of these macromolecules will be discussed in detail.

Chondroitin sulfate (CS) and Dermatan sulfate (DS) are sulfated linear GAGs which have a similar precursor in their biosynthesis. Chondroitin sulfate is composed of repeating subunits of glucuronic acid and N-acetylgalactosamine (GalNAc), while dermatan sulfate is structured by repeating L-iduronic acid N-acetylgalactosamine (GalNAc) disaccharides. CS and DS are heterogeneous molecules due to their various O-sulfation patterns and could be found in many mammals. Dermatan sulfate could be abundantly found in the human skin and the wall of the vessels, while chondroitin sulfate is mainly found in the articular cartilage and in nervous system. CS and DS play important roles in development, wound healing, differentiation, cardiovascular diseases, carcinogenesis, inflammation, infection and anticoagulation and fibrosis (Shirk et al. 2000; Maimone and Tollefsen 1990; Cöster 1991; Trowbridge and Gallo 2002; Kozma, Olczyk and Głowacki 2001; Watanabe, Yamada and Kimata 1998; McGee and Wagner 2003; Głowacki, Koźma and Olczyk 2004; Maeda et al. 2011; Calabrese et al. 2004).

Keratan sulfate (KS) is a short unbranched glycosaminoglycans constituted of an N-acetylglucosamine as well as galactose instead of uronic acid in its repeating disaccharides. KS could be mainly found in extracellular matrix of several tissues; however, it is majorly found in cornea, cartilage as well as central nervous system. Similar to other GAGs, KS involved in various cellular and biological processes such as development, osteoarticular disorders, corneal diseases and neurodegenerative disorders (Lester et al. 2001; Funderburgh, Caterson and Conrad 1986; Funderburgh et al. 1991; Lindahl et al. 1996; Funderburgh 2002; Greiling 1994).

Hyaluronan (HA) is large unsulfated negatively charged GAGs with high molecular weight that composed of repeating D-glucuronic acid and N-acetylglucosamine disaccharides. This molecule has an excellent lubricating characteristic as they could keep a large volume of fluid in extracellular matrix (ECM). Hyaluronan is a major component of synovial fluid, saliva, vitreous humor and extracellular matrix of loose connective tissues. These macromolecules are involved in some other important functions such as cell proliferation, wound healing, inflammation, immunity, angiogenesis and cancer progression (Gao et al. 2010; Slavkovsky et al. 2010; Maeshima et al. 2011; Bharadwaj et al. 2011; Meran et al. 2011; Swann et al. 1984; Pogrel, Lowe and Stern 1996; Cascone, Fonzi Dagger and Aboh 2002; Lu, Levick and Wang 2005; Cöster 1991; Maimone and Tollefsen 1990; Lindahl et al. 1996). As shown in Table 1.2, Proteoglycans are classified into several categories based on their core protein as well as their specific localization (Waddington and Embery 2001).

Table 1.2 Classification of proteoglycan (PGs) based on their core protein and localization (Waddington et al. 2001).

Localization	**Glycosaminoglycan chain**	**M_r of the core protein (kD)**	**Main members**
ECM	HA, CS, KS	225-250	Aggrecan, versican
Collagen-associated	CS, DS, KS	40	Decorin, biglycan, fibromodulin
Basement membrane	HS	120	Perlecan
Cell-membrane	HS, CS	33[(1)]-60[(2)]-92[(3)]	Syndecans[(1)], Glypican[(2)], Betaglycan[(3)], CD44E, cerebroglycan
Intracellular granules	Heparin, CS	17-19	Serglycin

HS, heparan sulfate; KS, keratan sulfate; CS, chondroitin sulfate; DS, dermatan sulfate; HA, hyaluronic acid, ECM; extracellular matrix.

1.3 Heparan Sulfate Proteoglycans (HSPG)

1.3.1 Introduction to Heparan Sulfate (HS)

As stated above, heparan sulfate is a highly sulfated macromolecule which expresses ubiquitously on the cell membrane as well as extracellular matrix of all mammals. This linear polysaccharide with a highly negative charge composed of repetitive disaccharide and covalently attaches to the serine residue of various core proteins. HSPGs are categorized to several classes based on their core protein. On the cell surface, heparan sulfate majorly bind with two main families of core proteins: Syndecan (Syndecan 1-4) and Glypican (Glypican 1-6). Syndecan are transmembrane proteins whose C- terminal domains are highly conserved. HS connect to syndecan via a serine residue in the distal part of the core protein. Chondroitin sulfate (CS) chains sometime accompany the HS on the syndecan and bounds to the proximal part of the core protein. Glypican core proteins are globular proteins stabilized by disulfide links on the cell surface and attach to cell membrane via Glycophosphatidylinositol (GPI) linkage. HS attaches to the glypican core protein near the plasma membrane. Secreted syndecan or glypican into the extracellular matrix are called Perlecans and Agrin which could be found in extracellular matrix (ECM) (Figure 1.7). Despite syndecans, glypicans and perlecans merely accompany heparan sulfate chains (Whitelock and Iozzo 2005; Kramer and Yost 2003).

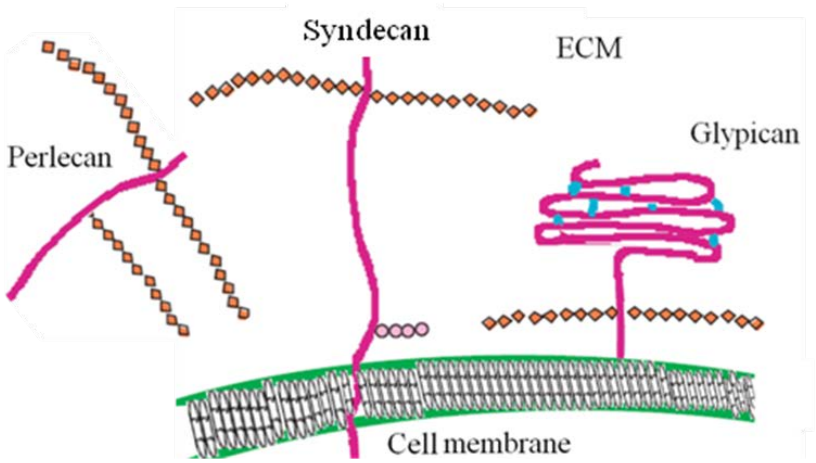

Figure 1.7. Main types of heparan sulfate proteoglycans (HSPGs). Syndecans composed of a transmembrane core protein (red), while the core globular protein (red) of glypicans attaches to the cell membrane via a glycosylphosphatidylinositol (GPI) linkage. Chondroitin sulfate (CS) chains sometime accompany the HS on the syndecan and bounds to the proximal part of the core protein. Blue dots represent disulfide bond in glypican core protein. Perlecans are shedded heparan sulfate proteoglycans (HSPGs).

Heparan sulfate is the most biologically active GAG in human and thus play a significant role in several biological and cellular processes. It interacts with several growth factors and cytokines and therefore mediates a variety of the complicated biological processes in cellular events such as proliferation, adhesion, migration and differentiation. The heparan sulfate may function as a receptor or co-receptor to mediate these cellular processes by internalizing the cell signals (Bernfield et al. 1999). Therefore, the level of expression of heparan sulfate may potentially influence the signal transduction. It was reported that expression of the HS on cell surface could critically regulate the development of different organs during embryonic period. This regulation may start from early blastula to the latest stages of organogenesis (Tumova, Woods and Couchman 2000; Sutherland et al. 1991; Litwack et al. 1998). Therefore, any change in the expression pattern of heparan

sulfate might lead to a variety of the growth and developmental disorders (Silveri et al. 1991; Cano-Gauci et al. 1999; Ng et al. 2009).

On the other hand, the quantitative changes of heparan sulfate expression may contribute in tumorogenesis process; because these changes could potentially alter the interaction between the cell membrane heparan sulfate and several ligands such as cytokines and growth factors. Heparan sulfate expression was reported to be involved in the malignant process of several cancers such as breast cancer, pancreatic cancer, colorectal cancer, brain cancer and lung cancer. For example, a high expression of syndecan 1 in breast cancer was shown to be associated with more aggressive nature of tumor cells (Vlodavsky et al. 1988; Iozzo 1988; Naor, Sionov and Ish-Shalom 1997; Lo et al. 2011; Suzuki et al. 2010; Umezu et al. 2010; Barbareschi et al. 2003; Tátrai et al. 2010; Lv et al. 2007; Chatzinikolaou et al. 2008; Raman and Kuberan 2010).

Heparanase is an enzyme that cleaves the cell surface and extracellular heparan sulfate. Studies has shown that over-expression of heparanase may result in various malignancies such as breast cancer, leukemia and brain cancer (Nadir, Vlodavsky and Brenner 2008; Theodoro et al. 2007). Other studies showed that shedding of syndecan 1 that is enhanced by heparanase, could significantly stimulate the growth and metastasis of the breast cancer cells (Su et al. 2007).

Apart from quantitative changes, qualitative alterations in the structure of HS could significantly affect the interaction between the heparan sulfates on the cell surface with

several growth factors. Hence, having a deep understanding about the structure of the heparan sulfate and its modification during biosynthesis seems to be necessary.

1.3.2 Heparan sulfate biosynthesis

Heparan sulfate is a heterogeneous macromolecule which consists of repeating disaccharide subunits of uronic acid and glucosamine and produces in Golgi apparatus inside the cells (Yang et al. 2007). Thus, heparan sulfate biosynthesis is a highly complex process that starts from the location in which it connects to the core protein. The attachment location usually composed of 2-4 Serine-Glycine sequence on the core protein.

The biosynthesis of HS is a sequential process which begins with chain initiation, continued by chain polymerization, and finally completed with chain modification. These steps are done by several enzymes such as glycosyltransferases, sulfotransferases, epimerase and acetylase. In the first step, assembly of a tetrasaccharide which is called linkage region on the serine residue of a core protein is started. The linkage region of heparin heparan sulfate, dermatan sulfate and chondroitin sulfate has similar structure. The catalysis of this step is sequentially accomplished by Xylose transferase (Xy1T), Galactose transferase I (GalIT), II (GalIIT) and Glucoronic acid transferase by adding each sugar to non-reducing side of the chain. By the end of first step, the tetrasaccharide is made and composed of glucoronic acid (GlcA)-galactose (Gal)-galactose (Gal)-Xylose (Xyl).

Polymerization of heparan sulfate specifically begins with addition of at least one α1, 4 glucuronic acid to the linkage region by α -glucoronic acid transferase II (GlcAT-II) and then followed by inserting N-acetylglucosamine by GlcNAc transferase II (GlcNAcT II). Thus, polymerization continues with addition of alternating disaccharide units (up to 200 disaccharides) by glycosyltransferases (EXTs) to form the backbone of HS in the Golgi apparatus (Esko and Selleck 2002; Lamanna et al. 2007).

By completing the polymerization, modification of heparan sulfate chain starts. These modifications happen in sequence, starting from Glucuronic acid N-deacetylation and N-sulfation to C5 epimerization of glucuronic acid into iduronic acid and then several O-sulfations. The latter is done by Sulfotransferases, the enzymes which specifically transfer the sulfate group from 3′-phosphoadenosyl-5′-phosphosulfate (PAPS) as a donor of sulfate group to the particular position in the sugar residues. O-sulfation begins at C2 of Iduronic acid (L-IdoA) and glucuronic acid (D-GlcA) residues (2-O-sulfation) with more preference for L-IdoA and then continued to C6 sulfation in glucuronic acid and N-acetylglucosamine (6-O-sulfation) and may finally end with C3 sulfation in glucuronic residues (3-O-sulfation).

Three isoforms have been recognized for heparan sulfate 6-O-sulfotransferases (HS6ST1-3). HS6ST isoforms have different substrate specificities. Thus, they may transfer the sulfate group to either GlcNSO3 or GlcNAc residues; additionally, HS6ST1 predominately act on C6 of GLcNOS3 residue of the HexA-GlcNOS3, but HS6ST2 prefer C6 of GlcNOS3 residue of the IdoA (2SO4)-GlcNO3 and HS6ST3 may act on

both depending on the substrate concentration. Furthermore, HS6ST isoforms express in a tissue-specific manner because HS6ST1 express in epithelial and neural-derived tissues, while HS6ST2 mainly expresses in mesenchymal tissues and HS6ST3 may express in a restricted manner during the later stages of embryonic period. (McCormick et al. 2000; Lin 2004; Kramer and Yost 2003; Izumikawa et al. 2006; Esko and Lindahl 2001; Hagner-McWhirter et al. 2004; Gorsi and Stringer 2007; Habuchi, Habuchi and Kimata 2004).

There are other important enzymes which are able to modify the heparan sulfate 6-O-sulfation in human; called endosulfatases (SULFs). Human SULF1 and SULF2 are enzymes known by their arylsulfatase activities that specifically remove sulfate group from C6 in heparan sulfate chain. SULFs are able to desulfate the HS both intracellular (Golgi apparatus) and extracellular (cell membrane and ECM). It was shown that trisulfated IdoA2S-GlcNS6S disaccharide in the heparan sulfate chain is a preferred substrate for both of the endosulfatases (Sedita, Izvolsky and Cardoso 2004; Frese et al. 2009; Ai et al. 2006).

All of the mentioned modifications provide a wide heterogeneity in heparan sulfate macromolecules. Sulfation pattern of heparan sulfate chain is a significant factor that determines the interactions between HS and variety of the ligands such as cytokines, and growth factors and therefore, the function of HS is critically dependent on its sulfation pattern (Morimoto-Tomita et al. 2002; Gama et al. 2006; Jastrebova et al. 2010; Allen, Filla and Rapraeger 2001). The sulfation seems to play a crucial role in cell signaling

which results in growth and development in mammals. Failure of any of these modifications may result in growth disorders or fatal developmental abnormalities during the embryonic period (Sugaya et al. 2008; Lin et al. 2000; Stickens et al. 2005; Carlsson et al. 2008; Habuchi et al. 2007; Habuchi, Habuchi and Kimata 2004; Kobayashi et al. 2007; Garg et al. 2003; Ford-Perriss et al. 2002; Habuchi and Kimata 2010; Pratt et al. 2006).

On the cellular basis, most of the biologically active growth factors need heparan sulfate to regulate the cellular processes such as proliferation, adhesion and migration. For this purpose, heparan sulfation pattern plays a critical role in determining the spatial configuration and the binding site of HS for interacting with growth factors. Recently, researcher showed that dysregulation of the heparan sulfation pattern may involve the cells in the malignant process of carcinogenesis (Sousa et al. 2008; Kozlowski and Pavao 2011; Tátrai et al. 2010; Jastrebova et al. 2010; Sanderson et al. 2005). Other researchers demonstrated that the heparan sulfation pattern could actively promote or inhibit tumor invasion as well as its metastasis (Kozlowski and Pavao 2011; Gama et al. 2006).

1.3.3 Heparan sulfate 6-O-sulfation and cancer

In the following section, enzymes which are involved in 6-O-sulfation of heparan sulfate chain and their significance in tumorogenesis are reviewed. Thus, we firstly will focus on critical role of 6-O-sulfotransferases (HS6STs) which transfer sulfate group into C6 position of N-acetylglucosamine (GlcNAc) residues of heparan sulfate. Then,

endosulfatases (SULFs) which remove sulfate group from the similar position will be discussed.

One of the most important sulfation modifiers of heparan sulfate is 6-O-sulfotransferase (HS6ST) that specifically transfers sulfate group from 3'-phosphoadenosine 5'-phosphosulfate (PAPS) to C6 position of N-acetylglucosamine (GlcNAc) residues of HS. As discussed, three HS6ST isoforms have been described in humans with differences in their tissue distribution. Each isoform plays an important role in modifying a tissue-specific 6-O-sulfation in heparan sulfate chain (Habuchi et al. 2000). Changes of the expression of each HS6ST isoforms were shown to be associated with an altered HS domain structure that may affect the molecular interactions and signaling processes (Do et al. 2006). Several studies have demonstrated that HS 6-O-sulfotransferases are involved in important biological processes such as embryonic organogenesis, postnatal growth and development (Kamimura et al. 2001; Sedita, Izvolsky and Cardoso 2004; Habuchi et al. 2007; Izvolsky et al. 2008). Tissue-specific expression of HS6ST isoforms at different time points of embryonic period indicates that their timely expression is significantly required for growth factor-related development during organogenesis (Sedita, Izvolsky and Cardoso 2004). In addition, to the embryonic development, HS6ST isoforms seem to influence the anticoagulant characteristic of heparan sulfate during its biosynthesis (Zhang et al. 2001). Of the few studies, remarkable over-expression of HS6ST2 has been demonstrated in serous, papillary, clear cell carcinoma of ovary as well as cervical and corpus cancer of uterine (Kanoh et al. 2006; Seko et al. 2009). Song et al. recently found that down-regulation of HS6ST2 could inhibit the growth and progression of the pancreatic cancer (Song et al. 2011). Therefore, a new insight has been provided

for identifying the potential role of HS6ST isoforms in tumorogenesis, but limited efforts were performed to clarify their function in the malignant process of tumorogenesis.

Endosulfatases (SULFs) are other potent sulfation modifying enzymes which specifically edit 6-O-sulfation on the cell surface and extracellular matrix by removing the sulfate group from C6 position of N-acetylglucosamine in heparan sulfate chain and thereby modulating the biological activity of heparan sulfate (Holst et al. 2007). SULF1 and SULF2 are two isoforms of endosulfatases which have been identified in humans. Recently, a growing body of research has focused on expression pattern of SULF1 and SULF2 in a variety of malignancies, since it was identified that the expression of these two enzymes were dysregulated in a number of human malignancies including breast cancer. It has also been distinguished that up or down regulation of human endosulfatases modulates the cellular behavior of many cancers by inducing an alteration in sulfation pattern of carbon C6 in heparan sulfate chain. This means that the sulfation pattern of C6 position in N-acetylglucosamine residues has an important role that crucially determines the binding site and interaction of heparan sulfate chain with various growth factors. Several researchers observed a remarkable suppression in tumor proliferation, invasion, migration and angiogenesis in response to over expression of SULF1 in a variety of cancers like myeloma, hepatocellular cancer, head and neck cancer, breast and ovarian carcinomas (Safaiyan, Lindahl and Salmivirta 1998; Lai et al. 2004; Dai et al. 2005; Sanderson et al. 2005; Morimoto-Tomita et al. 2005; Timson et al. 2006; Lai et al. 2006; Narita et al. 2007; Liu et al. 2009), while some others found that over expression of SULF1 could result in an enhanced tumor cell progression in few different malignancies such as lung, pancreatic and gastric carcinomas (Abiatari et al. 2006; Lemjabbar-Alaoui

et al. 2010; Junnila et al. 2010). These events are due to dramatic influence of endosulfatase enzymes on 6-O-sulfation pattern of heparan sulfate chain. To date, the expression pattern of SULF1 and SULF2 in breast cancer has been described in a few studies, but they have not explained the functional role of editing enzymes of 6-O-sulfation in breast carcinogenesis. Narita et al. observed that SULF1 is down regulated in their in situ hybridization with lobuar morphology predominance (Narita et al. 2007). Prior to that, they understood that the expression of SULF1 reduce angiogenesis as well as tumorogenesis of breast cancer *in vivo* (Narita et al. 2006). Later, Chen, Zhao et al. found that SULF1 gene is silenced due to the hypermethylation of its promoter in breast carcinomas (Chen et al. 2009). Functional hypermethylation of SULF1's promoter provided a logical mechanistic solution for SULF1 down regulation in breast cancer as well as other malignancies, but how SULF1 down regulation is involved in breast carcinogenesis, is limited to a few simple correlations. Unlike SULF1, there are some evidences implying that the expression of SULF2, on the other hand, is proangiogenic in the breast (Morimoto-Tomita et al. 2005). Therefore, it seems that SULF1 and SULF2 functionally behave differently in breast cancer in terms of their genomic pathway outcomes.

As stated above, although 6-O-sulfation induced by endosulfatases may play a paradoxical role in different human malignancies, its involvement in the malignant process of many cancers and specifically in breast cancer is potentially evident. In addition, it was consistently observed that the activity of SULF1 is diminished in breast

cancer as well as other cancers. Thereby, it is inferable that 6-O-sulfation within heparan sulfate chain may have a reverse relationship with SULF1 expression.

Herein, according to the significant involvement of SULF1 in the malignant process of breast carcinogenesis and based on the limited knowledge about the potential role of HS6ST isoforms in carcinomas, it is thus deducible that changes in the expression HS6ST isoforms may lead to a functional alteration of breast cancer cellular phenotypes. However, little is understood about the function of HS6ST isoforms in generating specific HS protein-binding sequences, expression pattern, and function, specifically in the malignant process of breast carcinogenesis.

1.4 Scope of the study

A growing body of researches has focused on the significant role of GAGs in the malignant process of the carcinogenesis. This study was mainly performed on the heparan sulfate glycosaminoglycan (HSGAG), the most diverse and biologically active GAG in regulating the interactions of cell to cell as well as cell to extracellular matrix (ECM). Modifications of heparan sulfate chain in the final stage of its biosynthesis are of great importance. Of several modifications, sulfation has attracted attentions, because sulfation critically determines the spatial configuration and thus the biding site for interaction of HS with other ligands such as growth factors. Recently, a few studies showed that 6-O-sulfation could be potentially involved in the malignant process of carcinogenesis. HS6STs and SULFs are the main editors of 6-O-sulfation within heparan sulfate chain. Similar to endosulfatases, HS6ST isoforms may similarly act on 6-O-

sulfation within heparan sulfate chain; however, their functional outcomes may vary in carcinogenesis. This study was specifically restricted to represent the expression, functional and genomics role of HS6ST3 in breast cancer. Thus, the functional role of the other isoforms was not central to this study. In addition, the involvement of HS6ST3 in other cancers was beyond the scope of our research.

1.5 Hypothesis

1- HS6ST3 may modulate the breast cancer growth and progression.

2-HS6ST3 expression may correlate with the clinicopathological parameters in breast cancer.

3-SULF1 expression may correlate with the clinicopathological parameters in breast cancer.

1.6 Aim of the study

In this study, it was mainly aimed to elucidate the functional role of HS6ST3 in T47D and MCF7 breast cancer cell lines. Thus, the results of this study may provide a novel pathway map for the down-stream gene(s) involved in proliferation, cell cycle, apoptosis, adhesion, migration and invasion of T47D and MCF7 cell lines after silencing *HS6ST3*. Furthermore, the immunohistochemical expression of HS6ST3 and SULF1 were examined on clinical samples of ductal breast carcinoma by using immunohistostaining

technique. The latter approach may significantly contribute to introduce novel diagnostic and/or prognostic biomarkers for breast cancer as well as other malignancies. Together, specific objectives of this research are as following:

1-To elucidate the functional roles of HS6ST3 in T47D and MCF7 breast cancer cell lines.

2-To study the effect of HS6ST3 silencing on heparan sulfate synthesis in T47D and MCF7 cell lines.

3-To explore a genomic pathway downstream to the *HS6ST3* which regulates the cancer growth and progression in T47D and MCF7 breast cancer cell lines.

4-To examine the influence of silencing of *HS6ST3* on sensitizing T47D cell line to the cytotoxic effect of cisplatin and 5-fluorouracil.

5- To determine the association between HS6ST3 expression and clinicopathological features of the patients with invasive ductal carcinoma

6- To investigate whether the expression of HS6ST3 could be used as a novel prognostic or diagnostic biomarker in breast cancer.

7- To determine the association between SULF1 expression and clinicopathological features of the patients with invasive ductal carcinoma.

8- To investigate whether the expression of SULF1 could be used as a novel prognostic or diagnostic biomarker in breast cancer.

In the next chapter, the methods of experiments and materials used in this study will be discussed. In chapter 3, results will be presented in detail. After that, conclusion and discussion will be presented in chapter 4.

CHAPTER 2

METHODS AND MATERIALS

2.1 Cell culture

Non-cancerous human epithelial breast cell lines including MCF12A (ATCC no: CRL-10782), and MCF-10A (ATCC no: CRL-10317); breast cancer cell lines including T47D (ATCC no: HTB-133, MCF7 (ATCC no: HTB-22) and MDA-MB 231 (ATCC no : HTB-26) cell lines were taken from American Tissue Culture Collection (ATCC, Manassas, VA, USA). MCF12A, an spontaneously immortalized non-cancerous human mammary epithelial cell line was taken from MCF-12M, a mortal cell line which was obtained from a mammary tissue with focal locations of intraductal hyperplasia taken during a reduction mammoplasty surgery of a nulliparous female who developed a fibrocystic disease (Paine et al. 1992).

MCF-12A cell lines was cultured in its specific culture condition, a 1:1 mixture of Dulbecco's modified Eagle's medium and F12 medium known as DMEM-F12 (Invitrogen, Carlsbad, CA, USA) which was supplemented with 5% FBS (Hyclone, Logan, Utah), 0.5µg/ml hydrocortisone, 20 ng/ml EGF, 10µg/ml insulin, 40µg/ml gentamicin (Invitrogen, Carlsbad, CA, USA) and 100 ng/ml cholera toxin. MCF-10A was cultured in a 1:1 mixture of Dulbecco's modified Eagle's medium and F12 medium known as DMEM-F12 (Invitrogen, Carlsbad, CA, USA) supplemented with 5% horse serum, 0.5µg/ml hydrocortisone, 20ng/ml EGF, 10µg/ml insulin, Pen/Strep (Invitrogen, Carlsbad, CA, USA) and 100 ng/ml cholera toxin.

T47D, a less invasive mammary carcinoma cell line was obtained from the pleural effusion sample of a 54-year-old female with invasive ductal adenocarcinoma in her breast (Keydar et al. 1979). T47D was cultured in RPMI 1640 medium (Sigma Aldrich, USA) supplemented with 10% Fetal Bovine Serum (Hyclone, Logan, UT, USA). MCF7, a moderately invasive breast carcinoma cell line was taken from the pleural effusion sample of a 69-year-old woman with metaplastic breast adenocarcinoma who had borne mastectomy for two times during a time span of 5 years (Levenson and Jordan 1997). MDA-MB 231, a highly invasive breast carcinoma cell line was taken from the pleural effusion sample of a 51-year-old woman with infiltrative breast adenocarcinoma (Cailleau, Olivé and Cruciger 1978). MCF7 and MDA-MB 231 were ordinarily cultured in DMEM supplemented with 10% fetal bovine serum (FBS). All of the above cell lines were cultured in humidified atmosphere incubator with 5% CO_2.

2.1.1 Thawing of human breast cancer cell lines

The frozen tube containing human mammary carcinoma cells was taken from liquid nitrogen storage tank and rapidly thawed using mechanical shaking in 37ºC. Cells were transferred to 15ml centrifuging tube. Complete culture medium that was pre-warmed later added to the cells. The tube was then centrifuged at ~ 56 x g (1000 rpm) for 5min in order to remove the dimethyl sulphoxide (DMSO). Next, the cells were resuspended in 5ml of complete culture medium. In the end, the cell suspension was fully transferred to 25 cm^2 culture flask and then incubated in 5% CO_2, 37ºC incubator. The culture medium was refreshed with pre-warmed fresh complete medium every 2-3 days.

2.1.2 Subculturing of human breast cancer cell lines

Once the monolayer breast cancer cells became 80-90% confluent in their culturing flask, they were subcultued. Therefore, the old culturing medium was removed from the flask. Next, the cells were washed once with 1x PBS (PBS, Sigma, U.S.A.) in order to wash away the dead cells as well as debris. In order to detach the adherent breast cancer cells from the bottom of culturing flask, 1x pre-warmed trypsin-EDTA added to the cells and then incubated at 37ºC incubator for 5min. However, MCF-12A cells were detached using 5x pre-warmed trypsin-EDTA at 37ºC incubator for 5min. In order to inactivate the trypsin, 10% FBS-supplemented complete culturing medium was added to the tripsinized cells. After that, the cell suspension was centrifuged at ~ 56 x g (1000 rpm) for 5min to remove the trypsin. In the end, the cells were resuspended in fresh complete culturing medium and then incubated in 5% CO_2, 37ºC incubator.

2.1.3 Cryopreservation of human breast cancer cell lines

Once the cells in culturing flask became 80-90% confluent, they were trypsinzed by adding of trypsin and then resuspend in 10% FBS-supplemented comlete culturing medium as mentioned above. Folloing of centrifuging the cell suspension at ~ 56 x g (1000 rpm) for 5min, the cells were resuspended in a fresh complete culturing medium containing 10% DMSO and 20% FBS and transferred into cryovial tubes. The cryovial tubes were put into Mr. Frosty container (Nalgene, Rochester, NY) to gradually decreasing the temperature as for 1ºC permin in a -80ºC freezer overnight. Next day, the cryovial tubes were finally stored in nitrogen tank for later usage.

2.2 Gene silencing

2.2.1 siRNA transfection

Firstly, T47D and MCF7 cell lines were separately cultured in 10% FBS-supplemented RPMI or DMEM respectively. Two pre-designed double stranded silencer siRNAs for targeting *HS6ST3* and one negative non-targeting siRNA (scrambled siRNA) were ordered from Ambion (Ambion, USA). The sequences of these 21-mer siRNAs were shown in Table 2.1. The sense and antisense sequences of each siRNA were blasted in NCBI (http: //blast.ncbi.nlm.nih.gov/Blast.cgi) to confirm that they specifically target *HS6ST3* gene. Reverse transfection method was performed based on Ambion protocol. Main parameters of transfection including cell seeding number, final concentration of transfection reagent, final siRNA concentration and duration time of exposure after transfection were all optimized. Three wells of 6-well culture plate were transfected with HS6ST3 siRNA (Ambion, USA) and the other three wells were transfected with scrambled siRNA. In brief, a total of $3.5x10^5$ cells for T47D cell line and $2x10^5$ cells for MCF7 cell line were seeded in each well of 6-well plate (Nunclon, Denmark) at 24 hours before the day of transfection. A cell confluency of 40-50% was considered as optimal for transfecting the cells using Oligofectamine (Invitrogen, USA) based on the manufacturer's protocol. For T47D, 10µl of 20µM siRNA was diluted in 100µl Opti-MEM I Reduced Serum Medium (Invitrogen, USA) and a mixture of 10µl Oligofectamine in 100µl Opti-MEM I was incubated for 5min at room temperature. For MCF7, 5µl of 20 µM siRNA was diluted in 180µl Opti-MEM I and then a mixture of 5µl Oligofectamin in 10µl Opti-MEM I was incubated at room temperature for 5min. The

two diluents were then combined gently and then incubated for 20min at room temperature to let siRNA-oligofectamine complex formation. The old culture medium of each well of 6-well was then removed and substituted with 780µl and 800µl Opti-MEM I for T47D and MCF7 respectively. A total of 220µl and 200µl siRNA-oligofectamin complex were finally added drop by drop into each well for T47D and MCF7 respectively. Then, T47D and MCF7 plates were incubated in 5% CO_2, 37ºC for 10 hours and 8 hours respectively. Following the incubation, 500µl of 30% FBS-supplemented RPMI and DMEM were added to each well of 6-well plate for T47D and MCF7 respectively to stop transfection. At 24 post-transfection, the old medium of each well was substituted with fresh culturing medium supplemented with 10% FBS. The cells were incubated untill 72 hours after transfection for continuing further experiments. For MCF12A, reverse transfection method was performed as recommended by Ambion. MCF12A cells were transfected by using Ambion silencer *HS6ST3* siRNA and siPORT Amine (Ambion, USA). For this purpose, 6.25µl of 20 µM siRNA was diluted in 93.75µl Opti-MEM I and a mixture of 8µl siPORT Amine in 92µl Opti-MEM I was incubated at room temperature for 25min. The two diluents were then combined gently and incubated for 10min at room temperature to allow siRNA-siPORT Amine complex formation. A total of 200µl of siRNA-siPORT Amine complex was finally added dropwise into 2.3ml ($1x10^5$ cells per ml) of MCF12A cells suspended in Opti-MEM I in each well of 6-well plate. MCF12A plate was then incubated in 5% CO_2, 37ºC for 8 hours. Following the incubation, the old medium was replaced with 3ml of DMEM supplemented with 5%, 0.5µg/ml hydrocortisone, 20 ng/ml EGF, 10µg/ml insulin, 40µg/ml gentamicin and 100 ng/ml cholera toxin. The plate was incubated for 48 and 72 hours post transfection for

doing further experiments. The silencing efficiencies were measured using RT-PCR. In addition, transfection efficiencies were also measured by using Cy3 labeled Negative control siRNA (Ambion, USA) by means of overlapping bright field and fluorescent field under Nikon Digital Sight DS-L1 camera (Nikon, Japan). Furthermore, the percentage of the live cells was estimated more than 90% at 72 hours post transfection among negative control groups.

Table 2.1. Two different pre-designed siRNA sequences for silencing human HS6ST3.

HS6ST3 siRNA	Ambion siRNA ID	*Sense*	*Antisense*
Sequence 1	#40347	*GGAAGACACAGUUUCUCUUtt*	*AAGAGAAACUGUGUCUUCCtc*
Sequence 2	#40437	*GGCACAUUGACUUUCUGUUtt*	*AACAGAAAGUCAAUGUGCCtg*

2.2.2 shRNA Preparation

Five sequenced of shRNA were purchased from Qiagen (Qiagen, SABioscience, USA) including four sequences for *XAF1* knocking down and one sequence as a negative control. 1µL of the plasmids (30 ng/µl) were used to transform 50µl DH5α competent E. coli cells. The sequences of XAF1 shRNA and negative control shRNA were shown in Table 2.2.Transformed DH5α was spread to LB plates containing 100 µg/ml Ampicillin (SIGMA-ALDRICH, USA). The LB plate was incubated at 37ºC overnight. Following the incubation, colony-PCR was performed for each sequence by using T4 and SP6 primers. Once the transformation of the plasmid into the DH5α was confirmed by colony-

PCR, the same colonies were picked and grown in 5ml LB medium supplemented with 100 µg/ml Ampicillin over a shaker (200-250 rpm) at 37ºC overnight. Next day, bacterial stocks were provided and preserved in and then the plasmids were extracted from bacteria by QIAprep Spin Miniprep kit (QIAGEN, USA). The concentrations of extracted plasmid of each colony were measured in NanoDrop ND-1000 (Thermo Fisher Scientific, Wilmington, USA).

Table 2.2. Sequences of shRNA used for silencing XAF1and negative control shRNA.

shRNA	**Insert sequence**
Sequence 1	*CTGTCATTATTGCAACCAAAT*
Negative control	*GGAATCTCATTCGATGCATAC*

2.2.3 shRNA transfection

Transfection of MCF7 was carried out by using shRNA and Lipofectamine 2000. Thus, transfection parameters were optimized by designing several experiments. One day prior to transfection, 2 x10^5 of MCF7 cells were seeded in each well of 24-well plate to have a 90-95% cell confluency at the time of transfection. 0.6µg shRNA was top upped with Opti-MEM I to 50µl and a mixture of 1.5µl Lipofectamine 2000 in 48.5µl Opti-MEM I was incubated at room temperature for 5min. The two diluents were then combined gently and incubated for 20min at room temperature to allow shRNA-Lipofectamine complex formation. A total of 100µl shRNA-Lipofectamine complex were finally added dropwise into 400µl Opti-MEM I provided in each well of 24-well plate. The plate was

then incubated in 5% CO_2, 37ºC for 6 hours and then the old medium was replaced with 1ml DMED supplemented with 10% FBS and 0.125 µg/ml Puromycin (Invitrogen, USA). One day after transfection, the cells were reseeded as for $1x10^4$ cells per each well of new 24-well plate. The old medium was replaced with similar but fresh medium supplemented with Puromycin every 2-3 days for two weeks to let all of untransfected cells be killed. Two weeks after transfection, a single colony of cells was picked from each wells and grown in 96-well plate. Fresh medium supplemented with 0.125 µg/ml Puromycin replaced again with old medium every 2-3 days for two weeks. After two weeks incubation, the content of each well was reseeded in 24-well plate and grown with similar medium until reaching to 80% cell confluency. Finally, the silencing efficiencies were measured using RT-PCR. The cells were cultured for proceeding further experiments as well as providing for frozen stock.

2.3 Quantitative Real Time PCR (RT-PCR)

2.3.1 Extraction of total RNA

The RNA was isolated at 72 hours post-transfection from mono layer cells in the 6-well plate with RNeasy using mini and/or micro kit (QIAGEN, Hilden, Germany). The provided extraction protocol was followed from the user manual of the kit. Firstly, each well was washed with 1X PBS to remove the old medium. The cells were lysed with a mixture of 350µl RLT buffer containing 1% ß-mercaptoethanol (ß-ME). The lysed cells were collected by cell scrapper and homogenized with 21# gauge needle applied on

RNase-free syringe. Similar volume of 70% ethanol added to the lysate and transferred to the RNeasy MicroElute spin column in 2ml provided collection tube. The column was centrifuged at ~ 9447 x g (13,000 rpm) for 30 sec. The flow through was discarded; 350µl of RW1 buffer was added to the column for washing the spin column. Thus, the column was centrifuged at ~ 9447 x g (13,000 rpm) for 30 sec. After discarding the flow through, RNA was then treated with 10µl RNase-free DNase I (QIAGEN, Hilden, Germany) diluted in 70µl RDD buffer and incubated for 15min at room temperature in order to remove all genomic DNA. Next, the column was washed with 350µl RW1 Buffer and centrifuged at ~ 9447 x g (13,000 rpm) for 30 sec and the flow through was discarded. After that, 500µl RPE buffer was pipetted to the spin column and then centrifuged again. Following that, 500µl of 80% ethanol was applied on the column for further wash and centrifuged at ~ 9447 x g (13,000 rpm) for 2min. In the next step, the open-lid column was dried by another centrifuging at ~ 9447 x g (13,000 rpm) for 5min to remove any carryover of the ethanol. Then, the column was placed in provided 1.5 ml collection tube and finally 14µl RNase-free water (for RNeasy Micro Kit) and 30µl (for RNeasy Mini Kit) was pipetted onto the center of silica membrane inside the column and centrifuged the column at ~ 9447 x g (13,000 rpm) for 1min.

2.3.2 RNA concentration and purity

The RNA concentration and purity was measured by NanoDrop ND-1000 (Thermo Fisher Scientific, Wilmington, USA). Briefly, the sampling arm was opened. 1µl of RNA sample was pipetted onto the lower measurement pedestal. Then the sampling arm was

gently closed and spectral measurement was started. The optical density (OD) ratio (260: 280) RNA was indicating the purity and integrity. OD ratio between 1.8 and 2.2 were considered ideal for RNA. The RNA concentration was automatically generated by ND-1000 software and given as ng/µl in the outputting report.

2.3.3 Synthesis of first strand cDNA

First strand cDNA was sensitized by using SuperScript III first strand synthesis system (Invitrogen, USA). Firstly, a total of 2 µg of RNA was mixed with 1µl random hexamer primer (50ng/µl), 1µl of dNTP (10mM) and added up with DEPC-treated water up to a total volume of 10µl. Reverse transcription was performed in thermo cycler (Thermo Hybrid, UK) based on following steps:

Step 1: The mixture was incubated at 65 ºC for 5min and then at 4ºC for 5min. Next, the master mix containing 2µl RT Buffer (10x), 4µl Mgcl2 (25mM), 2µl DTT (0.1M), 1µl RNase out, 1µl Superscript III RT was added to PCR tube and incubated at 4ºC for at least 1min. The cocktail was then sequentially incubated at 25ºC for 5min and 50ºC for 50min followed by inactivation SuperScript III at 85ºC for 5min.

The cDNA was diluted 10 times with autoclaved deionized water to have 0.01 µg/µl concentration for doing the RT-PCR. Diluted cDNA was then stored in -20ºC.

2.3.4 Quantitative real time polymerase chain reaction (qRT-PCR)

Primers were designed in Primer 3 version 0.4.0 (http://frodo.wi.mit.edu/) and Blasted in NCBI database (http://blast.ncbi.nlm.nih.gov/Blast.cgi) to check their specificity. Intron-spanning quality was considered during the primer designation. The designed primers were ordered to 1st Base for synthesis (First Base, Singapore). Light Cycler System (Roche, ID, USA) was employed for RT-PCR using Quanti Tect SYBR Green PCR kit (QIAGEN, Hilden, Germany). The sequence of all primers selected for qRT-PCR is shown in Table 2.3.

A master mix solution was prepared containing 5µl SYBR Green, 1µl of diluted cDNA (0.01 µg/µl), 0.5µl of each forward and reverse primers (10 µM stock) and DEPC- treated water to have a total volume of 10µl. The master mix was applied on RT-PCR micro capillary tube (Roche).

The RT-PCR was performed firstly by activation of polymerase at 95ºC for 15 followed by amplification of the target sequence in 45 cycles of a three-step process:

Step 1: Denaturation at 94ºC for 15 sec

Step 2: Annealing at 60ºC for 25 sec (primer-dependent)

Step 3: Extension at 72ºC for 12 sec (sequence-length dependent).

At the end of each annealing step, fluorescent intensity was detected by the device.

Melting curve analysis was then performed in order to check any unspecific amplification. Melting cure was generated in a plot by interfacing florescence versus

temperature in LightCycler software. Generated a single sharp peak confirmed the specificity of amplified sequence. The specificity of the products was further confirmed by performing a 2% agarose gel electrophoresis.

2.3.5 Quantitative analysis of qRT-PCR data

The gene expressions were analyzed by applying the given Ct values in $2^{\wedge (-\Delta\Delta ct)}$ method (Livak and Schmittgen 2001) to calculate the relative fold changes of gene of interest against reference gene (housekeeping gene). In this method, the Ct value stands for a threshold cycle in which the SYBR fluorescent signal exceeds the level of background noise during the process of amplification. ΔΔct is the difference of (Ct_{target}- $Ct_{reference}$) of treated and (Ct_{target}- $Ct_{reference}$) of control group. The results were normalized using GAPDH and/ or β-actin as a housekeeping genes in both groups. Finally, the relative fold of change was calculated by $2^{\wedge (-\Delta\Delta ct)}$ which is indicative of the relative expression of the gene of interest.

Table 2.3. Sequence of all primers selected for qRT-PCR.

Gene Symbol	Forward primer	Reverse primer	Product size (bp)
ADD3	tttcgggaagacttggaatg	gcaccaggaaggtcattgat	176
APOL1	cctggaaatgagcagaggag	gactttgccccctcatgtaa	117
ARHGAP11A	gagggacttttcacccctc	ttatcctttggggactgctg	183
ARHGAP19	ttgccactttgctgaagatg	aggaggagggagaatgagga	102
ATL3	tccgagatcttgatgtggtg	ttgaatggccactttccttc	117
CASP1	tgttcctgtgatgtggagga	acttcctgcccacagacatt	169
CBX5	acagtgccgatgacatcaaa	tcaccacaggaatctgttgc	118
CCL5	Ctgctgctttgcctacattg	acacacttggcggttctttc	124
CDCA7L	tgcaggatttacgcagagtg	ctcttcctcgctcaccaaag	109
CEP55	tgccatcacagagccattag	gctttcattgagtgcagcag	100
CFB	Tctgcctgatgccctttatc	tcttggagaagtcggaagga	136
COL12A1	cgacctctcagcagacacag	atatccacaccacgtgagca	135
CTNNAL1	ccatgctgatcatgtggttc	cgacaggtctcaacaagctg	123
DRAM	Catccccatgattgtctgtg	aaaggccactgtccattcac	118
FANCD2	tccgacttgacccaaacttc	caacttctcccgaagctcag	161
FCF1	gaccgggacctgaaaagaag	aatcgaggggctccataatc	113
GAPDH	gaaggtgaaggtcggagtcaacg	tgccatgggtggaatcatattgg	157
GPC6	ggaccatgccacaaaaactt	ggtccccacagatagctgaa	175
HIF1AN	tttaagccgaggtccaacag	atcttcctgcccacagtgtc	134
HMMR	cagcaaaaggaggaacaagc	gttcagcctccttccctttc	115
HS6ST1	ggcccttcatgcagtacaat	tacagctgcatgtccaggtc	128
HS6ST2	ccctggtaggctgctacaac	aaactcagtgaggccgaaga	115
HS6ST3	catctccccttcacacagt	ctcgtaaagctgcatgtcca	111
IFI27	gtcctccatagcagccaaga	gaacttggtcaatccggaga	127
IFIH1	ggggcatggagaataactca	ctgcccatgttgctgttatg	133
IFIT2	ctgcaaccatgagtgagaaca	tcacgattctgaaactcagtcc	133
IFIT3	aggaagggtggacacaactg	attgccagtccagaggagaa	112
IFITM1	tcgcctactccgtgaagtct	atgaggatgcccagaatcag	156
IGF1R	Tccatctgatcatcgctctg	cagaggcatacagcactcca	126
IL1R1	aaactacccgttgcaggaga	tttcagccacattcatcacg	175
IL29	ggagctagcgagcttcaaga	acctggagaagcctcaggtc	117
KLF4	Tcccatctttctccacgttc	agtcgcttcatgtgggagag	112
MX1	ggaatcttgacgaagcctga	ctcagctggtcctggatctc	143
NFKBIA	ctacaccttgcctgtgagca	gacacgtgtggccattgtag	118
NUPR1	atagcctggcccattcctac	ctctcttggtgcgacctttc	111
OAS1	tgtgtgtgtccaaggtggtaa	tctctctttgacaggcttcca	180
OAS2	cgagatccagaagtcccttg	cacccagcaatgcttactca	112

OASL	gaaacatcggccaactaagc	tcccatctgtacccttctgc	121
ODC1	gtggctttcctggatctgag	cgggctcagctatgattctc	120
PLDN	cgacgcctggtttaagtgac	gggcttgttttgatctctgc	138
PRKAR2A	actcagggtgaaaaggctga	caatctcgacctcctggttc	115
PRR11	agctccaggaagcactgaag	tctccaggggtgatcagaac	121
RARRES3	gtgagcaggaactgtgagca	caaaagagcatccagcaaca	136
RSAD2	ctcgccagtgcaactacaaa	agaaatggctctccacctga	148
S100A8	atcaggaaaaagggtgcaga	acgcccatctttatcaccag	104
SFXN2	Ccccgcactgtctttgtatc	cagcttcttggcatacagca	123
SHCBP1	aactctgattccgagcagga	gatcttctgaccgctggaac	180
SHISA5	ctgctgctgcctttacaaga	gtggtagccctggtagcttg	142
SLC7A11	cccagatatgcatcgtcctt	cctgggtttcttgtcccata	184
STAT1	caatggtgtggcaaagagtg	gggcattctgggtaagttca	140
TNFSF10	gcaagtcaagtggcaactcc	tgtgttgcttcttcctctgg	172
TTK	cggttcacttgggcatttac	catcttgtggtggcatgttc	104
UTRN	catgaagccagtcctgacaa	ggtggtttcccactctttga	137
XAF1	tcaccctccatgaggcttac	cacatcgtacacccaacctg	127
β-actin	tggcaccacaccttctacaat	gatagcacagcctggatagca	166

2.3.6 Agarose gel electrophoresis for RT-PCR products

Agarose gel electrophoresis was performed to further evaluate the specificity of amplified sequence by estimating the product size of each given band. The RT-PCR product was transferred to eppendorf tube by inverting the capillary and doing a short spin. 5 µl of RT-PCR product was added to 1µl loading dye (Blue/ 6x) and loaded into the well of 1.2% Agarose gel (0.6g Agarose and 1µl ethidium bromide in 50ml TAE which contains 40mM Tris-acetate, 1mM EDTA, PH: 8.1-8.3). A 100 bp ladder was also pipetted in into the first well. The samples were run on the gel at 120V for 40min. Then, the bands were demonstrated by Gel Documentation Image Analysis System V6.03 (ChemiGenius SynGene, Cambridge, UK). Finally, the given band was compared with the ladder for size verification.

2.4 Genome-wide expression profiling using Microarray Gen Chip

2.4.1 Microarray procedure by using Affymetrix Human Gene 1.0ST arrays

For this purpose, total RNAs were extracted from T47D cell line 72 hours after siRNA transfection by using RNeasy Micro Kit (N=3). The RNA concentration and purity were measured by NanoDrop. The silencing efficiency was checked by One-step RT-PCR kit (Qiagen, USA). The quality of RNAs was further determined using an Agilent Bioanalyzer according to Standard Operating Procedure (SOP).

The RNA samples were processed based on the Affymetrix recommended protocol for whole transcript analysis. Briefly, 300 ng of total RNA was reverse transcribed to produce cDNA, which was subsequently used as a template to create cRNA which was then converted to single stranded (ss) DNA. The ss-DNA was biotin labeled, fragmented and hybridized to Affymetrix Human Gene 1.0ST arrays for 16 hours at 45ºC with rotation at 60 rpm. Arrays were washed **a**nd stained using the FS450_0007 fluidics protocol and scanned using an Affymetrix 3000 7G scanner. Hybridization efficiency was inspected by scanned images and CEL files generated from GCOS (GeneChip Operating Software) were imported into Expression Console (EC) 1.1 software for array QC. RMA normalization was performed on the samples to generate the quality control (QC) metrics that routinely used to determine data quality. These include, perfect match mean (PM_Mean), background mean (Bgd_Mean), positive and negative probes (POS vs NEG AUC), bacterials spike controls, and polyA controls. Brief description for reagent used in the gene microarray profiling experiment was summarized in the Table 2.4.

Table 2.4. Reagent used in the gene microarray profiling experiment.

Reagent	**Manufacturer**	**Lot number**
GeneChip Eukaryotic Poly-A RNA Control Kit	Affymetrix	0806008
GeneChip WT cDNA Synthesis and Amplification Kit	Affymetrix	4060471
GeneChip WT Terminal Labeling Kit	Affymetrix	4060386
GeneChip Sample Cleanup Module	Affymetrix	127149657
GeneChip Hybridization Control Kit	Affymetrix	4055504
GeneChip Hybridization, Wash and Stain Kit	Affymetrix	0712009

2.4.2 Microarray gene expression data analysis

2.4.2.1 Genespring data analysis

The Genespring 7.0 (Silicon Genetics, CA, USA) was used to normalize Affymetrix .cel files of the Human Gene 1.0 ST Array to the median (50 percentile) intensity of the same array. After that, median value of genes in control samples was used to normalize the intensity of corresponding gene in the silenced group. Three algorithmic models (RMA, PLIER, iterPLIER) were performed in Genespring for processing the .cel files.

2.4.2.2 Expression console data analysis

Expression Console version 1.1.1 (Affymetrix) was used to summarizing the probe set as well as checking initial data quality. Thus, by importing probe cell intensity files (*.CEL), probe level summarization files (*.CHP) was created. For this purpose, necessary library files were downloaded for the Human Gene 1.0 ST Array. By creating a

new study CEL files was imported and selected for analysis. RMA-Sketch was selected as a default method for probe summarization and then the analysis was started. By completing the processing, CHP files appear and intensities of all probe set were reported after normalization. In RMA-Sketch, the data were normalized with the median intensity of the same array; however, other summarization methods such as PLIER (Probe Logarithmic Intensity Error) and iterativePLIER (iterPLIER) were used as different method for background correction. In PLIER and iterPLIER, Perfect match (PM) and PM-GCBG were used rather than PM-MM only model.

2.4.2.3 DNA-chip data analysis (dChip)

DNA-chip Analyzer 2008 (dChip) software was used to normalizing and also summarizing the probe levels (Schadt et al. 2001). Thus, the .cel files were imported to the software. dChip normalized the probe set intensities by using a model-based approach to adjust the image contamination and handle the cross-hybridization by detecting the outliers. In this model probe level perfect match (PM) and mismatch (MM) was inspected by performing PM selection. Then, the normalized values were logged to base 2 and then the samples were compared based on stringent filtering criteria that would be discussed later.

2.4.2.4 Robust Multi-array Analysis (RMA)

Robust multi-array analysis (RMA) is an algorithmic method (Irizarry et al. 2003) with robust linear model for normalization of the intensity at probe level. RMA was used to minimizing the difference of probe-specific affinity by reducing the variance across the

dynamic change as well as increasing the sensitivity to small changes between control and silenced group. Adjustment of background based on PM distribution, normalization and summarization were three main steps performed in RMA. Thus, imported .cel files were processed in RMA algorithm and then converted to comparable gene expression values. Compared to other methods, RMA could detect the differential changes very well with a higher reproducibility capacity over the single array analysis.

2.4.2.5 Probe Logarithmic Intensity Error Estimation (PLIER)

Probe Logarithmic Intensity Error Estimation or PLIER is another algorithmic method which generates the signals based on what was experimentally observed in probe levels and thus, adjusting the error at low and high signal values. Unlike RMA, PLIER provides a higher accuracy for background adjustment but at the cost of increasing the signal variance. Therefore, for detecting small changes in the relative gene expression (fold of change), PLIER is highly sensitive with more accuracy compared to RMA; however, the variances are not so stable at the Log scale. The PLIER method was used in Genespring and Expression Console software independently. Iterative PLIER or iterPLIER is very similar to PLIER; however, it does not perform the summarization on all of the probes, but it selects the good probes regardless of bad probes (Therneau and Ballman 2008; Qu, He and Chen 2010; Seo and Hoffman 2006).

2.4.2.6 Filtering criteria for gene selection

Following the primary array analysis, secondary analysis was performed to filter the differentially expressed gens as flowing:

1ST filter: Present call (P call) more than 100 at least in control or silenced group.

2nd filter: Fold of change of relative gene expression was considered at least 2.

3nd filter: p value< 0.05 after comparing intensities of silenced group against control group using t-test.

4th filter: The gene lists retrieved from several softwares by using different algorithmic models were overlapped.

5th filter: The genes were categorized based on their relevant biological function by using Gene Ontology database, Affymetrix database and David functional annotation database.

2.4.2.7 Statistical analysis

The filtering criteria were applied using various softwares and then the filtered genes were overlapped. Student t-test was performed to compare the silenced versus control group. P< 0.05 was considered statistically significant.

2.4.2.8 Gene pathway analysis

Extensive literature review was performed to find the relevant gene or genes justifying the biological cellular behaviors after silencing the *HS6ST3* gene. Selected filtered genes were also imported to Pathway Studio Version 5 software (Ariadne Genomics) to find the most probable links among the identified genes. The functional linkage between *HS6ST3* and downstream genes was validated by extending of the experiments.

2.5 Functional Genomic analysis of *HS6ST3* silencing in T47D and MCF7 cell lines

2.5.1 Proliferation assay

MTS method was performed for proliferation assay. For this purpose, each well was gently washed once with 1ml of 1 X PBS at 72 hours post-transfection (N=5). Next, 3ml complete medium (RPMI or DMEM containing 10% FBS for T47D and MCF7, respectively) was added to each well. Then, 600µl of AQueous One Solution (Promega, Madison, USA) was added (1: 5 ratio) to each well. After that, the 6-well plate was incubated in 5% CO_2, 37ºC for 1-4 hours and the absorbances were measured at 490 nm wave length in SpectraMax M5 plate reader (Molecular devices, USA) at several time points. The measurement was based on the amount of tetrazolium compound [3-(4,5-dimethylthiazol-2-yl)-5-(3-carboxymethoxyphenyl)-2-(4-sulfophenyl-2H-tetrazolium), inner salt; MTS] which was converted to formazan by the mitochondria of living cells. The formazan quantities were proportionally expressed the number of living cells inside each well. Absorbance values, generated in SpectraMax software were normalized with blank absorbance value of similar medium in 6-well plate. Finally, the given values of treated group were compared with control group by operating t-test ($p< 0.05$) in GraphPad Prism 5.00 software.

2.5.2 Cell cycle assay

Cell flow cytometry was employed for this assay. In the first step, the old medium was collected in 15ml tubes (in order to collect the dead cells) 72 hours post-transfection from 6-well plate (N=3). Trypsin was added to the wells; and then inactivated with complete culture medium. The cells were transferred to the corresponding 15ml tubes and centrifuged at ~ 56 x g (1000 rpm) for 5min. The supernatant was discarded; the cells were resuspended in 5ml 1 X PBS centrifuged at ~ 56 x g (1000 rpm) for 5min; and the washing process repeated once again to remove the old medium. After final centrifugation, the pelleted cells were resuspended in 0.5ml 1 X PBS. The cell suspension was added dropwise to a new 15ml tubes containing 4.5ml ice-cold ethanol. The tubes were left at 4ºC fridge overnight. In the second step, the tubes were centrifuged at ~ 56 x g (1000 rpm) for 5min and the supernatants were discarded. Next, the pelleted cells were resuspended in 5ml 1 X PBS and centrifuged once or twice in order to remove the ethanol. The supernatants were completely discarded. The cells in each tube were resuspended in 1ml of prepared Propidium iodide (1 mg /ml) cocktail (8ml cold 1 X PBS, 10µl Triton-X 100, 2ml RNase A and 200µl PI). Then, the tubes were shielded from light. PI stained the DNA of fixed cells. Finally, the DNA contents of fixed cells were measured in Beckman Coulter Epics Altra (Beckman, USA) and Dako Cytomation Cyan LX (Dako, USA) with laser excitation in 488nm wavelength. The given data were imported to winMDIv2.8 and Summit 4.3 softwares and then analyzed by comparing the DNA content of treated versus control groups in different phases of cell cycle by operating t-test ($p < 0.05$) in GraphPad Prism 5.00 software.

2.5.3 Apoptosis assay

Caspase-Glo 3/7 and 8 assays (Promega, Madison, USA) were used to measure the relative activity of Caspase 3/7 and 8, separately. For these purpose, the cells were firstly trypsinised in 6-well plate at 72 hours post-transfection and then inactivated with complete culture medium (N=3). The suspended cells were centrifuged at ~ 56 x g (1000 rpm) for 5min to remove the trypsin. The supernatants were discarded. Pelleted cells were resuspended in complete culture medium. For T47D and MCF7 cells, 2 x 10^4 cells were reseeded in each well of white-walled 96-well plate at a total volume of 100µl (N=5). The content of Caspase-Glo® 3/7 Buffer bottle was totally transferred into the amber bottle containing Caspase-Glo® 3/7 Substrate and mixed thoroughly. Then, 100µl of the Caspase-Glo® 3/7 mixture was added to each well. The content of the plate was gently mixed at 300-500 rpm for 30 sec. Then, the plate was covered with aluminum foil and incubated for 1-3 hours at room temperature. The activity of Caspase 3, 7 and 8 cleaved the luminogenic substrate containing DEVD sequence. The cleavage of caspase substrate released a substrate for luciferase (aminoluciferin) and resulting in luciferase reaction that produce a light. After this incubation, the luminescence was measured at all wavelengths in the SpectraMax M5 plate reader using the integration time of 1 sec. All of the luminescence values generated in SpectraMax software were normalized with blank luminescence value of similar medium in 96-well plate. The luminescence values were then divided by the average luminescence value of negative control group. The newly calculated values were finally compared in two groups by operating t-test ($p< 0.05$) in GraphPad Prism 5.00 software.

2.5.4 Transmission Electron Microscopy (TEM)

Cellular morphology of T47D cells were checked by Transmission Electron Microscopy (TEM). For this purpose, each well was gently washed once with 1ml of 1 X PBS after 72 hours siRNA transfection (N=3). The cells were trypsinised in 6-well plate 72 hours post-transfection and then inactivated with complete culture medium. The suspended cells were centrifuged at ~ 56 x g (1000 rpm) for 5min to remove the trypsin. The supernatants were discarded. Pelleted cells were washed once in 1 X PBS and centrifuged at ~ 56 x g (1000 rpm) for another 5min. Pelleted cells were resuspended in 0.5ml 1 X PBS and then 0.5ml 2.5% Glutaraldehyde in PB (pH 7.4) was added to the cell suspension in 1.5ml tubes. The tubes were then incubated at 4ºC for 1 hour and then centrifuged at ~ 503 x g (3000 rpm) for 10min. The supernatant was discarded in order to remove Glutaraldehyde. The cells were washed trice in 1ml 1 X PB and centrifuged at ~ 503 x g (3000 rpm) for 10min. Finally, 1ml 1 X PB was added over the pellet and kept at 4ºC overnight. Next day, the cells were post-fixed 1% osmium tetroxide (OsO4, pH 7.4) for one hour at room temperature. The cells were then washed trice with 1 X PBS and centrifuged at ~ 14 x g (500 rpm) for 10min. After washing, the cells were dehydrated in ethanol graded series each time for 10min at room temperature. After dehydration, 100% Aceton was added to the cells. Aceton made the cell penetrable to resin; thus, 1: 1 ratio of acetone to resin was added for 30min at room temperature followed by addition of 1: 6 ratio of acetone to resin was added at room temperature overnight. The old resin was changed with fresh resin for three times. For the first time, fresh resin was added to the cells and incubated at 45ºC for 45-60min. For second change, fresh resin was added to

the cells and incubated at 50ºC for 60min followed by third resin change at 55ºC for 30-60min. Embedded cells in fresh resin polymerized at 60ºC for 24 hours. Then, specimens were cut in 100 nm thickness by ultra-microtone (Leica, Germany) and mounted on copper grids (150-mesh). Grids were double stained by uranyl acetate and lead citrate, and then the grids were visualized under TEM 208 transmission electron microscope (Philips, England) at 100 Kv. Five random fields were selected and captured from each sample for further analysis. Physiologic cell death (apoptosis) was assessed in control and silenced group by considering cytoplasm shrinkage, cell membrane asymmetry, chromatin condensation, aggregation of chromatin at nuclear membrane, mitochondrial aggregation, cytoplasmic vacuolization, formation of cell membrane budding (apoptotic body formation), nuclear collapse, terminal fragmentation of the cells to the smaller bodies, nuclear fragmentation. Finally, physiological cell death was compared between control and silenced group by operating t-test ($p < 0.05$) in GraphPad Prism 5.00 software.

2.5.5 Adhesion assay

96-well plate (Nunclon, Denmark) was pre-coated with collagen I (20 µg/ml) or fibronectin (20 µg/ml) diluted in 1 X PBS in a total volume of 100µl per well and incubated at 4ºC overnight. Next day, the wells were washed trice with 1 X PBS and blocked with 100µl of 1% BSA. The wells were washed twice with 1 X PBS and air-dried inside the hood and finally pre-warmed in 37ºC incubators for 1 hour. T47D and/or MCF7 cells were trypsinised in 6-well plate at 72 hours post-transfection and then inactivated with complete medium (N=6). The suspended cells were centrifuged at ~ 56 x

g (1000 rpm) for 5min to remove the trypsin. The supernatants were discarded. The pelleted cells were resuspended in serum-free culture medium. A total number of 2.5x 10^4 cells in 100µl were seeded inside each well of 96-well plate coated with collagen I or fibronectin. The cells were then allowed to attach to the bottom of wells in 5% CO_2, 37º C incubators for 30min. After that, the medium of half of the wells were gently discarded and washed with 1 X PBS for three times. Each well was filled with100µl complete medium; then, 20µl MTS AQueous One Solution was added to each well. The 96-well plate was then incubated in 5% CO_2, 37ºC for 1-4 hours. The absorbance was measured at 490 nm in the SpectraMax M5 plate reader. The absorbance of two groups was compared after normalization with blank group as well as unwashed wells by operating t-test ($p< 0.05$) in GraphPad Prism 5.00 software.

2.5.6 F-actin staining

T47D and MCF7 cells were grown on coverslips in 6-well plate and 24 hours later the cells were transfected with *HS6ST3* siRNA. At 72 hours post transfection, the cells were washed trice in 1x PBS (pH 7.6). Then, they were fixed with 4% paraformaldehyde for 15min. Next, the cells were washed and permeabilized trice in PBS- Triton-X 0.2% (PBS-TX). After that, the cells were incubated with fluorescein isothiocyanate (FITC) conjugated with phalloidin (1:50 dilution) for 1 hour at room temperature. The coverslips were washed trice in1x PBS (pH 7.6) and then mounted on slides with Vectashield fluorescent mounting medium (Vector laboratories, USA). Five random fields were

selected from each replicate under Leica microscope (Leica DM 6000M, Germany). The distribution pattern of F-actin was observed in both control and silenced group.

2.5.7 Migration assay

2.5.7.1 Wound healing assay (scratch assay)

The wound healing assay was performed by scratch method on T47D cell line. Firstly, the cells trypsinised in 6-well plate 24 hours post-transfection and then inactivated with complete medium. The suspended cells were centrifuged at ~ 56 x g (1000 rpm) for 5min to remove the trypsin. The supernatants were discarded. The pelleted cells were resuspended in serum-free culture medium. $4x10^5$ cells were seeded inside each well of collagen I coated (20 µg/ml) 24-well plate (Costar, Corning, NY, USA) blocked with1% bovine serum albumin (BSA, Sigma, St.Louis, Mo, USA). The plate was incubated in 5% CO_2, 37ºC for 12 hours. Then, the monolayer cells were scratched by sterile 10µl plastic pipette tip. The suspended detached cells were gently washed by 1X PBS. The cells were continued to culture with complete medium in 5% CO_2, 37ºC. Gap closure was monitored at 0, 24, 48 and 72h after scratching by using Nikon Digital Sight DS-L1 camera. The average of each gap size was measured at ten randomly selected sites by Image J software. Finally, the cell wound closure were calculated by comparing the gap-size difference at the mentioned time-points by operating t-test ($p < 0.05$) in GraphPad Prism 5.00 software.

2.5.7.2 Transwell Migration assay

6.5 mm transwell polycarbonate membrane inserts with 8- µm pore size (Costar, USA) were used to perform cell migration assay. T47D and MCF7 cells were trypsinised in 6-well plate 48 hours post-transfection and then inactivated with complete medium. The suspended cells were centrifuged at ~ 56 x g (1000 rpm) for 5min to remove the trypsin. The supernatants were discarded. The pelleted cells were resuspended in culture medium supplemented with 10% FBS. At the same time, the migration chambers were hydrated in culture medium (RPMI for T47D and DMEM for MCF7) in 5% CO_2, 37ºC for 2 hours. A total number of 5x 10^4 cells were seeded in a total volume of 200µl into upper the chamber of the migration transwell. The lower chamber was filled with 600µl culture medium (RPMI for T47D and DMEM for MCF7) supplemented with 30% FBS. Cells were allowed to migrate in 5% CO_2, 37ºC for 24 hours. Following the incubation, the old medium was gently discarded from upper and lower migration chambers. Then, the cells were washed thrice with 1 X PBS and fixed in 600µl of methanol for 15min. The chambers were gently washed with 1 X PBS and air-dried. After that, the cells were stained with 600µl of 0.5% crystal violet for 30min. In order to remove the excess of crystal violet the inserts were immersed tap water inside a beaker. Non-migrated cells on the upper part of polycarbonate membrane were removed by using a cotton swab. Migrated cells on the lower surface of polycarbonate membrane were visualized under stereo microscope (Nikon SMZ 1500, DXM1200F) using 9 x objective. Pictures were taken from five random fields. Migrated cells were then counted in control group (N=3) and treated group (N=3). The average of migrated number of the cells in treated group

was finally compared to the control group by operating t-test ($p < 0.05$) in GraphPad Prism 5.00 software.

2.5.8 Invasion assay

The invasion assay was performed in BD BioCoat invasion Matrigel chamber with 8- µm pore size (BD Biosciences, CA, USA). The procedure of invasion assay was performed on T47D and MCF7 cells just similar to the procedure of migration assay discussed in previous section. Finally, the invaded cells were counted in control group (N=3) and treated group (N=3). The average of invaded number of the cells in treated group was compared to the control group by operating t-test ($p < 0.05$) in GraphPad Prism 5.00 software.

2.5.9 IGF1R receptor blocking assay

MCF7 cells were trypsinised in 6-well plate 10 hours post-transfection and then inactivated with complete medium. The suspended cells were centrifuged at ~ 56 x g (1000 rpm) for 5min to remove the trypsin. The supernatants were discarded. In order to remove the old serum, the pelleted cells were resuspended in 1 X PBS and centrifuged twice and finally resuspended in serum-free DMEM. For proliferation assay, a total number of 1×10^4 cells were seeded inside each well of 96 well-plate in two row for either silenced and control cells; then IGF1R blocking antibody (Rand D SYSTEMS, USA) was added to one row of either silenced and control group to reach a final

concentration of 10 µg/ml and then incubated in 5% CO_2, 37ºC for 1 hours. Following the incubation, the cell's medium was supplemented with FBS to a final concentration of 10%. The 96-well plate was then incubated in 5% CO_2, 37ºC. After 72 hours incubation, the proliferation assay was performed by using MTS solution as mentioned in proliferation assay section. The mean absorbance of IGF1R-treated cells were compared with untreated cells in either silenced and control groups. Similar to the proliferation assay, for adhesion assay the silenced and control cells were incubated with IGF1R antibody followed by addition of FBS and then incubated in 5% CO2, 37ºC. Following 72 hours incubation, a total number 3x 10^3 MCF7 cells were seeded in each well of 96-well plate coated with collagen I, and then adhesion assay was performed similar to what discussed before in adhesion assay section. Finally, the difference absorbance of washed and unwashed cells in silenced group was compared to control group. Similarly, in migration and invasion assays, the cells were incubated with IGF1R antibody followed by addition of FBS and then incubated in 5% CO_2, 37ºC. At 48 hours post transfection, a total number of 5x 10^4 MCF7 cells were seeded in migration and invasion chambers and incubated in 5% CO_2, 37ºC for 24 hours. During all stages of migration and invasion assays, the final concentration of IGF1R antibody was kept at 10 µg/ml level in cell culturing medium. The Migration and invasion's procedure were carried out similar to the migration and invasion assays that previously discussed.

2.6 Western blotting

2.6.1 Total protein extraction

Protein extraction was performed on T47D and MCF7 cells at 72 hours post transfection. Thus, the old medium was removed from each well. The wells were washed twice with ice-cold 1X PBS. A total volume of 100-200µl M-PER mammalian protein extraction reagent (Thermo SCIENTIFIC, USA) supplemented with 10µl/ml Halt Protease Inhibitor cocktail (Thermo SCIENTIFIC, USA) and 10µl/ml EDTA solution was added to each well. Halt protease Inhibitor functioned by inhibiting a variety of proteases. In addition, EDTA inhibited metallo- proteases by chelating divalent cations. After that, the 6-well plate was gently shaken on ice for 5min and then the cells were scrapped in each well. The cell lysate were centrifuged in 1.5ml tube at ~ 9447 x g (13000 rpm), 4ºC, for 10min. The supernatant was collected and stored at -20º C.

2.6.2 Quantification of total protein

Total protein concentration was measured by BCA (bicinchoninic acid) protein assay kit (Thermo SCIENTIFIC, USA). In this colorimetric method, reduction of Cu^{2+} to Cu^{+} was induced by proteins in an alkaline medium. Chelating one cu^{+} with two molecule of BCA produced a purple-colored water-soluble product that exhibited a strong absorbance at 562 nm. The total protein concentration is directly proportional to the measured absorbance. In order to plot a linear standard curve, a standard BSA (Bovine Serum Albumin) was diluted to a broad working range of 20 to 2000 µg/ml. The total protein extracted from the cells was also diluted for ten times. 25µl of protein (BSA standard protein and the extracted protein) was added to each well in 96-well plate. After that,

200µl of BCA working reaction including 50 part of BCA reagent A (sodium carbonate, sodium bicarbonate, bicinchoninic acid and sodium tartrate in 0.1 M sodium hydroxide) and 1 part of BCA reagent B (1% cupric sulfate) was added to each well and mixed thoroughly with the protein samples over a shaker for 30 sec . The plate was incubated at 37ºC for 30min and then cooled at room temperature for 5min. Finally, the absorbance was measured at 562 nm. The absorbance was normalized with blank and plotted against the known concentration of BSA standard protein. The linear curve was used to determine the concentration of the extracted protein.

2.6.3 SDS- polyacrylamide gel preparation (SDS-PAGE)

2.6.3.1 Preparation of separating gel

1.0 mm spacer, comb and glass plate were washed and wiped with 70% ethanol. 10ml of 10% separating gel was prepared by addition of 4ml deionised water, 3.3ml of 30% acrylamide mix, 2.5ml of Tris (1.5 M, Ph 8.8), 100µl of 10% Sodium dodecyle sulfate (SDS), 100µl of 10% ammonium persulfate (APS) and 4µl of N,N,N',N'-tetramthylenediamine (TEMED). The space between spacer and the glass plate was gently filled with the above mixture up to 1 cm below the comb level. Deionised water was pipetted over the mixture to remove bobbles and provide an even surface. The gel was polymerized at room temperature for 30min.

2.6.3.2 Preparation of stacking gel

When separating gel was completely polymerized, 5ml of 5% stacking gel was prepared by addition of 3.4ml of deionised water, 830µl of 30% acrylamide mix, 630µl of Tris

(1.0M, Ph 6.8), 50µl of 10% Sodium dodecyle sulfate (SDS), 50µl of 10% ammonium persulfate (APS) and 5µl TEMED. The deionised water over the separating gel was drained off by inverting the cast. Immediately, the mixture was added over the separating gel and then the comb was inserted into the stacking gel solution. The solution was allowed to polymerize for 30min.

2.6.4 Electrophoresis of SDS-polyacrylamide gel

The protein sample (20 µg of total protein) was mixed with 5x SDS gel loading buffer containing 10% SDS, 30% glycerol, Tris-Hcl (250mM, pH 6.8), 5% dithiothretol (DTT) and 0.02% bromophenol blue. The mixture was heated at 95ºC for 5min and then allowed to be cooled at room temperature. Following the gel polymerization, the comb was removed and the electrophoresis device and was filled with 1x Tris-glycine buffer. Precision protein standard marker (Bio-Rad, Hercules, CA, USA) and protein samples were loaded to the wells. Electrophoresis was performed at 80 V until the blue line reached to the end of separating gel.

2.6.5 Protein transfer to PVDF membrane

A polyvinyl difluoride (PVDF) membrane (Amersham Biosciences, Germany) was soaked firstly in methanol for 10 sec and then hydrated in deionised water for 5min and finally soaked in 1x transfer buffer. From top to the bottom a Whatman's paper, SDS-PAGE gel, PVDF membrane and another piece of Whatman's paper were sequentially placed on the cassette of Semi-Dry transfer cell (Bio-Rad, USA). A glass band was rolled

over the “gel-sandwich” to remove any trapped air bobble. Transferring of the protein was performed at 15 v for 45min.

2.6.6 Incubation in primary and secondary antibody

Following the transferring of protein, the PVDF membrane was rinsed twice in TBST buffer (150mM sodium chloride, 10mM Tris-Hcl; pH 7.5 and 1% Tween-20). The membrane was then blocked with 5% non-fat milk in 1x TBST at 4ºC overnight. The membrane was then incubated with primary antibody diluted in 5% non-fat milk for one hour at room temperature. The membrane was washed trice with 1x TBST buffer each time for 15min to remove the excess of primary antibody. After that, the membrane was incubated with secondary antibody conjugated with horseradish peroxidase (HRP) diluted in 5% non-fat milk for one hour at room temperature. The membrane was washed trice with 1x TBST buffer each time for 15min to remove the excess of secondary antibody.

2.6.7 Development of the band by Enhanced Chemiluminescence (ECL)

Enhanced Chemiluminescence method was performed by using West Femto and/ or West Pico Substrate System (Thermo Scientific, USA). For this purpose, peroxide solution and luminal solution were mixed in a 1:1 ratio. Then the mixture was incubated for 3-5min at room temperature. The mixture was pipetted over the PVDF membrane placed in a film cassette. Membrane was wrapped between the protector plastic sheets. A piece of X-ray film was exposed to the membrane for optimal time and then developed in Medical Film Processor SRX-101A (Konica MINOLTA, USA). The details of primary and secondary antibodies used for western blotting were summarized in the Table 2.5.

Table 2.5. Dilution of primary and secondary antibodies used in western blotting.

Primary antibody	Antibody dilution	Secondary antibody	Antibody dilution
H6ST3 Poly Clonal rabbit IgG (Santa Cruz)	1: 200	Goat anti rabbit IgG HRP-conjugated antibody (Dako)	1: 10 000
IGF1R Goat recombinant IgG (RandD)	1: 1000	Mouse anti goat IgG HRP-conjugated (Millipore)	1: 2000
XAF1 Polyclonal Rabbit IgG (Abcam)	1: 500	Goat anti rabbit IgG HRP-conjugated antibody (Dako)	1: 10 000
β-actin Monoclonal mouse IgG (Sigma-Aldrich)	1: 15 000	Sheep anti mouse IgG HRP-conjugated (GE healthcare)	1: 20 000

2.6.8 Densitometric analysis of the developed band

The developed bands over the film were scanned in Image Densitometer (Bio-Rad, GS-710, CA, USA) and the intensities were measured by using Quantity-one Image Analysis software version 4.62 (Bio-Rad, Ca, USA). To normalize and quantify the protein expression, the intensity of each band was divided by the β-actin intensity of the corresponding lane.

2.7 Immunohistochemistry (IHC) of human breast cancer

2.7.1 Immunohistostaining procedure

The following immunohistochemical protocol was used:

First day

1. 4µm thick paraffin-embedded tissue microarray sections (TMA) were dewaxed and hydrated with graded Series of alcohol and Histoclear.

2. Sections were treated with 3% hydrogen peroxide (H2O2) for 30minutes to suppress endogenous peroxidase activity.

3. Antigen Retrieval methods used for optimization would be discussed later (for SULF1 staining no antigen retrieval was used, while for HS6ST3 staining heating in Sodium Citrate buffer for 20min was performed).

4. Sections were blocked with 1% normal Gout serum in Tris-buffered saline (TBS) at pH 7.6 for 60min.

5. Sections were incubated with primary antibody overnight at 4°C (rabbit polyclonal antibody for HS6ST3 and SULF1).

Second day

1. The excess of the primary antibody was washed trice with Tris-buffered saline each time for 15min.

2. Slides were incubated with secondary antibody Polymerized with horseradish peroxidase (HRP) at room temperature for 20min (EnVision™ Detection Systems Peroxidase/DAB, Rabbit/Mouse kit for SULF1 staining and ImmPRESS™ UNIVERSAL polymer kit for HS6ST3 staining).

3. The excess of the secondary antibody was washed trice with Tris-buffered saline each time for 15min.

4. Slides were incubated in 1:10 diluted DAB (3,3'-diaminobenzidine) as a chromogen HRP's substrate supplemented with 33µL of H2O2 (6min for SULF1staining and 20min for HS6ST3 staining).

5. Hematoxylin counterstaining was performed

6. Slides were counterstained with Hematoxylin.

7. Tissues were dehydrated with histoclear and ethanol graded Series.

8. Slides were mounted in Permount and left to dry overnight.

9. Quality of slides was examined under Leica DM 6000 microscope (Leica, Germany).

Details of the primary and secondary antibodies used in the immunohistochemical staining were summarized in the Table 2.6. The immunohistostaing procedure was simultaneously performed on a single negative control breast cancer section without addition of the primary antibody to confirm the specificity of the IHC procedure and to reassure about the lack of any nonspecific background staining.

Table2.6. Dilution of primary and secondary antibodies used in Immunohistostaining.

Primary antibody	**Antibody dilution**	**Secondary antibody**	**Antibody dilution**
H6ST3 Poly Clonal rabbit IgG (Santa Cruz)	1: 25	ImmPRESS™ UNIVERSAL Anti-Mouse/Rabbit Ig Kit (VECTOR)	Ready to use
SULF1 Poly Clonal rabbit IgG (Santa Cruz)	1: 50	EnVision Detection Systems, Dual Link System-HRP (DAB+) Peroxidase/DAB, Rabbit/Mouse kit + (Dako)	Ready to use

2.7.2 Antigen retrieval

To restore the immunoreactivity of the paraffin-embedded tissues, proteolytic digestion and heat-induced antigen retrieval methods were performed.

2.7.2.1 Tris-EDTA buffer and Citrate buffer antigen retrieval

Steamer or water bath was preheated with staining dish containing Tris-EDTA Buffer or Sodium Citrate Buffer (pH 6) until temperature reaches 95-100 °C. Then, slides were immersed in the staining dish. While, the lid was loosely placed on the staining dish and incubated for 20-40minutes. After that, the steamer or water bath was turned off and the staining dish was removed to room temperature and the slides were allowed to cool for 20minutes. Finally, the sections were rinsed twice in PBS Tween 20 each time for 2min.

2.7.2.2 Proteinase K antigen retrieval

The sections were covered with Proteinase K working solution and incubate for 10-20min at 37ºC humidified chamber. Then, the sections were allowed to cool at room temperature for 10min. Finally, the slides were rinsed twice in PBS Tween 20 each time for 2min.

The citrate-based, Tris-EDTA-based and Proteinase K Antigen Retrieval were three methods that were able to break the protein cross-links, and thus enhancing the staining intensity by unmasking the antigens.

2.7.3 Immunohistochemical scoring

Cellular and extra cellular components including epithelial cells, stroma matrix and Stromal cells were examined by pathologist. The percentage of staining of the whole part

of each section was described from strong staining (+3), moderate staining (+2), weak staining (+1) to no staining (0) separately. Once the scoring was completed, Immunoreactivity scoring (IRS) or H-score method was hired by using the following formula: (3x % strong staining) + (2x % moderatestaining) + (1x % weak staining). Therefore, IRS of each component ranged from minimum 0 to maximum 300. Additionally, Weighted Average Index (WAI) was calculated by dividing IRS of each component by total stained percentage of each tissue component.

2.7.4 Statistical analysis

Data management and statistical analysis were performed using Microsoft excels 2007 and IBM PASW Statistics 18 for windows. Fisher exact test was used to find associations between the HS6ST3 and SULF1 immunohistochemical staining and clinicopathological parameters. Disease free survival (DFS) and overall survival (OS) were characterized as the length of time from date of diagnosis to recurrence or death respectively. The length of time between the dates of recurrence to death was also defined as survival after recurrence (SAR). Survival analysis was carried out to determine the prognostic values of SULF1 expression and clinicopathological parameters for DFS, OS and SAR by using univariate Cox regression proportional hazard model. Multivariate Cox regression analysis was performed to obtain hazard ratios (HRs) within 95% confidence interval (CI) by including known prognostic variables such as Age, tumor size, tumor side, histograde and lymph node status. Backward stepwise model was hired in performing multivariate survival analysis. All analytical tests were set at p-value less than 0.05. Unavailable information was considered as missing data.

2.8 Immunocytochemistry (ICC) of human breast cancer cell line

For immunocytostaining, a total $3.5x10^5$ of T47D and $2x\ 10^5$ of MCF7 cells were seeded over treated coverslips in 6-well plates and cultured for 24 hours. *HS6ST3* was silenced in T47D and MCF7 by using Ambion siRNA. At 72 hours post-transfection, the old medium was discarded and the cells were washed trice with 1x PBS. The cells were fixed in 4% paraformaldehyde for 15min. After fixing, the wells were washed trice with 1x PBS (pH 7.6). Then, the cells were permeabilized in PBS- Triton-X 0.2% (PBS-TX) and gently washed trice with PBS-TX. Next, 0.5% H_2O_2 diluted in methanol (200µl /well) was pipetted over the coverslips and incubated for 30min at room temp in the dark. H_2O_2 was washed away with PBS-TX thrice each time for 5min. Coverslips were blocked with 1% normal gout serum in 1x PBS for 1 hour and then incubated with primary antibody (HS6ST3, HEPSS1 and 10E4) diluted in PBS-TX at 4o C overnight by slow shaking. Next day, the excess of primary antibody was washed with PBS-TX thrice. The secondary antibody conjugated with HRP (EnVision™ Detection Systems Peroxidase/DAB, Rabbit/Mouse kit for HS6ST3 staining and ABC kit for HEPSS and 10E4) was pipetted over the coverslips and incubated for 1 hour at room temperature. The excess of secondary antibody was washed with 1x TBS (Ph 7.6) thrice. Following the secondary antibody addition, for HEPSS and 10E4 staining, ABC solution (400µl/well) was added and incubated for 1 hr at room temp. Wash with PBS thrice instead. In the next step, 400µl 1:10 diluted DAB (3,3'-diaminobenzidine) was pipetted to each well and incubated at room temperature (10min for HS6ST3 and 20min for HEPSS1 and 10E4 staining). The cells were then washed with 1x TBS once for 5min. Hematoxylin counterstaining was performed on coverslips. The coverslips were then

gently rinsed with tape water for a few seconds. Cells were dehydrated with histoclear and ethanol graded Series. Finally, the coverslips were mounted on glass slides by using permount medium. The slides were left to dry overnight. The scoring and analysis was performed similar to immunohistostaing. Thus, five random fields were selected from each replicate under Leica microscope (Leica DM 6000M, Germany). The IRS of each staining was calculated and then compared between control and silenced groups (N=3) by operating t-test ($p< 0.05$) in GraphPad Prism 5.00 software. Details of the primary and secondary antibodies used in immunocytostainings were summarized in the Table 2.7.

Table 2.7. Table Dilution of primary and secondary antibodies used in immunocytostaining.

Primary antibody	**Antibody dilution**	**Secondary antibody**	**Antibody dilution**
H6ST3 Poly Clonal rabbit IgG (Santa Cruz)	*1: 50*	EnVision Detection Systems, Dual Link System-HRP (DAB+) Peroxidase/DAB, Rabbit/Mouse kit + (Dako)	*Ready to use*
HEPSS1 monoclonal mouse IgM (SEIKAGAKU)	*1: 800*	ABC kit, anti-mouse secondary antibody (Vector Laboratories)	*1: 200*
10E4 monoclonal human IgM (SEIKAGAKU)	*1: 800*	ABC kit, anti-mouse secondary antibody (Vector Laboratories)	*1: 200*

2.9 Cell cytotoxicity assay

2.9.1 LD50 (Lethal dose 50%) measurement

Lethal dose 50% (LD50) is a drug dose in which 50% of cells could be killed.

To find LD50, a total number of 7x 10^3 T47D cells were seeded in each well of 96 well plate. 24 hours after seeding, the cells were treated with 0, 5, 10, 15, 20, 25, 30, 35 µg/ml of Cisplatin (Sigma, USA) diluted in 0.9% sterile sodium chloride (N=6) and 0, 2.5,20,40,60, 80, 100 µg/ml of 5-flurouracil (5-fu) (Sigma, USA) diluted in filtered DMSO (N=6) (the final concentration of DMSO was kept at 0.0025 µl/ml level in the cell culturing medium). Later, the cells were inculcated in 5% CO_2, 37ºC for 48 hours. Then, MTS solution was added to each well in 1: 5 ratios and then the absorbance was measured at 490 nm in SpectraMax M5 plate reader following incubating of the 96-well plate in 5% CO_2, 37ºC for 1-4 hour(s). The absorbances were normalized with blank and then the cytotoxic effects of Cisplatin and 5-fu was measured in Microsoft excel and finally dose-response curves were plotted by non-linear regression method in GraphPad Prism 5.00 software to find the LD50.

2.9.2 Cisplatin and 5-fu cytotoxicity assay after silencing *HS6ST3* in T47D

In the first step, the old medium was discarded 12 hours after transfecting T47D cells by *HS6ST3* siRNA in 6-well plate (N=3). Trypsin was added to the wells; and then inactivated with complete culture medium. The cells were transferred to the 15ml tubes and centrifuged at ~ 56 x g (1000 rpm) for 5min. The supernatant was discarded; the cells were resuspended in complete culture medium. A total number of 7x 10^3 of control and silenced T47D cells were seeded each in two rows inside 96 well plates (N=9). At 24

hours post-transfection, one row of the silenced and one row of control cells were treated with 13 µg/ml of Cisplatin (LD50 for Cisplatin) or 28 µg/ml of 5-fu (LD50 for 5-fu). The plates were incubated in 5% CO_2, 37ºC for 48 hours. After 72 hours post-transfection, MTS solution was added (1: 5 ratio) to each well in 96-well plate. After that, the absorbance was measured at 490 nm in SpectraMax M5 plate reader following incubating of the 96-well plate in 5% CO_2, 37ºC for 1-4 hour(s). Next, the absorbances were normalized with blank and then the absorbance of each drug-treated well in control and/ or silenced group was subtracted from the mean absorbance of the corresponding untreated group. Cell cytotoxicity of Cisplatin and 5-fu was measurd by substracting of the relative percentage of the live cells in drug-treated cells from non drug-treated cells in each of the silenced or control groups. The result of subtractions shows the percentage of dead cells due to the cytotoxic effect of Cisplatin and 5-fu. Finally, t-test ($p< 0.05$) was performed to compare the values between silenced and control group in GraphPad Prism 5.00 software.

2.9.3 Cisplatin and 5-fu cytotoxicity assay after silencing *HS6ST3* in MCF12A

To find the effect of Cisplatin and 5-fu after silencing *HS6ST3* in MCF12A, similar procedure was designed by silencing *HS6ST3* in MCF12A and treating with 13 µg/ml Cisplatin and/ or 28 µg/ml 5-fu. Finally, t-test ($p< 0.05$) was performed to compare the cytotoxicity effect of Cisplatin and 5-fu after silencing *HS6ST3* in MCF12A between silenced and control group in GraphPad Prism 5.00 software.

2.9.4 Imatinib cell cytotoxicity assay

To find a maximum non-toxic dose of imatinib (LC Laboratories, USA) on T47D cell growth, a total number of 7x 10^3 T47D cells were seeded in each well of 96 well plate. 24 hours after seeding, the cells were treated with 0, 1, 2, 3, 4, 5, 6 µM of Imatinib.

The cells were inculcated in 5% CO_2, 37ºC for 48 hours. Then, MTS solution was added to each well in 1: 5 ratios and then the absorbance was measured at 490 nm in SpectraMax M5 plate reader following incubating of the 96-well plate in 5% CO_2, 37ºC for 1-4 hour(s). The absorbances were normalized with blank and then the cytotoxic effects of Imatinib was measured in Microsoft excel to find the maximum ineffective dose of Imatinib on cell growth in T47D cell line.

2.9.5 Imatinib and Cisplatin cytotoxicity assay after silencing *HS6ST3* in T47D

For this assay, the old medium was discarded 12 hours after transfecting T47D cells by *HS6ST3* siRNA in 6-well plate (N=3). Trypsin was added to the wells; and then inactivated with complete culture medium. The cells were transferred to the 15ml tubes and centrifuged at ~ 56 x g (1000 rpm) for 5min. The supernatant was discarded; the cells were resuspended in complete culture medium. A total number of 7x 10^3 of control and silenced T47D cells were seeded each in four rows inside 96 well plates (N=9). At 24 hours post transfection, one row out of four rows of the silenced and/ or control group was treated with 13 µg/ml of Cisplatin (LD50 for Cisplatin). The second row was treated with 1mM Imatinib. The third row was treated with 13 µg/ml Imatinib and 1mM Imatinib. The final row was left un-treated. The plates were incubated in 5% CO_2, 37ºC for 48 hours. After 72 hours post-transfection, MTS solution was added (1: 5 ratio) to

each well in 96-well plate. After that, the absorbance was measured at 490 nm in SpectraMax M5 plate reader following incubating of the 96-well plate in 5% CO_2, 37ºC for 1-4 hour(s). Next, the absorbances were normalized with blank and then the relative percentage of the live cells of each double -treated well in control and/ or silenced group was again normalized with the mean percentage of live cells of the corresponding untreated group. Finally, t-test ($p< 0.05$) was performed to compare the percentage of the live cells between Cisplatin-treated cells and Cisplatin-Imatinib-treated cells in GraphPad Prism 5.00 software.

CHAPTER 3

RESULTS

In the first section of the current chapter, functional role of *HS6ST3* in breast cancer growth and progression was examined. In addition, the influence of *HS6ST3* knocked-down on the expression of heparan sulfate was examined by immunocytostaining in breast cancer cell lines. In the second section, Genome-wide expression profiling was presented in breast cancer after silencing *HS6ST3* by using Microarray Gene Chip. Based on gene microarray analysis, important downstream genes to *HS6ST3* were verified at genome level, protein expression level and finally at their functional relevance. In the third section, the critical effect of silencing *HS6ST3* was examined in breast cancer cellular response to Cisplatin, 5-fluracil and Imatinib. In the final sections, immunohistochemical expression of HS6ST3 and SULF1 was analyzed in clinical breast cancer specimens.

Section 1: Functional role of *HS6ST3* in growth and progression of T47D and MCF7

3.1 HS6STs expression in T47D, MCF7 and MDA-MB-231, breast cancer cell lines

The expression of *HS6ST* isoforms was measured in T47D, MCF7 and MDA-MB-231, relative to MCF-10A, normal epithelial breast cell line by performing two-step RT-PCR. Figure 3.1 shows that compared to MCF-10A, *HS6ST3* was significantly up-regulated in T47D, MCF7 and MDA-MB-231 for more than two hundred forty, twenty two and three times respectively. The two other isoforms had no significant changes in T47D, while *HS6ST1* and *HS6ST2* were up-regulated in MCF7 for more than two and two hundred times respectively. The expression pattern of *HS6ST3* in the breast cancer cell lines was indicative that *HS6ST3* was up-regulated in breast cancer, with the highest expression in the less invasive cell line (T47D) and the lowest expression in the highly invasive cell line (MDA-MB-231). Thus, it was hypothesized that *HS6ST3* might be potentially involved in regulating of the breast cancer phenotype. Therefore, in the next steps *HS6ST3* was silenced in T47D and MCF7 cell lines and then the functional role of this gene was evaluated in breast cancer.

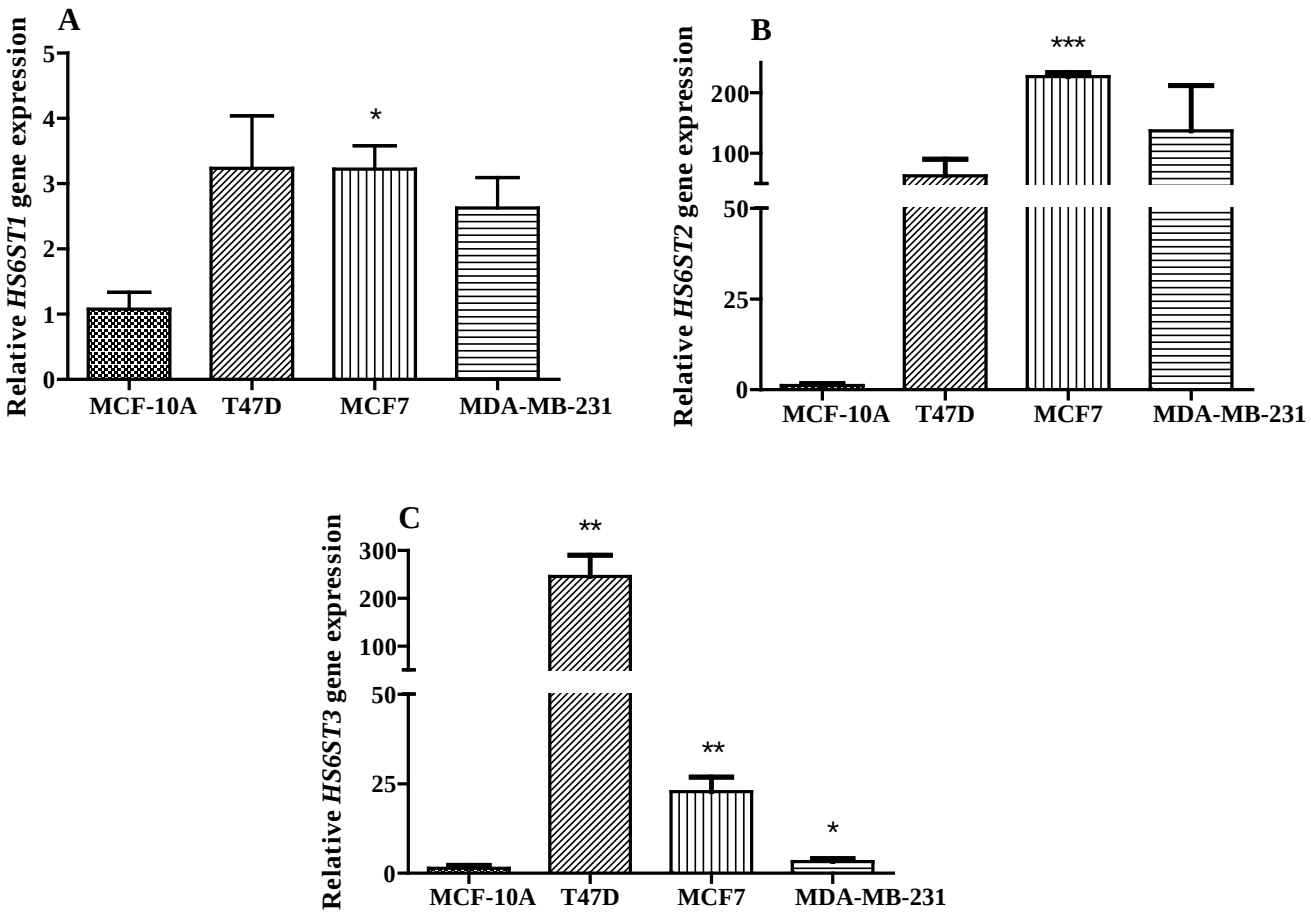

*Figure 3.1. Quantitative real time PCR (RT-PCR) expression analysis of HS6ST isoforms in T47D, MCF7 and MDA-MB231 breast cancer cell lines (N=3). All values are relative to the expression of HS6ST isoforms in MCF-10A, normal epithelial breast cell line.GAPDH housekeeping gene was used to normalize the expression level of all the HS6ST isoforms.Data was shown as mean ± SE, * p <0.05, ** p <0.01, ***p<0.001, T test.*

3.2 Measurement of silencing and transfection efficiencies in T47D and MCF7 cell lines

3.2.1 Silencing of *HS6ST3* gene

siRNA technology was used to elucidate the biological and functional importance of *HS6ST3* gene expression in breast cancer. *HS6ST3* gene was silenced in T47D and MCF7

breast cancer cell lines by using two sequences of pre-designed *HS6ST3* siRNAs. T47D and MCF7 cells were transfected with negatine scrambled siRNA as a control. In the first step, transfection efficiency was measured in order to examine the penetration of the siRNA into T47D and MCF7 cell lines by using fluorescent siRNA. As illustrated in Figure 3.2, the transfection efficiency was more than eighty percent in T47D and more than ninety percent in MCF7 at 72 hours post transfection. As shown in Figure 3.3, HS6ST3 was knocked down for more than 85% in T47D (A, B) and more than 71% in MCF7 cell line (C, D) on the basis of quantitative RT-PCR results. The highest silencing efficiency was achieved by using the first sequence of siRNA. Cell viabilities were more than 90% at 72 hours post-transfection in control groups. In addition, agarose gel electrophoresis showed a remarkable reduction in the corresponding intensity of silenced band compared to non-silenced (control) band (Fig. 3.4).

After this stage, functional studies were sequentially performed by silencing *HS6ST3* in T47D and MCF7 cell lines.

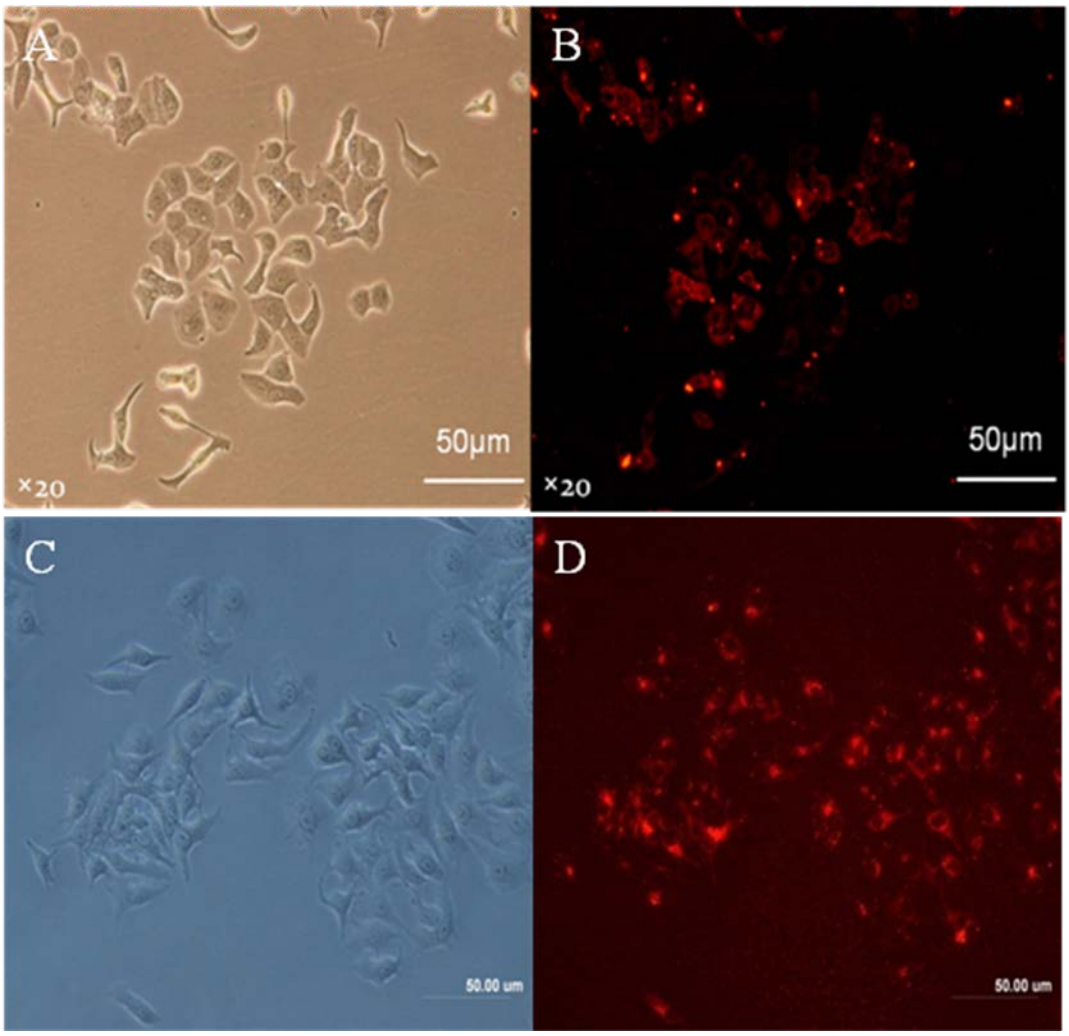

Figure 3.2. Measurement of transfection efficiency in T47D (A, B) and MCF7 (C, D) cell lines 72 hours post-transfection using fluorescent siRNA (Cyanine 3 labeled negative control siRNA) (N=3). The left photos represent the bright field and the right photo represents the same fluorescent field. Transfection efficiency was more than 80% in T47D and more than 90% in MCF7 (P-value <0.05, T test).

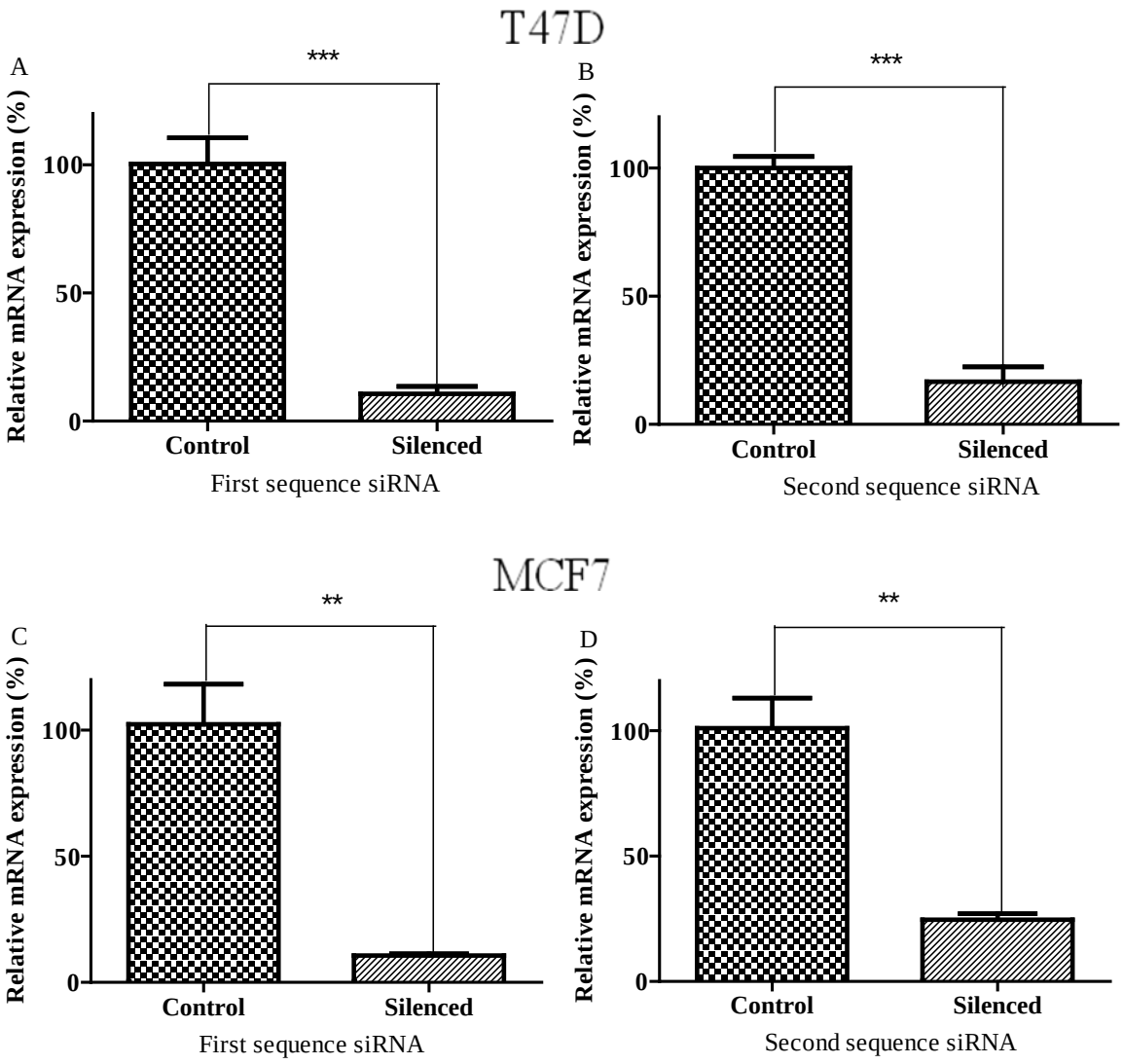

Figure 3.3. *Silencing efficiency of HS6ST3 genes in T47D (A, B) and MCF7 (C, D) breast cancer cell lines using two sequences of siRNA (N=3). The percentages were calculated based on the relative quantitation in RT-PCR. Data was shown as mean ± SE, * p <0.05, ** p <0.01, ***p<0.001, T test.*

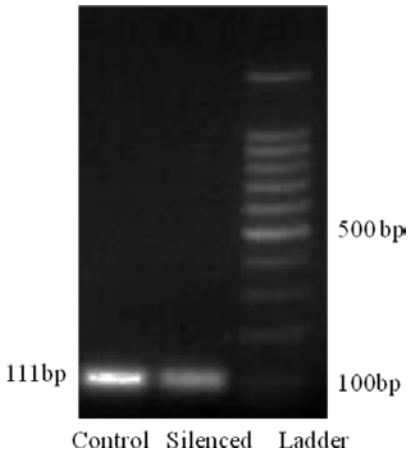

Figure 3.4 RT-PCR products were run on 1.2% Agarose gel 72 hours post-transfection. 100bp ladder was used on the right side.

3.2.2 Examining the specificity of silencing *HS6ST3* in T47D and MCF7 cell lines

Expression of all HS6ST isoforms were measured after silencing *HS6ST3* in T47D and MCF7 breast cancer cell lines by performing quantitative real time PCR (RT-PCR) (Figure 3.5).

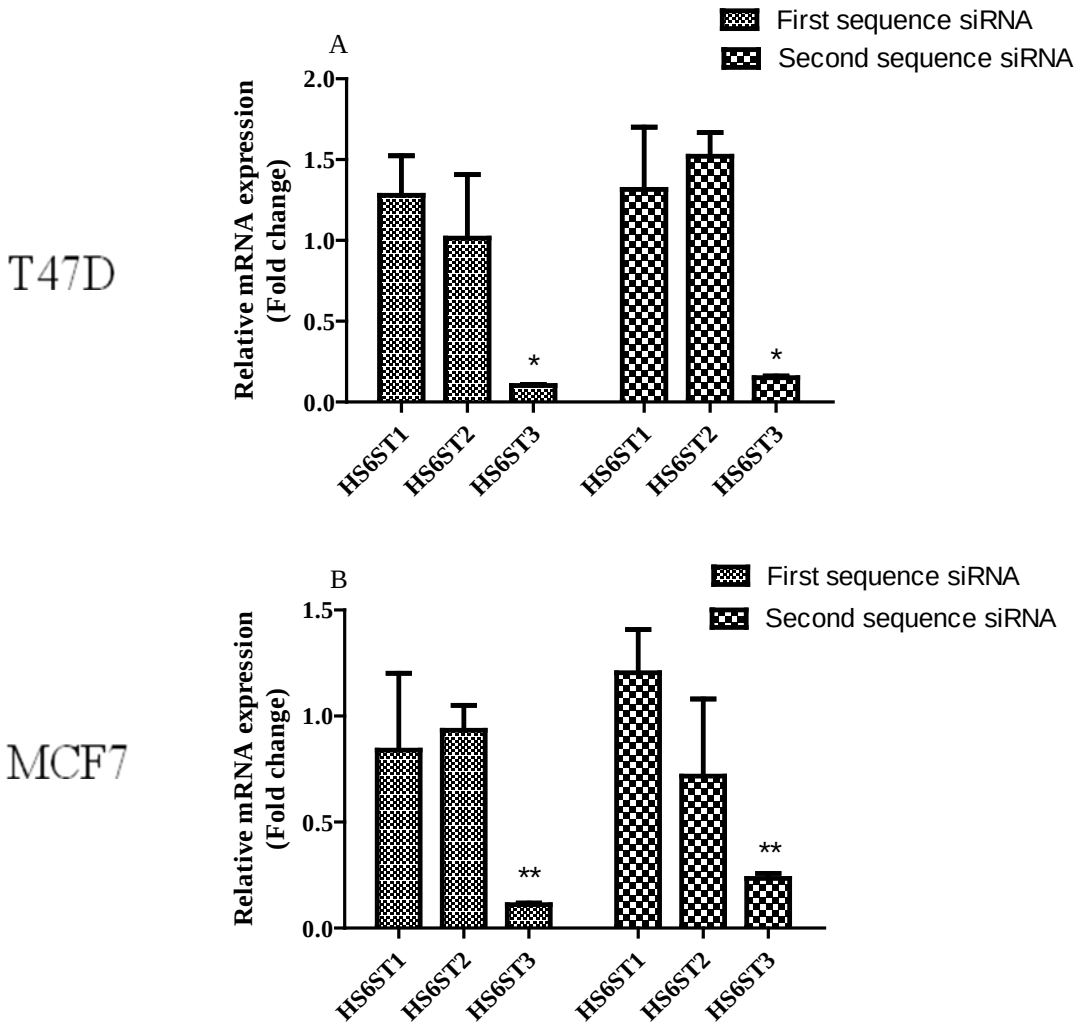

*Figure 3.5. Using two sequences of HS6ST3 siRNAs specifically silenced HS6ST3 without changing the expression of HS6ST1 and HS6ST2 in both T47D (A) and MCF7 (B) cell lines. The values in silenced groups were compared to negative control groups (transfected with scrambled siRNA). Data was shown as mean ± SE, * p <0.05, ** p <0.01, T test.*

3.3. HS6ST3 protein expression after silencing *HS6ST3* in T47D and MCF7

The expression of HS6ST3 was measured at protein level at 72 hours after transfecting T47D and MCF7 by western blotting and immunocytostaining. The expression values were normalized with the expression of β-actin, housekeeping protein in western blotting. As shown in Figure 3.6 and 3.7 the expression of HS6ST3 had a significant reduction at 72 hours after silencing *HS6ST3* gene in T47D and MCF7 cell lines.

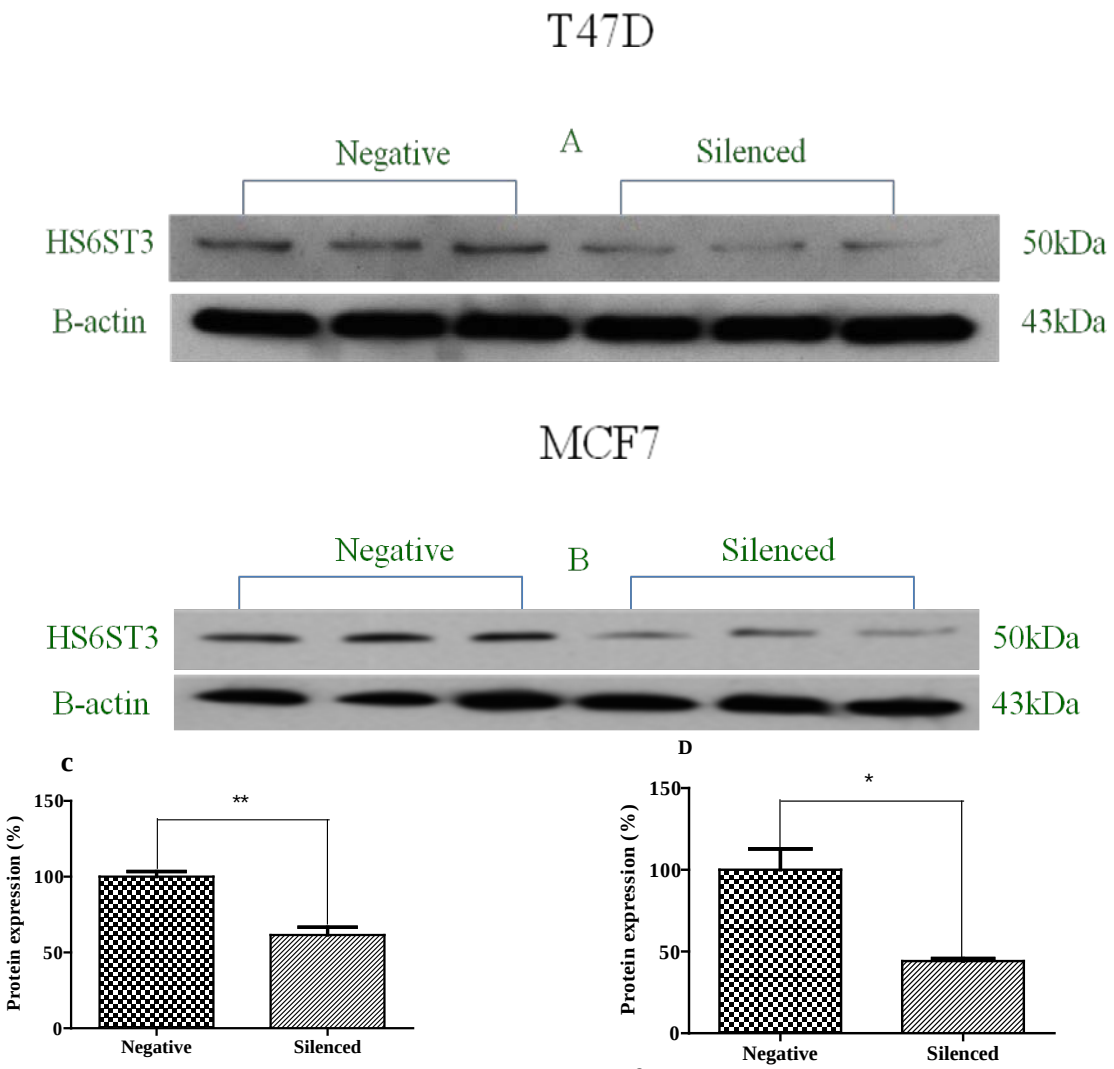

*Figure 3.6. Western blotting (WB) analysis of HS6ST3 protein expression at 72 hours after silencing HS6ST3 gene in T47D (A) and MCF7 (B) cell lines. Silencing HS6ST3 gene significantly reduced the protein expression by 38.5% and 55% in T47D (C) and MCF7 (D) respectively. Data was shown as mean ± SE, * p <0.05, ** p <0.01, T test.*

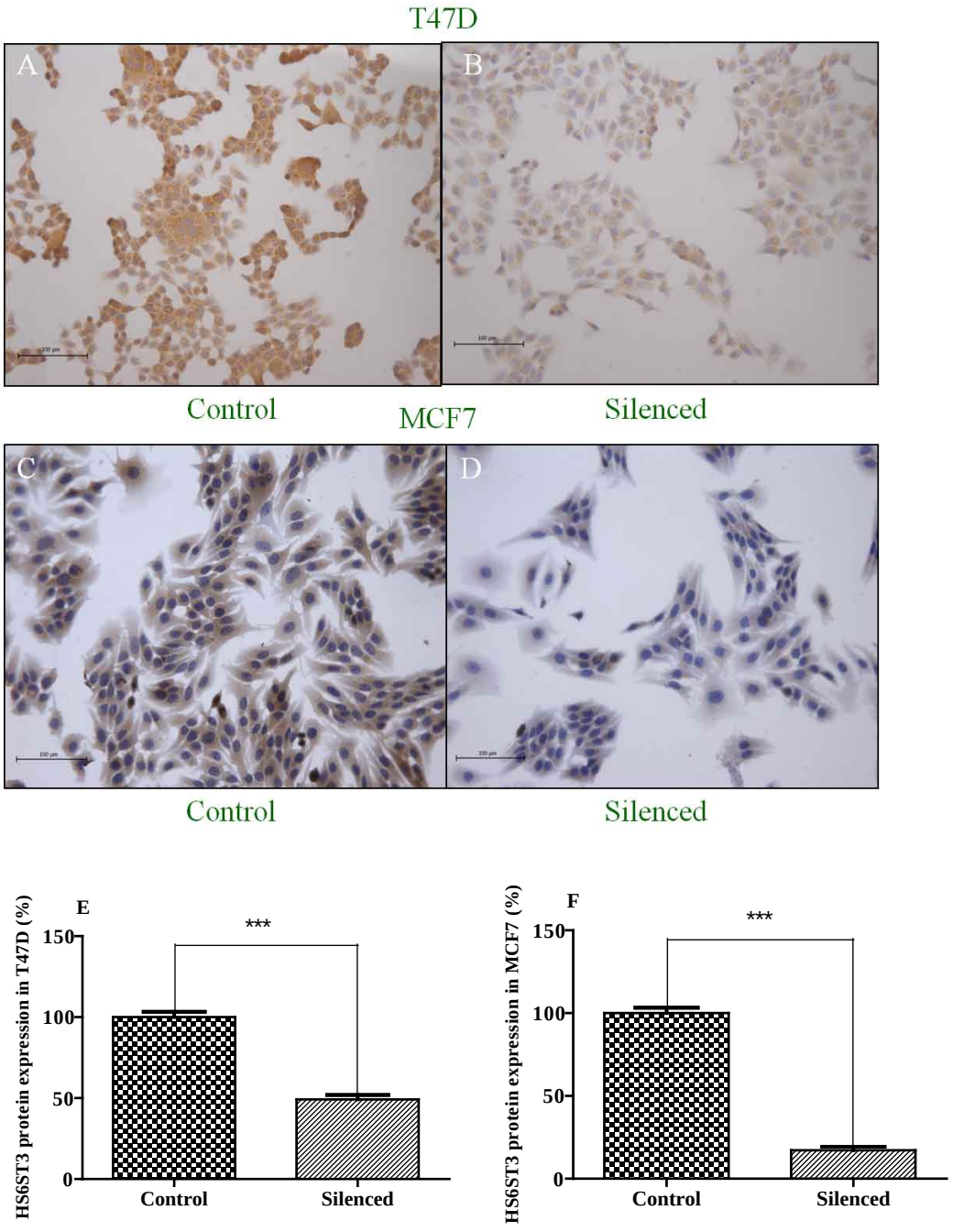

Figure 3.7. Immunocytostaining (ICC) analysis of HS6ST3 protein expression at 72 hours after silencing HS6ST3 gene in T47D (A, B) and MCF7 (C, D) cell lines. Silencing HS6ST3 gene significantly reduced the HS6ST3 *protein expression by 50.7% and 82.8% in T47D (C) and MCF7 (F) respectively. Data was shown as mean ± SE ,***p<0.001, T test.*

3.4 Effect of *HS6ST3*-knocking down on heparan sulfate expression in breast cancer cells

3.4.1 Analysis of HepSS1 expression after silencing *HS6ST3* in T47D and MCF7

A total $3.5x10^5$ of T47D and $2x\ 10^5$ of MCF7 cells were seeded over treated coverslips in 6-well plates and cultured for 24 hours. *HS6ST3* was silenced in T47D and MCF7 by using Ambion siRNA. At 72 hours post-transfection, immunocytostaining procedure (discussed in previous chapter) was performed. Then, the immunoreactivity score (IRS) was measured in five random fields of either control or silenced group. Comparison between the IRS of control and silenced groups showed that silencing *HS6ST3* inhibited the expression of HepSS1 epitope on the cell surface of T47D and MCF7 by 31.62% and 93.97% respectively (Figure 3.8).

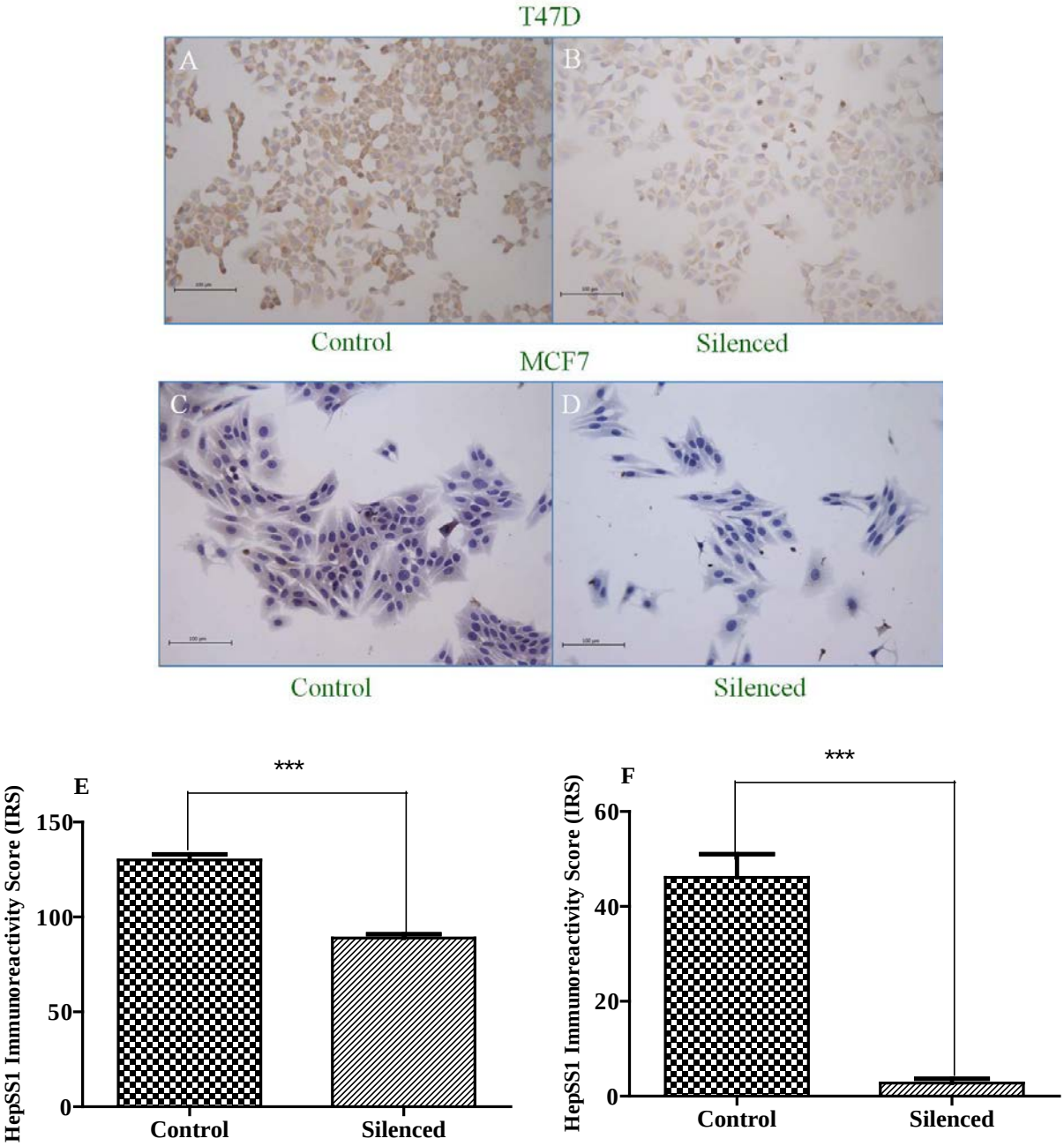

Figure 3.8. Immunocytostaining (ICC) analysis of HepSS1 epitope expression at 72 hours after silencing HS6ST3 gene in T47D (A, B) and MCF7 (C, D) cell lines. Silencing HS6ST3 gene significantly reduced the HepSS1 *epitope expression by 31.62% and 93.97% in T47D (C) and MCF7 (F) respectively (N=3). Data was shown as mean ± SE ,***p<0.001, T test.*

3.4.2 Analysis of 10E4 expression after silencing *HS6ST3* in T47D and MCF7

A total $3.5x10^5$ of T47D and $2x\ 10^5$ of MCF7 cells were seeded over treated coverslips in 6-well plates and cultured for 24 hours. *HS6ST3* was silenced in T47D and MCF7 by using Ambion siRNA. At 72 hours post-transfection, immunocytostaining procedure (discussed in previous chapter) was performed. Then, the immunoreactivity score (IRS) was measured in five random fields of either control or silenced group. Comparison between the IRS of control and silenced groups showed that silencing *HS6ST3* reduced the expression of 10E4 epitope on the cell surface of T47D and MCF7 by 19.23% and 98.14% respectively (Figure 3.9). The reduced expression of HepSS1 and 10E4 consistently showed that silencing *HS6ST3* potently diminish the expression of heparan sulfate on the cell surface. Thus, this observation could be suggestive of the modulatory effect of *HS6ST3* on heparan sulfate expression on the cell surface.

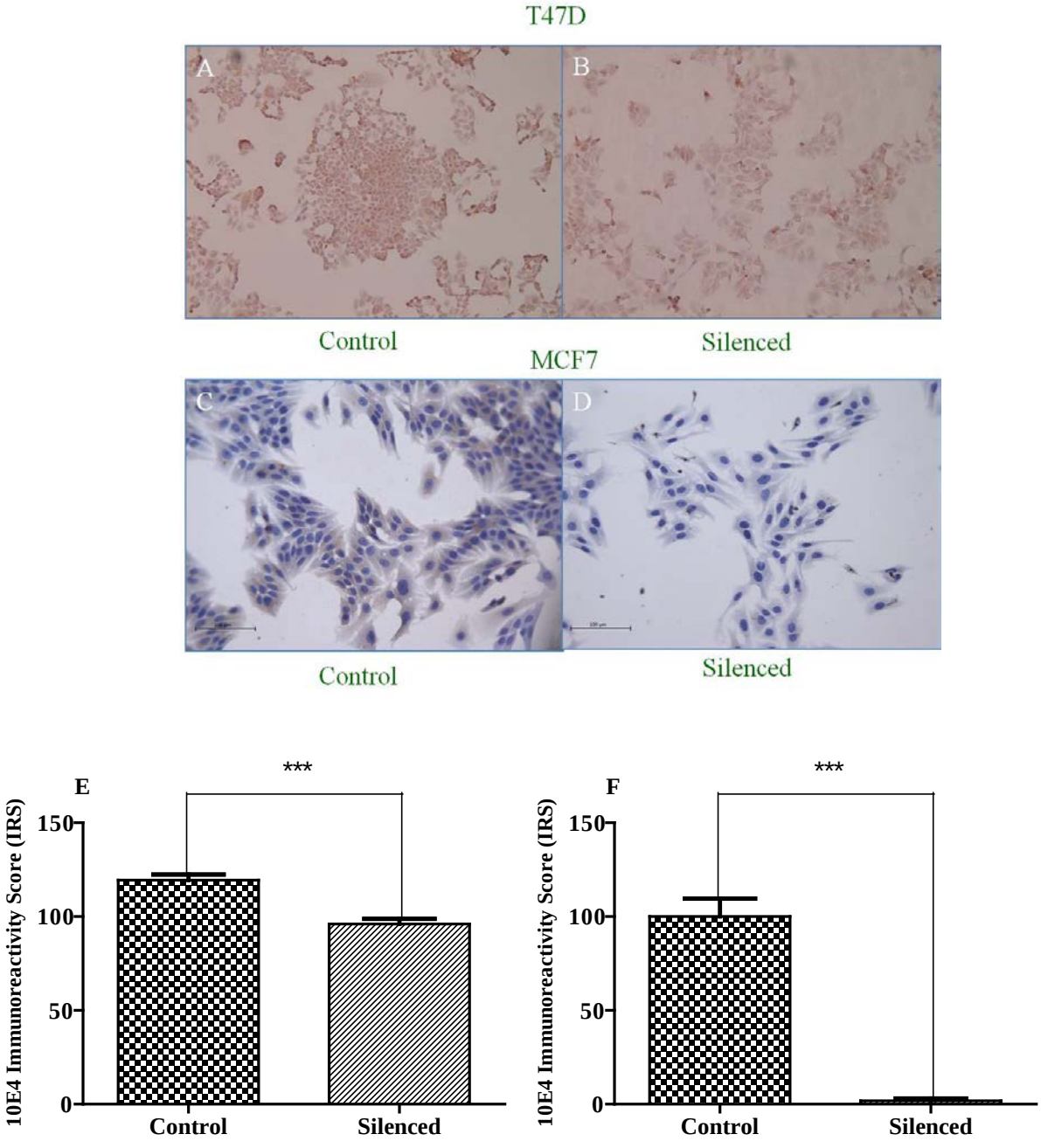

Figure 3.9. Immunocytostaining (ICC) analysis of 10E4 epitope expression at 72 hours after silencing HS6ST3 gene in T47D (A, B) and MCF7 (C, D) cell lines. Silencing HS6ST3 gene significantly reduced the 10E4 epitope *expression by 19.23% and 98.14% in T47D (C) and MCF7 (F) respectively (N=3). Data was shown as mean ± SE ,***p<0.001, T test.*

3.5 Analysis of cell Proliferation after silencing *HS6ST3* in breast cancer

To test whether silencing of *HS6ST3* gene is involved in breast cancer cell proliferation, the relative percentage of the live cells were measured at 72 hours after silencing *HS6ST3* in T47D and MCF7. Analysis showed a significant reduction in the relative percentage of live T47D and MCF7 cells at 72 hours after silencing *HS6ST3*. The silenced T47D cells exhibited nearly about 40.8-53.5% reduction in number of living cells compared to control group. Similarly, silencing *HS6ST3* reduced the relative percentage of the live MCF7 cells by 39.4-66.2% compared to the control group (Figure 3.10). The result suggested that expression of *HS6ST3* may positively modulate the cell growth in breast cancer. One plausible reason for reduction of the viable cells after silencing of *HS6ST3* is the regulatory effect of *HS6ST3* gene on other genes that influence the cell growth. Thus, in the next steps flow cytometry was performed to identify the influence of *HS6ST3* knock down on cell cycle regulation.

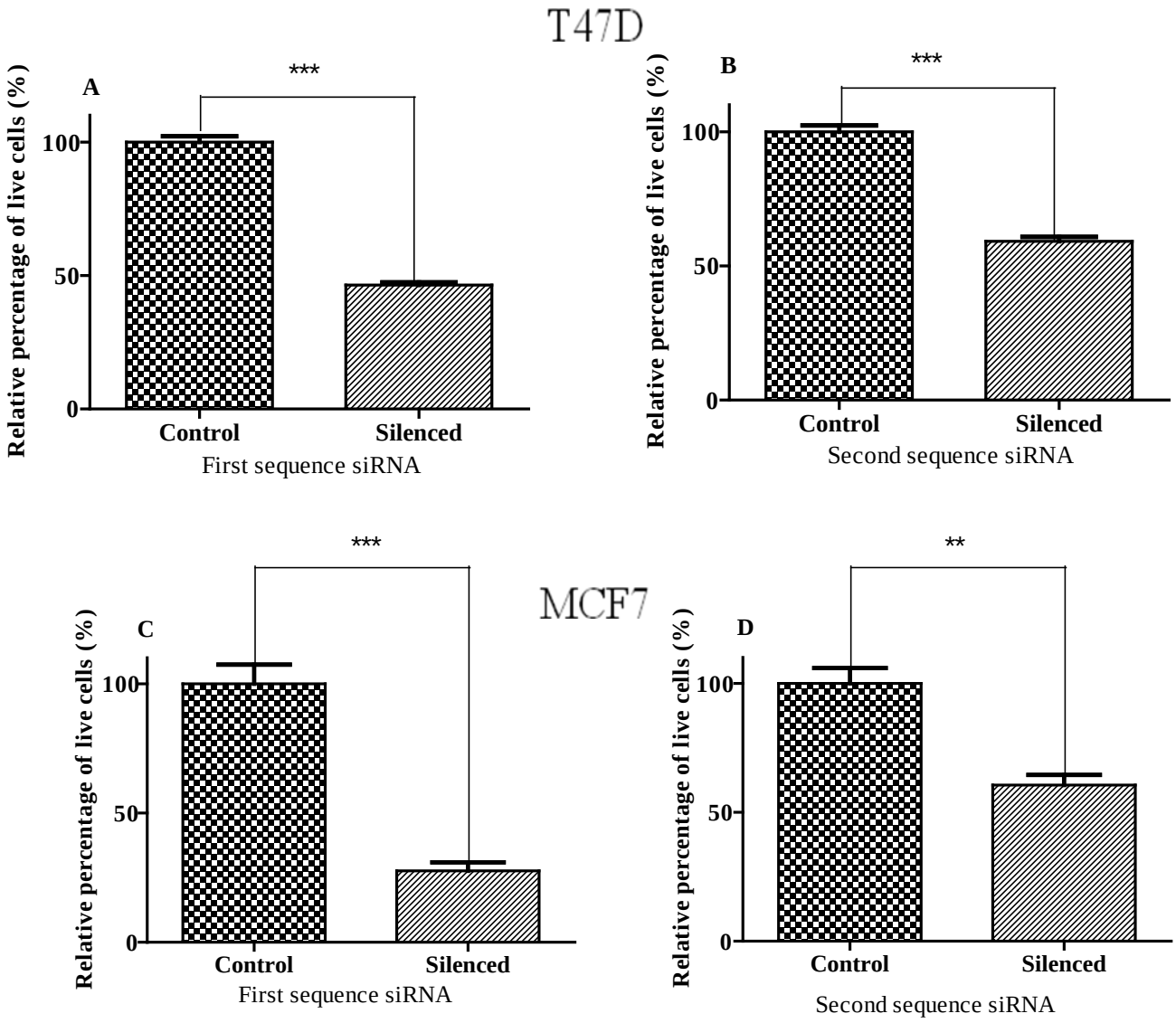

*Figure 3.10. Relative percentage of the live cells cells was measured based on absorbance of formazan produced by T47D (A, B) and MCF7 (C, D) cells at 72 hours post-transfection in control and silenced group (N=5). The relative percentage of the live cells reduced after silencing HS6ST3 by 40.8-53.5% and 39.4-66.2% in T47D and MCF7 respectively. Data was shown as mean ± SE, ** p <0.01, ***p<0.001, T test.*

3.6 Analysis of cell cycle phases after silencing *HS6ST3* in breast cancer

Proliferation assay showed a significant reduction in the relative percentage of the live cells after silencing *HS6ST3* in both T47D and MCF7. Cell cycle flow cytometry which is a direct reflection of cell proliferation was performed to examine whether down-regulation of *HS6ST3* influence the cell cycle progression. Therefore, this assay was performed at 72 hours post-transfection in T47D and MCF7 cell lines by using two sequences of siRNA. A total number of 10,000 cell events were acquired from control and silenced groups after silencing *HS6ST3* in both T47D and MCF7 cell lines. As shown in Figure 3.11, the numbers of the cells in G0 and G1 phases were respectively increased by 3% and 15% in silenced group compared to control group indicating a cell cycle arrest in G1 as well as slight increase in the number of pre-apoptotic cells; and consequently, more cells were seen in S and G2 phases in control group (Figure 3.11: I, II, Figure 3.12: A, B). Besides, silencing *HS6ST3* in MCF7 showed an induction of apoptosis pathway as the number of pre-apoptotic cells increased in G0 phase by 8-29%; and thus the living cells in G1, S and G2 phases was decreased compared to the control (Figure 3.11: III, IV, Figure 3.12: C, D). Furthermore, in this assay it was shown that the relative percentage of the live cells of all control groups (transfected with scrambled siRNA) were more than 95% at 72 hours after silencing *HS6ST3* in both T47D and MCF7 cell lines; and therefore, indicating that the cells in the control groups were not significantly affected by transfection reagent and scrambled negative siRNA.

The results of cell cycle assay could confirm the observed differences in proliferation assay. However, as the number of the pre-apoptotic cells of G0 phase was increased in

silenced group of both T47D and MCF7 cell lines, a complementary apoptosis assay was performed.

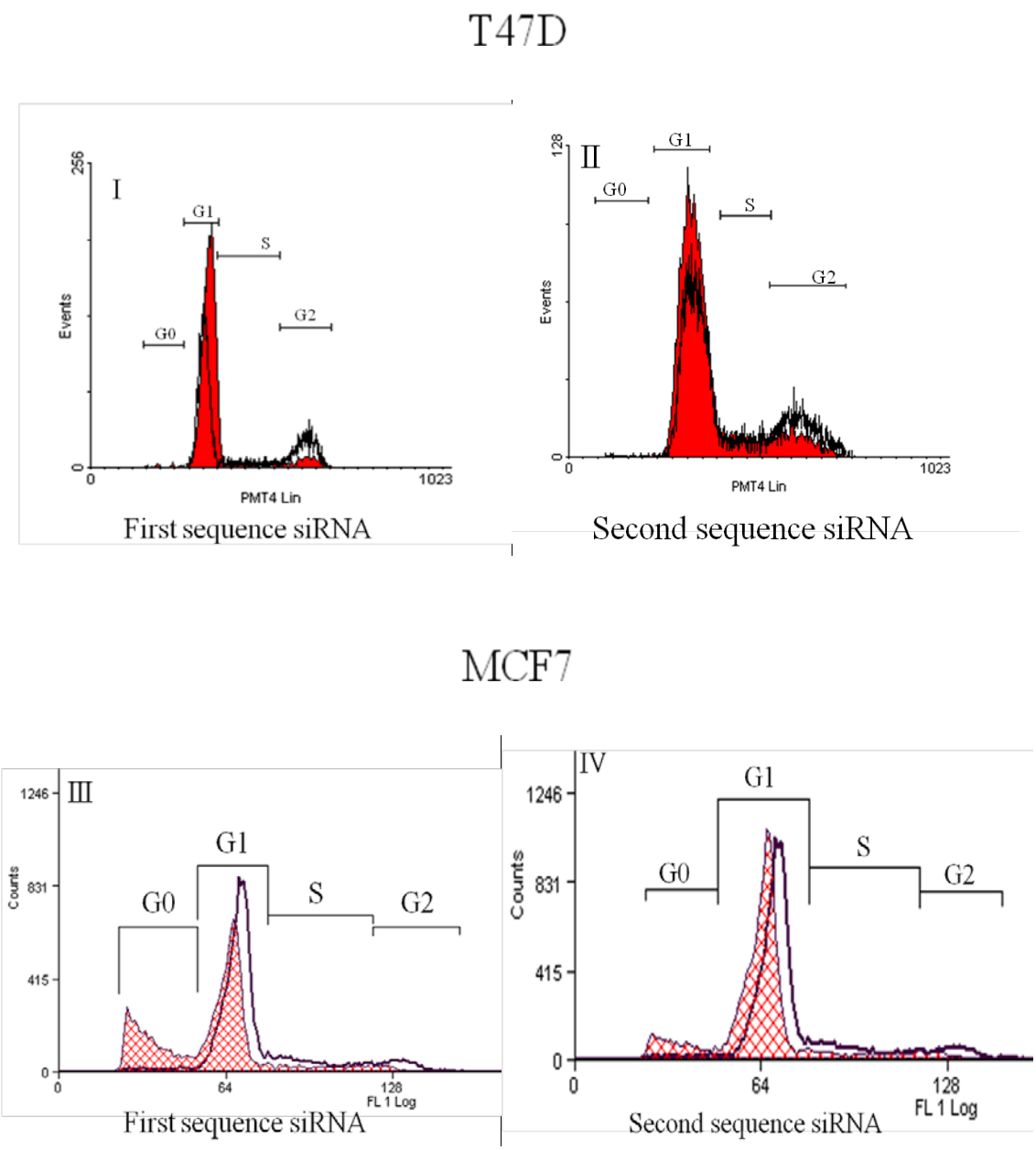

Figure 3.11. Representative histograms of T47D and MCF7 cell cycle analysis 72 hours after silencing HS6ST3. White histogram represents the control and the red histogram represents the silenced group. G0, G1, S, and G2 stand for cell cycle phases. G1 arrest in silenced cells is remarkable in T47D (I, II), while the number of pre-apoptotic cells were increased in G0 phase in MCF7 (III, IV).

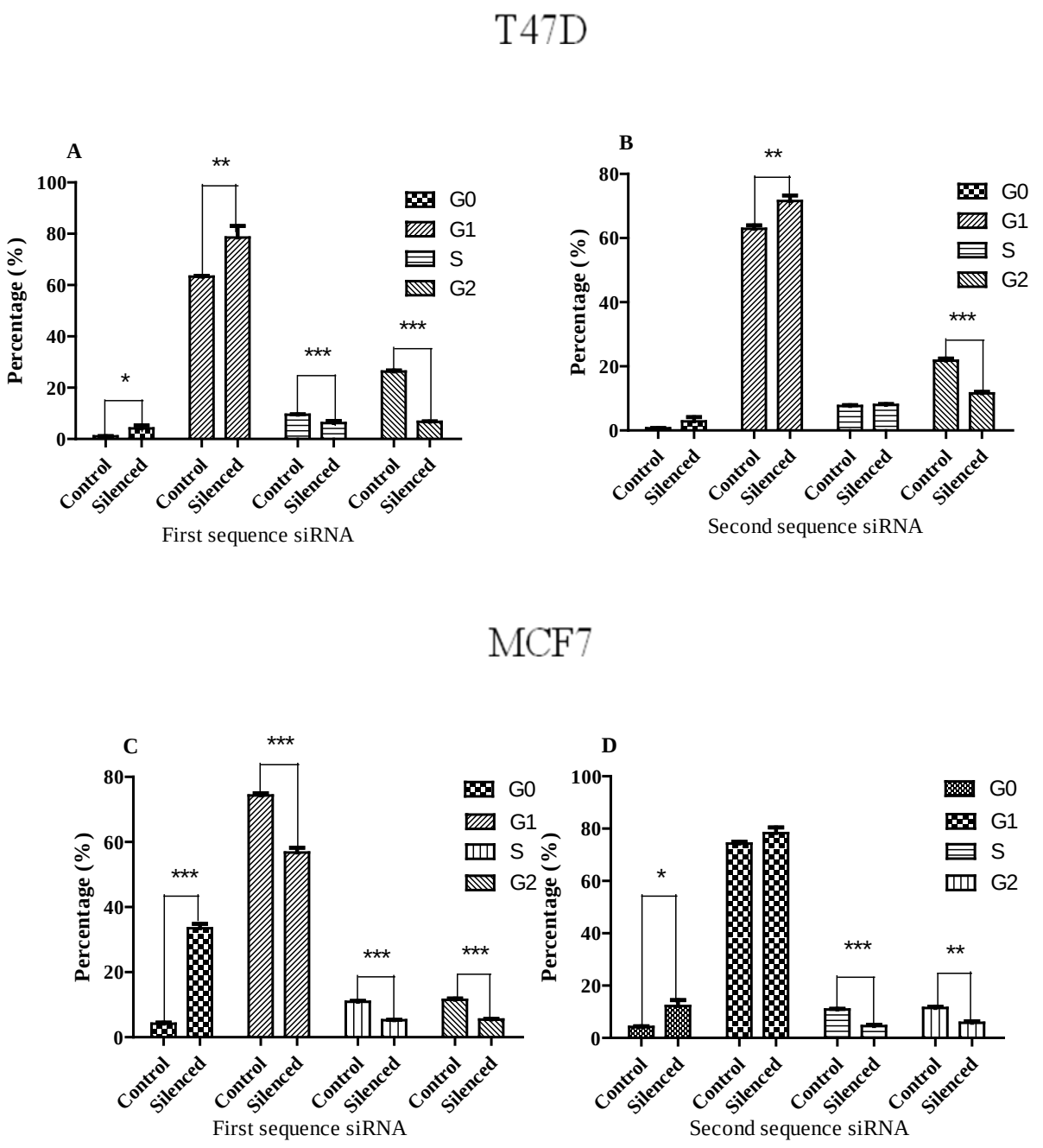

*Figure 3.12. Effect of HS6ST3 silencing on cell cycle phases in T47D and MCF7 cell lines at 72 hours post-transfection (N=3). G1 arrest in silenced cells is remarkable in T47D (A, B), while the number of pre-apoptotic cells were increased in G0 phase in MCF7 (C, D). Data was shown as mean ± SE, * p <0.05, ** p <0.01, ***p<0.001, T test.*

3.7 Analysis of Apoptosis assay after silencing *HS6ST3* in breast cancer

In order to find a possible reason for the observed differences between silenced and control group in proliferation and cell cycle assays, apoptosis assay was performed at 72 hours after silencing *HS6ST3* by using Caspase-Glo® 3/7 and 8 kits separately. Two sequences of siRNA were used to silence *HS6ST3* in T47D and MCF7 cell lines. As shown in Figure 3.13, silencing *HS6ST3* increased the relative activity of Caspase 3/ 7 (A) and 8 (B) in T47D by 16-44% and 22-32% respectively. In addition, a dramatic increase was observed in relative activity of Caspase 3/ 7 (C) (50-172%) and 8 (D) (185-270%) in MCF7 cell line. Thus, it seems that *HS6ST3* expression could have a strong inhibitory effect on apoptotic pathways regulated by apoptotic genes. In the other words, *HS6ST3* may play an important role to secure the survival of the breast cancer cells. Nevertheless, to find whether *HS6ST3* could function as an oncogene in the progression of the breast cancer we performed some further experiments such as adhesion, migration and invasion assays.

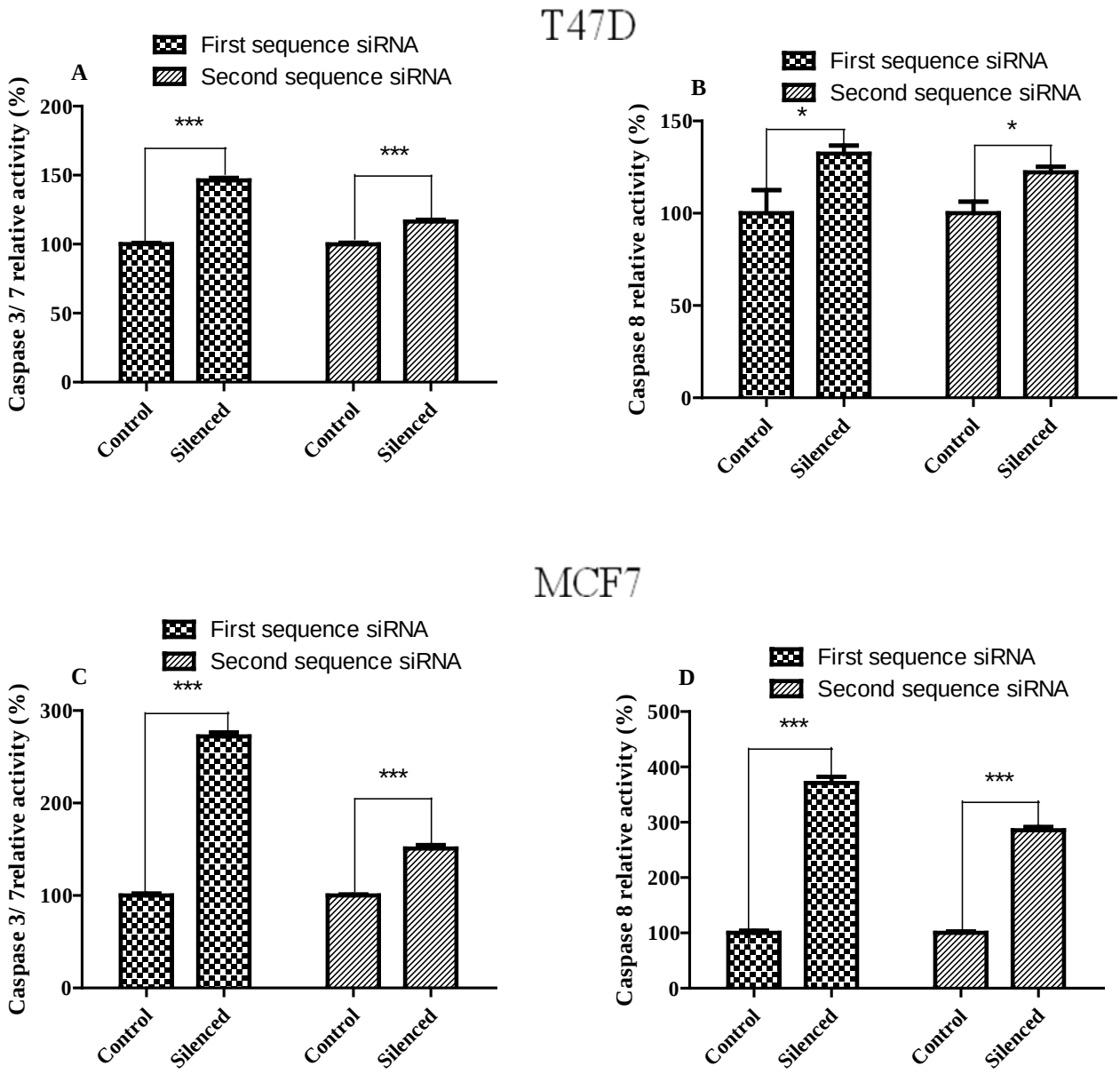

*Figure 3.13. Effect of HS6ST3 knock down on induction of apoptosis in T47D and MCF7 cell lines at 72 hours post-transfection (n=5). Apoptosis assay was performed by using Caspase-Glo® 3/7 and 8 kits. A remarkable increase was observed in the relative activity of Caspase 3/7 and 8 after silencing of HS6ST3 gene in T47D (A, B) and MCF7 (C, D) cell lines. In addition, a dramatic increase was observed in relative activity of Caspase 3/ 7 (C) (50-172%) and 8 (D) (185-270%) in MCF7 cell line. Data was shown as mean ± SE, * p <0.05, ***p<0.001, T test.*

3.8 Transmission Electron microscopy (TEM) analysis after silencing *HS6ST3* in T47D

Cell cycle and apoptosis assays revealed that silencing *HS6ST3* could induce the apoptosis in breast cancer. To visualize this observation, cellular morphology of T47D cells were selected by Transmission Electron Microscopy (TEM). Five random fields were selected and captured from each sample for further analysis. Physiologic cell death (apoptosis) was assessed in control and silenced group by considering cytoplasm shrinkage, cell membrane asymmetry, chromatin condensation, aggregation of chromatin at nuclear membrane, mitochondrial aggregation, cytoplasmic vacuolization, formation of cell membrane budding (apoptotic body formation), nuclear collapse, terminal fragmentation of the cells to the smaller bodies, nuclear fragmentation (Figure 3.14). Analysis of the TEM-based apoptosis revealed that silencing *HS6ST3* in T47D could increase the apoptosis by 21.8 % compared to negative control group (Figure 3.15). This observation was in agreement with the results of the cell cycle and apoptosis assays which were discussed in previous sections.

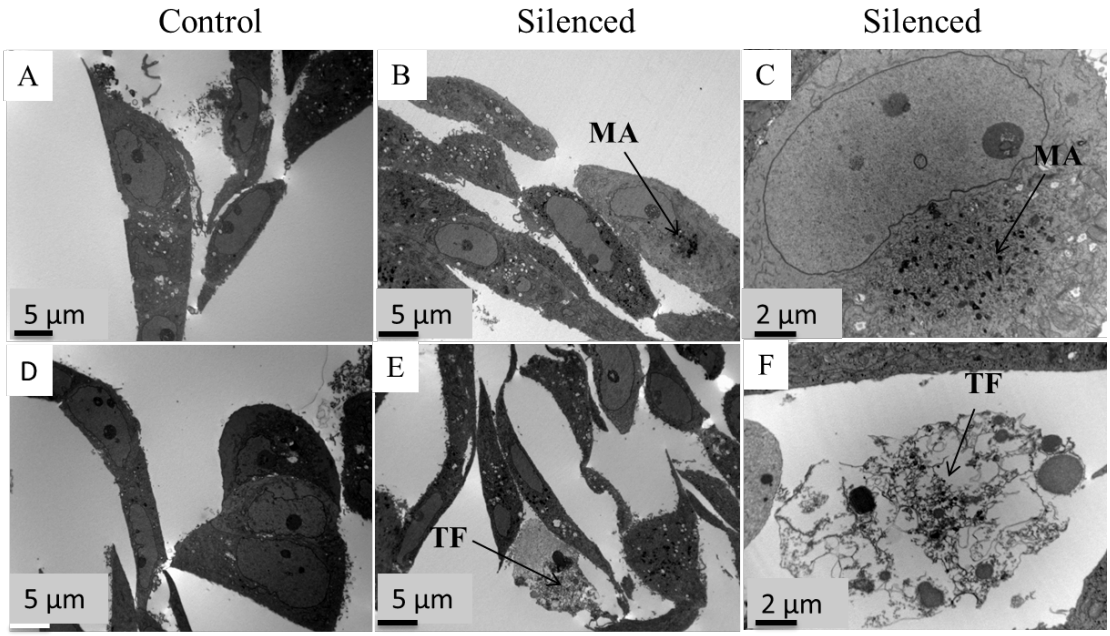

Figure 3.14. Visualization of cell morphology at 72 hours after silencing HS6ST3 in T47D. Silencing HS6ST3 induced apoptosis in T47D cell line. Figure B and C show Mitochondria Aggregation (MA). Figure E and F show Terminal Fragmentation (TF) of T47D cells after silencing HS6ST3.

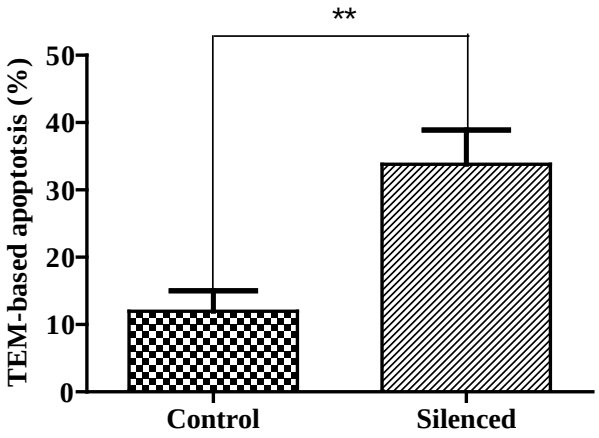

*Figure 3.15. Analysis of the cellular apoptosis percentage at 72 hours after silencing HS6ST3 in T47D based on TEM images. Silencing HS6ST3 increased the apoptosis in T47D by 21.8% compared to negative control group. Data was shown as mean ± SE, **p<0.01, T test.*

3.9 Analysis of adhesion assay after silencing *HS6ST3* in breast cancer

Similar to the cell motility, adhesion is one of the most important characteristics of tumor cells for progression. Adhesion assay was performed to investigate the potential effect of *HS6ST3* for changing the adhesion capacity of tumor cells into extracellular matrix (ECM). In this experiment the collagen I and fibronectin were used to coat the wells before seeding breast cancer cells. Analysis of the data revealed that the adhesion capacity of the T47D cells to collagen I was slightly increased by 5-10% in silenced group compared to control after silencing *HS6ST3* (Figure3.16: A); while this capacity was interestingly enhanced by 27-36% in MCF7 cell line (Figure3.16: C). Similarly, silencing of *HS6ST3* in T47D increased the adhesion capacity of this cell line to fibronectin by 9.2-14.4% (Figure3.16: B), while the similar capacity of MCF7 cells enhanced by 13-35% in silenced group compared to control (Figure3.16: D).

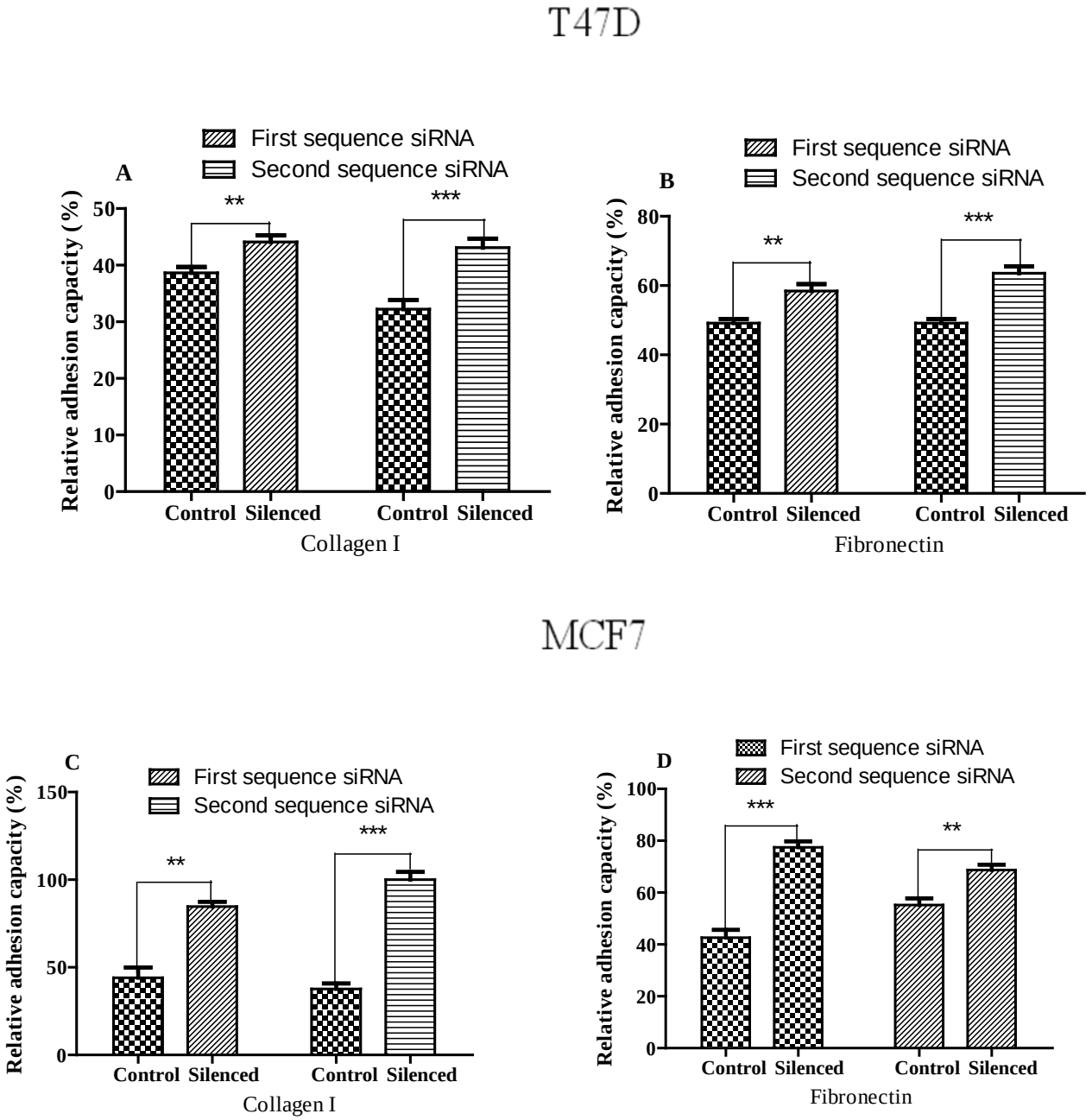

*Figure 3.16. Effect of silencing HS6ST3 on adhesion capacity of breast cancer cell lines. Silencing HS6ST3 slightly enhanced the adhesion capacity in T47D cell line toward collagen I and fibronectin (A, B); while, adhesion capacity of MCF7 cells remarkably increased toward Collagen I and fibronectin after silencing HS6ST3 (N=6) (C, D). Data was shown as mean ± SE, ** p <0.01, *** p<0.001, T test.*

3.10 Analysis of the cellular F-actin density in *HS6ST3*- knocked down cells

Analysis of adhesion assay showed that cell adhesion increased after silencing *HS6ST3* in breast cancer cell lines. Thus, we stained F-actin fibers in T47D and MCF7 breast cancer cell lines at 72 hours after silencing *HS6ST3*. However, it seems that silencing of *HS6ST3* did not affect the staining pattern of F-actin in T47D and MCF7 (Figure 3.17).

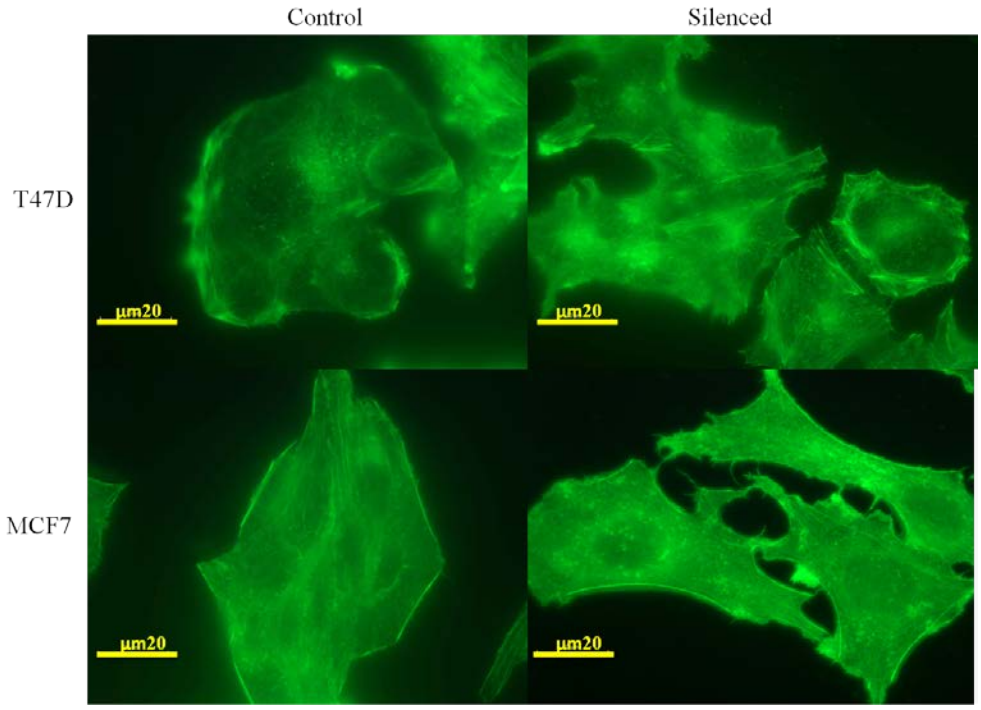

Figure 3.17. Effect of silencing HS6ST3 on F-actin assembly in breast cancer cell lines. F-actin fibers were probed by green color of fluorescein isothiocyanate (FITC-conjugated phalloidin). Silencing HS6ST3 did not change the distribution of F-actin in T47D and MCF7.

3.11 Analysis of Migration assay after silencing *HS6ST3* in breast cancer

This assay was performed to evaluate the functional role of *HS6ST3* in breast cancer cell motility. Wound healing (scratch assay) and transwell migration assays were two method that were employed to examine the migratory behavior of breast cancer cells after silencing *HS6ST3* with two sequence of siRNA. Firstly, migration assay was performed by transwell migration chambers for both T47D cell lines. Since T47D cells exhibited no migration through the migration inserts after silencing *HS6ST3*, we performed wound healing (scratch assay). Thus, *HS6ST3*-transfected T47D cells were seeded in 24 well plates and scratched 36 hours post-transfection and the gap sizes were measured by taking serial photos at 0, 24, 48 and 72 hours after scratch (Figure 3.18). The statistical analysis exhibited no significant differences at 24, 48 hours post-scratching; while, the gap size at 72 hours after scratching was significantly smaller in control compared to silenced group (Figure 3.19). The results showed that the scratch healing was delayed in silenced cells compared to control group. This change indicates that silencing of *HS6ST3* may potentially decrease the motility of cancer cells and consequently reduce the tumor progression; however we primarily concluded that this observed change might be attributable to the cellular proliferation rather than migration alone. In order to have a better understanding about cellular phenotype, we decided to perform invasion assay on MCF7 after silencing *HS6ST3*.

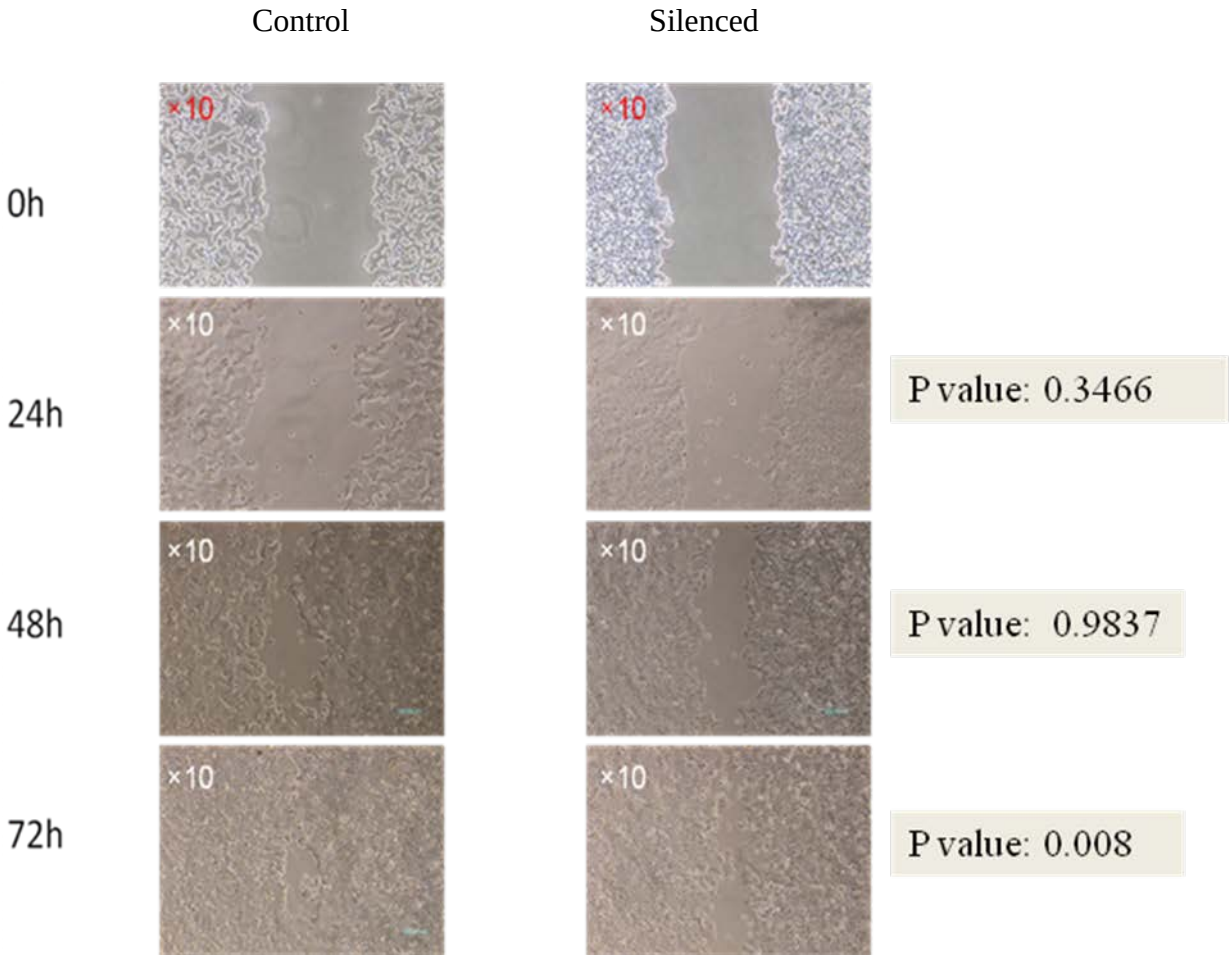

Figure 3.18. *Effect of HS6ST3 silencing on migration of T47D cell line at different time points (N=9). Although there were no significant differences at 24 and 48 hours post-scratching, the gap closure was delayed in silenced group compared to control group at 72 hours post-scratching (p< 0.01, T test).*

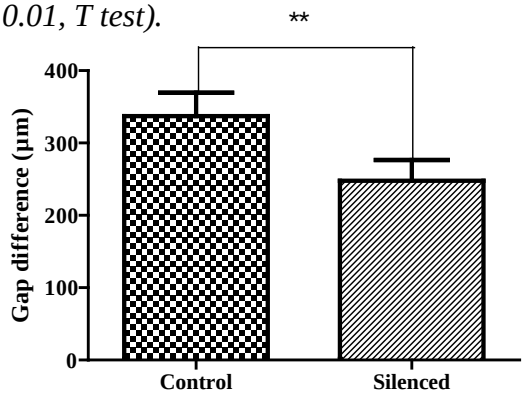

*Figure 3.19. Silencing HS6ST3 gene delayed the migration in silenced group at 72 hours post-scratching compared the control group (N=9, P< 0.01). Data was shown as mean ± SE, ** p <0.01, T test.*

Transwell migration inserts were employed to perform migration assay 72 hours after silencing *HS6ST3* in MCF7. Thus, the MCF7 cells were seeded in migration inserts at 48 hours post transfection and the cells were allowed to migrate through the inserts in 5% CO_2, 37ºC for 24 hours (Figure 3.20: A, B and C). Analysis revealed that cellular migration was significantly reduced after silencing *HS6ST3* compared to control group (Figure 3.20: D). The reduction in migratory cells confirmed the result of previous observation in scratch assay.

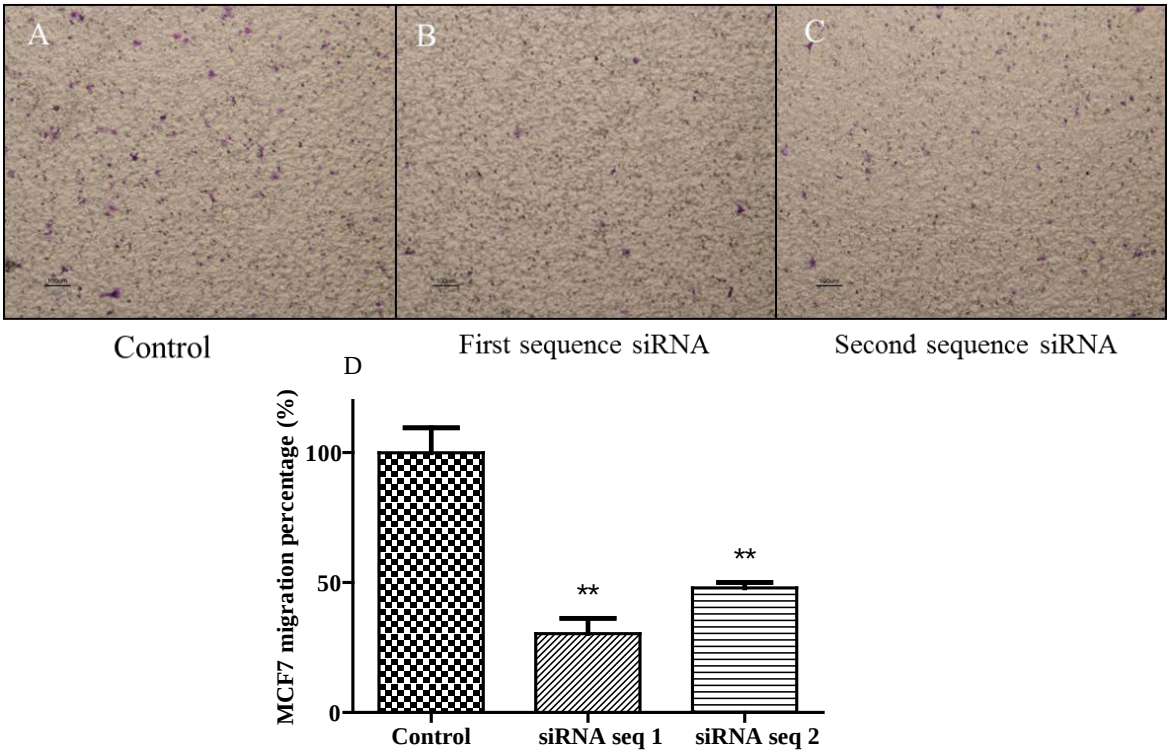

*Figure 3.20. The effect of HS6ST3 down-regulation on migration of MCF7 cells. A total number of 5x 10^4 cells were seeded in a total volume of 200µl into upper the chamber of the migration transwell. The lower chamber was filled with 600µl culture medium (RPMI for T47D and DMEM for MCF7) supplemented with 30% FBS. Cells were allowed to migrate in 5% CO_2, 37ºC for 24 hours. The migratory behavior of MCF7 cells were remarkably reduced in the silenced groups (B, C) compared to the control group (A) by 52-69% (D) (N=3). Data was shown as mean ± SE, ** p <0.01, T test.*

3.12 Analysis of breast cancer cellular invasion after silencing *HS6ST3*

Invasion is clinically an important characteristic of cancer cells which leads to metastasis. Metastasis occurs when the tumor cells invade the basement membrane to expand their proliferation to adjacent tissues as well as other organs. Invasion assay was performed on T47D and MCF7 cell lines after silencing *HS6ST3*. This assay provided an *in vitro* simulation model for cancer cell invasiveness by using Matrigel coated membrane. Analysis revealed no invasion in silenced or control group of T47D cell line. Then we performed invasion assay on MCF7 cell line to examine whether *HS6ST3* could affect the cellular invasiveness phenotype. Figure 3.21 show that silencing *HS6ST3* in MCF7 significantly reduced the invasiveness capacity of the cells by 52-71%.

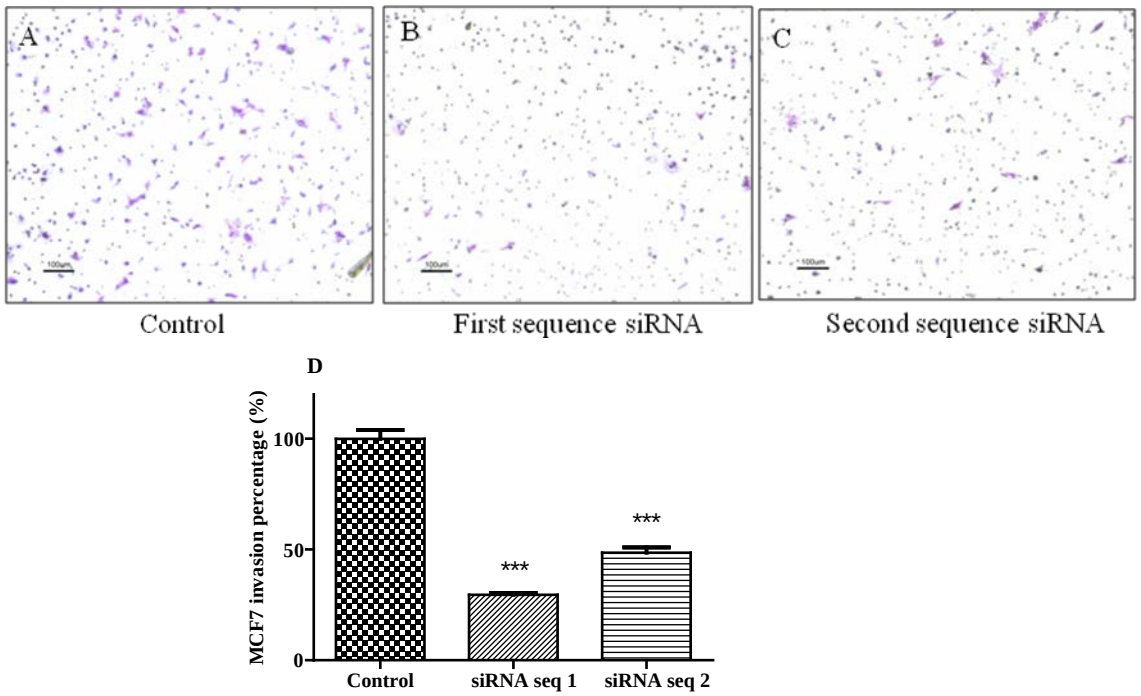

*Figure 3.21.Down-regulation of HS6ST3 in MCF7 significantly reduced the cellular invasiveness. The number of invaded cells across the matrigel membrane was evidently lower in silenced group compared to control (D) (N=3). Data was shown as mean ± SE, *** p <0.001, T test.*

Section 2: Genome-wide expression profiling in *HS6ST3*-knocked down T47D cells

As stated, it was identified that *HS6ST3* was highly up-regulated in breast cancer with the highest expression in the less invasive cell line (T47D). Thus, *HS6ST3* was silenced in T47D and then Genome-wide microarray was performed to identify the significant alteration in the expression of *HS6ST3*-related genes to find the potential pathway(s) in which *HS6ST3* was involved in the malignant process of carcinogenesis. T47D cells were transfected with negative scrambled siRNA as a negative control.

3.13 RNA yield, quality and integrity for T47D cells after silencing *HS6ST3*

The quality and integrity of RNA samples were important factors affecting the success of gene microarray hybridization. The quality of RNA samples defined by 260/ 280 absorbance ratios and also the RNA integrity number (RIN) were summarized in Table 3.2. All samples showed 260/ 280 absorbance ratios between 2.055 to 2.081 with concentration ranging from 478.52 to 970.21 ng/ µl. The mean RNA concentration of the silenced group was more than control group which was due to the effect of silencing *HS6ST3* on the relative percentage of the live cells. RIN ranged from 1 (degraded RNA) to 10 (intact RNA) was calculated based on the ratio of 28S/ 18S ribosomal RNA (rRNA) in Agilent 2100 Bioanalyzer. Analysis showed that all of the samples had a RIN of 8.2 to 9.4 indicating that RNA samples were of good quality (Table 3.1).

Electropherograms illustrated in Figure 3.22 (A) showed good integrity of RNA samples as they had two sharp peaks at18S and 28S. Furthermore, an image of depicted pseudo

gel revealed two specific distinct bands, one for 18S and another for 28S ribosomal subunit. Thus, the RNA samples were qualified to be used for next steps for synthesis of cDNA and cRNA in microarray procedure.

Table 3.1. *Quality and integrity of RNA samples for microarray procedure. Data was shown as mean ± SE.*

Sample	**Control**	**Silenced**
RIN	9.66± 0.033	9.10± 0.450
Conc. measured (ng/µl)	895.67± 39.107	496.74± 13.641
260/280	2.07± 0.007	2.06± 0.006

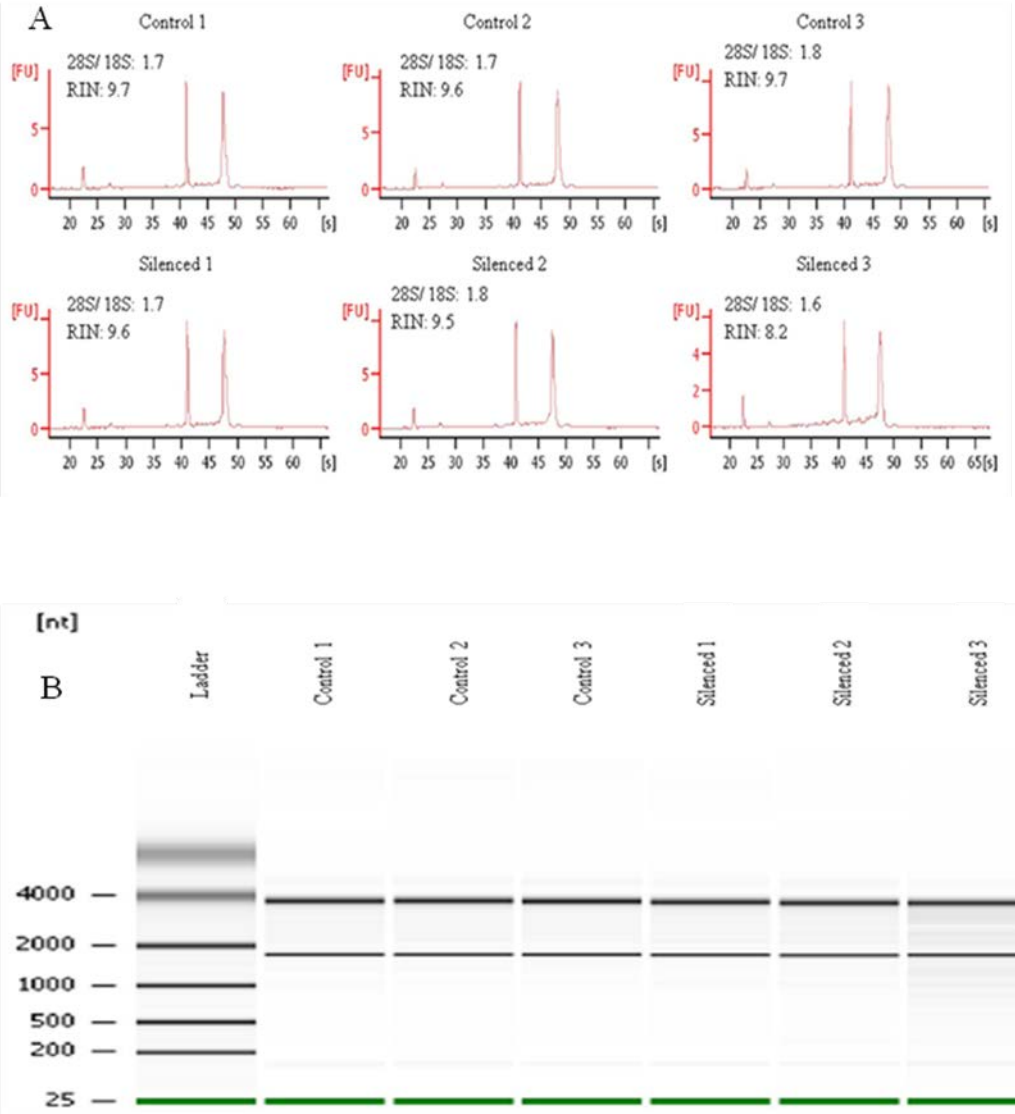

Figure 3.22. *Analysis of total RNA quality after silencing HS6ST3 in T47D by Agilent bioanalyzer. A) The spectrum analysis of 6 samples. Sharp peaks at 18S and 28S indicated highly intact RNA. B) The pseudo gel image from Agilent Bioanalyzer analysis showed two distinct bands (upper band: 28S subunit, lower band: 18S subunit). Samples include: Ladder, Control 1, Control 2, Control 3, Silenced 1, Silenced 2 and Silenced 3.*

3.14 Target preparation

300 ng of each total RNA sample was used for the whole transcript assay. The spectrophotometric reading results of sample processing were summarized in Table 3.2.

and Table 3.3. At each QC stage all the samples have good purity with high concentration.

Table 3.2. Spectrophotometric details of purified cRNA. Data was shown as mean ± SE.

Sample	Control	Silenced
260/280 Ratio	2.09± 0.002	2.09± 0.000
Concentration (mg/ml)	5.34± 0.160	4.58± 0.228
Yield (µg)	64.12± 1.925	54.96± 2.737

Table.3.3. Spectrophotometric details of purified single stranded cDNA. Data was shown as mean ± SE.

Sample	Control	Silenced
260/280 Ratio	1.77± 0.017	1.84± 0.054
Concentration (mg/ml)	273.55± 3.596	268.28± 11.867
Yield (µg)	7.66± 0.101	7.51± 0.332

3.15 Analysis of gene Microarray data

Synthesized Biotin-labeled cRNA were hybridized to the Human Gene 1.0 ST Gene Chips. Arrays were then washed and stained and finally scanned in Affymetrix 3000 7G scanner. Scanning provided an image file as well as raw signal intensities for all probe

sets. Expression Console, Genespring and dChip softwares were hired to processing the microarray data. Additionally, RMA, PLIER and iterPLIER algorithms were separately used in Expression Console and Genespring.

As discussed in method and material chapter, RMA was used to minimizing the difference of probe-specific affinity by reducing the variance across the dynamic change as well as increasing the sensitivity to small changes between control and silenced group. Adjustment of background based on PM distribution, normalization and summarization were three main steps performed in RMA. Unlike RMA, PLIER provides a higher accuracy for background adjustment but at the cost of increasing the signal variance. Therefore, for detecting small changes in the relative gene expression (fold of change), PLIER is highly sensitive with more accuracy compared to RMA; however, the variances are not so stable at the Log scale. The PLIER method was used in Genespring and Expression Console software independently. Iterative PLIER or iterPLIER is very similar to PLIER; however, it does not perform the summarization on all of the probes, but it selects the good probes regardless of bad probes (Therneau and Ballman 2008; Qu, He and Chen 2010; Seo and Hoffman 2006).

By using several stringent criteria (based on p-value, fold of change and probe intensity) for gene filtering in three softwares, we found significant alteration in expressions of 297 genes (Fig. 12) after silencing *HS6ST3* gene in T47D. The genes categorized into two groups: (i) 107 down-regulated genes; and (ii) 190 up-regulated genes (Figure 3.23).

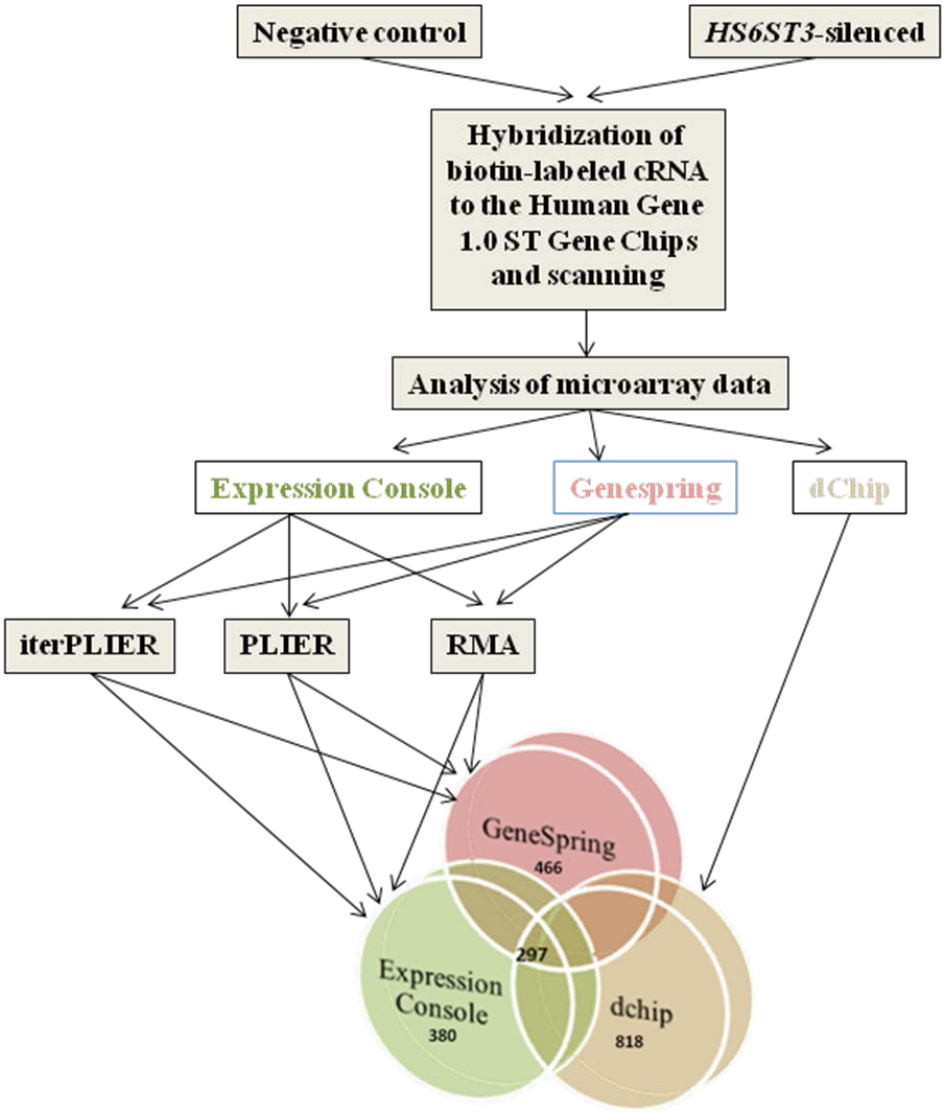

Figure 3.23. Overlapping the filtered genes after using three analytical microarray softwares (Expression Console, Genespring and dchip). Using three different algorithmic analyses in Expression Console and Genespring together with the data given from dChip provided seven sets of data for filtered gene which were finally overlapped together. T47D cells were transfected with negative scrambled siRNA as a negative control.

3.16 Functional categorization of target genes

Visualization and Integrated Discovery (DAVID) functional annotation (DAVID, Bioinformatics Resources, 2008) and Affymetrix NetAffx database were hired to find the

functional categorization of filtered genes. Up-regulated and down-regulated genes together were classified based on their genomic function in Table 3.4.

Table 3.4. F*unctional categorization of filtered genes after silencing HS6ST3 gene based on DAVID gene ontology and Affymetrix NetAffx database. Relative expression is fold change of gene after silencing HS6ST3. Negative values in relative gene expression indicate Down-regulation, while positive values show Up-regulation.*

Function	Gene Symbol	Gene Name	Relative Expression	Entrez ID
Apoptosis (33 genes)	APOL1	apolipoprotein L, 1	27.53	8542
	APOL6	apolipoprotein L, 6	5.43	80830
	BIRC3	baculoviral IAP repeat-containing 3	6.87	330
	CASP1	caspase 1, apoptosis-related cysteine peptidase (interleukin 1, beta, convertase)	4.58	834
	CCL5	chemokine (C-C motif) ligand 5	46.27	6352
	CD74	CD74 molecule, major histocompatibility complex, class II invariant chain	10.69	972
	CXCR4	chemokine (C-X-C motif) receptor 4	4.64	7852
	DRAM	damage-regulated autophagy modulator	2.33	55332
	EIF2AK2	eukaryotic translation initiation factor 2-alpha kinase 2	2.44	5610
	HERC5	hect domain and RLD 5	8.34	51191
	IFI6	interferon, alpha-inducible protein 6	9.31	2537
	IFIH1	interferon induced with helicase C domain 1	11.53	64135
	IGF1R	insulin-like growth factor 1 receptor	(-)2.37	3480
	IL28A /// IL28B	interleukin 28A (interferon, lambda 2) /// interleukin 28B (interferon, lambda 3)	4.08	282616 /// 282617
	IL29	interleukin 29 (interferon, lambda 1)	7.75	282618
	JAK2	Janus kinase 2 (a protein tyrosine kinase)	2.54	3717
	KLF4	Kruppel-like factor 4 (gut)	4.4	9314
	MX1	myxovirus (influenza virus) resistance 1, interferon-inducible protein p78 (mouse)	12.6	4599
	MYD88	myeloid differentiation primary response gene (88)	2.47	4615
	NFKBIA	nuclear factor of kappa light polypeptide gene enhancer in B-cells inhibitor, alpha	2.67	4792
	NUPR1	nuclear protein 1	2.35	26471
	OPTN	Optineurin	2.95	10133
	PML	promyelocytic leukemia	3.49	5371
	RARRES3	retinoic acid receptor responder (tazarotene induced) 3	19.11	5920

	SHISA5	shisa homolog 5 (Xenopus laevis)	2.81	51246
	SOD2	superoxide dismutase 2, mitochondrial	2.97	6648
	STAT5A	signal transducer and activator of transcription 5A	7.07	6776
	TLR3	toll-like receptor 3	4.81	7098
	TNFAIP3	tumor necrosis factor, alpha-induced protein 3	4.65	7128
	TNFSF10	tumor necrosis factor (ligand) superfamily, member 10	5.8	8743
	TP53I3	tumor protein p53 inducible protein 3	(-)2.59	9540
	UBE4B	ubiquitination factor E4B (UFD2 homolog, yeast)	(-)2.89	10277
	XAF1	XIAP associated factor 1	29.84	54739
Proliferation (25 genes)	BST2	bone marrow stromal cell antigen 2	3.19	684
	CCL5	chemokine (C-C motif) ligand 5	46.27	6352
	CD74	CD74 molecule, major histocompatibility complex, class II invariant chain	10.7	972
	CEP55	centrosomal protein 55kDa	(-)2.62	55165
	CXCL10	chemokine (C-X-C motif) ligand 10	13.9	3627
	CXCR4	chemokine (C-X-C motif) receptor 4	4.65	7852
	EIF2AK2	eukaryotic translation initiation factor 2-alpha kinase 2	2.44	5610
	IFITM1	interferon induced transmembrane protein 1 (9-27)	14.45	8519
	IGF1R	insulin-like growth factor 1 receptor	(-)2.37	3480
	IL29	interleukin 29 (interferon, lambda 1)	7.75	282618
	JAK2	Janus kinase 2 (a protein tyrosine kinase)	2.54	3717
	KLF4	Kruppel-like factor 4 (gut)	4.4	9314
	LAMP3	lysosomal-associated membrane protein 3	15.07	27074
	MYD88	myeloid differentiation primary response gene (88)	2.47	4615
	NFKBIA	nuclear factor of kappa light polypeptide gene enhancer in B-cells inhibitor, alpha	2.67	4792
	NUPR1	nuclear protein 1	2.35	26471
	ODC1	ornithine decarboxylase 1	(-)3.01	4953
	OGFR	opioid growth factor receptor	3.61	11054
	PML	promyelocytic leukemia	3.49	5371
	RARRES3	retinoic acid receptor responder (tazarotene induced) 3	19.11	5920
	SKAP2	src kinase associated phosphoprotein 2	(-)3.02	8935
	SOD2	superoxide dismutase 2, mitochondrial	2.97	6648
	STAT5A	signal transducer and activator of transcription 5A	7.07	6776
	TTK	TTK protein kinase	(-)2.21	7272
	ZFP106	zinc finger protein 106 homolog (mouse)	(-)2.17	64397
Adhesion (12 genes)	RND1	Rho family GTPase 1	5	27289
	CCL5	chemokine (C-C motif) ligand 5	46.27	6352

	CITED2	Cbp/p300-interacting transactivator, with Glu/Asp-rich carboxy-terminal domain,2	2.63	10370
	COL12A1	collagen, type XII, alpha 1	(-)2.8	1303
	CTNNAL1	catenin (cadherin-associated protein), alpha-like 1	(-)3.04	8727
	ICAM1	intercellular adhesion molecule 1	3.05	3383
	LGALS3BP	lectin, galactoside-binding, soluble, 3 binding protein	10.23	3959
	LGALS9 /// LGALS9B /// LGALS9C	lectin, galactoside-binding, soluble, 9 /// lectin, galactoside-binding, soluble, 9B /// lectin, galactoside-binding, soluble, 9C	6.33	3965 /// 284194 /// 654346
	PCDHB14	protocadherin beta 14	(-)2.85	56122
	PCDHB16	protocadherin beta 16	(-)2.53	57717
	PCDHB6	protocadherin beta 6	(-)3.18	56130
	STAT5A	signal transducer and activator of transcription 5A	7.07	6776
Migration (11 genes)	ABHD2	abhydrolase domain containing 2	(-)2.8	11057
	CXCR4	chemokine (C-X-C motif) receptor 4	4.65	7852
	HLA-C /// HLA-B /// FAM20B /// MICA /// LOC730410 /// HLA-A /// XXbac-BPG181B23.1	major histocompatibility complex, class I, C /// major histocompatibility complex, class I, B /// family with sequence similarity 20, member B /// MHC class I polypeptide-related sequence A /// similar to HLA class I histocompatibility antigen, B-18 alpha chain precursor (MHC class I antigen B*18) /// major histocompatibility complex, class I, A /// MHC class I polypeptide-related sequence A	3.74	3107 /// 3106 /// 9917 /// 4276 /// 730410 /// 3105 /// 100129668
	HLA-C /// HLA-B /// FAM20B /// MICA /// LOC730410 /// HLA-A /// XXbac-BPG181B23.1	major histocompatibility complex, class I, C /// major histocompatibility complex, class I, B /// family with sequence similarity 20, member B /// MHC class I polypeptide-related sequence A /// similar to HLA class I histocompatibility antigen, B-18 alpha chain precursor (MHC class I antigen B*18) /// major histocompatibility complex, class I, A /// MHC class I polypeptide-related sequence A	3.84	3107 /// 3106 /// 9917 /// 4276 /// 730410 /// 3105 /// 100129668
	HLA-C /// HLA-B /// MICA /// XXbac-BPG181B23.1	major histocompatibility complex, class I, C /// major histocompatibility complex, class I, B /// MHC class I polypeptide-related sequence A /// MHC class I polypeptide-related sequence A	3.58	3107 /// 3106 /// 4276 /// 100129668
	HMMR	hyaluronan-mediated motility receptor (RHAMM)	(-)2.56	3161
	ICAM1	intercellular adhesion molecule 1	3.05	3383
	IGF1R	insulin-like growth factor 1 receptor	(-)2.37	3480
	PARP9	poly (ADP-ribose) polymerase family, member 9	8.07	83666
	SDCBP	syndecan binding protein (syntenin)	2.26	6386
	SP100	SP100 nuclear antigen	3.98	6672
Cell Cycle (26 genes)	ATM /// NPAT	ataxia telangiectasia mutated /// nuclear protein, ataxia-telangiectasia locus	(-)2.67	472 /// 4863

CDCA7L	cell division cycle associated 7-like	(-)2.69	55536
CEP55	centrosomal protein 55kDa	(-)2.62	55165
CITED2	Cbp/p300-interacting transactivator, with Glu/Asp-rich carboxy-terminal domain, 2	2.63	10370
DSCC1	defective in sister chromatid cohesion 1 homolog (S. cerevisiae)	(-)2.89	79075
FANCD2	Fanconi anemia, complementation group D2	(-)2.5	2177
HERC5	hect domain and RLD 5	8.34	51191
HLA-DRB3 /// HLA-DRB5 /// hCG_1998957 /// HLA-DRB4 /// HLA-DRB1 /// LOC730415 /// HLA-DQB1 /// HLA-DQB2 /// HLA-DRB2 /// ZNF749 /// RNASE2	major histocompatibility complex, class II, DR beta 3 /// major histocompatibility complex, class II, DR beta 5 /// major histocompatibility complex, class II, DR beta 5 /// major histocompatibility complex, class II, DR beta 4 /// major histocompatibility complex, class II, DR beta 1 /// hypothetical protein LOC730415 /// major histocompatibility complex, class II, DQ beta 1 /// major histocompatibility complex, class II, DQ beta 2 /// major histocompatibility complex, class II, DR beta 2 (pseudogene) /// zinc finger protein 749 /// ribonuclease, RNase A family, 2 (liver, eosinophil-derived neurotoxin)	5.04	3125 /// 3127 /// 731247 /// 3126 /// 3123 /// 730415 /// 3119 /// 3120 /// 3124 /// 388567 /// 6036
IGF1R	insulin-like growth factor 1 receptor	(-)2.37	3480
IL1R1	interleukin 1 receptor, type I	(-)2.4	3554
IRF1	interferon regulatory factor 1	4.68	3659
NCAPD2	non-SMC condensin I complex, subunit D2	(-)2.2	9918
PML	promyelocytic leukemia	3.49	5371
PSMB10 /// CTRL	proteasome (prosome, macropain) subunit, beta type, 10 /// chymotrypsin-like	2.28	5699 /// 1506
PSMB8	proteasome (prosome, macropain) subunit, beta type, 8 (large multifunctional peptidase 7)	5.17	5696
PSMB8	proteasome (prosome, macropain) subunit, beta type, 8 (large multifunctional peptidase 7)	5.17	5696
PSMB8	proteasome (prosome, macropain) subunit, beta type, 8 (large multifunctional peptidase 7)	5.17	5696
PSMB9	proteasome (prosome, macropain) subunit, beta type, 9 (large multifunctional peptidase 2)	6.96	5698
PSMB9	proteasome (prosome, macropain) subunit, beta type, 9 (large multifunctional peptidase 2)	6.96	5698
PSMB9	proteasome (prosome, macropain) subunit, beta type, 9 (large multifunctional peptidase 2)	6.96	5698
PSME1	proteasome (prosome, macropain) activator subunit 1 (PA28 alpha)	2.38	5720
SP100	SP100 nuclear antigen	3.98	6672
STAT5A	signal transducer and activator of transcription 5A	7.07	6776
TP53I3	tumor protein p53 inducible protein 3	(-)2.59	9540

	TTK	TTK protein kinase	(-)2.21	7272
	XAF1	XIAP associated factor 1	29.84	54739
Signal Transduction (28 genes)				
	ARHGAP11A	Rho GTPase activating protein 11A	(-)2.42	9824
	ARHGAP19	Rho GTPase activating protein 19	(-)2.48	84986
	ATM /// NPAT	ataxia telangiectasia mutated /// nuclear protein, ataxia-telangiectasia locus	(-)2.67	472 /// 4863
	BIRC3	baculoviral IAP repeat-containing 3	6.87	330
	C3	complement component 3	6	718
	CASP1	caspase 1, apoptosis-related cysteine peptidase (interleukin 1, beta, convertase)	4.57	834
	CCL5	chemokine (C-C motif) ligand 5	46.27	6352
	CD74	CD74 molecule, major histocompatibility complex, class II invariant chain	10.7	972
	CLOCK	clock homolog (mouse)	(-)2.66	9575
	CXCL10	chemokine (C-X-C motif) ligand 10	13.9	3627
	CXCR4	chemokine (C-X-C motif) receptor 4	4.65	7852
	GNG12	guanine nucleotide binding protein (G protein), gamma 12	(-)2.13	55970
	HLA-DRB3 /// HLA-DRB5 /// hCG_1998957 /// HLA-DRB4 /// HLA-DRB1 /// LOC730415 /// HLA-DQB1 /// HLA-DQB2 /// HLA-DRB2 /// ZNF749 /// RNASE2	major histocompatibility complex, class II, DR beta 3 /// major histocompatibility complex, class II, DR beta 5 /// major histocompatibility complex, class II, DR beta 5 /// major histocompatibility complex, class II, DR beta 4 /// major histocompatibility complex, class II, DR beta 1 /// hypothetical protein LOC730415 /// major histocompatibility complex, class II, DQ beta 1 /// major histocompatibility complex, class II, DQ beta 2 /// major histocompatibility complex, class II, DR beta 2 (pseudogene) /// zinc finger protein 749 /// ribonuclease, RNase A family, 2 (liver, eosinophil-derived neurotoxin)	5.04	3125 /// 3127 /// 731247 /// 3126 /// 3123 /// 730415 /// 3119 /// 3120 /// 3124 /// 388567 /// 6036
	IFITM1	interferon induced transmembrane protein 1 (9-27)	14.45	8519
	IGF1R	insulin-like growth factor 1 receptor	(-)2.37	3480
	IRF9	interferon regulatory factor 9	2.86	10379
	LGALS3BP	lectin, galactoside-binding, soluble, 3 binding protein	10.23	3959
	MX1	myxovirus (influenza virus) resistance 1, interferon-inducible protein p78 (mouse)	12.6	4599
	OPTN	Optineurin	2.95	10133
	PML	promyelocytic leukemia	3.49	5371
	PRKAR2A	protein kinase, cAMP-dependent, regulatory, type II, alpha	(-)2.8	5576
	RND1	Rho family GTPase 1	5	27289

	SKAP2	src kinase associated phosphoprotein 2	(-)3.02	8935
	STAT1	signal transducer and activator of transcription 1, 91kDa	4.55	6772
	STAT2	signal transducer and activator of transcription 2, 113kDa	3.34	6773
	STAT5A	signal transducer and activator of transcription 5A	7.07	6776
	TLR3	toll-like receptor 3	4.81	7098
	TNFSF10	tumor necrosis factor (ligand) superfamily, member 10	5.8	8743
Others				

3.17 Validation of gene expression by RT-PCR

297 genes were further filtered to 50 genes (25 down-regulated and 25 up-regulated genes) regarding their functional categories and the most up- and down-regulated change. To check the accuracy of microarray results, quantitative RT-PCR was performed on the 50 genes. For this purpose, forward and reverse primers were designed in Primer 3 software and then their specificity was checked in NCBI Blast.

After designing specific primers, RT-PCR was performed on 50 genes out of 297 genes to validate their expression. The results of RT-PCR for all of the up- and down-regulated genes were consistent with that of microarray results (Table 3.5). For further verification, the direction of the regulation of the genes and the quantitative level of up- and down-regulation (fold of change) was plotted in Figure 3.24. The main focus of this study was on the above mentioned gene list; however, based on the extensive literature review, changes of a few other genes (after silencing *HS6ST3)* were considered from non-overlapped list of genes (using iterPLIER of Expression Console) which will be discussed in the discussion chapter.

Table 3.5. *Validation of 50 differentially expressed genes in Microarray analysis by RT-PCR.* ↑ stands for up-regulation and ↓ *stands for down-regulation.*

	Gene Symbol	Gene Name	Microarray	RT-PCR
Up-regulated genes				
	CFB /// C2	complement factor B /// complement component 2	↑	↑
	CCL5	chemokine (C-C motif) ligand 5	↑	↑
	OASL	2'-5'-oligoadenylate synthetase-like	↑	↑
	IFIT3	interferon-induced protein with tetratricopeptide repeats 3	↑	↑
	IFIT2	interferon-induced protein with tetratricopeptide repeats 2	↑	↑
	XAF1	XIAP associated factor 1	↑	↑
	APOL1	apolipoprotein L, 1	↑	↑
	OAS2	2'-5'-oligoadenylate synthetase 2, 69/71kDa	↑	↑
	IFI27	interferon, alpha-inducible protein 27	↑	↑
	S100A8	S100 calcium binding protein A8	↑	↑
	RSAD2	radical S-adenosyl methionine domain containing 2	↑	↑
	MX1	myxovirus (influenza virus) resistance 1, interferon-inducible protein p78 (mouse)	↑	↑
	RARRES3	retinoic acid receptor responder (tazarotene induced) 3	↑	↑
	IFITM1	interferon induced transmembrane protein 1 (9-27)	↑	↑
	IFIH1	interferon induced with helicase C domain 1	↑	↑
	IL29	interleukin 29 (interferon, lambda 1)	↑	↑
	STAT1	signal transducer and activator of transcription 1, 91kDa	↑	↑
	KLF4	Kruppel-like factor 4 (gut)	↑	↑
	SHISA5	shisa homolog 5 (Xenopus laevis)	↑	↑
	NFKBIA	nuclear factor of kappa light polypeptide gene enhancer in B-cells inhibitor, alpha	↑	↑
	DRAM	damage-regulated autophagy modulator	↑	↑
	NUPR1	nuclear protein 1	↑	↑
	OAS1	2',5'-oligoadenylate synthetase 1, 40/46kDa	↑	↑
	TNFSF10	tumor necrosis factor (ligand) superfamily, member 10	↑	↑
	CASP1	caspase 1, apoptosis-related cysteine peptidase (interleukin 1, beta, convertase)	↑	↑

Down-regulated genes	FCF1	FCF1 small subunit (SSU) processome component homolog (S. cerevisiae)	↓	↓
	CBX5	chromobox homolog 5 (HP1 alpha homolog, Drosophila)	↓	↓
	PRR11	proline rich 11	↓	↓
	ATL3	atlastin 3	↓	↓
	ODC1	ornithine decarboxylase 1	↓	↓
	CTNNAL1	catenin (cadherin-associated protein), alpha-like 1	↓	↓
	IGF1R	insulin-like growth factor 1 receptor	↓	↓
	COL12A1	collagen, type XII, alpha 1	↓	↓
	PRKAR2A	protein kinase, cAMP-dependent, regulatory, type II, alpha	↓	↓
	CDCA7L	cell division cycle associated 7-like	↓	↓
	PLDN	pallidin homolog (mouse)	↓	↓
	CEP55	centrosomal protein 55kDa	↓	↓
	ARHGAP19	Rho GTPase activating protein 19	↓	↓
	UTRN	Utrophin	↓	↓
	FANCD2	Fanconi anemia, complementation group D2	↓	↓
	HMMR	hyaluronan-mediated motility receptor (RHAMM)	↓	↓
	SFXN2	sideroflexin 2	↓	↓
	HIF1AN	hypoxia-inducible factor 1, alpha subunit inhibitor	↓	↓
	ARHGAP11A	Rho GTPase activating protein 11A	↓	↓
	SHCBP1	SHC SH2-domain binding protein 1	↓	↓
	TTK	TTK protein kinase	↓	↓
	SLC7A11	solute carrier family 7, (cationic amino acid transporter, y+ system) member 11	↓	↓
	GPC6	glypican 6	↓	↓
	ADD3	adducin 3 (gamma)	↓	↓
	IL1R1	interleukin 1 receptor, type I	↓	↓

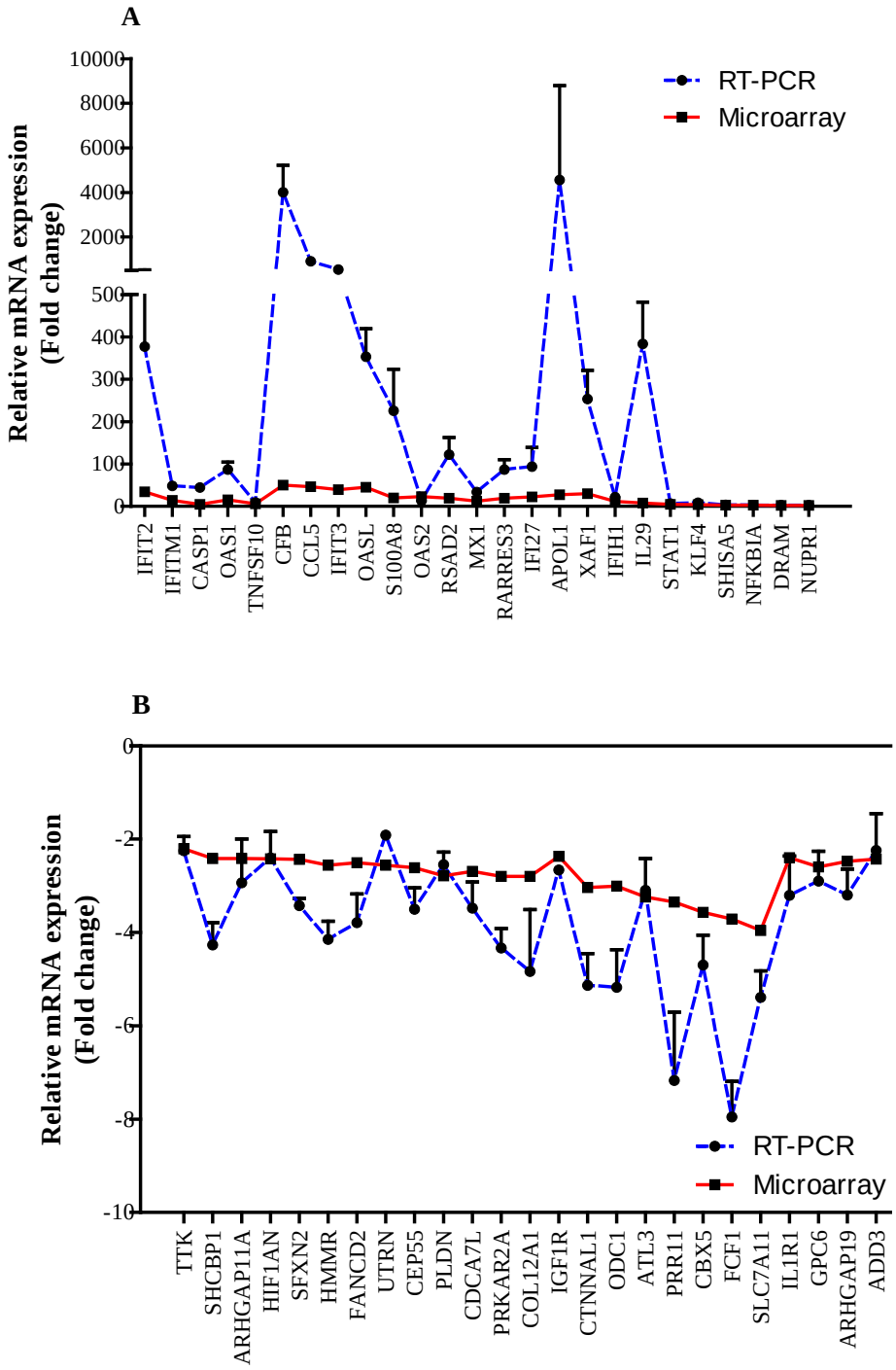

Figure 3.24. Quantitative RT-PCR agreement of the expression direction of the filtered genes with microarray results. Up-regulated genes revealed with positive values (A), while down-regulated genes illustrated with negative values (B). Data was shown as mean ± SE, T test.

3.18 Gene pathway analysis

Extensive literature review performed to verify the function(s) of 50 selected genes. Then, the genes with relevant functions were further evaluated. Thus, out of 50 verified genes, a few of them found to be potentially involved in observed phonotypical changes (discussed in the first section of this chapter) after silencing *HS6ST3* in the breast cancer. One of the most important of them was Insulin-like growth factor receptor I (*IGF1R*) gene which was down-regulated after silencing *HS6ST3* in breast cancer. IGF1R is a transmembrane tyrosine kinase receptor comprising two extracellular alpha and two beta subunits which critically modulate several biological events such as growth and development. The other significant gene was XIAP-associated factor 1 (XAF1) which was considerably up-regulated in *HS6ST3*-knocked down T47D cells. XIAP-associated factor 1 or XAF1, a zinc finger protein, is known as a tumor suppressor that antagonizing XIAP, an antiapoptotic protein, and thus induce the cell death.

Both IGF1R and XAF1 were identified as candidate genes that seemed to be potentially involved in cancer cell growth and progression. Therefore, in order to validate these findings we firstly rechecked the expression pattern of *IGF1R* and *XAF1* genes in T47D and MCF7 cell lines. Then, western blotting was performed to examine IGF1R and XAF1 expression at the protein level after silencing *HS6ST3* in T47D and MCF7. After that, various functional assays were performed on *HS6ST3*-knocked down cells after blocking IGF1R receptors or double silencing with XAF1 shRNA. All of the functional assays in latter step were performed on MCF7 cells because firstly, we found that blocking IGF1R receptor in MCF7 is much more effective than T47D cells by using our

available blocking antibody; and secondly the higher growth rate of MCF7 enabled us to pick a single colony for clone selection after transfecting MCF7 with XAF1 shRNA plasmid, while similar procedure was not feasible in T47D due to its lower growth rate compared to MCF7.

3.19 Quantitative real time (RT-PCR) analysis of *IGF1R* expression after silencing *HS6ST3* in T47D and MCF7

Relative expression pattern of *IGF1R* gene was measured by performing RT-PCR at 72 hours after silencing *HS6ST3* in T47D and MCF7 cell lines in triplicate. Analysis revealed that *IGF1R* expression was significantly decreased by 47.6% and 38.4% in *HS6ST3*-knocked down T47D and MCF7 respectively (Figure 3.25).

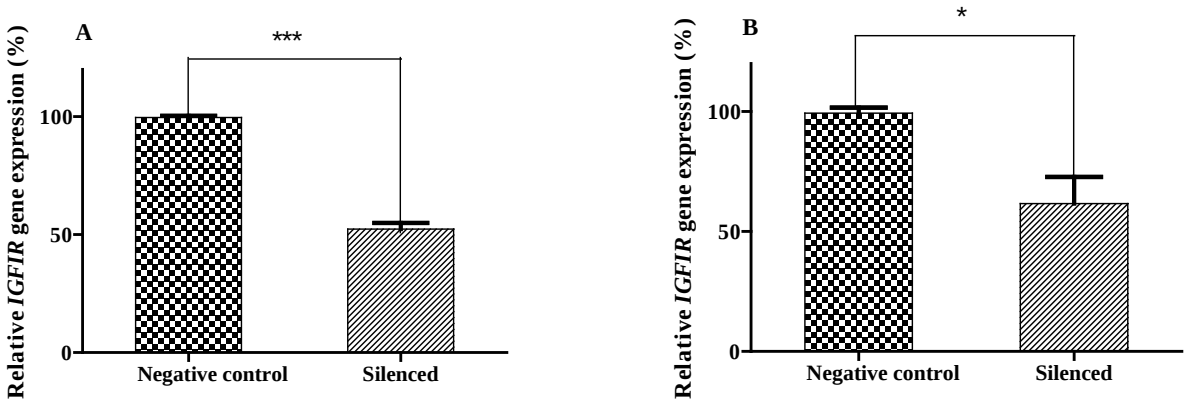

*Figure 3.25. Effect of HS6ST3 silencing on relative mRNA expression of IGF1R gene in T47D (A) and MCF7 (B) cells (N=3). Data was shown as mean ± SE, * p <0.05, *** p <0.001, T test.*

3.20 Western blotting analysis of IGF1R expression in *HS6ST3*-knocked down cells

The expression of IGF1R was measured at protein level at 72 hours after silencing *HS6ST3* in T47D and MCF7 by western blotting. The expression values were normalized with the expression of β-actin, housekeeping protein in western blotting. As shown in Figure 3.26, the expression of IGF1R had a significant reduction by 46.9% at 72 hours after silencing *HS6ST3* gene in T47D and MCF7 cell lines.

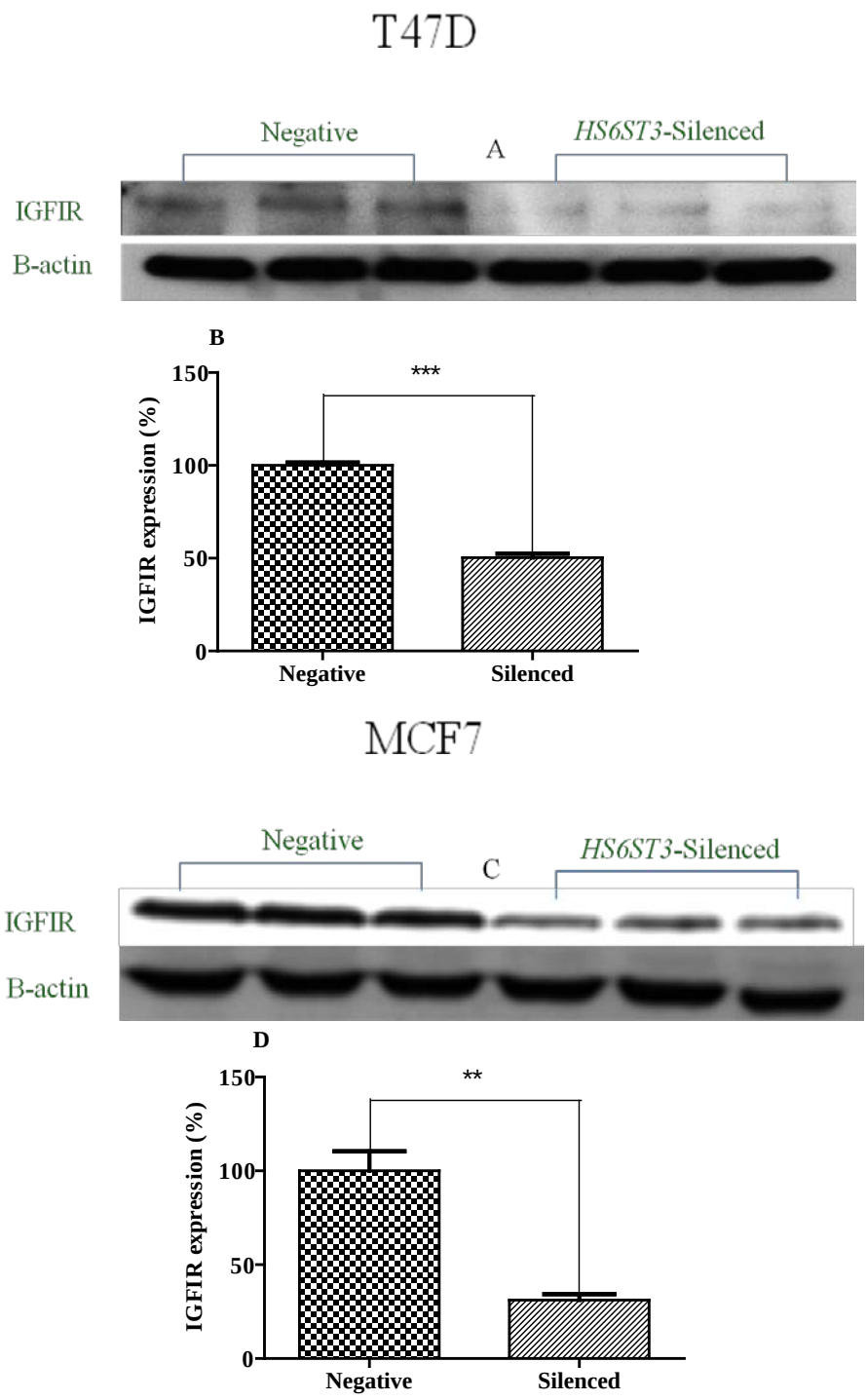

Figure 3.26. *Western blotting (WB) analysis of IGF1R protein expression at 72 hours after silencing HS6ST3 gene in T47D (A) and MCF7 (C) cell lines. Silencing HS6ST3 gene significantly reduced the* IGF1R *protein expression by 46.9% and 68% in T47D (B) and MCF7 (D) respectively (N=3). Data was shown as mean ± SE, ** p <0.01, *** p <0.001, T test.*

3.21 Analysis of the effect of IGF1R receptor blocking on cell proliferation

Insulin-like growth factor I receptor (IGF1R) is a transmembrane tyrosine kinase receptor that critically modulate several biological events such as growth and promotion of malignant cells. It is understood that restoration of IGF1R expression increases the malignant cell proliferation, migration and invasion; while it reduces the apoptosis (Tang et al. 2007; Cullen et al. 1990; Werner and Le Roith 1997; Burtscher and Christofori 1999; Yanochko and Eckhart 2006; Carboni et al. 2005; Dunn et al. 1998; Sachdev et al. 2004; Samani et al. 2004; Sachdev et al. 2010; Zhang et al. 2010; Kang et al. 2010; Linnerth et al. 2009; Avnet et al. 2009; Párrizas, Saltiel and LeRoith 1997; Guvakova and Surmacz 1999) .

Non-transfected T47D and MCF7 cells were washed and incubated in FBS-free medium in 5% CO_2, 37ºC for 1 hour. Serial recommended concentration of IGF1R antibody was used to find the dose at which 50% of the cell survived. Following the incubation, FBS was added at a final concentration of 10% in culture medium and incubated in 5% CO2, 37ºC for 72 hours. Finally, cell proliferation assay was performed by adding MTS solution and then the absorbances were measured at 490 nm. Figure 3.27 revealed the effect of blocking of the IGF1R on the relative percentage of the live T47D and MCF7 cell lines.

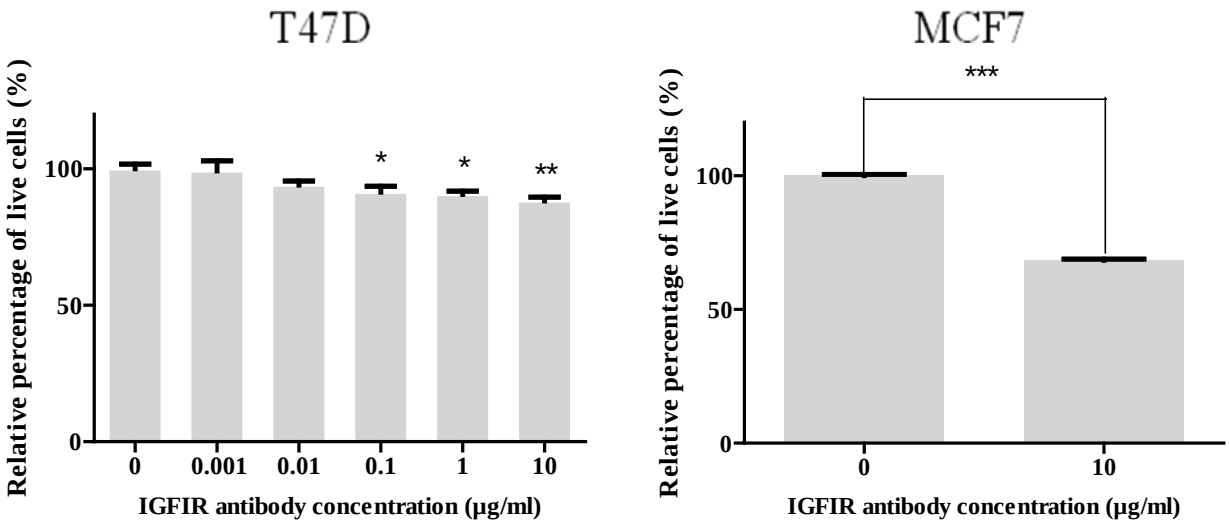

*Figure 3.27. Effect of IGF1R blocking antibody on the relative percentage of live T47D (A) and MCF7 (B). Various recommended concentration (0, 0.001, 0.01, 1 and 10 µg/ml) of IGF1R blocking antibody were used on T47D cells; however, a maximum recommended dose of 10 µg/ml was much more effective in MCF7 compared to T47D cells (N=3). Data was shown as mean ± SE, * p <0.05, ** p <0.01, ***p<0.001, T test.*

3.22 Analysis of the effect of blocking IGF1R receptor on the relative percentage of live *HS6ST3*-knocked down MCF7 cells

MCF7 cells were transfected for silencing *HS6ST3*. At 10 hours post-transfection, the IGF1R receptors on the cell surface were blocked with 10 µg/ml of blocking antibody in a serum-free culture medium. Next, serum (FBS) was added at a final concentration of 10% and then the cells were incubated in 5% CO_2, 37ºC for 72 hour. Then, the relative percentage of the live cells was measured by using MTS method. There was no significant difference in the relative percentage of live *HS6ST3*-silenced group which were blocked for IGF1R receptor, while non-silenced group revealed reduction in their relative percentage of live cells by 37.8% after blocking IGF1R receptor (Figure 3.28).

The observed difference might be due to the lower expression of IGF1R receptor after silencing *HS6ST3* in MCF7.

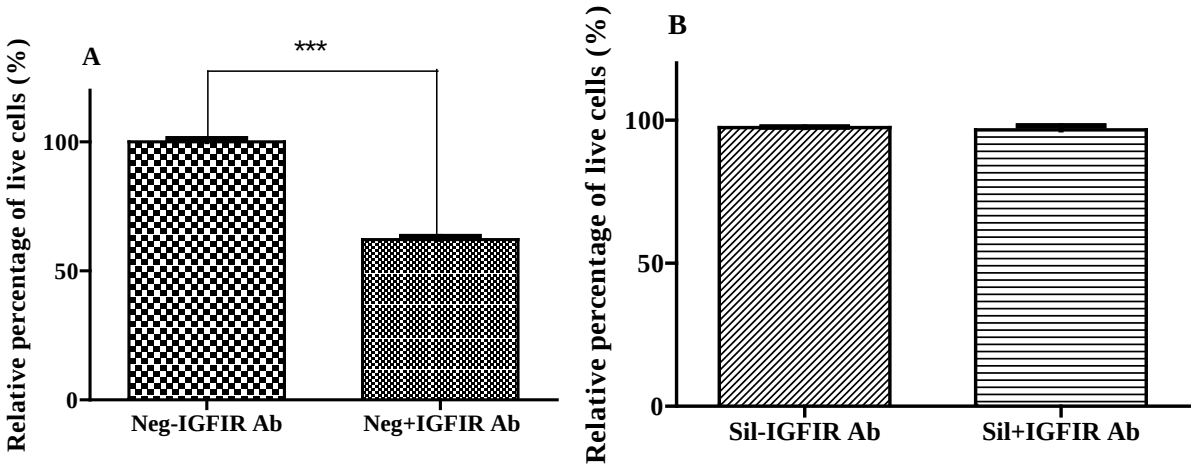

*Figure 3.28. Effect of IGF1R blocking antibody on the relative percentage of the live HS6ST3-knocked down MCF7. While IGF1R blocking antibody had no influence on relative percentage of live silenced cells, it reduced the relative percentage of live cells in negative siRNA-transfected MCF7 cells by 37.8% (N=3). Data was shown as mean ± SE, ***p<0.001, T test.*

3.23 Analysis of adhesion assay after blocking IGF1R receptor in HS6ST3-silenced MCF7

MCF7 cells were transfected for silencing *HS6ST3*. At 10 hours post-transfection, the IGF1R receptors on the cell surface were blocked with 10 µg/ml of blocking antibody in a serum-free culture medium. Next, serum (FBS) was added at a final concentration of 10% and then the cells were incubated in 5% CO_2, 37ºC for 72 hour. Adhesion assay was performed in 96-well plate coated with collagen I (discussed in previous chapter). Interestingly, adhesion of both silenced and control group were increased at 72 hours after silencing *HS6ST3* and blocking IGF1R receptor in MCF7; however, statistically no significant difference was observed between silenced and control group (Figure 3.29).

The result of this assay was indicative of a potential role for IGF1R receptor in cell adhesion.

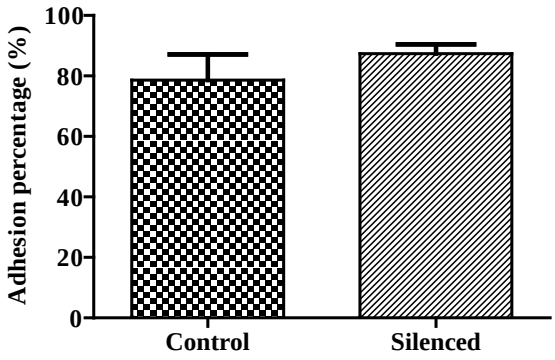

Figure 3.29. Effect of IGF1R blocking antibody on adhesion of HS6ST3-knocked down MCF7. IGF1R blocking antibody increased the cell adhesion at 72 hours after blocking IGF1R in MCF7 for both control and silenced groups. However, no statistical difference was observed between silenced and control groups (N=3). The control group was transfected with negative control siRNA and treated with IGF1R antibody. Each group of the control or silenced group was normalized to its corresponding un-washed cells during the adhesion assay. Data was shown as mean ± SE, T test.

3.24 Analysis of migration and invasion assays after blocking IGF1R receptor in *HS6ST3*-silenced MCF7

MCF7 cells were transfected for silencing *HS6ST3*. At 10 hours post-transfection, the IGF1R receptors on the cell surface were blocked with 10 µg/ml of blocking antibody in a serum-free culture medium. Next, serum (FBS) was added at a final concentration of 10% and then the cells were incubated in 5% CO_2, 37ºC. At 48 hours post transfection, a total number of 5x 10^4 MCF7 cells were seeded in migration and invasion chambers and incubated in 5% CO_2, 37ºC for 24 hours. During all stages of migration and invasion assays, the final concentration of IGF1R antibody was kept at 10 µg/ml level in cell

culturing medium. Both migration (Figure 3.30 A, B) and invasion (Figure 2.31 A, B) were evidently decreased in control and silenced groups compared to non-IGF1R blocked cells. However, no significant differences were found between silenced and control group in both migration (Figure 3.30 C) and invasion (Figure 3.31 C) assays. This observation was suggestive of contribution of IGF1R in cellular migration and invasion.

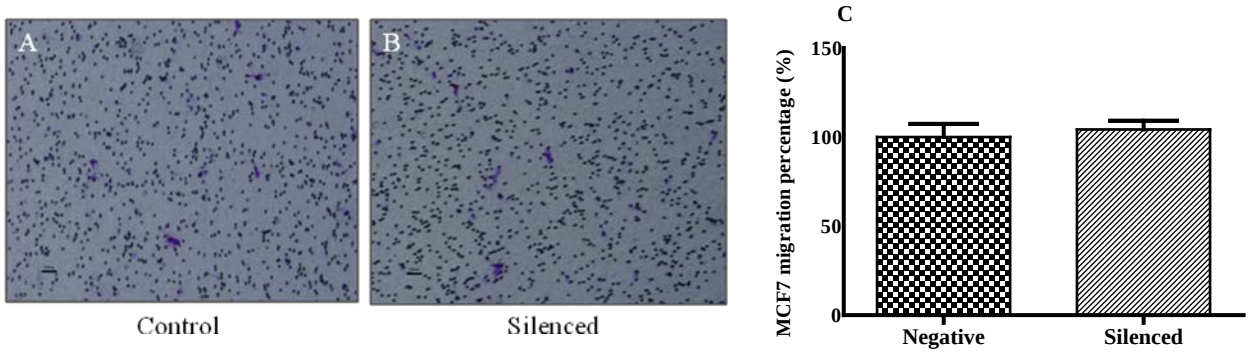

Figure 3.30. Effect of IGF1R blocking antibody on migration of HS6ST3-knocked down MCF7 cells (N=3). The control group was transfected with negative control siRNA and treated with IGF1R antibody. Data was shown as mean ± SE, T test.

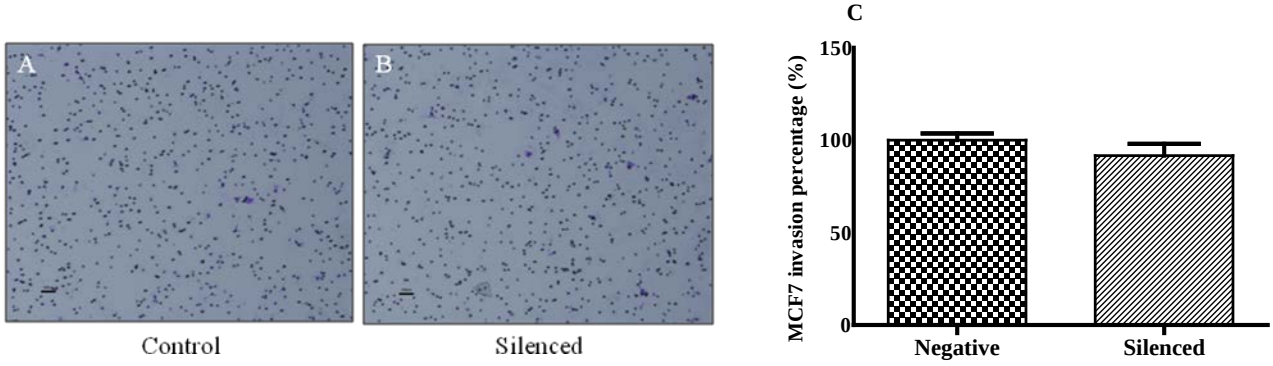

Figure 3.31. Effect of IGF1R blocking antibody on invasion of HS6ST3-knocked down MCF7 cells (N=3). The control group was transfected with negative control siRNA and treated with IGF1R antibody. Data was shown as mean ± SE, T test.

3.25 Quantitative real time (RT-PCR) analysis of *XAF1* expression after silencing *HS6ST3* in T47D and MCF7

Relative expression pattern of *XAF1* gene was measured by performing RT-PCR at 72 hours after silencing *HS6ST3* in T47D and MCF7 cell lines in triplicate. Analysis revealed that *XAF1* was significantly over-expressed by 253 and 3472 times in *HS6ST3*-knocked down T47D and MCF7 respectively (Figure 3.32).

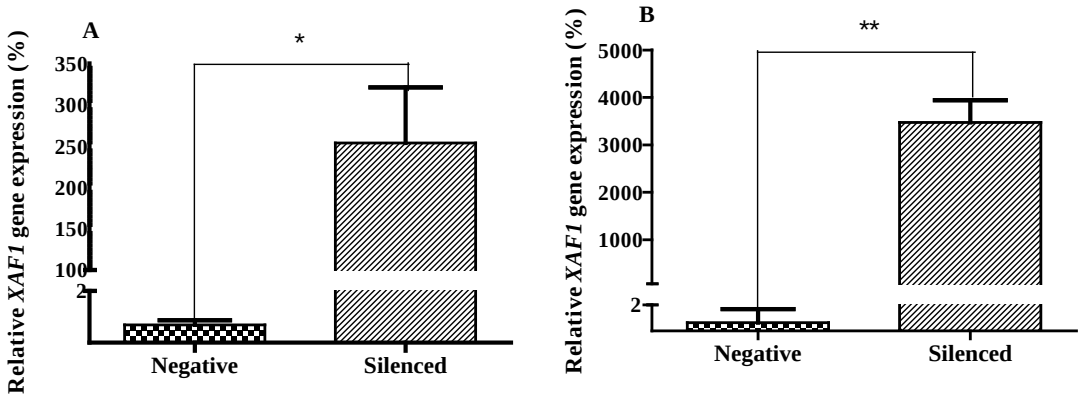

*Figure 3.32. Effect of HS6ST3 silencing on relative mRNA expression of XAF1 gene in T47D (A) and MCF7 (B) cells (N=3). Data was shown as mean ± SE, * p <0.05, ** p <0.01, T test.*

3.26 Western blotting analysis of XAF1 expression in *HS6ST3*-knocked down cells

The expression of XAF1 was measured at protein level at 72 hours after silencing *HS6ST3* in T47D and MCF7 by western blotting. The expression values were normalized with the expression of β-actin, housekeeping protein in western blotting. At 72 hours after silencing *HS6ST3* gene, the expression of XAF1 significantly increased by 102% and 670.8% in T47D and MCF7 cell lines respectively (Figure 3.33).

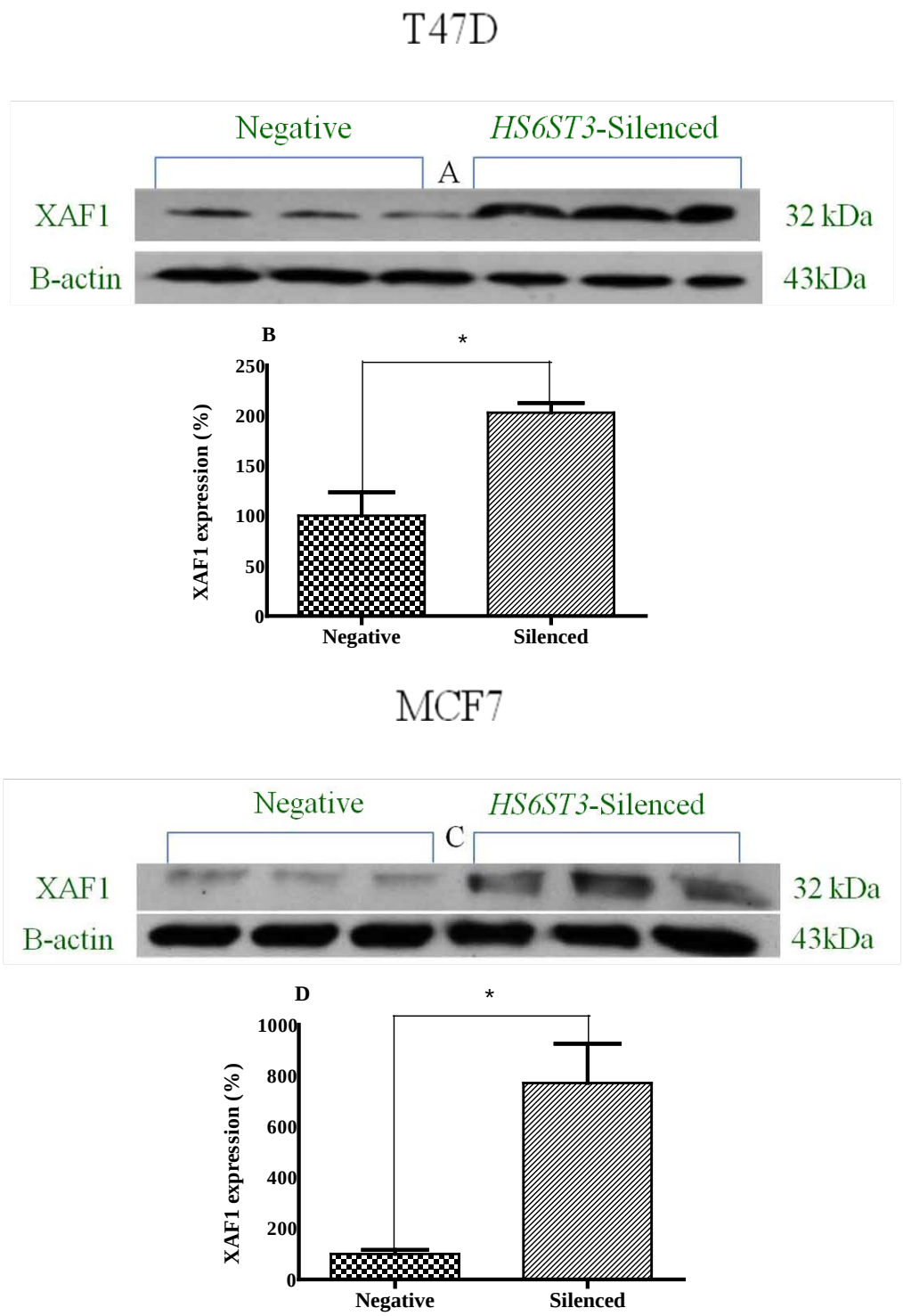

Figure 3.33. Western blotting (WB) analysis of XAF1 *protein expression at 72 hours after silencing HS6ST3 gene in T47D (A) and MCF7 (C) cell lines. Silencing HS6ST3 gene significantly up-regulated* XAF1 *protein expression in T47D (B) and MCF7 (D) respectively (N=3). Data was shown as mean ± SE, * p <0.05, T test.*

3.27 Quantitative real time (RT-PCR) analysis of *XAF1* expression after silencing in MCF7

XIAP-associated factor 1 or XAF1, a zinc finger protein, is known as a tumor suppressor that antagonizes XIAP, an antiapoptotic protein, and thus induce the cell death. XAF1 could be detected ubiquitously in many tissues; however, its expression is suppressed *in vitro* and *in vivo* in several cancers such as gastric cancer, skin cancer, colorectal cancer, prostate cancer, blood cancer, kidney cancer, bladder cancer, liver cancer and testicular cancer (Sakemi et al. 2007; Ng et al. 2004; Byun et al. 2003; Ma et al. 2005; Chen et al. 2006; Lee et al. 2006; Gao et al. 2006; Zou et al. 2006; Shibata et al. 2007; Yu et al. 2007; Chung et al. 2007; Li et al. 2007; Kempkensteffen et al. 2007; Li et al. 2008; Kempkensteffen et al. 2008; Pinho et al. 2009; Huang et al. 2010). Researchers understood that loss of XAF1 expression was associated with poor prognosis in several malignancies (Chen et al. 2006; Huang et al. 2010). On the other hand, over-expression of XAF1 could redistribute the cytosolic XIAP into nucleus and therefore trigger the apoptosis pathway and induce cell cycle arrest at specific check points (Liston et al. 2001; Wang et al. 2009).

XAF1 was silenced in MCF7 using shRNA plasmid. Thus, the mRNA of transfected cells was extracted and then quantitative real time PCR (RT-PCR) was performed to compare the silencing efficiency. Analysis of RT-PCR data showed that *XAF1* was silenced in MCF7 by 82% by using XAF1 shRNA (Figure 3.34).

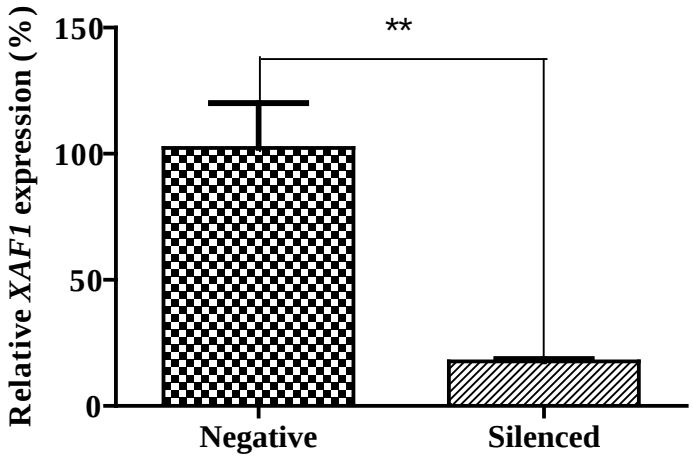

*Figure 3.34. Silencing efficiency of XAF1 genes in MCF7 cell line using shRNA (N=3). The percentages were calculated based on the relative quantitation in RT-PCR. Negative control group was transfected with negative shRNA. Data was shown as mean ± SE, ** p <0.01, T test.*

3.28 Western blotting analysis of XAF1 expression after silencing *XAF1* in MCF7

The expression of XAF1 was measured at protein level in *XAF1*-knocked down MCF7 by western blotting. The expression values were normalized with the expression of β-actin, housekeeping protein in western blotting. Analysis revealed that the expression of XAF1 protein significantly diminished by 56.6% in MCF7 after silencing *XAF1* by shRNA (Figure 3.35).

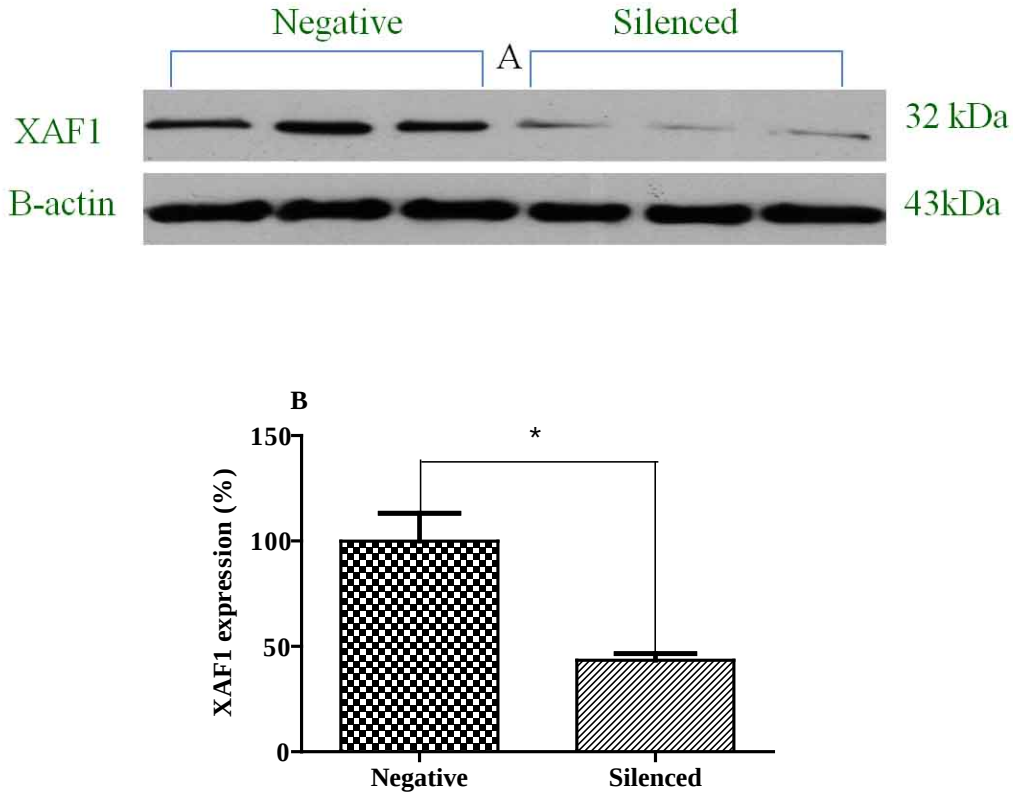

Figure 3.35.Western blotting (WB) analysis of XAF1 *protein expression hours after silencing XAF gene in MCF7 cell lines. Silencing XAF1 gene significantly reduced* XAF1 *protein expression in MCF7 (N=3) Negative control group was transfected with negative control shRNA. Data was shown as mean ± SE, * p <0.05, T test.*

3.29 Analysis of proliferation assays after silencing *XAF1* in MCF7

This assay was performed to evaluate of the effect of silencing of *XAF1* gene on MCF7 proliferation. Thus, a total number of 1X 10^4 of *XAF1*-silenced MCF7 and negative shRNA transfected cells were seeded in 96 well plate. Proliferation assay was performed at 72 hours after seeding MCF7cells, by using MTS method. The proliferation of *XAF1*-knoked down MCF7 was slightly increased by 10.6% compared to negative control

(Figure 3.36). The result of this assay could be indicative of an inhibitory role of *XAF1* on cellular proliferation or its effect on inducing of the apoptosis.

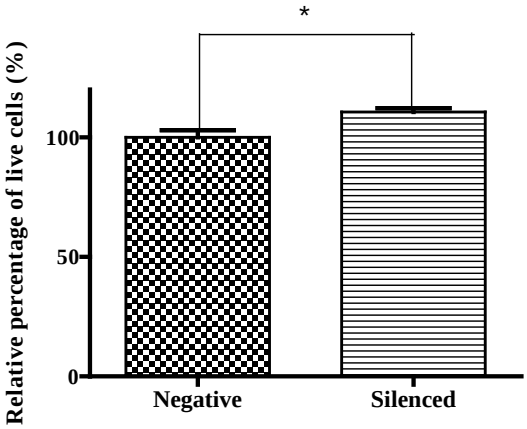

*Figure 3.36. Effect of silencing XAF1 on proliferation of MCF7. Negative control group was transfected with negative control shRNA. In the other group cells were silenced with XAF1 shRNA (N=5). Data was shown as mean ± SE, * p <0.05, T test.*

3.30 Analysis of proliferation assays after silencing *HS6ST3* in *XAF1*-knocked down MCF7

This assay was performed for evaluating the effect of silencing *HS6ST3* gene on the proliferation of *XAF1*-silenced MCF7. For this purpose, a total number of 2 X 10^5 of *XAF1*-silenced MCF7 and negative shRNA transfected cells were seeded in two 6-well plates separately. *HS6ST3* was silenced in both groups by using *HS6ST3* siRNA. Negative control groups were transfected with negative control siRNA. At 72 hours post-transfection, proliferation assay was performed by using MTS method. Analysis of the data showed that silencing *HS6ST3* in *XAF1*-silencved MCF7 severely reduced the relative percentage of the live cells by 78% (Figure 3.37: B), while silencing *HS6ST3* in negative control shRNA-transfected cells reduced the relative percentage of the live cells by 59% that was similar to the effect of silencing *HS6ST3* in non-transfected MCF7 cells

(Figure 3.37: A). The result of this experiment was contradictory to the results of previous observation; however, the reduction in the relative percentage of the live cells might be due to an unknown synergistic effect of double silencing of *XAF1* and *HS6ST3* in MCF7.

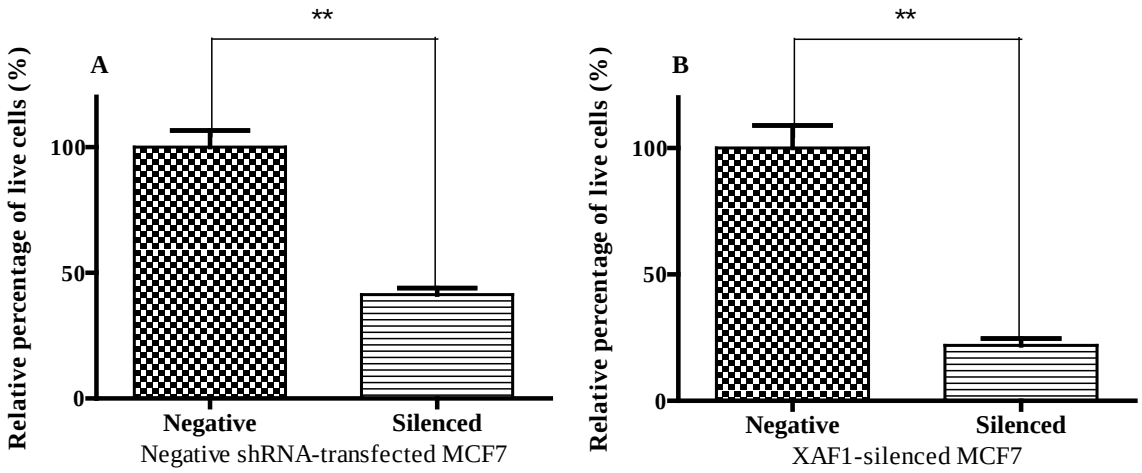

Figure 3.37. Effect of double silencing XAF1 and HS6ST3 on proliferation of MCF7 cells. ***A)*** *Negative shRNA-transfected MCF7 cells were transfected by negative control siRNA (Negative) or HS6ST3 siRNA (Silenced) (N=3).* ***B)*** *XAF1-silenced MCF7 cells were transfected by negative control siRNA (Negative) or HS6ST3 siRNA (Silenced) (N=3). Data was shown as mean ± SE, ** p <0.01, T test.*

3.31 Analysis of adhesion assays after silencing *HS6ST3* in *XAF1*-knocked down MCF7

Adhesion assay was performed to investigate the potential effect of *XAF1* for changing the adhesion capacity of tumor cells into extracellular matrix (ECM) in *HS6ST3*-knocked down MCF7. This assay was performed at 72 hours after silencing *HS6ST3* in *XAF1*-silenced MCF7 cells. In this experiment collagen I and fibronectin were used to coat the wells before seeding breast cancer cells. Analysis of the data revealed that double silencing *XAF1* and *HS6ST3* decreased the adhesion capacity of MCF7 to collagen I (A)

and fibronectin (B) and thus no significant differences were observed between control (single silenced for *XAF1*) and silenced (double silenced for *XAF1* and *HS6ST3*) group (Figure 3.38).

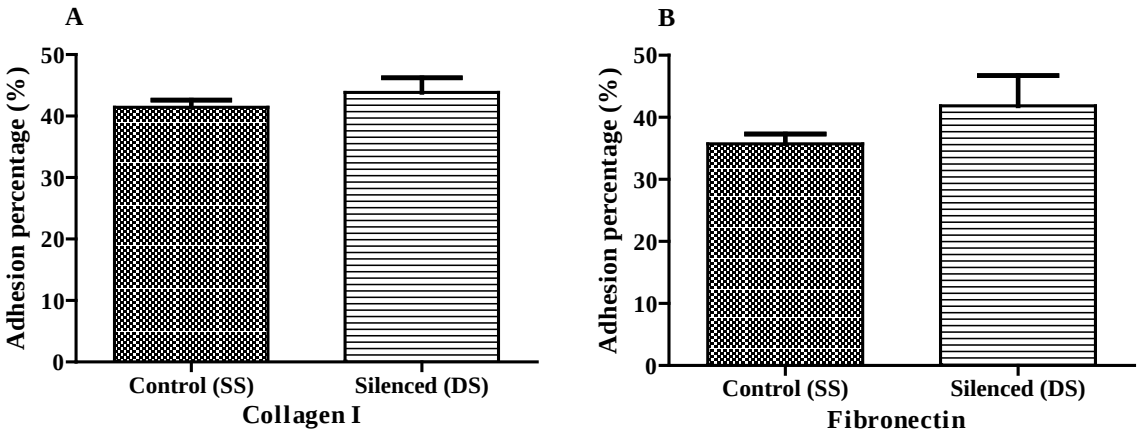

Figure 3.38. Effect of double silencing XAF1 and HS6ST3 on adhesion of MCF7. SS: Single silenced for XAF1, Negative controls were just silenced for XAF1. DS: Double silenced for XAF1 and HS6ST3. Each group of the control or silenced group was normalized to its corresponding un-washed *cells during the adhesion assay (N=6). Data was shown as mean ± SE, T test.*

3.32 Analysis of migration assays after silencing *HS6ST3* in *XAF1*-knocked down MCF7

Migration assay was performed for evaluating the effect of double silencing *XAF1* and *HS6ST3* on migration capacity of MCF7 cells compared to the cells silenced just for *HS6ST3* in negative shRNA-transfected MCF7. Thus, *XAF1*-silenced MCF7 and also negative control shRNA-transfected cells were silenced for *HS6ST3*. At 48 hours after silencing *HST6ST3*, the cells were re-seeded into migration chambers and allowed to migrate for 24 hours (discussed in previous chapter). As shown in figure 3.39, double

silencing *XAF1* and *HS6ST3* interestingly increased the migratory capacity of MCF7 cells by 188% compared to the similar capacity in *HS6ST3*-knocked down MCF7 (C).

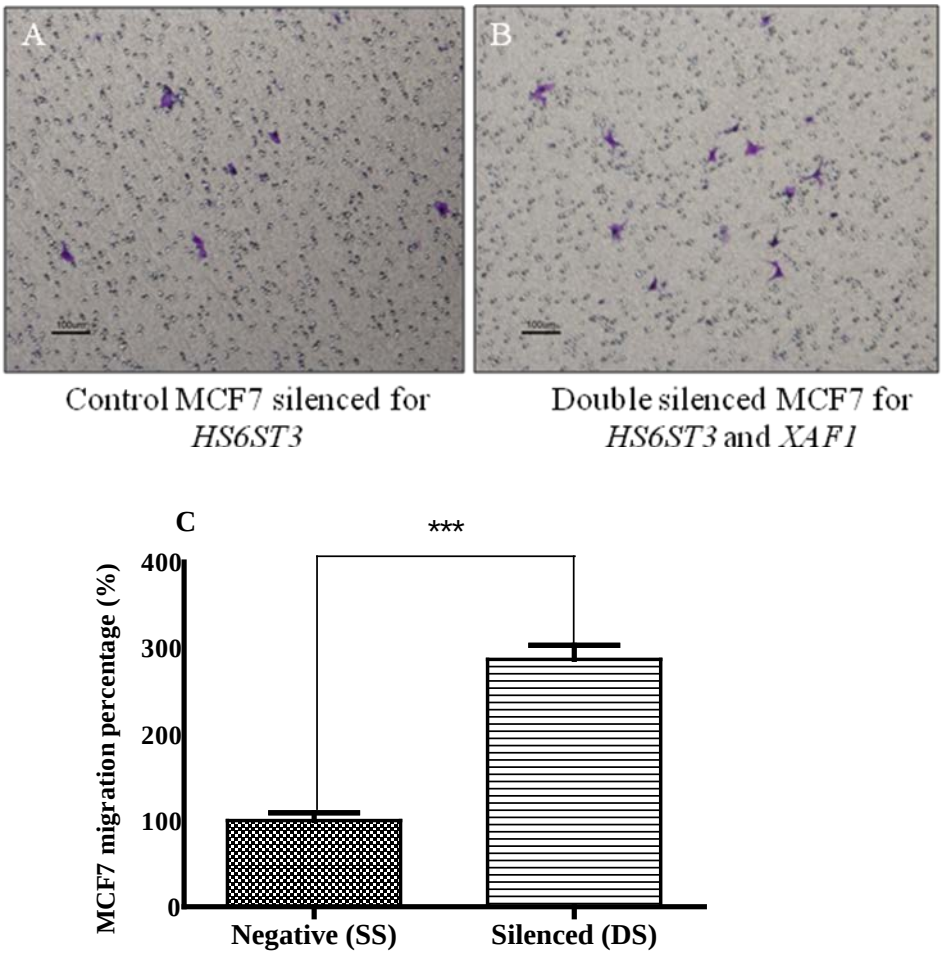

*Figure 3.39. Effect of double silencing XAF1 and HS6ST3 on migration of MCF7. SS: Single silenced for HS6ST3, DS: Double silenced for XAF1 and HS6ST3. Double silencing MCF7 cells considerably increased the migration of MCF7 cells through migration inserts (N=3). Data was shown as mean ± SE, *** p <0.001, T test.*

3.33 Analysis of invasion assays after silencing *HS6ST3* in *XAF1*-knocked down MCF7

Migration assay was performed to assess the effect of double silencing *XAF1* and *HS6ST3* on migration capacity of MCF7 cells compared to the cells silenced just for

HS6ST3 in negative shRNA-transfected MCF7. Thus, *XAF1*-silenced MCF7 and also negative control shRNA-transfected cells were silenced for *HS6ST3*. At 48 hours after silencing *HST6ST3*, the cells were re-seeded into invasion chambers and allowed to migrate for 24 hours (discussed in previous chapter). Similar to migration assay, silencing *XAF1* and *HS6ST3* significantly enhanced the cellular invasiveness by 90% compared to the cells only silenced for *HS6ST3* in MCF7 cells (Figure 3.40).

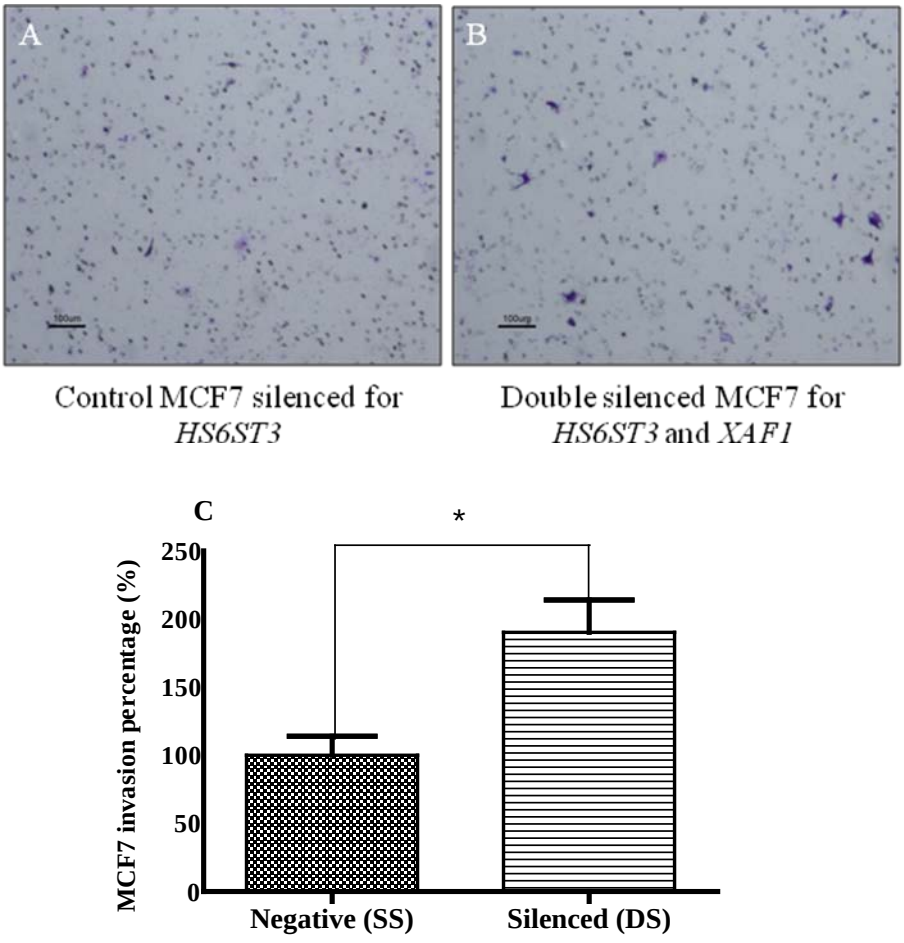

*Figure 3.40. Effect of double silencing XAF1 and HS6ST3 on invasiveness of MCF7. SS: Single silenced for HS6ST3, DS: Double silenced for XAF1 and HA6ST3. Double silencing XAF1 and HS6ST3 transformed the MCF7 nature to a highly invasive cells (N=3). Data was shown as mean ± SE, * p <0.05, T test.*

Section 3: Analysis of the effect of silencing *HS6ST3* on sensitivity of T47D breast cancer cell line to Cisplatin and 5-fluorouracil

3.34 Measurement of LD50 concentration of cisplatin and 5-Flurouracil (5-fu)

To find LD50, a total number of 7x 10^3 T47D cells were seeded in each well of 96 well plate. 24 hours after seeding, the cells were treated with 0, 5, 10, 15, 20, 25, 30, 35 µg/ml of Cisplatin and 0, 2.5,20,40,60, 80, 100 µg/ml of 5-flurouracil (5-fu). Later, the cells were inculcated in 5% CO_2, 37ºC for 48 hours. Then, relative percentage of live cells was measured by using MTS method. The absorbances measured in MTS assay were then normalized with blank and then the cytotoxic effects of Cisplatin and 5-fu was measured in Microsoft excel and finally dose-response curves were plotted by non-linear regression method in GraphPad Prism 5.00 software to find the LD50. Non-linear model is generally used for the response of specific drugs such as antimetabolites which influence the cell cycle phases and finally lead to a plateau for their cytotoxicity effect that means the greater doses does not result in more cell death. Using non-linear regression analysis, we found high coefficients of correlation that showed strong negative relationships between doses versus cell survival ($R^2 > 0.9$). LD50 of 28 ug/ml and 13 ug/ml were determined for 5-fu and Cisplatin respectively (Figure 3.41).

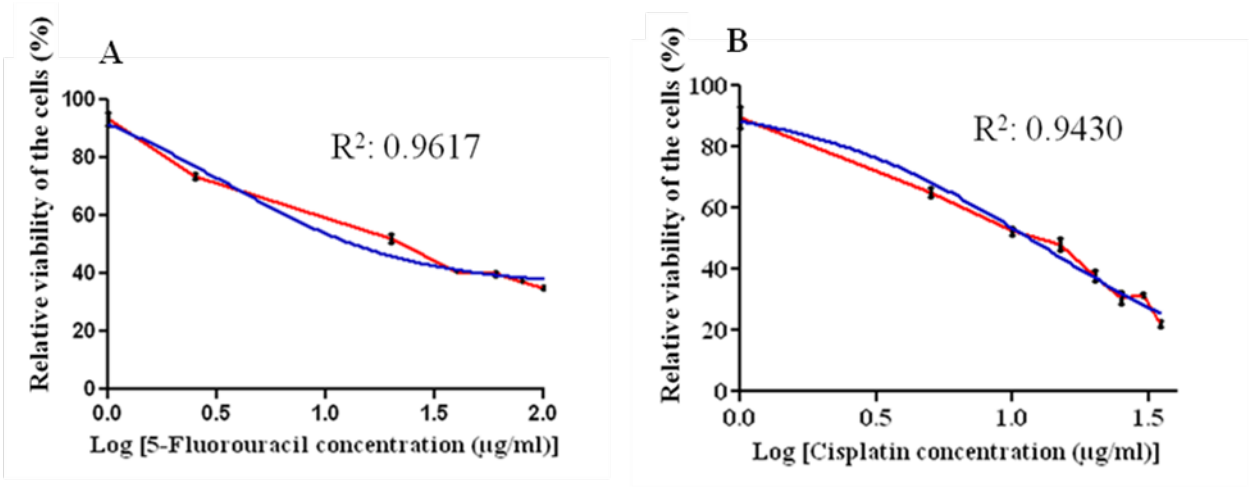

Figure 3.41.Logarithmic curves illustrating LD50 of 5-Flurouracil (A) and Cisplatin (B) in dose-response model by using non-linear regression method (N=6).

3.35 Analysis of Cisplatin and 5-fu cytotoxicity assay after silencing *HS6ST3* in T47D

T47D cells were silenced by two sequence of *HS6ST3* Ambion siRNA. At 12 hours post-transfection, a total number of 7x 10^3 of control and silenced T47D cells were seeded each in two rows inside 96 well plates. At 24 hours post-transfection, one row of the silenced and one row of control cells were treated with 13 µg/ml of Cisplatin (LD50 for Cisplatin) or 28 µg/ml of 5-fu (LD50 for 5-fu). The plates were incubated in 5% CO_2, 37ºC for 48 hours. After 72 hours post-transfection, relative percentage of the live cells was measured using MTS method. Cell cytotoxicity of Cisplatin and 5-fu was measurd by substracting of the relative percentage of the live cells in drug-treated cells from non drug-treated cells in each of the silenced or control groups. Analysis of the results showed that silencing *HS6ST3* in T47D sensitized the cancer cells to the cytotoxic effect of Cisplatin and 5-fu. Thus, *HS6ST3*-knocked down T47D cells were killed by 9.05-11.75% more than control after treating with 13 µg/ml of Cisplatin (Figure 3.42).

Similarly, *HS6ST3*-knocked down T47D cells were killed by 18.31-23.2% more than control after treating with 28 µg/ml of 5-fu (Figure 3.43).

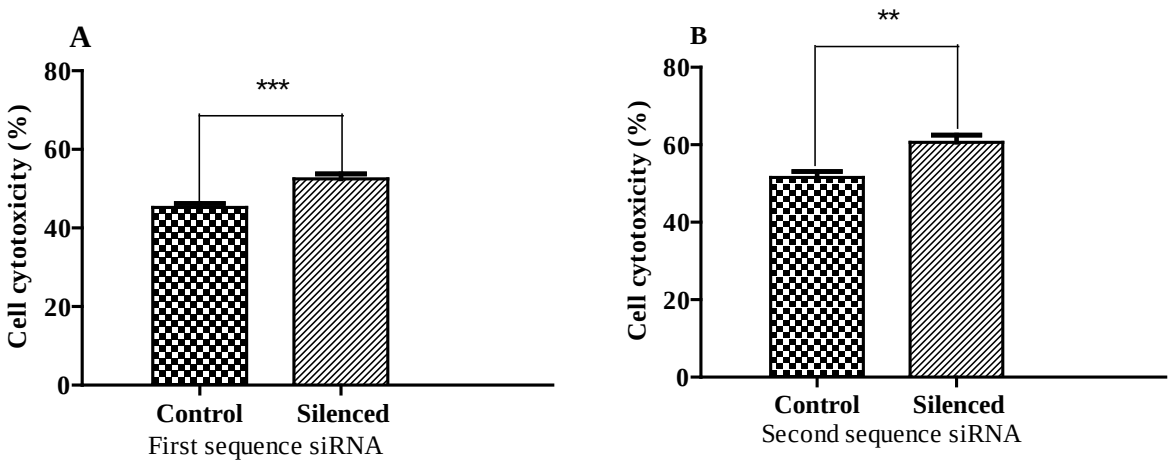

*Figure 3.42. The cytotoxic effect of Cisplatin after silencing HS6ST3 in T47D. The values of treated groups with Cisplatin were normalized with the values in non-treated control or silenced groups (N=9). Data was shown as mean ± SE ,**p<0.01, ***p<0.001, T test.*

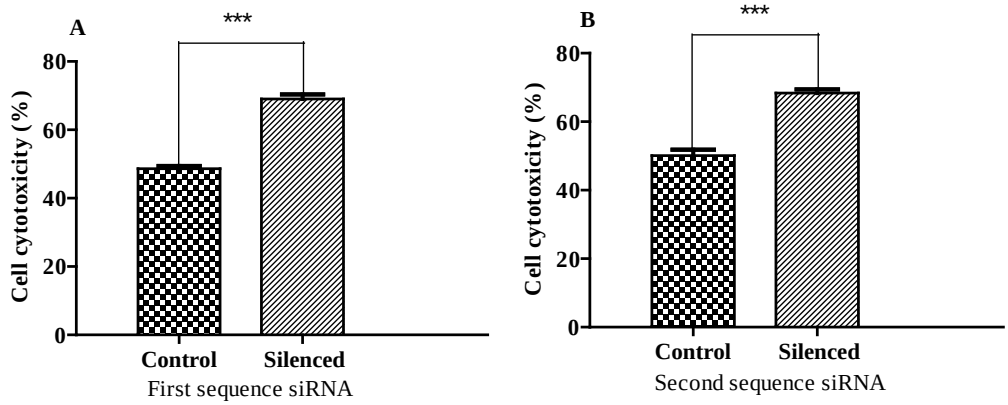

*Figure 3.43. The cytotoxic effect of 5-fu after silencing HS6ST3 in T47D. The values of treated groups with Cisplatin were normalized with the values in non-treated control or silenced groups (N=9). Data was shown as mean ± SE, ***p<0.001, T test.*

3.36 Analysis of Cisplatin and 5-fu cytotoxicity assay after silencing *HS6ST3* in MCF-12A

MCF12-A, normal epithelial cell line was silenced by two sequences of Ambion *HS6ST3* siRNA. At 10 hours post-transfection, a total number of 7x 10^3 of control and silenced MCF-12A cells were seeded each in two rows inside 96 well plates (N=9). At 24 hours post-transfection, one row of the silenced and one row of control cells were treated with 13 µg/ml of Cisplatin (LD50 for Cisplatin) or 28 µg/ml of 5-fu (LD50 for 5-fu). The plates were incubated in 5% CO_2, 37ºC for 48 hours. After 72 hours post-transfection, the relative percentage of the live cells was measured using MTS method. Unlike T47D, analysis of the results showed that silencing *HS6ST3* in MCF12-A did not statistically change the sensitivity of the cells to Cisplatin (Figure 3.44). It was also found that silencing *HS6ST3* in MCF-12A did not sensitized the normal epithelial cells to 5-fu (Figure 3.45).

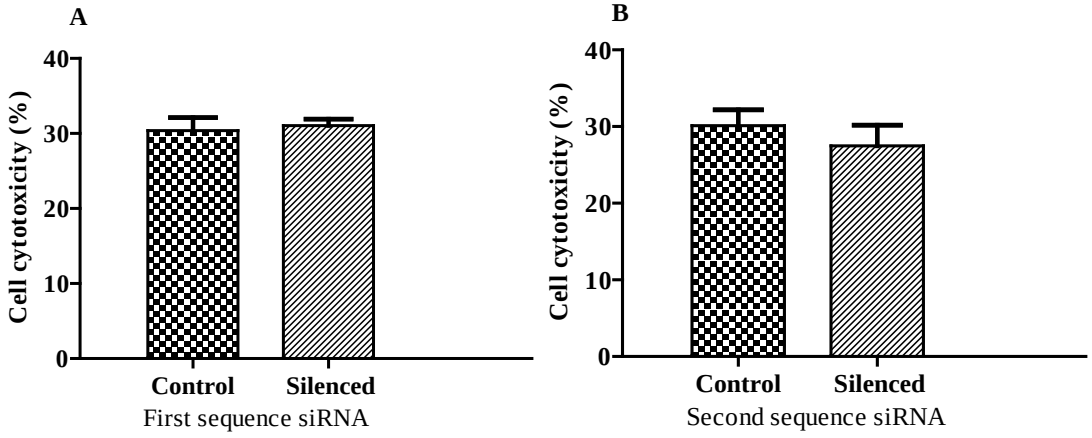

Figure 3.44. The cytotoxic effect of Cisplatin on HS6ST3-silenced MCF-12A. The values of treated groups with Cisplatin were normalized with the values in non-treated control or silenced groups (N=6). Data was shown as mean ± SE, T test.

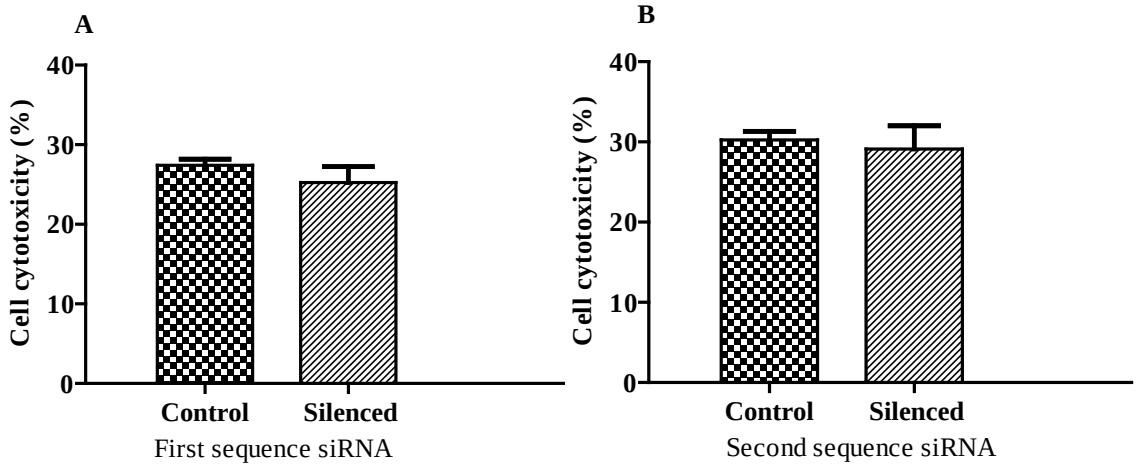

*Figure 3.45. The cytotoxic effect of 5-fu on HS6ST3-silenced MCF-12A. The values of treated groups with Cisplatin were normalized with the values in non-treated control or silenced groups (N=6). Silencing HS6ST3 in MCF-12A by first sequence siRNA made the cells more resistant to 5-fu by 13% compared to control. Data was shown as mean ± SE, **p<0.01, T test.*

3.37 p63/ p73-mediated cytotoxicity

Activation of BCL2 superfamily might be mediated by p63/ p73 network in response to cisplatin treatment .TAp63 promote the survival of the breast cancer cells, while TAp73 induce apoptosis by activating BCL2 superfamily (Carroll et al. 2006). However, TAp73 and TAp63 may co-express in the cancer cells and then bind to each other. Dissociation of these proteins is a determining factor that could regulate the relative percentage of the live cells (Leong et al. 2007). Imatinib is a drug that inhibits the dissociation of TAp63 from TAp73. In order to find if the sensitization of T47D cells to Cisplatin after silencing *HS6ST3* is mediated by p63/ p73 network, imatinib was used to inhibit the dissociation of TAp63 from TAp73.

3.38 Analysis of Imatinib cell cytotoxicity on T47D cell line

To remove the cytotoxic effect of Imatinib as a confounding factor, a maximum non-toxic dose of Imatinib was measured on T47D. For this purpose, a total number of 7x 10^3 T47D cells were seeded in each well of 96 well plate. 24 hours after seeding, the cells were treated with 0, 1, 2, 3, 4, 5, 6 µM of Imatinib. The cells were inculcated in 5% CO_2, 37ºC for 48 hours. Then, the relative percentage of the live cells was measured by using MTS method. The absorbances were normalized with blank and then the cytotoxic effects of Imatinib was measured in Microsoft excel to find the maximum ineffective dose of Imatinib on cell growth in T47D cell line. The result of this experiment showed that the maximum dose of 1 µM was non-toxic to the live cells (Figure 3.46). Thus, this dose was used for next cytotoxicity assay during treating *HS6ST3*- silenced T47D cells with Cisplatin and Imatinib.

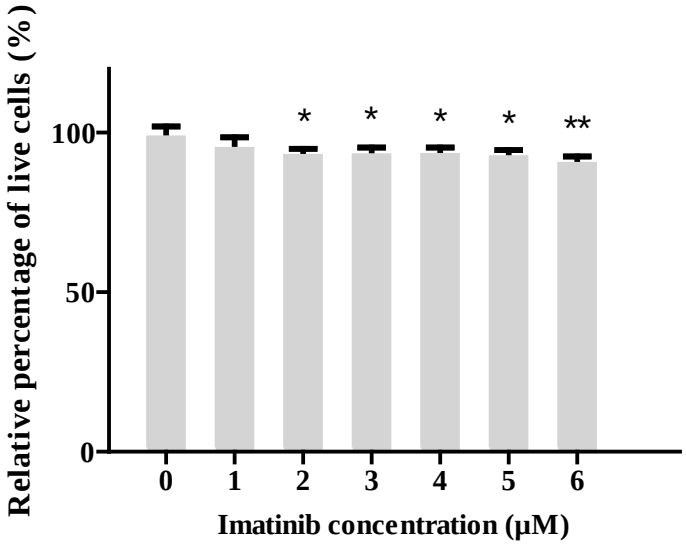

*Figure 3.46. The cytotoxic effect of Imatinib on T47D cell line. T47D cells were treated by serial concentration of Imatinib in 96-well plate. The absorbance values of treated cells were normalized with non-treated T47D cells (N=5). Data was shown as mean ± SE, *p<0.05, **p<0.01, T test.*

3.39 Analysis of Imatinib effect on cisplatin sensitivity pathway in *HS6ST3*-silenced T47D cells

T47D cells were silenced by two sequence of *HS6ST3* Ambion siRNA. At 12 hours post-transfection, a total number of 7x 10^3 of control and silenced T47D cells were seeded each in four rows inside 96 well plates. At 24 hours post-transfection, one row of the silenced and/ or control cells were treated with 13 µg/ml of Cisplatin. The second row was treated with 1mM Imatinib. The third row was treated with 13 µg/ml Imatinib and 1mM Imatinib. The final row was left un-treated. The plates were incubated in 5% CO_2, 37ºC for 48 hours. After 72 hours post-transfection, cell relative percentage of the live cells was measured using MTS method. Analysis of this assay showed that Imatinib reduced the cytotoxic effect of Cisplatin on non-silenced T47D by 11-17% (Figure 3.47: A, C), while Imatinib had no significant effect on the cytotoxicity of Cisplatin in *HS6ST3*-silenced T47D (Figure 3.47: B, D). These observations were indicative of the influence of down regulation of *HS6ST3* on the Imatinib pathway. On the other hand, reviwing our microarray data revealed that Tap73 was significantly up-regulated by 58% ($p<0.01$) after silencing *HS6ST3* in breast cancer, while no significant change occoured in the expression of Tap63. Thus, it could be postulated that silencing *HS6ST3* could sensitize the breast cancer cells to the cytotoxic effect of Cisplatin in a TAP73-dependent manner.

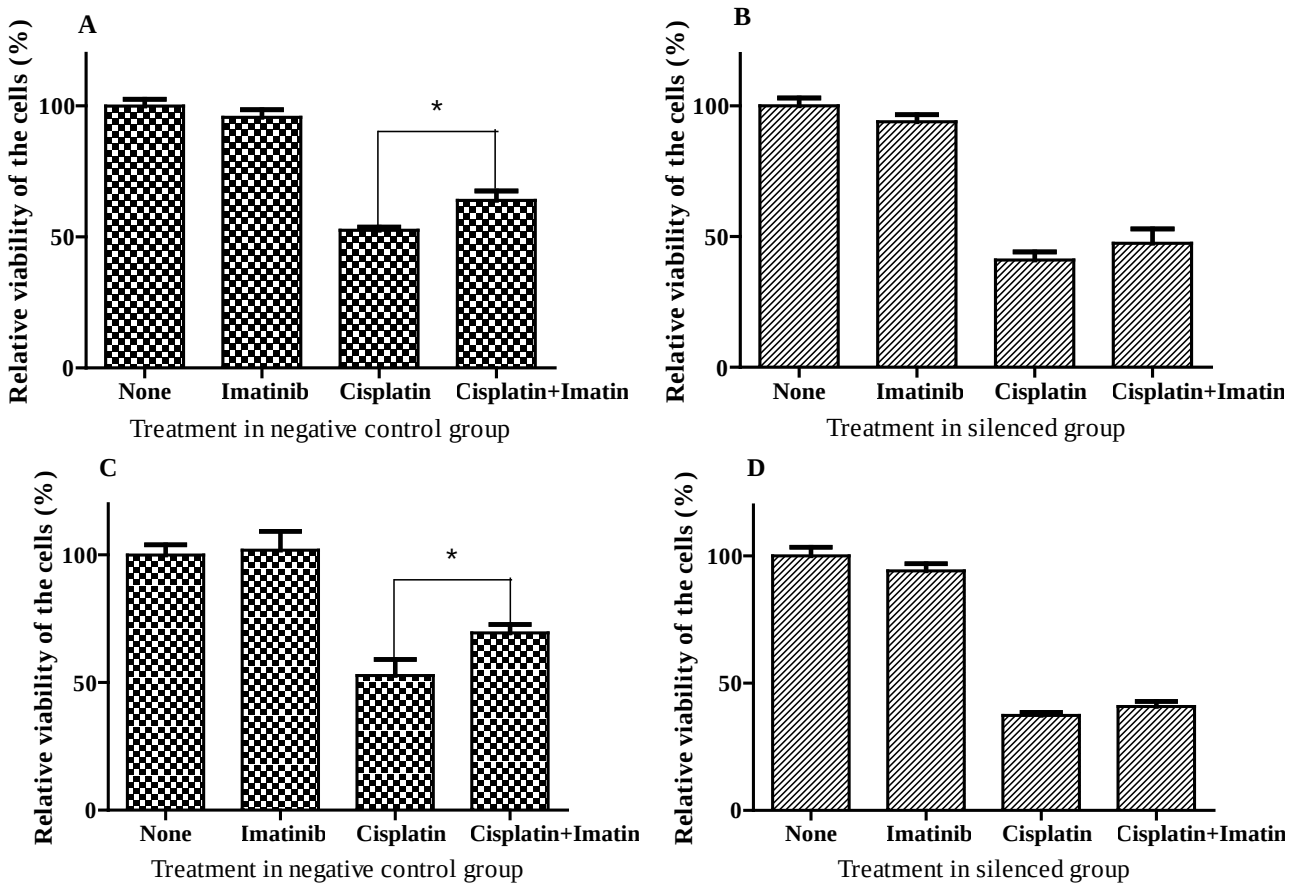

*Figure 3.47. The cytotoxic effect of Cisplatin and Imatinib on HS6ST3-silenced T47D. Two sequences of siRNA were used to silence HS6ST3 in T47D. Figure A, C) T47D was transfected with negative control siRNA. Figure B) T47D was silenced using first sequence of siRNA. Figure D) T47D was silenced using second sequence of siRNA. The absorbance values of treated cells were normalized with non-treated T47D cells (N=5). Data was shown as mean ± SE, *p<0.05, T test.*

Section 4: Immunohistochemical analysis of human HS6ST3 expression in human clinical breast cancer sections of ductal carcinoma

3.40 Clinicopathological features of breast cancer sections

In this cohort study, immunohistostaining was performed on a total of 258 paraffin embedded tissue microarray cases (TMA) of archival blocks of diagnosed cases of breast adenocarcinoma which were collected in the Department of Pathology of Singapore

General Hospital, between 1998 and 2004. In addition to the study population, 43 sections were collected from non cancerous (normal) breast biopsies. Clinicopathological features of cases including race, age, tumor side, tumor size, histotype, histograde, lymph node status, associated ductal carcinoma in situ (DCIS) nuclear grade, associated DCIS nuclear grade extent as well as immunohistochemical markers such as estrogen receptor, progesterone receptor and HER2 were collected. Other information such as diagnosis date, recurrence date and also date of death were retrieved from patient's records. The study follow up was set up from January 1998 to the end of June 2009. This study was ethically approved by Institutional Review Board, Singapore General hospital.

In this study, most of the breast cancer specimens were from Chinese. In addition, majority of the cancer sections were diagnosed as ductal adenocarcinoma. The age of the breast cancer patients ranged from 23 to 88, with a mean age of 57.52. Tumor size was distributed from 1mm to 140mm among cases with median of 30mm. Details of clinicopathological features of all cases are summarized in Table 3.6. It must be mentioned that nearly all of the specimens were collected prior to any therapy. Thus, the expression of HS6ST3 enzyme was not affected by any available treatments.

Table 3.6. Clinicopathological features of 258 cases of breast cancer. Data represented the number and percentage of cases.

Clinicopathological features			**Clinicopathological features**		
	n	%		n	%
Age			**Involved Lymph nodes (LN)**		
≤ Mean age (57.5)	147	57	LN = 0	118	45.7
> Mean age (57.5)	111	43.0	≥1 LN 4 <	64	24.8
Race			≥ 4	61	23.6
Chinese	214	82.9	Unavailable	15	5.8
Malay	21	8.1	**Associated nuclear grade of DCIS**		
Indians	7	2.7	None	110	42.6
Others	16	6.2	Low	9	3.5
Laterality			Intermediate	56	21.7
Right	121	46.9	High	81	31.4
Left	137	53.1	Unavailable	2	.8
Unavailable	0	0	**DCIS nuclear grade extent**		
Tumor size (TS)			None	28	10.9
TS ≤ 20	64	24.8	Minimal	61	23.6
> 20	186	72.1	Extensive	25	9.7
Unavailable	8	3.1	Unavailable	144	55.8
Histotype			**ER expression**		
IDC	231	89.5	Negative	96	37.2
Non-IDC	6	2.3	Positive	158	61.2
Unavailable	21	8.1	Unavailable	4	1.6
Histograde			**PR expression**		
1	23	8.9	Negative	116	45.0
2	97	37.6	Positive	138	53.5
3	129	50.0	Unavailable	4	1.6
Unavailable	9	3.5	**HER2 expression**		
			Negative	169	65.5
			Positive	81	31.4
			Unavailable	8	3.1

3.41 Expression of HS6ST3 in normal and cancerous human breast tissue

In benign human breast tissues, HS6ST3 expresses itself both in the cytoplasm of epithelial cells as well as extracellular compartments including stroma matrix and stromal cells (Figure 3.49: A). In invasive ductal adenocarcinoma, HS6ST3 seemed to be differentially expressed in epithelial and stromal components of human ductal adenocarcinoma (Figure 3.48). Although HS6ST3 basically expressed in cytoplasm of epithelial cells, the cytoplasmic expression of HS6ST3 positively correlates with its stromal existence ($p < 0.01$).

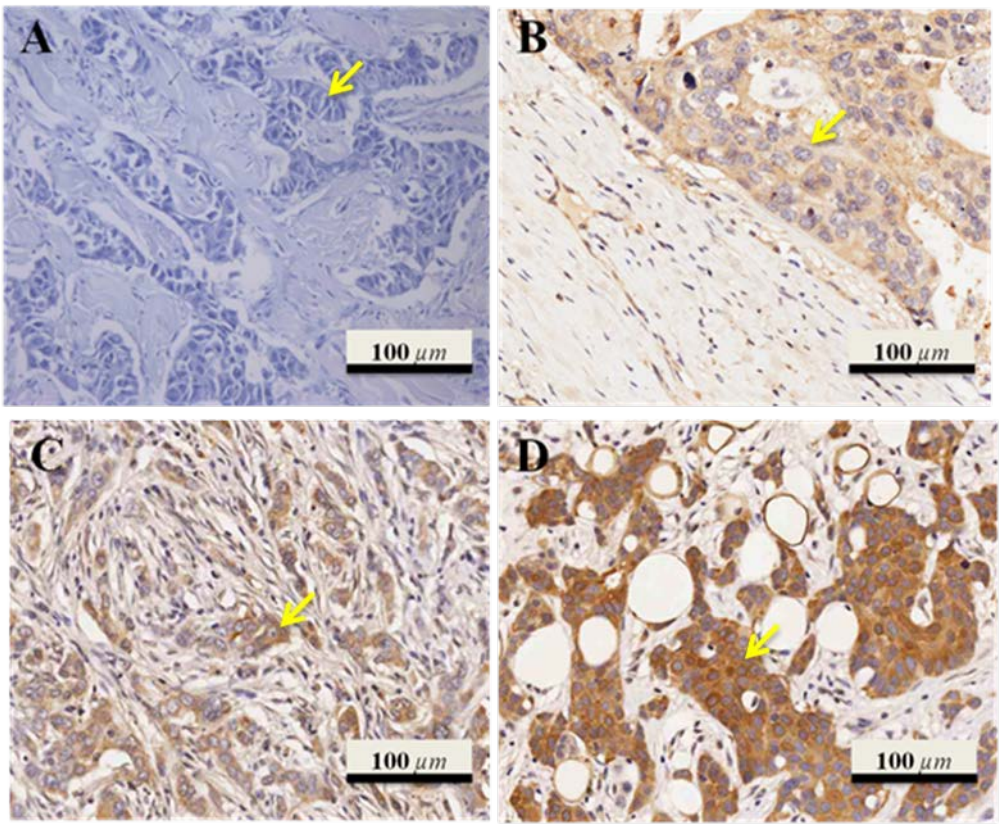

Figure 3.48. Immunohistochemical staining of HS6ST3 in tissue microarray sections of breast cancer. (A) 0 or negative epithelial staining (B) +1 or weak staining (C) +2 or moderate staining (D) +3 or strong staining.

3.42 Immunohistochemical expression of HS6ST3 in epithelial and stromal components of breast ductal adenocarcinoma

HS6ST3 expresses itself both in the cytoplasm of epithelial cells as well as extracellular compartments including stroma matrix and stromal cells of normal and breast cancer cells. Analysis revealed that the mean staining intensity of stroma matrix of normal tissues (42.209 ± 3.290) were discriminatively higher than cancer sections (15.969 ± 1.338) (Figure 3.49); however, no significant difference was found for the similar comparison in epithelial and stromal cell components (Table 3.7).

Table 3.7. Immunoreactivity scoring (IRS) among all tissue sections, T test.

IRS		Tissue type	Mean	Std. Error	95% Confidence Interval		P value
					Lower Bound	Upper Bound	
Tissue component	Epithelial cells	Normal	44.651	5.602	33.627	55.675	0.853
		Cancer	45.775	2.287	41.275	50.276	
	Stroma matrix	Normal	42.209	3.290	35.735	48.683	**0.000***
		Cancer	15.969	1.338	13.336	18.602	
	Stromal cells	Normal	42.791	4.275	34.379	51.203	0.433
		Cancer	46.415	1.745	42.981	49.849	

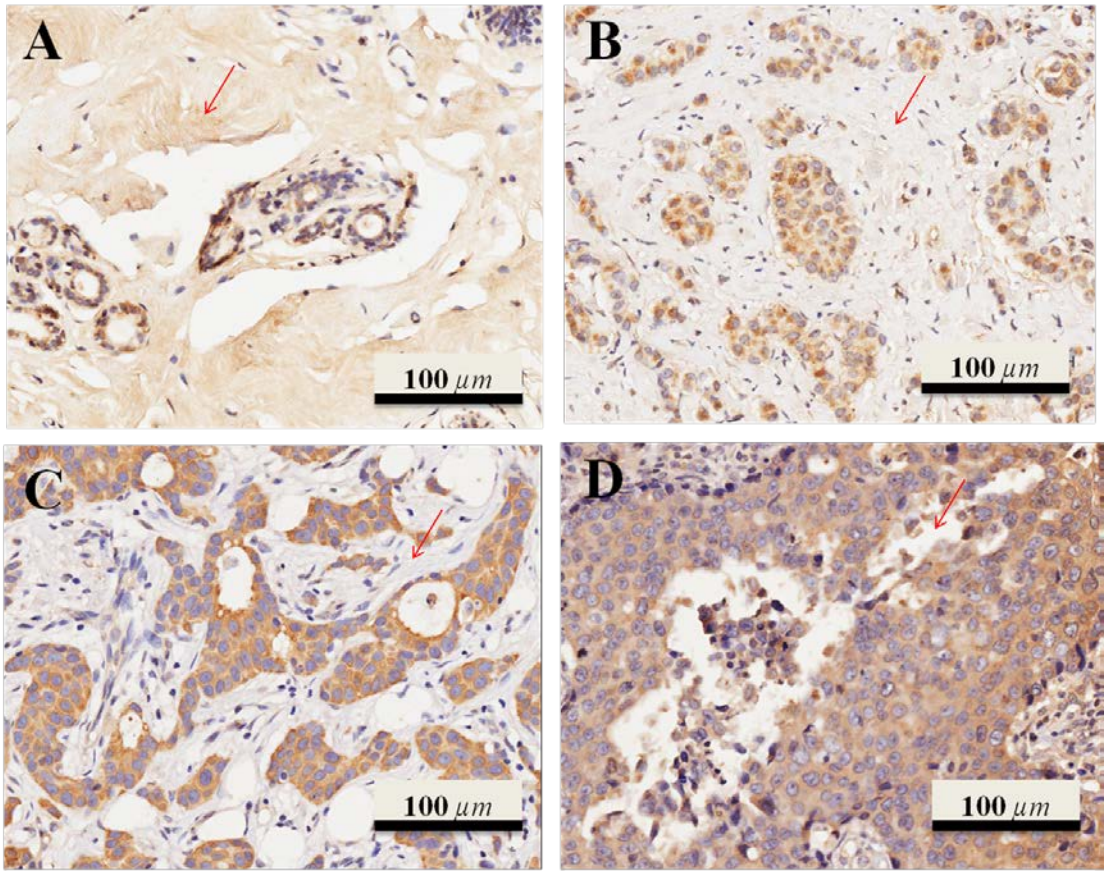

Figure 3.49. A) Normal breast tissue. B) IDC grade I C) IDC grade II D) IDC grade III. Arrows indicating the expression of HS6ST3 which was significantly reduced in stroma matrix of cancer sections compared to normal breast tissues.

3.43 Association analysis of HS6ST3 immunoreactivity with clinicopathological parameters

The staining intensity of different tissue compartments were compared with clinicopathological features. Data shown in Table 3.8, 3.9, and 3.10 represented associations between the expression of HS6ST3 and clinicopathological parameters of breast cancer patients such as age, tumor size, histograde, histotype, lymph node status, estrogen receptor and progesterone receptor. The results suggested that patients whose ages were above the mean of age expressed more HS6ST3 in their epithelial cell and stromal cells, while no associations were found in stroma matrix. In addition, tumors smaller than 20mm showed to have higher staining intensities in their stroma matrix. Furthermore, histograde 2 had a significantly higher staining intensity compared to histograde 1 and 3 in stroma matrix (Table 3.8). Invasive ductal carcinoma (IDC) exhibited more HS6ST3 in their stromal cells compared to DCIS. Tumor which metastasized to more than three lymph nodes had also a higher staining intensity in their stroma matrix. Interestingly, HS6ST3 expressed more in stroma matrix compartments of breast cancer specimens which were positive for estrogen and progesterone receptors. There was no significant association between the expression of HS6ST3 and tumor side, nuclear grade and HER2 in tissue compartments.

Table 3.8. Correlations between expression of HS6ST3 using IRS cut off 25 and clinicopathological features of breast cancer, Fisher's exact test.

Clinicopathological parameter		IRS Epithelial cells		P value	IRS Stroma matrix		P value	IRS Stromal cell		P value
		≤25	**>25**		**≤25**	**>25**		**≤25**	**>25**	
Age	**≤ mean (57.5)**	66	81	0.373	119	28	0.535	46	101	**0.031***
	> mean (57.5)	43	68		86	25		21	90	
Race	**Chinese**	89	125	0.738	170	44	1	55	159	0.851
	Others	20	24		35	9		12	32	
Laterality	**Right**	47	74	0.315	96	25	1	28	93	0.394
	Left	62	75		109	28		39	98	
Tumor size	**≤ 20mm**	22	42	0.188	44	20	**0.013***	18	46	0.741
	> 20mm	82	104		155	31		47	139	
Histograde	**Grade 1**	12	11	0.636	20	3	**0.035***	4	19	0.173
	Grade 2	40	57		70	27		21	76	
	Grade 3	56	73		110	19		40	89	
Histotype	**IDC**	99	132	0.405	185	46	0.351	59	172	0.186
	DCIS	1	5		4	2		3	3	
Lymph node involvement	**≤ 3 nodes**	78	104	0.549	147	35	0.277	52	130	0.129
	> 3 nodes	23	38		45	16		11	50	
Associated nuclear grade of DCIS	**None**	47	63	0.477	86	24	0.498	23	87	0.349
	Low	6	3		8	1		2	7	
	Intermediate	23	33		48	8		16	40	
	High	32	49		62	19		26	55	
DCIS nuclear grade extent	**None**	11	17	0.318	23	5	0.354	7	21	0.846
	Minimal	25	36		52	9		18	43	
	Extensive	6	19		18	7		8	17	
Estrogen receptor	**Negative**	39	57	0.602	83	13	**0.026***	25	71	1
	Positive	70	88		118	40		40	118	
Progesterone receptor	**Negative**	53	63	0.446	98	18	0.063	31	85	0.773
	Positive	56	82		103	35		34	104	
HER2	**Negative**	72	97	1	129	40	0.134	40	129	0.354
	Positive	34	47		69	12		24	57	

Table 3.9. Correlations between expression of HS6ST3 using IRS cut off 45 and clinicopathological features of breast cancer, Fisher's exact test.

Clinicopathological parameter		IRS Epithelial cells		P value	IRS Stroma matrix		P value	IRS Stromal cell		P value
		≤45	**>45**		**≤45**	**>45**		**≤45**	**>45**	
Age	**≤ mean (57.5)**	89	58	**0.023***	137	10	0.37	82	65	**0.024***
	> mean (57.5)	51	60		100	11		46	65	
Race	**Chinese**	115	99	0.742	197	17	0.765	106	108	1
	Others	25	19		40	4		22	22	
Laterality	**Right**	68	53	0.617	113	8	0.496	58	63	0.62
	Left	72	65		124	13		70	67	
Tumor size	**≤ 20mm**	32	32	0.471	56	8	0.193	36	28	0.196
	> 20mm	103	83		173	13		87	99	
Histograde	**Grade 1**	14	9	0.769	22	1	0.425	7	16	0.143
	Grade 2	52	45		87	10		47	50	
	Grade 3	68	61		121	8		68	61	
Histotype	**IDC**	122	109	0.687	212	19	1	112	119	**0.014***
	DCIS	4	2		6	0		6	0	
Lymph node involvement	**≤ 3 nodes**	98	84	1	172	10	**0.028***	95	87	0.141
	> 3 nodes	33	28		52	9		25	36	
Associated nuclear grade of DCIS	**None**	61	49	0.417	100	10	0.331	51	59	0.549
	Low	7	2		9	0		6	3	
	Intermediate	30	26		54	2		26	30	
	High	40	41		72	9		43	38	
DCIS nuclear grade extent	**None**	11	17	0.281	26	2	0.076	14	14	0.681
	Minimal	32	29		58	3		36	25	
	Extensive	9	16		20	5		13	12	
Estrogen receptor	**Negative**	45	51	0.053	91	5	0.24	51	45	0.438
	Positive	94	64		142	16		75	83	
Progesterone receptor	**Negative**	63	53	1	111	5	**0.041***	60	56	0.311
	Positive	76	62		122	16		66	72	
HER2	**Negative**	92	77	1	153	16	0.47	84	85	1
	Positive	44	37		76	5		40	41	

Table 3.10. Correlations between expression of HS6ST3 using WAI cut off 1 and clinicopathological features of breast cancer, Fisher's exact test.

Clinicopathological parameter		WAI Epithelial cells		P value	WAI Stroma matrix		P value	WAI Stromal cell		P value
		≤1	>1		≤1	>1		≤1	>1	
Age	≤mean (57.5)	8	139	0.229	146	1	0.318	174	0	0.184
	> mean (57.5)	11	100		108	3		109	2	
Race	Chinese	18	196	0.213	210	4	1	212	2	1
	Others	1	43		44	0		44	0	
Laterality	Right	6	115	0.232	120	1	0.625	120	1	1
	Left	13	124		134	3		136	1	
Tumor size	≤ 20mm	3	61	0.575	63	1	1	64	0	0.405
	> 20mm	15	171		183	3		184	2	
Histograde	Grade 1	4	19		23	0		23	0	
	Grade 2	2	95	**0.016***	95	2	0.777	96	1	0.882
	Grade 3	12	117		127	2		128	1	
Histotype	IDC	16	215	0.363	227	4	1	229	2	1
	DCIS	1	5		6	0		6	0	
Lymph node involvement	≤ 3 nodes	12	170	1	181	1	0.156	181	1	0.44
	> 3 nodes	4	57		59	2		60	1	
Associated nuclear grade of DCIS	None	9	101	0.242	109	1	0.29	110	0	0.226
	Low	2	7		9	0		9	0	
	Intermediate	3	53		56	0		56	0	
	High	4	77		78	3		79	2	
DCIS nuclear grade extent	None	3	25	0.796	28	0	0.149	28	0	0.413
	Minimal	4	57		60	1		59	2	
	Extensive	2	23		23	2		25	0	
Estrogen receptor	Negative	10	86	0.218	94	2	0.634	.J12.	1	0.378
	Positive	9	149		156	2		158	0	
Progestrone receptor	Negative	12	104	0.151	113	3	0.334	115	1	0.457
	Positive	7	131		137	1		138	0	
HER2	Negative	12	157	1	167	2	0.597	169	0	0.324
	Positive	5	76		79	2		80	1	

3.44 Survival analysis of HS6ST3 expression in breast ductal carcinoma

Kaplan-Meier survival analysis was primarily performed in all of the possible strata of the histopathological parameters. Then, Univariate Cox regression proportional analysis was performed on strata which were detected as a significant factor ($p< 0.05$) for predicting the prognosis by Kaplan-Meier survival analysis. Disease free survival (DFS) and overall survival (OS) were defined as the length of time from date of diagnosis to recurrence or death respectively. The length of time between the dates of recurrence to death was also defined as survival after recurrence (SAR). Univariate Cox regression proportional analysis showed that staining intensity of tissue compartments is predictive of OS, DFS and SAR. The prognostic factors associated with the expression of HS6ST3 are summarized in Table 3.11. The survival analysis revealed that age, tumor size, histograde, progesterone and HER2 are predictive of the breast cancer prognosis. Thus, the OS of breast cancer cases whose ages were younger than 57.5 were significantly higher than those who developed breast cancer after 57.5. In addition, bigger tumors (> 34.1mm) were associated with poorer OS, DFS and SAR. As expected, higher histograde was associated with worse DFS, while lymph node metastasis could not significantly predict the prognosis. Unlike lymph node status, histograde was able to predict DFS; however, none of them was predictive of OS, while HS6ST3 expression was interestingly predictive of OS, DFS and SAR. In the other words, higher expression of HS6ST3 in stroma matrix of breast cancer predicted a worse prognosis for OS and DFS. Similarly, higher HS6ST3 expression in stroma matrix of breast cancer patients with tumor size bigger than 20mm or involvement of more than 3 lymph nodes or progesterone negativity was predictive of a shorter DFS. In contrast, higher expression of HS6ST3 of the stromal

cells predicted a longer survival for patients with less than 4 lymph node involvement or intermediate nuclear grade. Furthermore, higher expression of HS6ST3 in stromal cells of breast cancers in histograde 1 and histograde 2 predicted a better outcome in terms of their DFS, while it was predictive of worse SAR in breast cancer cases with positive HER2. The trends of survivals are shown in Figure 3.50 using Kaplan-Meier survival analysis.

Using a multivariate survival analysis interestingly revealed that the IRS and WAI of stroma matrix could independently be predictive of OS and DFS. In addition, it was shown that IRS of stromal cell compartment could independently predict the DFS of the breast cancer patients; however, none of the IRS or WAI was found predictive of SAR (Table 3.12).

Table 3.11. Univariate Cox regression analysis for prognostic clinicopathological factors in breast cancer.

	Overall survival			Disease-free survival			Survival after recurrence		
	HR	**95% CI**	**p Value**	**HR**	**95% CI**	**p Value**	**HR**	**95% CI**	**p Value**
Age ≤Mean (57.5) vs > Mean (57.5)	1.949	1.071-3.547	**0.029***	1.406	0.876-2.255	0.158	1.798	0.990-3.266	0.054
Tumor size (Mean) ≤ 34.1mm vs > 34.1mm	2.746	1.450-5.200	**0.002***	2.039	1.261-3.298	**0.004***	2.185	1.152-4.146	**0.017***
Histograde	1.654	0.989-2.767	0.055	1.577	1.068-20328	**0.022***	1.242	0.744-2.072	0.408
Lymph node status (metastasis) ≤ 3 nodes vs >3 nodes	1.199	0.832-1.727	0.33	1.212	0.908-1.617	0.192	1.069	0.737-1.551	0.724
Estrogen receptor Neg vs Pos	1.134	0.588-2.185	0.708	0.883	0.536-1.455	0.625	1.488	0.772-2.869	0.235
Progesterone receptor Neg vs Pos	0.529	0.283-0.989	**0.046***	0.584	0.360-0.945	**0.029***	0.643	0.341-1.210	0.171
HER2 Neg vs Pos	0.387	0.171-0.875	**0.022***	0.844	0.496-1.435	0.53	0.323	0.142-0.738	**0.007***
WAI stroma matrix ≤1 vs >1	4.593	1.101-19.129	**0.036***	4.626	1.443-14.826	**0.010***	2.01	0.428-8.377	0.338
IRS stroma matrix in ≤ 3 lymph nodes involvement ≤25 vs >25	0.163	0.022-1.207	0.076	0.282	0.087-0.913	**0.035***	0.207	0.028-1.534	0.123
IRS stromal cell in intermediate nuclear grade ≤25 vs >25	0.29	0.040-2.132	0.224	0.213	0.059-0.768	**0.018***	0.789	0.072-8.7.6	0.847
IRS stroma matrix in tumor size > 20mm ≤45 vs >45	2.077	0.805-5.354	0.13	2.723	1.334-5.557	**0.006***	1.065	0.403-2.814	0.900
IRS stroma matrix in ≥ 4 lymph nodes involvement ≤45 vs >45	2.145	0.682-6.743	0.192	3.357	1.356-8.309	**0.009***	0.942	0.279-3.184	0.924
IRS stroma matrix in PR negative ≤45 vs >45	2.439	0.570-10.441	0.23	3.89	1.358-11.144	**0.011***	1.094	0.254-4.714	0.905
IRS stromal cells in histograde 1, 2 ≤45 vs >45	0.412	0.149-1.135	0.086	0.448	0.208-0.967	**0.041***	0.513	0.186-1.415	0.197
IRS stromal cells in HER2 positive ≤45 vs >45	4.915	0.590-40.931	0.141	0.925	0.374-2.291	0.868	8.749	1.032-74.183	**0.047***

Table 3.12. Multivariate Cox regression analysis for prognostic clinicopathological factors in breast cancer using backward stepwise model.

Predictor		HR	95% CI	p Value
Overall survival (OS)				
Tumor size_34.1 (mean)		2.892	1.509-5.545	**0.001***
PR		0.509	0.267-0.971	**0.040***
HER2		0.293	0.128-0.671	**0.003***
WAI stroma matrix	≤ 1 vs > 1	5.882	1.349-25.654	**0.018***
Disease free survival (DFS)				
Tumor size_34.1mean		1.743	1.060-2.866	**0.028***
Progesterone receptor (PR)		0.619	0.375-1.022	**0.060***
WAI stroma matrix	≤ 1 vs > 1	5.054	1.556-16.417	**0.007***
IRS stroma matrix in ≤ 3 lymph nodes involvement	≤ 25 vs > 25	0.306	0.094-0.995	**0.049***
IRS stromal cells in intermediate nuclear grade	≤ 25 vs > 25	0.214	0.060-0.764	**0.017***
Histograde		1.640	1.015-2.649	**0.043***
IRS stroma matrix in tumor size > 20mm	≤ 45 vs > 45	2.648	1.189-5.894	**0.017***
IRS stroma matrix in PR negative	≤ 45 vs > 45	3.909	1.359-11.247	**0.011***
IRS stromal cells in histograde 1, 2	≤ 45 vs > 45	0.443	0.203-0.966	**0.040***
Survival after recurrence (SAR)				
Tumor size_ mean (34.1)		107800.291	0.000-8.00E150	0.946
IRS stromal cells in HER2 positive	≤45 vs >45	6.276	0.742-53.104	0.092

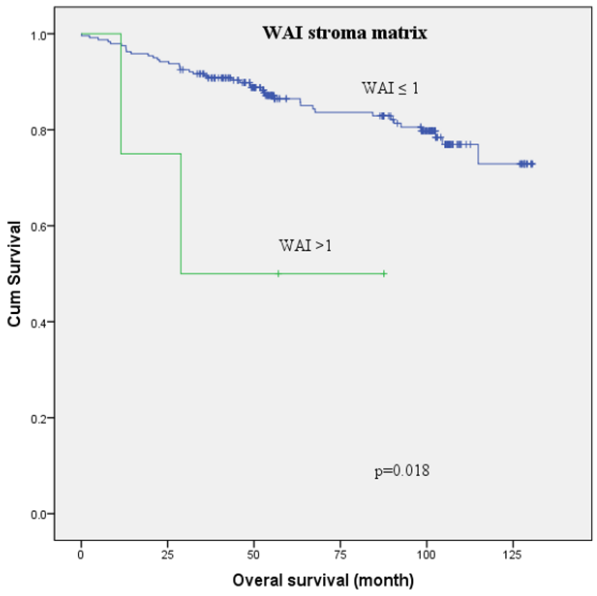

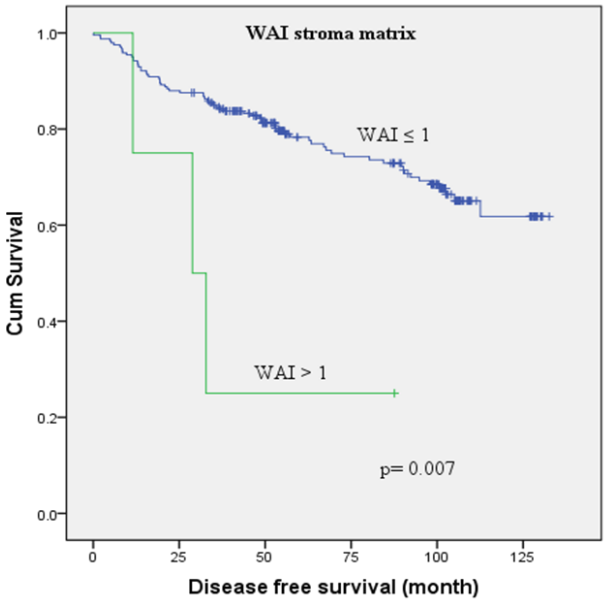

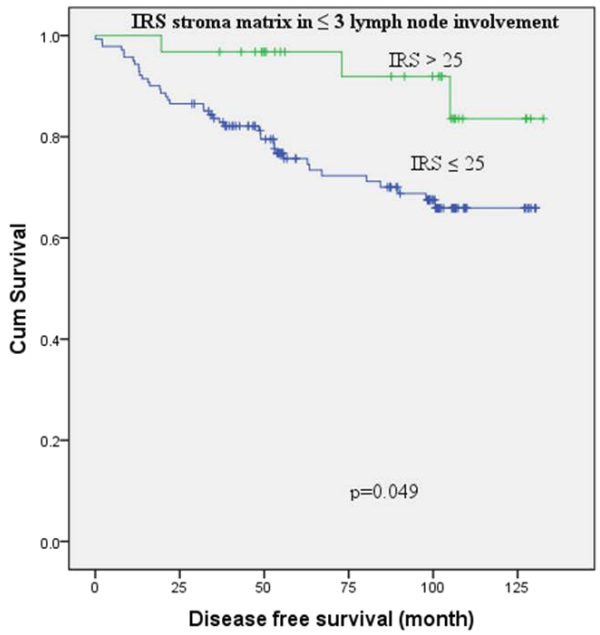

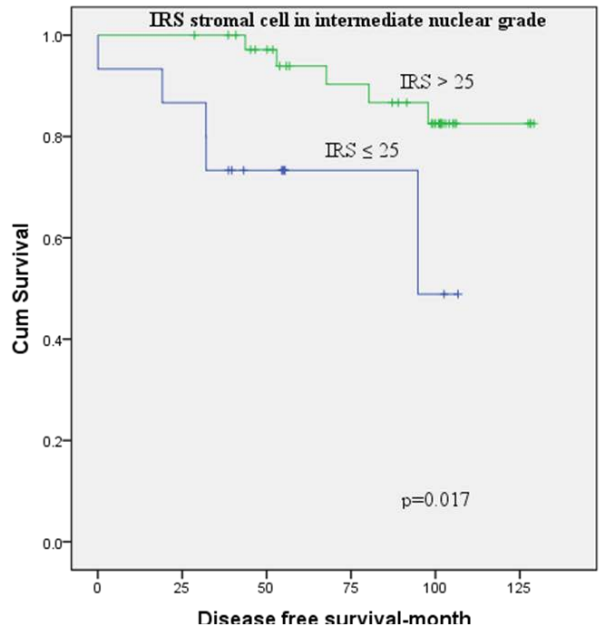

Figures continued into the next page……

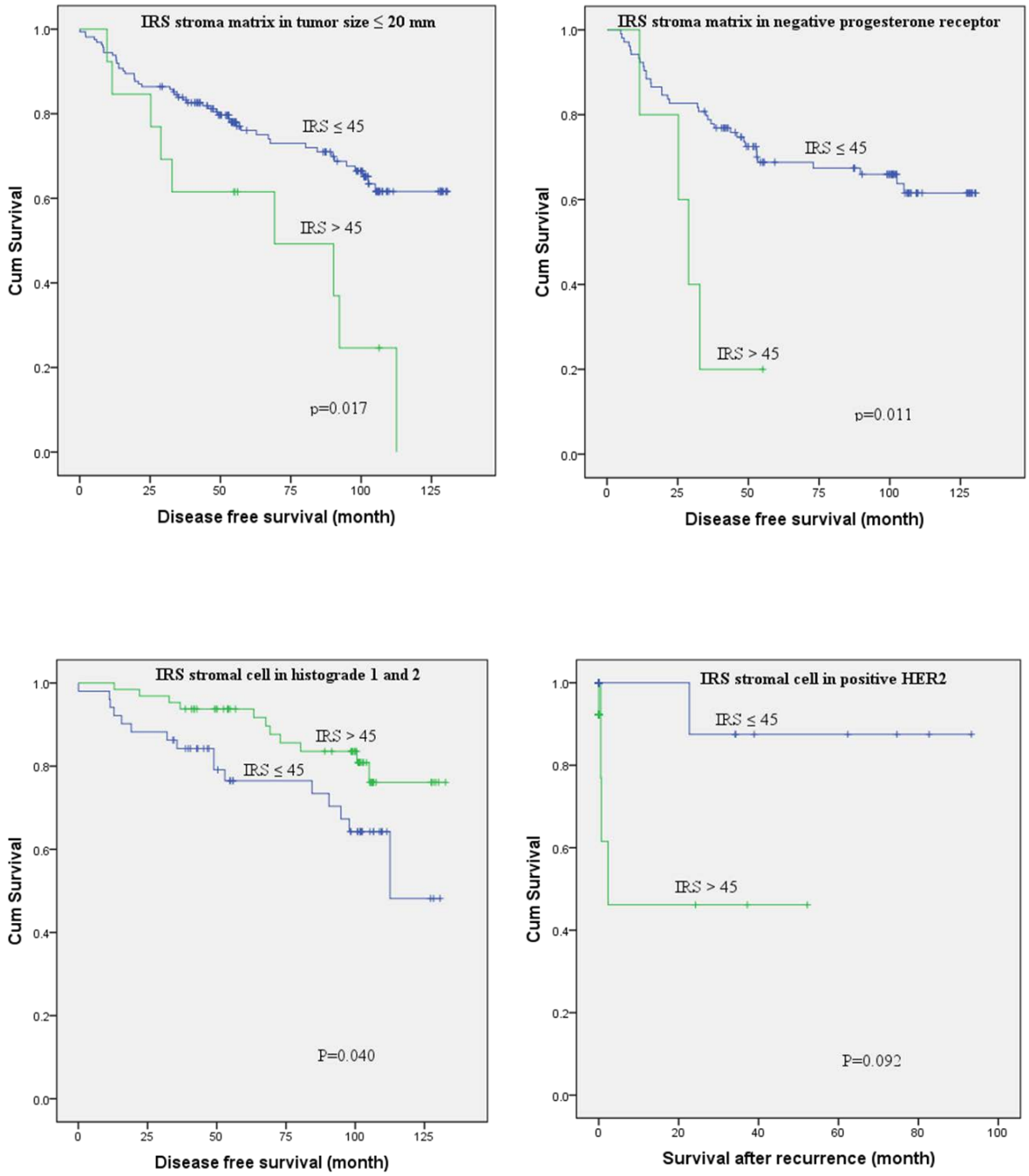

Figure 3.50. Kaplan-Meier survival analysis of the breast cancer using HS6ST3 as a biomarker. Survival analysis revealed that HS6ST3 staining in stroma matrix and stromal cells could predict the prognosis of the breast cancer. Thus, HS6ST3 staining in different tissue compartments was predictive of OS and DFS.

Section 5: Immunohistochemical analysis of human SULF1 expression in human clinical breast cancer sections of ductal carcinoma

3.45 Clinicopathological features of breast cancer sections

Human SULF1 is an enzyme known by its arylsulfatase activity that specifically removes sulfate group from carbon 6 position in heparan sulfate chain. In recent studies, it was identified that human SULF1 expression is dysregulated in several cancers. It lost its expression in cancers such as breast cancer, ovarian cancer, hepatocellular carcinoma and myeloma, while it is up-regulated in gastric cancer and primary pancreatic adenocarcinoma (Li et al. 2005; Lai et al. 2004; Lai et al. 2003; Narita et al. 2007; Abiatari et al. 2006; Narita et al. 2006; Staub et al. 2007; Junnila, 2010).

In this study, immunohistostaining was performed on a total of 267 paraffin embedded tissue microarray slides (TMA) of archival blocks of diagnosed cases of breast adenocarcinoma which were collected in the Department of Pathology of Singapore General Hospital, between 1998 and 2004. In addition to the study population, 39 sections were collected from non cancerous (normal) breast biopsies. Clinicopathological features of cases including race, age, tumor side, tumor size, histotype, histograde, lymph node status, associated ductal carcinoma in situ (DCIS) nuclear grade, associated DCIS nuclear grade extent as well as immunohistochemical markers such as estrogen receptor, progesterone receptor and HER2 were collected. Other information such as diagnosis date, recurrence date and also date of death were retrieved from patient's records. The

study follow up was set up from January 1998 to the end of June 2009. This study was ethically approved by Institutional Review Board, Singapore General hospital.

In this study, most of the breast cancer specimens were from Chinese. In addition, majority of the cancer sections were diagnosed as ductal adenocarcinoma. The age of the breast cancer patients ranged from 23 to 88, with a mean age of 57.26. Tumor size was distributed from 1mm to 140mm among cases with median of 30mm. Details of clinicopathological features of all cases are summarized in Table 3.13. It must be mentioned that nearly all of the specimens were collected prior to any therapy. Thus, the expression of SULF1 enzyme was not affected by any available treatments.

Table 3.13.Clinicopathological features of 267 cases of breast cancer. Data represented the number and percentage of cases.

Clinicopathological features			**Clinicopathological features**		
	n	%		n	%
Age			**Involved Lymph nodes (LN)**		
≤ Mean age (56)	136	50.9	LN = 0	127	47.6
> Mean age (56)	131	49.1	≥1 LN 4 <	66	24.7
Race			≥ 4	61	22.8
Chinese	218	81.6	Unavailable	13	4.9
Malay	21	7.9	**Associated nuclear grade of DCIS**		
Indians	11	4.1	None	109	40.8
Others	17	6.4	Low	11	4.1
Laterality			Intermediate	59	22.1
Right	132	49.4	High	85	31.8
Left	135	50.6	Unavailable	3	1.1
Unavailable			**DCIS nuclear grade extent**		
Tumor size (TS)			None	30	11.2
≤20	75	28.1	Minimal	61	22.8
>20	185	69.3	Extensive	29	10.9
≤30 (mean)	148	55.4	Unavailable	147	55.1
>30 (mean)	112	41.9	**ER expression**		
Unavailable	7	2.6	Negative	98	36.7
Histotype			Positive	164	61.4
IDC	239	89.5	Unavailable	5	1.9
Non-IDC	27	10.1	**PR expression**		
Unavailable	1	.4	Negative	124	46.4
Histograde			Positive	138	51.7
1	27	10.1	Unavailable	5	1.9
2	102	38.2	**HER2 expression**		
3	128	47.9	Negative	177	66.3
Unavailable	10	3.7	Positive	81	30.3
			Unavailable	9	3.4

3.46 Expression of SULF1 in normal and cancerous human breast tissue

In benign human breast tissues, SULF1 strongly expresses itself both in the cytoplasm of epithelial cells as well as extracellular compartments including stroma matrix and stromal cells (Figure 3.51, D). In ductal adenocarcinoma, SULF1 seemed to be differentially expressed in epithelial and stromal components of human ductal adenocarcinoma. Although SULF1 basically expressed in cytoplasm of epithelial cells, the cytoplasmic expression of SULF1 positively correlates with its stromal existence ($p< 0.001$).

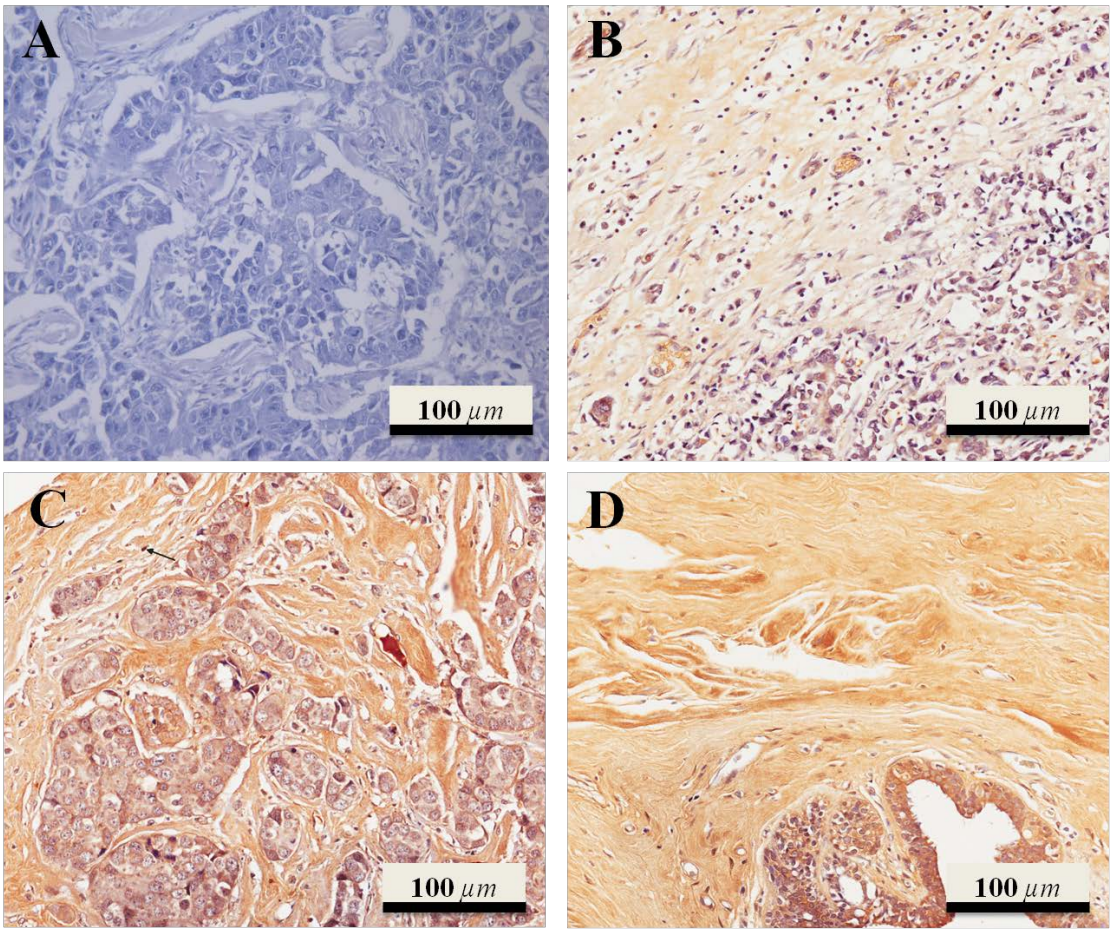

Figure 3.51. Immunohistochemical staining of SULF1 in tissue microarray sections of breast cancer. (A) 0 or negative epithelial and stromal staining (B) +1 or weak staining (C) +2 or moderate staining (D) +3 or strong staining. Picture A, B and C belong to cancer sections, while picture D was captured from normal breast tissue.

3.47 Immunohistochemical expression of SULF1 in epithelial and stromal components of breast ductal adenocarcinoma

SULF1 expresses itself both in the cytoplasm of epithelial cells as well as extracellular compartments including stroma matrix and stromal cells. However, the mean of staining intensity was evidently higher in epithelial cells (126.925±3.929) and stroma matrix (97.772±3.120) than stromal cells (66.498±2.790) among cancer specimens (P<0.001). Analysis of tissue microarrays revealed that the average staining intensity of normal tissues was overall stronger than cancer sections in extra cellular matrix; thus, this difference was significant in stroma matrix and stromal cells by 95% and 90% confidence interval respectively (Table 3.14).

Table 3.14. Immunoreactivity scoring (IRS) among all tissue sections, T test.

IRS	Type of breast tissue	Mean	Std. Error	95% Confidence Interval		P value
				Lower Bound	Upper Bound	
Epithelial cells	Normal	113.077	9.743	93.905	132.249	0.144
	Tumor	126.929	3.724	119.601	134.256	
Stroma matrix	Normal	112.564	8.164	96.498	128.630	**0.016***
	Tumor	97.772	3.120	91.631	103.912	
Stromal cells	Normal	69.103	7.300	54.738	83.467	0.073
	Tumor	66.498	2.790	61.008	71.988	

3.48 Association analysis of SULF1 immunoreactivity with clinicopathological parameters

The staining intensity of different tissue compartments were compared with clinicopathological features. Data shown in Table 3.8 represent associations between the expression of SULF1 and clinicopathological parameters of breast cancer patients such as age, tumor size, histograde, lymph node status, estrogen receptor, progesterone receptor and HER2. The results suggested that patients whose ages were above the mean of age express more SULF1 in their stromal cell, while no associations were found in epithelial cells and stroma matrix. In addition, tumors bigger than 20mm showed to have higher staining intensities in their epithelial cells. In contrast, WAI-based analysis at 1.2 cut off showed that SULF1 staining intensity is higher in stroma matrix of tumors which were smaller than 20mm ($p=0.007$) In addition, the latter analysis revealed that histograde 1 and 2 together have a significantly lower staining intensity compared to histograde 3 in stromal cell compartment (Table 3.15). Further, analysis revealed that the expression of SULF1 was higher in stroma matrix of the sections with higher lymph node metastasis (Table 3.16). There was no significant association between the expression of SULF1 and estrogen and progesterone receptors in tissue compartments. However, interestingly, SULF1 expressed more in epithelial cells and stroma matrix compartments of breast cancer specimens which were positive for HER2.

Table 3.15. Correlations between expression of SULF1 using IRS and clinicopathological features of breast cancer, Fisher's exact test.

Clinicopathological parameter		IRS Epithelial cells		P value	IRS Stroma matrix		P value	IRS Stromal cell		P value
		≤50	**>50**		**≤50**	**>50**		**≤50**	**>50**	
Age	**≤ mean (56)**	16	119	0.454	20	116	0.339	61	75	**0.002***
	> mean (56)	17	113		16	115		36	95	
Race	**Chinese**	28	188	0.811	32	186	0.353	79	139	1
	Others	5	44		4	45		18	31	
Laterality	**Right**	14	117	0.458	12	120	**0.048***	41	91	0.098
	Left	19	115		24	111		56	79	
Tumor size	**≤ 20mm**	16	59	**0.006***	9	66	0.37	29	46	0.408
	> 20mm	16	167		27	158		67	118	
Histograde	**Grade 1**~2	18	111	0.183	15	114	0.226	48	81	0.467
	Grade 3	12	114		20	108		46	82	
Histotype	**IDC**	25	213	**0.008***	31	209	0.671	86	154	0.651
	DCIS	3	4		1	6		2	5	
Lymph node involvement	**≤ 3 nodes**	25	168	0.248	27	166	0.273	74	119	0.436
	> 3 nodes	5	54		6	55		22	39	
Associated nuclear grade of DCIS	**None**	14	95	0.238	15	94	0.977	41	68	0.937
	Low	3	8		1	10		4	7	
	Intermediate	4	55		8	51		23	36	
	High	9	74		11	74		29	56	
DCIS nuclear grade extent	**None**	5	25	0.671	4	26	0.996	7	23	0.582
	Minimal	6	53		8	53		20	41	
	Extensive	4	25		4	25		10	19	
Estrogen receptor	**Negative**	14	84	0.338	16	82	0.224	29	69	0.054
	Positive	19	143		20	144		66	98	
Progesterone receptor	**Negative**	18	106	0.225	20	104	0.188	39	85	0.08
	Positive	15	121		16	122		56	82	
HER2	**Negative**	27	150	**0.014***	29	148	**0.035***	64	113	0.499
	Positive	4	75		6	75		30	51	

Table 3.16. Correlations between expression of SULF1 using WAI andclinicopathological features of breast cancer, Fisher's exact test.

Clinicopathological parameter		WAI Epithelial cells		P value	WAI Stroma matrix		P value	WAI Stromal cell		P value
		≤ 1.2	**>1.2**		**≤1.2**	**>1.2**		**≤1.2**	**>1.2**	
Age	**≤ mean (56)**	36	100	0.461	76	60	0.161	112	24	0.506
	> mean (56)	33	98		82	49		107	24	
Race	**Chinese**	60	158	0.21	134	84	0.112	175	43	0.15
	Otheres	9	40		24	25		44	5	
Laterality	**Right**	29	103	0.164	76	56	0.62	105	27	0.34
	Left	40	95		82	53		114	21	
Tumor size	**≤ 20mm**	21	54	0.353	35	40	**0.007***	63	12	0.359
	> 20mm	46	139		119	66		150	35	
Histograde	**Grade 1**~2	37	92	0.103	80	49	0.228	113	16	**0.022***
	Grade 3	27	101		74	54		99	29	
Histotype	**IDC**	57	183	0.673	141	99	1	196	4	1
	DCIS	2	5		4	3		6	1	
Lymph node involvement	**≤ 3 nodes**	47	146	0.444	122	71	**0.004***	158	35	0.577
	> 3 nodes	16	45		26	35		50	11	
Associated nuclear grade of DCIS	**None**	28	81	0.919	71	38	0.364	89	20	0.835
	Low	3	8		7	4		10	1	
	Intermediate	13	46		32	27		49	10	
	High	23	62		46	39		68	17	
DCIS nuclear grade extent	**None**	5	25	0.579	18	12	0.513	26	4	0.556
	Minimal	15	46		37	24		47	14	
	Extensive	8	21		14	15		23	6	
Estrogen receptor	**Negative**	25	73	0.467	59	39	0.524	82	16	0.41
	Positive	44	120		98	66		134	30	
Progestrone receptor	**Negative**	31	93	0.373	72	52	0.324	102	22	0.534
	Positive	38	100		85	53		114	24	
HER2	**Negative**	48	129	0.185	111	66	0.093	149	28	0.142
	Positive	17	64		43	38		63	18	

3.49 Survival analysis of SULF1 expression in breast ductal carcinoma

Kaplan-Meier survival analysis was primarily performed in all of the possible strata of the histopathological parameters. Then, Univariate Cox regression proportional analysis was performed on strata which were detected as a significant factor ($p < 0.05$) for predicting the prognosis by Kaplan-Meier survival analysis. Univariate Cox regression

proportional analysis showed that staining intensity of tissue compartments significantly associated with overall survival (OS), disease-free survival (DFS) as well as survival after recurrence (SAR). The prognostic factors associated with the expression of SULF1 are summarized in Table 3.10. The survival analysis revealed that age, tumor size, tumor laterality and the number of lymph node involvement are predictive of prognosis. Thus, the OS and SAR of breast cancer cases whose ages were younger than 60 were significantly higher than those who developed breast cancer after 60. In addition, bigger tumors (> 30mm) were associated with poorer SAR. As expected, more lymph node involvement was associated with worse OS and SAR. Interestingly, SULF1 expression was the only factor which was able to predict DFS in addition to OS in breast cancer. Therefore, higher expression of SULF1 in epithelial cells of grade1 of breast cancer predicted a better prognosis for DFS. Similarly, higher SULF1 expression in stroma matrix of breast cancer patients with less than 4 lymph node involvements was predictive for a longer OS and DFS. In contrast, higher expression of SULF1 in stromal cells of breast cancer patients below 60 years old predicted a worse outcome in terms of their DFS. The trends of survivals are shown in Figure 3.52 using Kaplan-Meier survival analysis.

Using a multivariate survival analysis interestingly revealed that the IRS of all of the tissue compartments could independently be predictive for OS and DFS; however, it was not predictive for SAR (Table 3.17).

Table 3.17. Univariate Cox regression analysis for prognostic clinicopathological factors in breast cancer.

	Overall survival			Disease-free survival			Survival after recurrence		
	HR	**95% CI**	**p Value**	**HR**	**95% CI**	**p Value**	**HR**	**95% CI**	**p Value**
Age ≤60 vs >60	2.266	1.222-4.202	**0.009***	1.613	0.976-2.666	0.062	1.862	1.007-3.443	**0.048***
Tumor size (mm) ≤ Median (30) vs > Median (30)	0.984	0.490-1.978	0.964	1.046	0.626-1.749	0.884	1.793	1.030-3.121	**0.039***
Tumor side Right vs Left	0.412	0.213-0.796	**0.008***	0.639	0.385-1.060	0.083	0.45	0.232-0.871	**0.018***
Lymph node metastasis pN0 vs PN1 to pN3	1.909	1.053-3.463	**0.033***	1.323	0.836-2.092	0.23	1.916	1.054-3.482	**0.033***
IRS Epithelial in Grade 1 ≤50 vs > 50	0.196	0.027-1.405	0.105	0.181	0.036-0.904	**0.037***	0.227	0.032-1.613	0.138
IRS Stroma matrix in PN1 to pN3 ≤50 vs > 50	0.249	0.085-0.729	**0.011***	0.231	0.087-0.616	**0.001***	0.377	0.119-1.192	0.097
IRS Stromal cell in Age below 60 ≤50 vs > 50	1.634	0.621-4.299	0.32	2.63	1.191-5.810	**0.017***	1.554	0.544-4.437	0.411

Table 3.18. Multivariate Cox regression analysis for prognostic clinicopathological factors in breast cancer using backward stepwise model.

Predictor		**HR**	**95% CI**	**p Value**
Overall survival (OS)				
IRS Stroma matrix in PN1 to pN3	≤50 vs > 50	0.157	0.049-0.506	**0.002***
Tumor side	Right vs Left	0.315	0.098-1.009	0.052
IRS Stroma matrix	≤50 vs > 50	0.461	0.209-1.017	0.055
Age	≤60 vs > 60	2.456	1.292-4.666	**0.006***
Tumor side	Right vs Left	0.352	0.176-0.705	**0.003***
Disease free survival (DFS)				
IRS Epithelial cell in Grade 1	≤50 vs > 50	0.02	0.001-0.465	**0.015***
Lymph node status		6.272	1.080-36.414	**0.041***
IRS Stroma matrix in PN1 to pN3	≤50 vs > 50	0.201	0.073-0.554	**0.002***
IRS Stromal cell in Age below 60	≤50 vs > 50	3.021	1.307-6.986	**0.010***

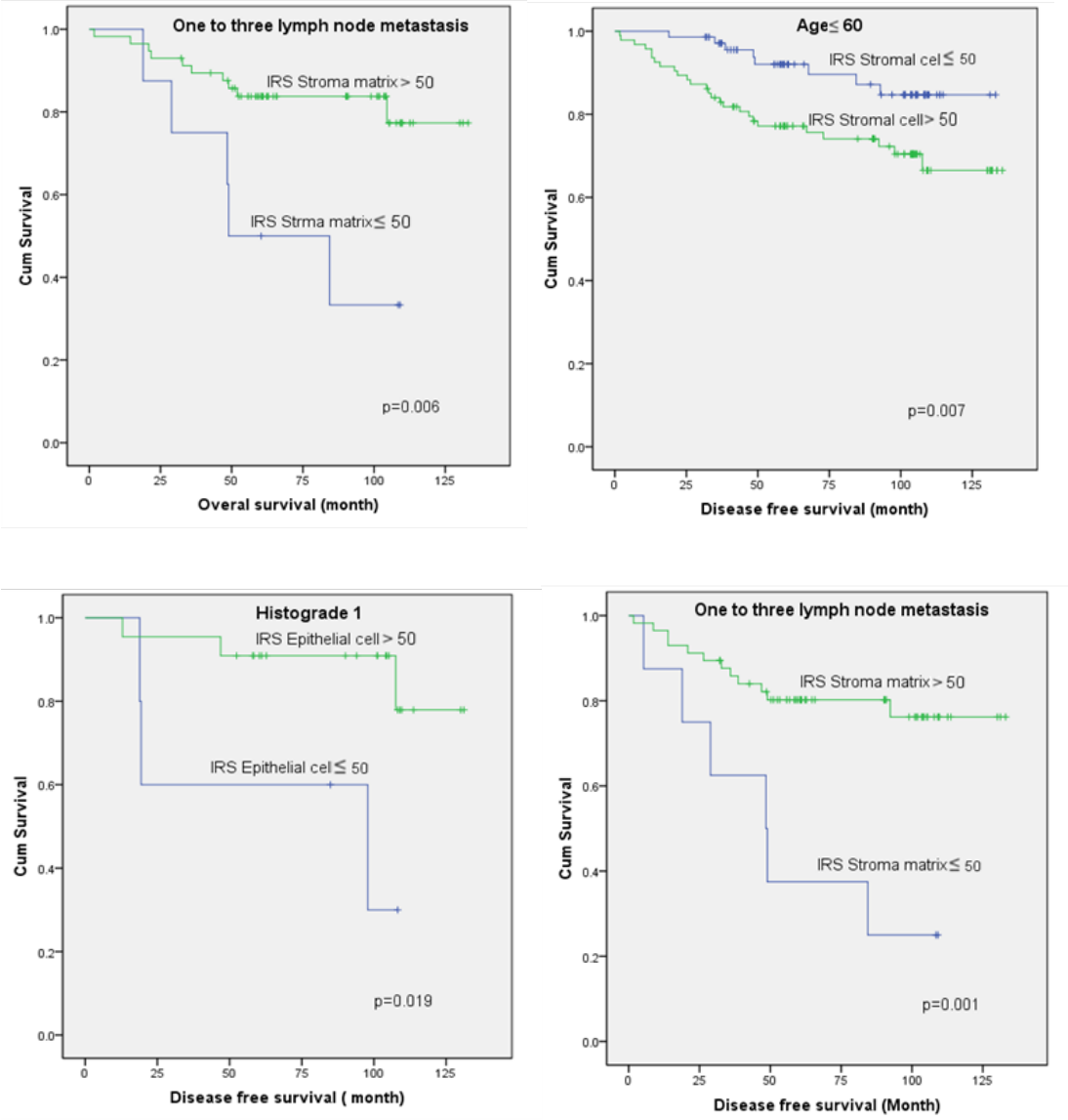

Figure 3.52. Kaplan-Meier analysis of the breast cancer survival using SULF1 as a biomarker. Analysis revealed that SULF1 positivity in epithelial cells and stroma matrix was associated with a longer survival, while similar expression in stromal cells was associated with poorer prognosis.

3.50 Analysis of the expression of HS6ST3 and SULF1 in breast cancer

The staining intensities of HS6ST3 and SULF1 of various tissue compartments revealed to have significant associations with clinicopathological parameters such as age, tumor size, histograde, histotype, lymph node status, estrogen receptor, progesterone receptor and HER2.

The breast cancer patients whose ages were above the mean of age expressed more HS6ST3 and SULF1 in their epithelial cells and stromal cells respectively. Tumors which were smaller than 20mm expressed more HS6ST3 in their stroma matrix, while they expressed less SULF1 in their epithelial cells. Similarly, tumors which were smaller than 20mm expressed more SULF1 in stroma matrix compartment. Besides, HS6ST3 expressed more in stroma matrix of the histograde 2 compared to histograde 1 and histograde 3. SULF1 expressed more in stromal cells of histograde 3 compared to histograde 1 and histograde 2. It was also identified that the expression of HS6ST3 was higher in stromal cells of invasive ductal carcinoma (IDC) compared to ductal carcinoma in situ (DCIS). However, there was no significant association between the expression of SULF1 and histotype. On the other hand, SULF1 expression was found higher in the epithelial cells and stroma matrix of tumors which were positive for HER2, while no association was identified between the expression of HS6ST3 and HER2. Furthermore, the analysis interestingly showed that the higher expression of HS6ST3 and SULF1 in stroma matrix associated with more lymph node metastasis.

Survival analysis showed that the expression of both HS6ST3 and SULF1 in different tissue compartments could independently predict the prognosis of the breast cancer patients.

Although the expression of HS6ST3 in epithelial cell was not predictive of prognosis, the similar expression in extracellular components could predict the prognosis of the breast cancer patients. Lower expression of HS6ST3 in stroma matrix of the breast cancer cells was predictive of a better survival; however, in tumors with less lymph node metastasis (≤ 3 lymph nodes involvement), higher expression of HS6ST3 was able to predict a longer survival. On the other hand, less staining of HS6ST3 in stromal cell compartments with positive HER2 was predictive of a better survival, while a higher expression of HS6ST3 in stromal cells of histograde 1, 2 sections were associated with a prolonged survival.

The expression of SULF1 in various tissue compartments was also predictive of survival of the breast cancer patients. Unlike the expression of HS6ST3, the expression of SULF1 in epithelial cells was predictive of the breast cancer survival. It was identified that higher expression of SULF1 in epithelial cells of the histograde 1 was associated with a better survival. Similarly, a higher expression of SULF1 in stroma matrix of the tumors with less lymph node metastasis (≤ 3 lymph nodes involvement) was associated with a longer survival. On the other hand, the expression of SULF1 in stromal cell compartment was able to predict the breast cancer prognosis. Thus, it was interestingly revealed that the

lower staining of SULF1 in the stromal cells of the patients below 60 years old was associated with a better survival.

CHAPTER 4

DISCUSSION

4.1 Expression analysis of HS6ST3 in breast cancer cell lines

This study was mainly aimed to highlight the significance of *HS6ST3* in breast cancer behavior. Thus, the modulatory role of *HS6ST3* was examined in T47D and MCF7 breast cancer cell lines by performing several functional experiments such as proliferation, cell cycle, apoptosis, adhesion, migration and invasion assays. The current research is the first comprehensive study which was performed to elucidate the potential role of *HS6ST3* in the malignant process of carcinogenesis. Hence, little is known about the involvement of *HS6ST3* in cancer in the literature. In addition, the function of other *HS6ST* isoforms was rarely studied in cancer. Seko et al. firstly showed that *HS6ST2* was over-expressed in mucinous adenocarcinomas, while *HS6ST3* was down-regulated in the same carcinomas (Seko et al. 2002). Later, labbe et al. revealed that targeting TGF-beta and Wnt signaling could increase the expression of *HS6ST2* in mammary and intestinal carcinomas (Labbé et al. 2007). Recently, song et al. found the significant involvement of *HS6ST2* in pancreatic cancer. They understood that shRNA silencing of *HS6ST2* diminished the growth, progression and angiogenesis of the pancreatic carcinoma. In addition, they proposed that *HS6ST2* could trigger the Notch signaling in PC. (Song et al. 2011).

In the current study, proliferation assay showed that silencing *HS6ST3* decreases the number of viable T47D and MCF7 cells in culture medium. It was postulated that *HS6ST3* knock down could result in diminished relative percentage of the live cells. However, this change might be attributable to diminished rate of cell proliferation or activation of apoptotic pathway(s). Whether this observed effect is due to diminished

proliferation or activation of apoptotic cascade, the finding indicates that silencing *HS6ST3* could potentially change the interactions between heparan sulfate and a variety of growth factors and cytokines. Consequently, cell signaling which is influenced by the latter process could potentially affect the relative percentage of the live cells. Lai et al. showed that the expression of SULF1, a heparan sulfate 6-O-sulfation editing enzyme, could reduce the proliferation and induce the apoptosis in the ovarian carcinoma (Lai et al. 2003). Therefore, it is plausible that 6-O-hypo sulfation of the heparan sulfate by inhibiting HS6ST(s) or over-expression of SULF1 could potentially alter the interaction of the heparan sulfate chain with other significant signaling molecules which regulate the cellular processes.

In order to find why the relative percentage of the live cells was diminished after silencing *HS6ST3*, cell cycle assay and apoptosis assays were performed respectively. Thus, cell cycle assay was carried out at 72 hours after *HS6ST3* knock down. Analysis revealed that the cellular population percentages of cell cycle phases were shifted after silencing *HS6ST3* in both T47D and MCF7. In T47D, this shift was remarkably obvious in G0 and G1 phases. In G0 phase which is indicative of pre-apoptotic cells, the cellular percentage was significantly increased after silencing *HS6ST3*. Similar trend was observed in G1 phase suggesting that *HS6ST3* knock down induced a G1 arrest. In other words, the percentage of viable cells in G1 was remarkably increased. As a result of G1 arrest, cellular transition from G1 to G2 phase was reduced in T47D; and in turn the relative number of viable cell was significantly diminished in S and G2 phases. In MCF7,

the shift in G0 was more prominent as the number of pre-apoptotic cells remarkably increased. However, G1 arrest was not observed after silencing *HS6ST3* in MCF7. These changes were consistent with the result of proliferation assay. Performing cell cycle assay showed that down regulation of *HS6ST3* may decrease the relative percentage of the live cells through various pathways in T47D and MCF7 as it mainly induced apoptosis and on the other hand, caused G1 arrest in the cell cycle.

Cell cycle assay showed that the numbers of pre-apoptotic cells increased after silencing *HS6ST3;* however, in order to verify the direct influence of apoptosis on the relative percentage of the live cells, apoptosis assay was performed. In this assay, the activity of caspase 3, 7 and caspase 8 were measured in T47D and MCF7. These caspases were previously chosen from the list of the genes which were up-regulated after silencing *HS6ST3* in gene microarray analysis. Luminescence measurement showed that the activity of these caspases was increased by knocking down *HS6ST3*. This observation was in agreement with the observations of proliferation and cell cycle assay and was indicative of the potential ability of *HS6ST3* knocked down on activation of apoptotic pathways. In other words, restoration of *HS6ST3* expression prevented the activation of the cascade of caspases.

Adhesion is an important characteristic of most cells. Malignant cells tend to have weaker adhesion compared to non-malignant cells; therefore, cancer cells may easily metastasize

into adjacent tissues of the involved organ as well as other organs (Ruoslahti 1984; Pauli et al. 1983; Sebestyén et al. 2000). In this study, we performed adhesion assay using collagen I or fibronectin coated plates. Analysis of this assay demonstrated a significant increase in cell adhesion after silencing *HS6ST3* in T47D and MCF7. This finding suggested that down-regulation of *HS6ST3* may result in over expressing adhesion molecule(s) which tends to adhere into collagen I and/ or fibronectin; and consequently, enhances the cellular adhesion. For example, based on our microarray data we identified that ICAM1 and paxillin, adhesion molecules, were overexpressed by 205.5% ($p< 0.001$) and 50% ($p< 0.05$) respectively after silencing *HS6ST3* in the breast cancer. Kawai et al. revealed that restoration of ICAM1 expression in lymphatic endothelial cells enhanced the adhesion of cancer cells to the lymphatic endothelial cells (Kawai et al. 2009). On the other hand, Schröder et al. explained that the expression of ICAM1 may increase the cell migration and invasion in the breast cancer (Schröder et al. 2011). However, the critical role of ICAM1 in the malignant process of tumorogenesis is still unknown.

Paxillin is another adhesion molecule that mechanically regulates the integrin bonds in vascular cell adhesion by contributing in the assembly of focal adhesion (Manevich et al. 2007). Chen et al. revealed that silencing of paxillin inhibited the cellular adhesion in the breast cancer (Chen and Kroog 2010).

Our microarray analysis showed that by silencing *HS6ST3,* the expression of several integrins such as alpha 3 ($p< 0.01$), alpha 2b ($p< 0.05$), beta 2 ($p< 0.05$), alpha 9 ($p< 0.05$), beta 8 ($p< 0.05$), alpha 8 ($p< 0.01$), beta 7 ($p< 0.01$), and alpha M ($p<0.05$)

increased. All of these observations could be suggestive of the potential effect of *HS6ST3* silencing in enhancing the cellular adhesion in the breast cancer. As an example, Slambrouck et al. showed that inhibition of integrin alpha 2 led to a poor adhesion and enhanced the invasion of the cells in prostate cancer (Van Slambrouck et al. 2009).

Malignant cells may move from their original location and reach to the blood vessels as well as lymphatic vessels and hence could potentially facilitate the metastasis of the cancer cells into the other tissues or organs (Brown and Bicknell 2001; Simpson et al. 2010; Moutasim, Nystrom and Thomas 2011). To assess how the cell motility was affected by *HS6ST3* knock down, migration assay was perform using wound healing or scratch assay. For this purpose, serial photos were captured at 12, 24, 48 and 72 hours after scratching the T47D cells. Analysis shows no significant different between silenced cells and control group at 12, 24 and 48 hours. On the other hand, significant difference was observed at 72 hours post scratch indicating that the wound healing was delayed in silenced cells compared to control group. However, since the time lag between scratch and cell motility at 72 hours after that was quite long, the observed difference could be attributable to cellular proliferation. In order to confirm whether the latter is due to proliferation or cell motility a different migration assay was performed by using migration inserts. The results of the transwell migration assay revealed no cellular migration through the inserts in either silenced or control groups of T47D cells. Unlike T47D, silencing *HS6ST3* diminished the cell migration in MCF7.

Invasiveness of the tumor cell is as a result of pathological interaction of the malignant cells with the other cells as well as extracellular matrix (ECM). Invasive cancers may metastasize to the adjacent tissues as well as other organs. These malignant cells are capable to invade the basement membrane that lines the epithelial or endothelial cells and infiltrate into the other tissues. In order to simulate this condition, we performed invasion assay by using matrigel invasion chambers (Kramer, Bensch and Wong 1986; Kleinman and Jacob 2001). Similar to the migration chamber, the results of the invasion assay revealed no cellular invasion through the inserts in either silenced or control group. However, silencing *HS6ST3* in MCF7 resulted in an interesting decrease in cellular invasiveness. The observed differences in migration and invasion between T47D and MCF7 cell lines might be due to their nature, size or other unknown factors (Karey and Sirbasku 1988; Edwards et al. 1989; Sheridan, Francis and Horwitz 1989; Ryde, Nicholls and Dowsett 1992; Mooney et al. 2002).

In addition, we found that silencing *HS6ST3* in T47D and MCF7 could significantly diminish the expression of heparan sulfate on the cell surface. The latter was revealed in immunocytostaining (ICC) by using two anti-heparan sulfate antibodies (10E4 and HepSS-1). Suppression of heparan sulfate synthesis could further justify the observed phenotypic alterations after silencing *HS6ST3* in T47D and MCF7; because cell surface heparan sulfate regulates a variety of signal transduction by interacting with several ligands such as growth factors, matrix components and cytokines (Lo et al. 2011; Iozzo 1988; van den Born et al. 2005; Pilkington et al. 1997; Fujita et al. 2010). In 2004, Maeda

et al. realized that over-expressing the syndecan-1 could enhance the tumoral proliferation in breast cancer (Maeda, Alexander and Friedl 2004). Park et al. understood that syndecan-2 was involved the process of tumorogenesis and this involvement was mediated by Focal Adhesion Kinase (FAK) in fibrosarcoma (Park et al. 2005). Later, Choi et al. examined the role of syndecan-2 on the cancer progression. They showed that over-expression syndecan-2 increased the collagen adhesion, migration and invasion of the rate intestinal epithelial cells (RIE1) (Choi et al. 2009). Earlier to these findings, Farooq and his colleagues found that the syndecan-3 could induce cell cycle arrest at G1; and thus they showed that by inhibiting the expression of syndecan-3, cellular proliferation could increase in Hep 3B (Farooq et al. 2003). Nikolova et al. showed that the syndecan-1 differentially expressed in the different stages of the breast cancer and therefore regulating the breast cancer progression (Nikolova et al. 2009).

In our microarray data we found that silencing *HS6ST3* did not affect the expression of any of the syndecans, while it significantly reduced the expression of the expression of glypican-6 ($p< 0.001$) by 61 % and increased the expression of glypican 1 ($p< 0.05$) and glypican 2 ($p< 0.01$) by 49% and 64% respectively. Therefore, we may deduce that during the process of carcinogenesis the expression of the glypican 1 and glypican 2 was diminished and the expression of the glypican 6 was increased so that it composed the major content of the heparan sulfate on the cell surface of the breast cancer cells. Thus, significant reduction of cell surface heparan sulfate after silencing *HS6ST3* in T47D and MCF7 could be attributable to the reduction in the content of the cell surface glypican 6.

Furthermore, we one possible way to justify the observed phenotypic change after silencing HS6ST3 is the regulatory role of glypican 6 in the malignant process of carcinogenesis.

Herein, we proposed two hypotheses: Firstly, the phenotypic alterations consistently indicated that silencing *HS6ST3* could significantly influence the interactions between heparan sulfate and several growth factors. This in turn affects the growth factor signals that adjust the cell growth, adhesion, apoptosis, migration as well as invasion; and thus diminish breast cancer progression. In our microarry analysis it was identified that silencing *HS6ST3* reduced the expression of IGF1R which will be fully discussed in the next section. Secondly, it might be possible that *HS6ST3* gene have a direct or indirect positive regulation on breast cancer oncogene(s) and a negative regulation on the breast cancer tumor suppressor gene(s). Thus, silencing *HS6ST3* may minimize the positive regulation of the oncogene(s), while tumor suppressor(s) could be activated and consequently these alterations influenced the cancer growth and progression. Osborne et al. introduced a number of oncogenes (such as Cyclin D1, Cyclin E) and tumor suppressor genes (such as CHK2) which could potentially contribute in breast cancer tumorogenesis (Osborne, Wilson and Tripathy 2004).

In the microarray analysis, we found that the expression of Cyclin D1 and Cyclin E, breast cancer oncogenes diminished by 40% ($p < 0.01$) and 37% ($p < 0.05$) respectively

after silencing *HS6ST3*. On the other hand, silencing *HS6ST3* over-expressed CHK2, a breast cancer suppressor gene, by 30% ($p < 0.05$).

These finding are of considerable significance since they have introduced an interesting gene which regulates breast cancer behavior. The significance of the current study is not restricted to the regulatory role of *HS6ST3* in breast cancer because it could be also used as a novel prognostic and/ or diagnostic biomarker in breast cancer. In addition, it might be useful as an effective therapeutic target for treating breast cancer as well as other malignancies. However, the results of our study were restricted to breast cancer cell line *in vitro*. Therefore, a direct extension of this study is required to explore the consistency of these findings *in vivo*. Applying similar studies *in vivo* could reveal the clinical significance of HS6ST3 in breast cancer as well as other malignancies.

4.2 Insulin-like growth factor 1 receptor (IGF1R)

Based on our microarray analysis, we found that IGF1R was down-regulated after silencing *HS6ST3*. This finding was further confirmed by RT-PCR in T47D and MCF7 breast cancer cell lines. Then, the downstream relationship of IGF1R and HS6ST3 was validated by designing several functional studies. After that, we found that blocking IGF1R with blocking antibody diminished the cellular proliferation, migration and invasion in breast cancer.

IGF1R is a transmembrane tyrosine kinase receptor comprising two extracellular alpha and two beta subunits which critically modulate several biological events such as growth and development. Hadsell et al. examined the role of insulin-like growth factor I on the development of mammary. They showed that targeting insulin-like growth factor I could result in incomplete breast development, diminished mammary gland branching and loss of secretory lobules (Hadsell et al. 1996; Richards et al. 2004). On the other hand, IGF1R is a key regulator of several cell processes in malignant cells, and thus play an important role in growth and progression of the cancers (Tang et al. 2007). Cullen et al. was firstly explained the expression and function of IGF1R in breast cancer. They concluded that IGF1R ubiquitously express in breast carcinoma and suggested a mitogenic function for this receptor (Cullen et al. 1990). Hence, the existence or even up-regulation of IGF1R seems to be essential for transforming the non-tumoral cellular phenotype into a malignant behavior (Werner and Le Roith 1997; Burtscher and Christofori 1999). Activation of IGF1R was shown to enhance the cellular proliferation and inhibit the apoptosis in several cell lines such as breast epithelial cells. (Yanochko and Eckhart 2006). Carboni et al. revealed that activation of IGF1R in transgenic mice could develop breast cancer, and then they detected the higher expression level of IGF1R in the mammary tumor at 8 weeks of age (Carboni et al. 2005). Jones et al. injected the breast cancer cells over-expressed for IGF1R into the mammary gland of wild type mice. After about two weeks they found a prominent tumor which was palpable in the mammary gland, while the control mice had the palpable tumor after about 12 weeks. Additionally, based on their microarray analysis they found that suppression of IGF1R diminished the expression of cyclin D1 protein *in vivo* and *in vitro*. Thus, they proposed that some

proliferative functions of IGF1R might be regulated by cyclin D1 as a downstream signaling factor (Jones et al. 2008). Cyclin D1 was reported to be aberrantly expressed in breast cancer as well as other cancer. High expression level of cyclin D1 associated with poorer prognosis in breast cancer cases. Over-expression of cyclin D1 was associated with invasive malignant transformation of non-invasive epithelial cells of the mammary gland (Wang et al. 2007). On the other hand, suppression of Cyclin D1 expression in breast cancer inhibited the tumor cell growth by inducing a G1 arrest in cell cycle and also promoted the apoptosis of the breast cancer cells (Wei et al. 2011). In our study, cyclin D1 was remarkably down-regulated by 40% *(*$p < 0.01$) after silencing HS6ST3 in the breast cancer; therefore, we postulate that the suppression of cyclin D1 could be due to the down-regulation of IGF1R which occurred after silencing *HS6ST3* in breast cancer cell line. Therefore, we may also presume that the suppression of the growth and development of the tumor cells in *HS6ST3* knocked down cells were partly due to the down-regulation of the cyclin D1.

In estrogen receptor expressing (ER) cell lines such as MCF7, IGF1R was shown to be involved in a crosstalk which synergistically leads to promote the cell cycle progression. Thus, the estrogen potentiates the effect of IGF1R signaling and enhances the cellular proliferation (Dupont and Le Roith 2001).

Metastasis of the breast cancer cells is a process in which the tumor cells invade the basement membrane and then migrate to the adjacent tissues or different organs. Apart from proliferation, IGF1R was reported to have a robust regulatory influence on the

migration and invasion of the breast carcinoma as well as other cancers. Suppression of IGF1R was firstly shown to reduce the invasion and thus the metastasis of the cancer cells (Dunn et al. 1998; Sachdev et al. 2004). Samani et al. revealed that genetically engineering of highly invasive cancer cells that expressed truncated IGF1R subunits could considerably neutralized the invasive characteristics of the malignant cells by blocking the IGF1R mediated signal transduction *in vivo*. In addition, they found that this method increased the disease free survival (DFS) of the mice comparing with the controls (Samani et al. 2004). Sachdev et al. found that IGF1R promotes the metastasis and survival of the tumor cells in breast cancer independent to the role which it has for primary tumor proliferation. The latter indicated that IGF1R is able to regulate multiple phenotypes in the process of tumorogenesis (Sachdev et al. 2010). The functional role of IGF1R has been extensively studied in breast carcinoma; however, similar scenario was observed in other cancers such as bladder cancer, colorectal cancer, Ewing tumor, lung cancer, prostate carcinoma and bone malignancies (Zhang et al. 2010; Kang et al. 2010; Linnerth et al. 2009; Avnet et al. 2009).

Insulin-like growth factor I (IGF-I), a potential specific ligand for IGF1R is similarly able to potentiate the cellular proliferation, while it inhibits the apoptosis via multiple signal transduction pathways such as kinase pathways (Párrizas, Saltiel and LeRoith 1997). The association between serum IGF1 levels and IGF1 binding proteins and increased risk of breast cancer was described in a few epidemiological studies (Goodwin et al. 2002). The risk of developing breast cancer was further increased when activation of IGF1R accompanied p53 mutation. In addition, clinical studies showed that IGF1R is a valuable

independent predictor of breast carcinoma specifically at its earlier stages (Mulligan et al. 2007; Toniolo et al. 2000).

Decreasing cellular adhesion is another important characteristic of invasive cells in different malignancies. It was reported in a few studies that expression of IGF1R was necessary for the cellular adhesion (Dunn et al. 1998; Mauro et al. 2003), while Guvakova et al. found that activation of the IGF1R induced disassembly of actin filament as well as tyrosine deposphorylation of paxillin and Focal adhesion kinase (FAK) in mammary epithelial cells. In their study, activation of IGF1R was associated with decreasing of the cell adhesion. They further found that increased activity of IGF1R promoted the cellular motility in MCF7 (Guvakova and Surmacz 1999). In another study, Mauro et al. showed that the expression of E-cadherin as a junctional protein is needed for IGF1R-dependent cell to cell adhesion in MCF7. They found that the assembly of E-cadherin (E-cad) was stimulated by over-activation of IGF1R in MCF7 but not in negative E-cad cell lines. Thus, they deduced that co-expression of E-cad and IGF1R could increase the intercellular adhesion (Mauro et al. 2001).

In the current study, we found that down-regulation of IGF1R in *HS6ST3*-silenced T47D cells increased the cellular adhesion. Based on our microarray analysis, we noticed that silencing *HS6ST3*, upregulated the paxillin by 50% ($p < 0.05$), while there was no statistically significant change in the expression of E-cad and FAK. This finding had a consistency with the other findings regarding the growth and progression of tumor cells in breast cancer.

Targeting IGF1R in breast cancer has been suggested as a novel therapeutic method in many studies. In antisense therapy, an anti sense RNA or oligonucleotide could target the genomic expression of IGF1R and decreases its expression in order to inhibit the tumoral growth and progression (Yang, Elliott and Head 2002; Samani et al. 2004). Recently, the scientist revealed that targeting IGF1R may induce the tumor supression, while it does not totally eradicate the preneoplastic changes in mammary tumor. Although they knew that targeting IGF1R could be an effective antitumor therapy, co-targeting IGF1R with other molecules was reported to be more potent against cancer growth and progression (Jones, Petrik and Moorehead 2010). For example, Chakraaborty et al. found that co-targeting IGF1R and HER2 dramatically inhibited the cell proliferation and efficiently induced the apoptosis in the breast cancer cells. Therefore, targeting IGF1R in combination with other signaling molecules might be beneficial in developing of anti-cancer treatment (Chakraborty, Liang and DiGiovanna 2008).

In this study, we showed that knocking down of *HS6ST3* down-regulated *IGF1R* expression in breast cancer. This effect may occur through inactivation of IGF1R transcription regulator. Alternatively, silencing *HS6ST3* might change the growth factor signaling due to possible alteration in 6-O sulfation pattern and this may down-regulate IGF1R expression. Overall down-regulation of IGF1R mediated the reduction in growth and progression of breast cancer after silencing *HS6ST3*.

4.3 X chromosome-linked inhibitor of apoptosis protein (XIAP)-associated factor 1 (XAF1)

Analysis of our microarray data showed that XAF1 was strongly up-regulated after silencing *HS6ST3*. Performing RT-PCR confirmed that the expression of *XAF1* significantly increased by 102% and 670.8% in T47D and MCF7 cell lines respectively. Then, the downstream relationship of *XAF1* and *HS6ST3* was validated by designing several functional studies. After that, we found that silencing *XAF1* enhance the cellular growth in MCF7. In addition, by performing double silencing for *XAF1* and *HS6ST3* it was unraveled that the suppression of *XAF1* might be involved in cell proliferation, adhesion, migration and invasion in breast cancer.

XIAP-associated factor 1 or XAF1, a zinc finger protein, is known as a tumor suppressor that antagonizing XIAP, an antiapoptotic protein, and thus induce the cell death. XIAP is an important member of intrinsic factors which diminish the apoptosis both *in vitro* and *in vivo*. The inhibition function of XIAP is done by binding to the caspase 3, 7, 8 and 9 (Chai et al. 2001; Huang et al. 2001; Riedl et al. 2001; Fong et al. 2000; Groebner et al. 2010). However, XAF1 prevent XIAP of binding to the caspases. For this purpose, XAF1 could bind to XIAP and facilitate degradation of Survivin which is an important anti-apoptotic protein (Arora et al. 2007). In our microarray analysis, we found that XIAP was significantly down-regulated by 31% ($p<0.01$) in *HS6ST3*-silenced breast cancer cells. When the changes in the expression of XAF1 and XIAP was identified in HS6ST3-knocked down cells, we luminometrically measured the activity of different caspases after silencing *HS6ST3* to evaluate whether the observed apoptosis was due to the

enhanced caspase(s) activity. Then, we found that the activity of caspase 3, 7 and 8 was remarkably increased after silencing *HS6ST3 in* T47D and MCF7. This observation might be attributable to the over-expression of XAF1 after silencing *HS6ST3* or the direct influence of *HS6ST3*-knocked down on the expression of the caspases. Douglas et al. suggested that the up-regulation the *XAF1* might be potently mediated by INF-beta and this up-regulation sensitized the cells to induce apoptosis; however, we found no significant change in the expression of INF-beta after silencing *HS6ST3* in breast cancer. Therefore, we hypothesized that up-regulation of XAF1 was occurred in *HS6ST3*-knocked down cells independent to INF-beta (Leaman et al. 2002; Wang et al. 2006; Micali et al. 2007). On the other hand, Sun et al showed that the promoter of the *XAF1* might be activated by the transcription regulator STAT1 in colon cancer (Sun et al. 2008). In this regards, we found that STAT1 was up-regulated up to 354% ($p< 0.001$) after silencing *HS6ST3* in breast cancer based on the microarray data. Hence, we could postulate that the over-expression of *XAF1* might be mediated by activation of STAT1 in *HS6ST3*-knocked-down cells in breast cancer.

Association between the absences of programmed cell death and carcinogenesis has been widely examined in many studies. It was proposed that the disrupted balance between XIAP and XAF1 expression might be a key element in cancer growth and progression (Fong et al. 2000; Yin, Cheepala and Clifford 2006). XAF1 could be detected ubiquitously in many tissues; however, its expression is suppressed *in vitro* and *in vivo* in several cancers such as gastric cancer, skin cancer, colorectal cancer, prostate cancer, blood cancer, kidney cancer, bladder cancer, liver cancer and testicular cancer (Sakemi et

al. 2007; Ng et al. 2004; Byun et al. 2003; Ma et al. 2005; Chen et al. 2006; Lee et al. 2006; Gao et al. 2006; Zou et al. 2006; Shibata et al. 2007; Yu et al. 2007; Chung et al. 2007; Li et al. 2007; Kempkensteffen et al. 2007; Li et al. 2008; Kempkensteffen et al. 2008; Pinho et al. 2009; Huang et al. 2010). Researches explained that low expression of XAF1 in tumor cells was attributable to the aberrant promoter hypermethylation which contribute in tumor progression (Jang et al. 2005; Murphy, Perry and Lawler 2008). They further found an inverse correlation between low XAF1 expression and mutation of p53 indicating that loss of XAF1 expression may accompany the p53 mutation in the process of carcinogenesis in malignancies such as gastric cancer (Byun et al. 2003). On the other hand, XAF1 and p53 which are known as tumor suppressors could modulate the expression of each other in cancer cells. In other words, it was shown that the over-expression of XAF1 suppressed the expression of p53 and the restoration of p53 inhibited the XAF1 transcription in gastrointestinal cancer (Zhang et al. 2010). However, in Zou's study it was revealed that over-expression of XAF1 resulted in activation of wild-type p53 and accumulation of wild type p53 led to apoptosis (Zou et al. 2011). In our microarray results it was noticed that tumor protein p53 inducible nuclear protein 2 (TP53INP2) was slightly up-regulated, while other p53-related proteins such as TP53RKB, TP53BP2, TP53I11, TO53I3, TP53TG1, PERP and PDRG1 were significantly down-regulated after silencing *HS6ST3* in breast cancer. Although we could not rule out the mutation of p53 in breast cancer, we may primarily hypothesize that over-expression of XAF1 reduced the growth and progression of breast cancer independent to p53. In a recent study, it was revealed that the autophagic cell death function of XAF1 was mediated by Beclin-1 in gastric cancer (Sun et al. 2011). Herein, we found that

autophagy/ beclin-1 regulator 1 (AMBRA1) was significantly up-regulated by 80% after silencing *HS6ST3* in our microarray data ($p< 0.001$). Hence, we think that Beclin-1 may also mediate the regulatory effect of XAF1 on tumoral growth and progression in breast cancer. Recently, Xing et al. examined the regulatory influence of somatostatin on XAF1. They realized that somatostatin inhibit the cell proliferation and induced the cellular apoptosis via regulating XAF1 (Xing et al. 2010). Somatostatin was found up-regulated after silencing *HS6ST3* in breast cancer by more than 50 %. Thus, it is postulated that somatostatin is an up-stream gene which inhibit the tumoral growth and progression by modulating XAF1 expression in breast cancer.

Researchers further examined the significance of XAF1 and found that up-regulation of XIAP or loss of XAF1 expression was associated poor prognosis in acute leukemia and pancreatic cancer (Chen et al. 2006; Huang et al. 2010). Similar to IGF1R, XAF1 was introduced as an independent prognostic factor which could predict the survival in gastric adenocarcinoma (Shibata et al. 2008). On the other hand, over-expression of XAF1 could redistribute the cytosolic XIAP into nucleus and therefore trigger the apoptosis pathway and induce cell cycle arrest at specific check points (Liston et al. 2001; Wang et al. 2009). Qiao et al. examine the role of XAF1 in the process of angiogenesis. They revealed that restoration of XAF1 expression inhibited the angiogenesis in the mouse endothelial cells (Qiao et al. 2008).

As discussed growing body of researches has been elucidated the critical role of XAF1 in programmed cell death; however, the potential role of the XAF1 and XIAP in other

cellular processes is still immature. Our findings importantly contributed in elucidating the role of XAF1 in critical cellular processes such as proliferation, cell cycle, adhesion, migration and invasion of the breast cancer.

Restoration of XAF1 expression has been shown as a potent inhibitor of tumor growth and progression in many cancers (Tu et al. 2009); therefore, regardless of its diagnostic and prognostic values it could be considered as an important therapeutic candidate for treating the malignancies in future (Liston et al. 2001; Holcik, Gibson and Korneluk 2001; Yang et al. 2003); however, further research should attempt to investigate the molecular mechanisms suppressing XAF1 expression in cancers and then examine the functional values of XAF1 in cancer growth and progression.

In the current study, it was revealed that XAF1 could mediate the behavior of the tumor cells after silencing *HS6ST3* in the breast cancer by changing the expression of several genes such as caspases, STAT1, p53-related proteins, Beclin-1, Somatostatin. Herein, we proposed that targeting *HS6ST3* might be useful therapeutic tool for treatment of breast cancer. This study elucidated the role of *HS6ST3* in breast cancer cell lines *in vitro*; however, *in vivo* examining of the influence of *HS6ST3* in regulating the breast cancer cell could be complementary to this work. On the other hand, *HS6ST3* might be a potential therapeutic target for malignancies other than breast cancer. Therefore, further studies are needed to achieve its potential antitumorigenic applications.

4.4 Identification of a novel molecular pathway in relation with *HS6ST3*

We identified the potential role of *HS6ST3* for regulating the cell phenotypes in breast cancer. Herein, we show a schematic diagram for the relationship of *HS6ST3*-related genome-wide genes which is based on our experimental observations and in agreement with the extensive literature review. (Appendix: Figure 4.1).

4.5 Analysis of the drug sensitivity of the breast cancer after silencing *HS6ST3*

We hypothesized that *HS6ST3* is involved in cancer growth and progression by modulating several relevant genes. Extensive analysis of our microarray data revealed that the regulation of some of the potential genes might sensitize tumor cells to chemotherapeutic reagents. We examined the candidacy of XAF1 as a tumor suppressor in breast cancer therapy. Therefore, we found that silencing *HS6ST3* in T47D modulated the cellular response to Cisplatin and 5-fluorouracil (5-fu) in breast cancer. In specific, it was identified that breast cancer cells were sensitized to the cytotoxic effect of cisplatin and 5-fu by silencing *HS6ST3*.

As discussed, suppression of the growth and progression of the breast cancer was mainly mediated by down-regulation of *IGF1R* and up-regulation of the *XAF1* after silencing *HS6ST3* as its downstream factors. In addition to this significant discovery, we noticed that the down-regulation of IGF1R and up-regulation of XAF1 were reported to sensitize the malignant cells to several chemotherapeutic reagents (Hellawell et al. 2003). IGF1R was over-expressed in many malignancies such as prostate cancer, melanoma ovary cancer and renal carcinoma and thus modulating the cancer growth and progression.

Therefore, several researchers hypothesized that IGF1R expression may contribute in tumor resistance to chemotherapy (Eckstein et al. 2009; Yavari et al. 2010; Zuo and Luo 2010). Liu et al. showed that stimulation of IGF1R in esophageal carcinoma induced chemoresistance to cisplatin, 5-fluorouracil (5-fu) and camptothecin (Liu et al. 2002). Other researchers understood that inhibition of IGF1R may enhance the cytotoxic effect of chemotherapeutic agents such as 5-fu on several cancers such as colorectal carcinoma and renal cancer (Dallas et al. 2009; Zeng et al. 2009; Yuen et al. 2009). Rochester et al. found that down-regulation of IGF1R sensitized the prostate cancer cells to DNA-damaging drugs (Rochester et al. 2005). Later, other researchers observed an enhanced chemosensitivity to cisplatin after silencing *IGF1R* in melanoma, ovary cancer, lung cancer, renal carcinoma, teratoid/ rhabdoid tumor, mesothelioma and skin tumors (Yeh, Bohula and Macaulay 2006; Gao et al. 2008; Dong et al. 2008; Yuen et al. 2009; D'cunja et al. 2007; Kai et al. 2009; Liu et al. 2010). Furthermore, the potent influence of *IGF1R* silencing on cancer chemosensitization was exhibited both *in vitro* and *in vivo* (Zeng et al. 2009).

Cisplatin is a chemotherapeutic drug which has been used in anti-tumor therapy for more than four decades. Although it is not included in traditional regime used for treatment of the breast cancer, it has been effectively used on several cancers in human. Cisplatin could induce the apoptosis by formation of DNA adducts and causing DNA damage (Milosavljevic et al. 2010; Maiani, Diederich and Gonfloni 2011). Although several theories were hypothesized for cisplatin function, its direct and indirect function on the

tumoral protein expression is still unclear (Gibson 2009; Krause-Heuer et al. 2009; Tabata et al. 2011).

Cyclin A2, an indicator of poor prognosis in several cancers, was introduced in Suzuki's study as an important factor which modulate the aggressiveness of tumor cells by activation of PI3K pathway and induced resistance to cisplatin (Suzuki et al. 2010). Herein, we noticed that cyclin A2 was down-regulated after silencing *HS6ST3* in our microarray data by more than 40% ($p< 0.01$). Thus, sensitization of tumor cells to cisplatin in the current study might be attributable to down-regulation of cyclin A2 after silencing *HS6ST3* in breast cancer. The Wilson disease protein (ATP7B) is an ATPase which adjusts copper transportation and hence regulates the copper homeostasis in the cells. Expression of ATP7B was shown to be associated with chemoresistance to cisplatin (Dmitriev 2011). Our microarray analysis revealed that ATP7B was down-regulated in *HS6ST3*-knocked down cells by 36% ($p< 0.05$). Therefore, the observed down-regulation might be another possible reason for sensitizing the breast cancer cells to cisplatin. Rouette et al. showed that cisplatin induce cell death by activating B-cell-lymphoma 2 (BCL2). They further indicated that over-expression of BCL2 could promote the treatment efficiency of cisplatin on endometrial cancer (Rouette et al. 2011). In the current study, we noticed that BCL2L1 and BCL2L14 which are the facilitator of the cellular apoptosis was up-regulated in *HS6ST3*- knocked down cells by 60% ($p< 0.001$) and 46% ($p< 0.05$) respectively. We think that the alteration in the expression of BCL2 subsets could potentiate the cisplatin function in breast cancer. Leong et al. showed that activation of BCL2 superfamily might be mediated by p63/ p73 network in response to

cisplatin treatment. TAp63 promote the survival of the breast cancer cells, while TAp73 induce apoptosis by activating BCL2 superfamily. However, TAp73 and TAp63 may co-express in the cancer cells and then bind to each other. Dissociation of these proteins is a determining factor that could regulate the relative percentage of the live cells. Breast cancers expressing both TAp63 and TAp73, exhibited cisplatin sensitivity that was closely TAp73-dependent. Cisplatin induces the dissociation of TAp73 from TAp63 through phosphorylating TAp73 and thus by activating BCL2 family induce the cell death (Leong et al. 2007; Carroll et al. 2006). By reviewing our microarray data we understood that TAp73 was up-regulated by 58% ($p<0.01$) after silencing *HS6ST3* in breast cancer, while no significant change occurred in the expression of TAp63. Hence, it is presumable that up-regulation of TAp73 induced an imbalance between TAp63 and TAp73 and therefore, over-expression of TAp73 could further augment the cytotoxic effect of cisplatin in breast cancer.

Imatinib is able to inhibit dissociation of TAp63 from TAp73. As stated, we found that silencing *HS6ST3* sensitized the breast cancer cells to the cytotoxic effect of cisplatin. In order to examine whether the observed sensitivity was occurred via p63/ p73 network, we tried to treat the breast cancer cells with maximum non-toxic dose of imatinib to inhibit the dissociation of TAp63 from TAp73. Then, it was identified that treating *HS6ST3*-silenced cells with imatinib and cisplatin was not significantly different from *HS6ST3*-silenced cells which was treated with cisplatin only, while the relative percentage of the live cells were significantly increased in control group which treated with imatinib and cisplatin compared to the control group which was treated with cisplatin only. This

observation indicates that silencing *HS6ST3* strongly promoted the dissociation of TAp63 from TAp73 in p63/ p73 pathway so that imatinib was not able to increase the cell survival by inhibiting of the dissociation. On the other hand, we further propose that up-regulation of Tap73 could independently enhance the cytotoxic effect of cisplatin on the breast cancer cells (Appendix: Figure 4.2).

As discussed, XAF1 has been shown to be down-regulated in many cancers. Over-expression of XAF1 was also shown as a potent inhibitor of cancer growth and progression. A few studies, examined the critical role of XAF1 expression on the sensitivity of the cancer cells to chemotherapeutic agents. Lee et al. understood that restoration of XAF1 expression sensitized the urogenital cancers (kidney, bladder and prostate) to the cytotoxic effect of etoposide and 5-fluorouracil (5-fu) (Lee et al. 2006). This effect was further confirmed in Pinho's study that examined the role of XAF1 expression on chemotherapy response of the bladder cancer (Pinho et al. 2009).

During the last decade, 5-fluorouracil (5-fu) has been widely used as a classic anti-tumor drug for treatment of solid tumor such as breast cancer, gastric cancer, colorectal cancer, prostate cancer, pancreatic cancer and urogenital carcinomas. 5-fu specifically acts on thymidylate synthase (TYMS) during the S phase and thus inhibiting the cell cycle by damaging DNA and RNA synthesis (Shahrokni, Rajebi and Saif 2009). Thymidylate synthase is an important enzyme which is actively involved in synthesis of DNA. (Longley, Harkin and Johnston 2003; Salk, Grogan and Chang 2006; Parker and Stivers 2011) Researchers suggested TYMS as a useful serological biomarker which could evaluate the chemotherapy responsiveness in colorectal cancer (Shebzukhov et al. 2005;

Gusella et al. 2009; Tan et al. 2011). TYMS was introduced as a critical gene which could modulate the chemoresistance to 5-fu and methotrexate. Three polymorphisms were discovered for thymidydlate synthase gene so that they could affect the expression of TYMS in several cancers (Shahrokni, Rajebi and Saif 2009; Fujishima et al. 2010). Kumar et al. revealed that polymorphisms of thymidydlate synthase gene significantly influenced the chemoresponsiveness of 5-fu in breast cancer (Kumar, Vamsy and Jamil 2010). Over-expression of TYMS was shown to be associated with resistance to 5-fu in several cancers such as colorectal cancer and esophageal cancer (Lecomte et al. 2004; Marsh 2005; Langer et al. 2007; An et al. 2007; Jensen et al. 2008; Peters et al. 2009; Martinez-Balibrea et al. 2010; Watson et al. 2010). Ichikawa et al. found that low expression of TYMS was associated with tumor shrinkage as well as longer survival of gastric cancer after chemotherapy (Ichikawa et al. 2006). Takagi et al. showed that a reduction in the expression of TYMS enhanced the chemosensitivity to 5-fu. More importantly, they understood that the expression of TYMS was regulated by cyclin-dependent kinase (CDK). Then, they concluded that inhibition of CDK expression by specific drug resulted in suppression of TYMS in a dose-dependent manner and sensitized the cancer cells to 5-fu in colorectal cancer (Takagi et al. 2008).

Our microarray analysis showed that by silencing *HS6ST3*, the expression of CDK-related genes (CDK2, CDK4, CDK7, CDK8, CDK9, CDK10, CDKAL1, CDKL3, CDKL5, CDK5RAP3, CDK2AP2, CDKN2AIP, and CDK5RAP2) was significantly decreased, while the expression of CDK-inhibitor genes (CDKN2B, CDKN2D and CDKN1C) was increased in breast cancer. Furthermore, we noticed that the expression of

TYMS was reduced by 53% ($p<0.01$) after silencing *HS6ST3* in breast cancer. Therefore, we may propose that silencing *HS6ST3* directly inhibited the expression of TYMS or indirectly by up-regulating the CDK-inhibitor genes and consequently down-regulation of CDK-related genes that modulates the TYMS expression. Together, it might be concluded that low expression of TYMS in *HS6ST3*-silenced breast cancer cells could effectively enhance the cell mediated cytotoxicity of 5-fu *in vitro*.

Silencing of *HS6ST3* showed that it could alter the expression of the several genes which are critical for chemosensitivity of the breast cancer cells to the cytotoxic effect of cisplatin and 5-fu. The significant role of *HS6ST3* on the treatment of breast cancer was unraveled *in vitro* in the current pre-clinical study; thus a direct extension of this work should be accomplished *in vivo*. In addition, the results of these findings should be validated on the other cancer cell lines. Together, the inclusion of *HS6ST3*-targeted treatment in chemotherapeutic regimes could provide an effective therapy for breast cancer as well as the other malignancies.

4.6 Expression analysis of HS6ST3 in clinical specimens of breast ductal carcinoma

HS6ST3 is a heparan sulfate sulfotransferase that specifically transfers sulfate group from 3'-phosphoadenosine 5'- phosphosulfate (PAPS) to C6 position of N-acetylglucosamine (GlcNAc) residues of heparan sulfate chain. HS6ST3 was shown to play an important role in modifying a tissue-specific 6-O-sulfation in heparan sulfate chain (Habuchi et al. 2000). Changes of the expression of HS6ST3 were reported to be associated with an altered heparan sulfate domain structure that may affect the molecular interactions and signaling processes (Do et al. 2006).

Several studies have demonstrated that 6-O-sulfotransferases are involved in important biological processes such as embryonic organogenesis, postnatal growth and development (Kamimura et al. 2001; Sedita, Izvolsky and Cardoso 2004; Habuchi et al. 2007; Izvolsky et al. 2008). Tissue-specific expression of HS6ST3 at different time points of embryonic period indicates that their timely expression is significantly required for growth factor-related development during organogenesis (Sedita, Izvolsky and Cardoso 2004). In addition to the embryonic development, HS6ST isoforms seem to influence the anticoagulant characteristic of heparan sulfate during its biosynthesis (Zhang et al. 2001).

Recently, researchers have shown an increased interest in identifying the potential role of 6-O-sulfotransferases in the malignant process of carcinogenesis. Of the few studies, remarkable over-expression of HS6ST2 has been demonstrated in serous, papillary, clear cell carcinoma of ovary as well as cervical and corpus cancer of uterine (Kanoh et al. 2006; Seko et al. 2009). However, the potential role of HS6ST3 has not been studied in any of the human malignancies. Thus, the significance of HS6ST3 was extensively explored on 258 cases of the breast cancer in the current study. In this study, it was revealed that HS6ST3 expressed in epithelial and extracellular matrix compartments with expression being the strongest in epithelial and stromal cell compartments. Immunoreactivity staining (IRS) analysis revealed that the expression of HS6ST3 was significantly diminished in stroma matrix of the breast adenocarcinoma compared to the normal sections. Analysis showed that by 95% confident interval, the lower and upper bound (13.336-18.602) of the staining intensity of HS6ST3 in the matrix stroma of the cancer sections had no overlapping with the lower and upper bound (35.735-48.683) of

similar staining in the normal section ($p< 0.001$). This finding was strongly suggestive of the diagnostic characteristics of HS6ST3 as a sensitive test for early detecting of the breast cancer.

Significant correlations were detected between the expression of HS6ST3 and several clinicopathological factors among all of the tissue compartments; however, it seems that the biological significance of HS6ST3 is compartment-specific in the cancer tissues as it differentially expressed in various tissue compartments. Analysis of the immunoreactivity staining (IRS) of the HS6ST3 showed a significant correlation between the expression of the HS6ST3 in stroma matrix of the cancer sections and histograde. In specific, the expression of HS6ST3 was significantly enhanced by increasing the histograde with expression being the weakest in histograde 1. On the other hand, immunoreactivity staining of HS6ST3 in epithelial and stromal cells revealed no correlation with histograde, while analysis of weighted average intensity (WAI) of the HS6ST3 of epithelial cells represented a significant correlation with histograde ($p=0.016$). In other words, the expression of HS6ST3 was enhanced by increasing the histograde with expression being the weakest in histograde 1. This finding was consistent with results we discussed earlier regarding the correlation of immunoreactivity staining of stroma matrix with histograde of the cancer sections. By moving from histograde 1 to histograde 2, the IRS and WAI were remarkably increased; however, by shifting from histograde 2 to histograde 3, a slight reduction occurred in the expression of the HS6ST3 in epithelial cells and matrix stroma of the breast cancer sections.

Survival analysis showed breast cancers were associated with poorer prognosis in older ages, bigger tumors, progesterone or HER2 negativity. Histograde weakly predicted the disease free survival (DFS) of the breast cancer patients, but it was not predictive for overall survival (OS) and survival after recurrence (SAR). In addition, we did not find any prognostic value for lymph node metastasis, estrogen receptor status and other clinicopathological parameters.

On the other hand, univariate survival analysis revealed that staining intensity of HS6ST3 in various tissue compartments could potentially predict the OS, DFS and SAR of the breast cancer patients. Performing multivariate survival analysis further confirmed that IRS and WAI of the tissue compartments could be used as a valuable prognostic factor for breast cancer. While multivariate analysis showed that the expression level of HS6ST3 could strongly predict the prognosis of the breast cancer patients in terms of OS and DFS, it was not independently able to predict the SAR of the breast cancer patients. Survival analysis interestingly showed that higher expression of HS6ST3 in stroma matrix resulted in shorter survival, while similar expression in stroma matrix of the tumors with less than three lymph nodes involvements was predictive of a better survival. On the other hand, it was identified that the higher expression of HS6ST3 in stromal cells of lower histograde and intermediate nuclear grade could valuably predict a longer survival for breast cancer patients. Therefore, we may hypothesize that during the process of carcinogenesis, the expression of HS6ST3 was firstly diminished in stroma matrix. By progressing of the tumor histograde, the epithelial and stromal cells expressed more HS6ST3; and thus the expression of the HS6ST3 increased in stroma matrix of the

cancerous tissue. Although by increasing of the higher histograde, the expression pattern of the HS6ST3 had an ascending trend in the epithelial cells and stroma matrix compartments, a slight reduction was observed in the expression of HS6ST3 of the histograde 3 compared to the histograde 2. Thus, it is postulated that the expression of HS6ST3 in stroma matrix could be regulated by epithelial and stromal cells. In other words, the expression of HS6ST3 in stromal matrix could be a consequent of HS6ST3 expression in epithelial or stromal cell. However, we think that the expression of the HS6ST3 in stroma matrix could directly play a crucial role in the malignant process of carcinogenesis because it could potentially edit the 6-O-sulfation of the cell surface and stroma matrix heparan sulfates and thus change the interactions of the heparan sulfate chain with a several ligands such as growth factors. This alteration in turn could affect the growth factor signaling pathway(s) which enhance the tumoral growth and progression.

This study was the first research which unraveled the clinical significance of the HS6ST3 in breast cancer. Herein, we understood that HS6ST3 was up-regulated in the breast cancer and could potentially regulate the growth and progression of this malignancy. Although the underlying molecular mechanisms are unclear, we think that HS6ST3 might have an important contribution in the malignant process of carcinogenesis. This contribution could be possibly due to the alteration of 6-O-sulfation of heparan sulfate chain which could potentially change the interactions between heparan sulfate molecules with a variety of signaling ligands such as growth factors.

Together, the current study is of valuable importance in terms of diagnosis the breast cancer at any grade or stage. In addition, it was provided a clinically significant insight

for clinician to predict the breast cancer prognosis and then decide about the timely ideal therapy.

This study was restricted to unravel the diagnostic and prognostic values of HS6ST3 in the breast cancer; but we did not explore the role of HS6ST3 in other malignancies. Thus, to achieve this goal further research is required.

4.7 Expression analysis of SULF1 in clinical specimens of breast ductal carcinoma

A variety of molecular changes has been identified in breast cancer; however, their clinical significance is poorly understood. SULF1 is a potent sulfation modifying enzymes which specifically edit 6-O-sulfation on the cell surface and extracellular matrix by removing the sulfate group from C6 position of N-acetylglucosamine in heparan sulfate chain and thereby modulating the biological activity of heparan sulfate (Holst et al. 2007). SULF1 is dysregulated in breast cancer as well as several other cancers. DNA methylation and histone acetylation are two proposed mechanisms for down regulation of SULF1 gene in epithelial cells of cancers such as ovarian, breast and hepatocellular carcinoma (Castro et al. 2008). Although, this alteration could potentially be a significant stage in tumorogenesis of breast cancer, the molecular basis for the involvement of SULF1 expression in malignant process is still unknown.

In this study, we have shown that SULF1 expresses in epithelial cells as well as extracellular matrix with expression being the weakest in stromal cells. Significant correlations were detected between the expression of SULF1 and several

clinicopathological factors among all of the tissue compartments; however, it seems that the biological significance of SULF1 is specific to tissue compartments since localization of this enzyme has a multimodal nature in different tissue compartments. In particular, we identified that the expression of SULF1 is differentially associated with various clinicopathological parameters in different tissue compartment of breast cancer specimens.

In this study, the clinical significance of SULF1 was extensively explored on 267 cases of the breast cancer. SULF1 was differentially expressed in epithelial cells and extra cellular matrix compartments. The expression of SULF1 in majority of epithelial cells of the cancer sections had an obvious reduction; however, due to the large variation in the expression of this enzyme in different grades we did not find any significant difference amongst the histogrades. Unlike the epithelial cells, the expression of SULF1 in stromal cells was statistically lower than other tissue compartments both in normal and cancer sections. This expression significantly increased when the breast cancer shifted from histograde 2 to the highest histograde (3) (P=0.049). Additionally, it was revealed that the stronger SULF1 expression in stromal cells is predictive of a poorer prognosis for breast cancer survival; while, a similar expression of SULF1 in epithelial cells and stroma matrix was observed to have a longer survival in breast cancer patients (Table 3.18). SULF1 express weaker in stromal cells than other tissue compartments; however, it seems that increasing the expression of SULF1 in stromal cells is clinically of great importance as a novel prognostic factor. Although SULF1 is less expressed in matrix stroma of breast cancer compared to normal breast tissue, it is postulated that increasing

SULF1 expression in stromal cells of more invasive cancers is concomitant with increasing the SULF1 shedding in stroma matrix. Thus, interpreting SULF1 staining intensity in all of the tissue compartments could be a more useful tool for predicting a cancer state specifically with regards to clinicopathological associations.

Survival analysis in our study showed that more lymph node infiltration and bigger tumor size were associated with poorer OS and DFS. However, we could not distinguish any association between histograde and survival of breast cancer patients. On the other hand, while none of the histopathological features were able to predict DFS in univariate survival analysis, the expression of SULF1 was able to significantly function as a valuable prognostic factor for predicting both OS and DFS. Tumor laterality was another prognostic factor which suggests that left sided breast cancer are significantly associated with a better prognosis. This observation might be due to the anatomical differences in vascular distribution between left and right auxiliary regions. Multivariate survival analysis further confirmed that the IRS of tissue compartments could be used as a valuable prognostic factor.

All together, these observations suggest a potential role for involvement of SULF1 in malignant process of carcinogenesis in breast cancer. Since, the expression of SULF1 is generally higher in normal breast tissue compared to cancerous tissue; we postulate that down regulation of SULF1 in breast cancer epithelial cells as well as other cancers could be a starting point in the chain of cancer tumorogenesis. A possible explanation is that under-expression or non-functionality of expressing SULF1 in epithelial cells of breast

tissue could result in over-sulfation of carbon 6 positions in heparan sulfate chain which in turn entertains a variety of signaling growth factors on the cell membrane of epithelial cells. Therefore, in the process of tumorogenesis, normal epithelial cells present invasive phenotype. However, once the cancer cells transform to higher histograde, stromal cells might be reactivated in response to the malignant state of stroma matrix microenvironment and thus the expression of SULF1 would be enhanced by stromal cells in order to modulate the malignant state by suppressing heparin-binding growth factor signaling. Besides, due to the rapid turnover of reactive stromal cells, the SULF1 content of stroma matrix is increased in higher grades of breast cancer (Appendix: Figure 4.3). Although, stromal cells may attempt to repress the rapidly growing rate of epithelial cells by expressing SULF1 (Lai et al. 2004), this inhibitory mechanism might not be strong enough to completely repress the uncontrolled invasive phenotypes of the tumor cells.

The newly developed biomarkers during the last decades have played an important role in identifying signaling pathway(s) involved in malignant process of breast tumorogenesis. In addition, some of these biomarkers have served as novel diagnostic or prognostic detection markers in breast cancer as well as other cancers. In fact, identifying new cancer biomarkers lead to early detection of cancer besides receiving optimal treatment. On the other hand, they could be potentially targeted as therapeutic molecule(s) to inhibit the pathological process of tumorogenesis (Shao et al. 2011). Currently, optimal treatment for breast cancer basically depends on the stage of disease at the time of diagnosis. An effective treatment further depends on availability of several biomarkers

profile such as estrogen receptor, progesterone receptor and HER2 (Alvarez Goyanes et al. 2010).

This study greatly has contributed to exploring an important prognostic role for SULF1 in breast cancer as it has provided guidelines for determining breast cancer survival. However, interpretation of interesting correlations of HER2 and tumor size with SULF1 expression which were observed in this study has remained unknown due to the lack of current knowledge about the biological role of SULF1 in human. Thus, we would like to suggest this study as a preliminary basis for further research on using human SULF1 as a diagnostic biomarker in breast cancer. Therefore, in the future, using SULF1 expression as a powerful tool may enable clinicians to decide their therapeutic strategies ranging from less invasive therapies to very invasive therapies such as total mastectomy as well as combinational chemotherapy and radiotherapy. However, further research is required to uncover the underlying molecular mechanisms for the involvement of SULF1 in breast carcinogenesis. Meanwhile, a direct extension of this work should be considered on other cancers as this study was mainly restricted to breast cancer.

CONCLUSION

AND

FUTURE STUDIES

In this study, we showed that that silencing *HS6ST3* could significantly diminish the tumor growth and progression in breast cancer by reducing the proliferation, migration and invasion, while inducing the apoptosis and enhancing the adhesion. Genome wide microarray analysis revealed that the expression of a number of genes was changed after silencing *HS6ST3* in the breast cancer. By performing extensive literature review, we found a few critical up- and down-regulated genes which might be involved in the malignant process of carcinogenesis in the breast cancer. Out of a few recognized genes, we understood that the functional role of *IGF1R* and *XAF1* had of great importance in the *HS6ST3* pathway. IGF1R was significantly down-regulated, while XAF1 was up-regulated after silencing *HS6ST3* in the breast cancer. To validate our hypothesis, several functional experiments were designed by silencing *HS6ST3* and blocking IGF1R or silencing *XAF1* in the breast cancer. Then, it was found that *IGF1R* and *XAF1* significantly could modulate the phenotypic behavior of the tumor cells in mammary cancer. Thus, we found that IGF1R and XAF1 critically mediated the modulatory function of the *HS6ST3* in the breast cancer.

Additionally, it was shown that silencing *HS6ST3* could diminish the expression of the heparan sulfate on the cell surface. Our microarray data revealed that the expression of glypican 6 was significantly reduced after silencing *HS6ST3* in the breast cancer, while syndecans bore no significant difference. Since silencing *HS6ST3* diminished the cytoplasmic heparan sulfate expression, it is plausible that glypican 6 comprised the

major content of heparan sulfate on the cell surface of the breast cancer cell line and thus silencing *HS6ST3* affected the expression of the glypican 6 in the breast cancer.

Our findings indicated that *HS6ST3* could regulate the breast cancer phenotypic behavior by regulating the expression of critical genes directly and/ or influence the interactions between heparan sulfate and several growth factors on the cell surface.

Based on our microarray data, we further noticed that changing the expression of specific genes might sensitize the tumoral cell to specific chemotherapeutic drugs. Then, by performing cytotoxicity assays it was identified that silencing *HS6ST3* could sensitize the breast cancer cells to the cytotoxic effect of Cisplatin and 5-fu.

Therapeutic targeting of IGF1R and XAF1 has attracted attentions in many studies. Herein, we found an important gene which could regulate *IGF1R* and *XAF1* and thus could target both of them at the same time while it could sensitize the breast cancer to Cisplatin and 5-fu. Thus, a new pathway was introduced that could be used as an effective therapy for the breast cancer.

The immunohistochemical findings on heparan sulfate editing enzymes using HS6ST3 and SULF1 antibodies in the breast cancer showed that the expression of SULF1 and HS6ST3 were dysregulated in breast cancer. Besides, it was identified that HS6ST3 could

be used as a novel diagnostic and prognostic tool for breast cancer, while SULF1 could be used as a prognostic factor in breast carcinoma.

These finding are of considerable significance since they have introduced an interesting gene which regulates breast cancer behavior. The significance of the current study is not limited to the regulatory role of *HS6ST3* in cellular processes because it could be also used as a novel prognostic and/ or diagnostic biomarker in breast cancer. In addition, it might be useful as an effective therapeutic target for treating breast cancer as well as other malignancies.

REFERENCES

References

Abiatari, I, Kleeff, J, Li, J, Felix, K, Büchler, MW and Friess, H, 2006, 'Hsulf-1 regulates growth and invasion of pancreatic cancer cells', J Clin Pathol, vol. 59, no. 10, pp. 1052-1058.

Ai, X, Do, AT, Kusche-Gullberg, M, Lindahl, U, Lu, K and Emerson, CP, 2006, 'Substrate specificity and domain functions of extracellular heparan sulfate 6-O endosulfatases, QSulf1 and QSulf2', J Biol Chem, vol. 281, no. 8, pp. 4969-4976.

Albrektsen, G, Heuch, I, Hansen, S and Kvåle, G, 2005, 'Breast cancer risk by age at birth, time since birth and time intervals between births: exploring interaction effects', Br J Cancer, vol. 92, no. 1, pp. 167-175.

Allen, BL, Filla, MS and Rapraeger, AC, 2001, 'Role of heparan sulfate as a tissue-specific regulator of FGF-4 and FGF receptor recognition', J Cell Biol, vol. 155, no. 5, pp. 845-858.

Allen, NE, Beral, V, Casabonne, D, Kan, SW, Reeves, GK, Brown, A, Green, J and Million Women Study Collaborators, 2009, 'Moderate alcohol intake and cancer incidence in women', J Natl Cancer Inst, vol. 101, no. 5, pp. 296-305.

Alonso Gordoa, T, García-Sáenz, JÁ, Rodríguez Moreno, JF, Hernández Pérez, FJ and Díaz-Rubio, E, 2011, 'Is trastuzumab-induced cardiotoxicity involved in onco-cardiology outcome?', Clin Transl Oncol, vol. 13, no. 7, pp. 451-459.

Althuis, MD, Dozier, JM, Anderson, WF, Devesa, SS and Brinton, LA, 2005, 'Global trends in breast cancer incidence and mortality 1973-1997', Int J Epidemiol, vol. 34, no. 2, pp. 405-412.

Alvarez Goyanes, RI, Escobar Pérez, X, Camacho Rodríguez, R, Orozco López, M, Franco Odio, S, Llanes Fernández, L, Guerra Yi, M and Rodríguez Padilla, C, 2010, 'Hormone receptors and other prognostic factors in breast cancer in Cuba', MEDICC review, vol. 12, no. 1, pp. 36-40.

American Cancer Society (2011a), Breast Cancer Facts and Figures, 2009-2010. http://www.cancer.org/Research/CancerFactsFigures/BreastCancerFactsFigures/breast-cancer-facts--figures-2009-2010, access date: 08/01/2011.

American Cancer Society (2011b), Cancer Facts and Figures, 2011-2012. http://www.cancer.org/acs/groups/content/@epidemiologysurveilance/documents/document/acspc-030975.pdf, access date: 08/01/2011.

American Cancer Society, (2011c), BreastCancer.ORG. http://www.cancer.org/Cancer/BreastCancer/index, access date: 08/01/2011.

An, Q, Robins, P, Lindahl, T and Barnes, DE, 2007, '5-Fluorouracil incorporated into DNA is excised by the Smug1 DNA glycosylase to reduce drug cytotoxicity', Cancer Res, vol. 67, no. 3, pp. 940-945.

Arnone, P, Zurrida, S, Viale, G, Dellapasqua, S, Montagna, E, Arnaboldi, P, Intra, M and Veronesi, U, 2010, 'The TNM classification of breast cancer: need for change', Updates in surgery, vol. 62, no. 2, pp. 75-81.

Arora, V, Cheung, HH, Plenchette, S, Micali, OC, Liston, P and Korneluk, RG, 2007, 'Degradation of survivin by the X-linked inhibitor of apoptosis (XIAP)-XAF1 complex', J Biol Chem, vol. 282, no. 36, pp. 26202-26209.

Autier, P, Boniol, M, La Vecchia, C, LaVecchia, C, Vatten, L, Gavin, A, Héry, C and Heanue, M, 2010, 'Disparities in breast cancer mortality trends between 30 European countries: retrospective trend analysis of WHO mortality database', BMJ, vol. 341, pp. c3620.

Avnet, S, Sciacca, L, Salerno, M, Gancitano, G, Cassarino, MF, Longhi, A, Zakikhani, M, Carboni, JM, Gottardis, M, Giunti, A, Pollak, M, Vigneri, R and Baldini, N, 2009, 'Insulin receptor isoform A and insulin-like growth factor II as additional treatment targets in human osteosarcoma', Cancer Res, vol. 69, no. 6, pp. 2443-2452.

Ballard-Barbash, R, Hunsberger, S, Alciati, MH, Blair, SN, Goodwin, PJ, McTiernan, A, Wing, R and Schatzkin, A, 2009, 'Physical activity, weight control, and breast cancer risk and survival: clinical trial rationale and design considerations', J Natl Cancer Inst, vol. 101, no. 9, pp. 630-643.

Bantema-Joppe, EJ, de Munck, L, Visser, O, Willemse, PHB, Langendijk, JA, Siesling, S and Maduro, JH, 2011, 'Early-Stage Young Breast Cancer Patients: Impact of Local Treatment on Survival', Int J Radiat Oncol Biol Phys, vol. 81, no. 4: 553-559.

Barbareschi, M, Maisonneuve, P, Aldovini, D, Cangi, MG, Pecciarini, L, Angelo Mauri, F, Veronese, S, Caffo, O, Lucenti, A, Palma, PD, Galligioni, E and Doglioni, C, 2003, 'High syndecan-1 expression in breast carcinoma is related to an aggressive phenotype and to poorer prognosis', Cancer, vol. 98, no. 3, pp. 474-483.

Barker, S, 2003, 'Anti-estrogens in the treatment of breast cancer: current status and future directions', Curr Opin Investig Drugs, vol. 4, no. 6, pp. 652-657.

Barth, A, Köchli, OR, Brenner, RJ, Giuliano, E and Castiglione, M, 1995, '[Ductal carcinoma in situ of the breast]', Schweiz Med Wochenschr, vol. 125, no. 4, pp. 103-112.

Bernfield, M, Götte, M, Park, PW, Reizes, O, Fitzgerald, ML, Lincecum, J and Zako, M, 1999, 'Functions of cell surface heparan sulfate proteoglycans', Annu Rev Biochem, vol. 68, pp. 729-777.

Betsill, WL, Rosen, PP, Lieberman, PH and Robbins, GF, 1978, 'Intraductal carcinoma. Long-term follow-up after treatment by biopsy alone', JAMA, vol. 239, no. 18, pp. 1863-1867.

Bharadwaj, AG, Goodrich, NP, McAtee, CO, Haferbier, K, Oakley, GG, Wahl, JK and Simpson, MA, 2011, 'Hyaluronan suppresses prostate tumor cell proliferation through diminished expression of N-cadherin and aberrant growth factor receptor signaling', Exp Cell Res, vol. 317, no. 8, pp. 1214-1225.

Bjelic-Radisic, V and Petru, E, 2010, '[Hormonal contraception and breast cancer risk]', Wien Med Wochenschr, vol. 160, no. 19-20, pp. 483-486.

Bohnet, HG and Bertram, M, 1989, '[The peripheral hormone level in premenopausal patients with benign breast changes and their modification by various hormone therapies]', Gynakologe, vol. 22, no. 4, pp. 255-261.

Boice, JD, Land, CE, Shore, RE, Norman, JE and Tokunaga, M, 1979, 'Risk of breast cancer following low-dose radiation exposure', Radiology, vol. 131, no. 3, pp. 589-597.

Bonaïti-Pellié, C, Andrieu, N, Arveux, P, Bonadona, V, Buecher, B, Delpech, M, Jolly, D, Julian-Reynier, C, Luporsi, E, Noguès, C, Nowak, F, Olschwang, S, Orsi, F, Pujol, P, Saurin, JC, Sinilnikova, O, Stoppa-Lyonnet, D and Thépot, F, 2009, '[Cancer genetics: estimation of the needs of the population in France for the next ten years]', Bull Cancer, vol. 96, no. 9, pp. 875-900.

Borràs, JM, Espinàs, JA and Castells, X, 2003, '[The evidence on breast cancer screening: the story continues]', Gac Sanit, vol. 17, no. 3, pp. 249-255.

Brown, NS and Bicknell, R, 2001, 'Cell migration and the boyden chamber', Methods Mol Med, vol. 58, pp. 47-54.

Burris, HA, 2011, 'Trastuzumab emtansine: a novel antibody-drug conjugate for HER2-positive breast cancer', Expert Opin Biol Ther, vol. 11, no. 6, pp. 807-819.

Burtscher, I and Christofori, G, 1999, 'The IGF/IGF-1 receptor signaling pathway as a potential target for cancer therapy', Drug Resist Updat, vol. 2, no. 1, pp. 3-8.

Byun, DS, Cho, K, Ryu, BK, Lee, MG, Kang, MJ, Kim, HR and Chi, SG, 2003, 'Hypermethylation of XIAP-associated factor 1, a putative tumor suppressor gene from the 17p13.2 locus, in human gastric adenocarcinomas', Cancer Res, vol. 63, no. 21, pp. 7068-7075.

Calabrese, GC, Alberto, MF, Tubio, R, Marani, MM, Fernández De Recondo, ME, Lazzari, M and Recondo, EF, 2004, 'A small fraction of dermatan sulfate with significantly increased anticoagulant activity was selected by interaction with the first complement protein', Thromb Res, vol. 113, no. 3-4, pp. 243-250.

Calle, EE, Feigelson, HS, Hildebrand, JS, Teras, LR, Thun, MJ and Rodriguez, C, 2009, 'Postmenopausal hormone use and breast cancer associations differ by hormone regimen and histologic subtype', Cancer, vol. 115, no. 5, pp. 936-945.

Canavese, G, Dozin, B, Vecchio, C, Tomei, D, Villa, G, Carli, F, Del Mastro, L, Levaggi, A, Rossello, C, Spinaci, S, Bruzzi, P and Catturich, A, 2011, 'Accuracy of sentinel lymph node biopsy after neo-adjuvant chemotherapy in patients with locally advanced breast cancer and clinically positive axillary nodes', Eur J Surg Oncol, vol. 37, no. 8, pp. 688-694.

Canfell, K, Banks, E, Moa, AM and Beral, V, 2008, 'Decrease in breast cancer incidence following a rapid fall in use of hormone replacement therapy in Australia', Med J Aust, vol. 188, no. 11, pp. 641-644.

Cano-Gauci, DF, Song, HH, Yang, H, McKerlie, C, Choo, B, Shi, W, Pullano, R, Piscione, TD, Grisaru, S, Soon, S, Sedlackova, L, Tanswell, AK, Mak, TW, Yeger, H, Lockwood, GA, Rosenblum, ND and Filmus, J, 1999, 'Glypican-3-deficient mice exhibit developmental overgrowth and some of the abnormalities typical of Simpson-Golabi-Behmel syndrome', J Cell Biol, vol. 146, no. 1, pp. 255-264.

Carboni, JM, Lee, AV, Hadsell, DL, Rowley, BR, Lee, FY, Bol, DK, Camuso, AE, Gottardis, M, Greer, AF, Ho, CP, Hurlburt, W, Li, A, Saulnier, M, Velaparthi, U, Wang, C, Wen, ML, Westhouse, RA, Wittman, M, Zimmermann, K, Rupnow, BA and Wong, TW, 2005, 'Tumor development by transgenic expression of a constitutively active insulin-like growth factor I receptor', Cancer Res, vol. 65, no. 9, pp. 3781-3787.

Carlsson, P, Presto, J, Spillmann, D, Lindahl, U and Kjellén, L, 2008, 'Heparin/heparan sulfate biosynthesis: processive formation of N-sulfated domains', J Biol Chem, vol. 283, no. 29, pp. 20008-20014.

Carroll, DK, Carroll, JS, Leong, CO, Cheng, F, Brown, M, Mills, AA, Brugge, JS and Ellisen, LW, 2006, 'p63 regulates an adhesion programme and cell survival in epithelial cells', Nat Cell Biol, vol. 8, no. 6, pp. 551-561.

Carter, BA and Page, DL, 2004, 'Phyllodes tumor of the breast: local recurrence versus metastatic capacity', Hum Pathol, vol. 35, no. 9, pp. 1051-1052.

Cascone, P, Fonzi Dagger, L and Aboh, IV, 2002, 'Hyaluronic acid's biomechanical stabilization function in the temporomandibular joint', J Craniofac Surg, vol. 13, no. 6, pp. 751-754.

Castro, NP, Osório, CABT, Torres, C, Bastos, EP, Mourão-Neto, M, Soares, FA, Brentani, HP and Carraro, DM, 2008, 'Evidence that molecular changes in cells occur before morphological alterations during the progression of breast ductal carcinoma', Breast Cancer Res, vol. 10, no. 5, pp. R87.

Chai, J, Shiozaki, E, Srinivasula, SM, Wu, Q, Datta, P, Alnemri, ES, Shi, Y and Dataa, P, 2001, 'Structural basis of caspase-7 inhibition by XIAP', Cell, vol. 104, no. 5, pp. 769-780.

Chakraborty, AK, Liang, K and DiGiovanna, MP, 2008, 'Co-targeting insulin-like growth factor I receptor and HER2: dramatic effects of HER2 inhibitors on nonoverexpressing breast cancer', Cancer Res, vol. 68, no. 5, pp. 1538-1545.

Champion, L, Brain, E, Giraudet, AL, Le Stanc, E, Wartski, M, Edeline, V, Madar, O, Bellet, D, Pecking, A and Alberini, JL, 2011, 'Breast cancer recurrence diagnosis suspected on tumor marker rising: value of whole-body 18FDG-PET/CT imaging and impact on patient management', Cancer, vol. 117, no. 8, pp. 1621-1629.

Chaney, AW, Pollack, A, McNeese, MD, Zagars, GK, Pisters, PW, Pollock, RE and Hunt, KK, 2000, 'Primary treatment of cystosarcoma phyllodes of the breast', Cancer, vol. 89, no. 7, pp. 1502-1511.

Chatzinikolaou, G, Nikitovic, D, Asimakopoulou, A, Tsatsakis, A, Karamanos, NK and Tzanakakis, GN, 2008, 'Heparin--a unique stimulator of human colon cancer cells' growth', IUBMB Life, vol. 60, no. 5, pp. 333-340.

Chen, GH, Lin, FR, Ren, JH, Chen, J, Zhang, JN, Wang, Y and Wang, J, 2006, '[Expression and significance of X-linked inhibitor of apoptosis protein and its antagonized proteins in acute leukemia]', Zhongguo Shi Yan Xue Ye Xue Za Zhi, vol. 14, no. 4, pp. 639-643.

Chen, PW and Kroog, GS, 2010, 'Leupaxin is similar to paxillin in focal adhesion targeting and tyrosine phosphorylation but has distinct roles in cell adhesion and spreading', Cell adhesion and migration, vol. 4, no. 4, pp. 527-540.

Chen, S and Parmigiani, G, 2007, 'Meta-analysis of BRCA1 and BRCA2 penetrance', J Clin Oncol, vol. 25, no. 11, pp. 1329-1333.

Chen, Z, Fan, JQ, Li, J, Li, QS, Yan, Z, Jia, XK, Liu, WD, Wei, LJ, Zhang, FZ, Gao, H, Xu, JP, Dong, XM, Dai, J and Zhou, HM, 2009, 'Promoter hypermethylation correlates with the Hsulf-1 silencing in human breast and gastric cancer', Int J Cancer, vol. 124, no. 3, pp. 739-744.

Choi, M, Craft, B and Geraci, SA, 2011, 'Surveillance and monitoring of adult cancer survivors', Am J Med, vol. 124, no. 7, pp. 598-601.

Choi, S, Kim, Y, Park, H, Han, IO, Chung, E, Lee, SY, Kim, YB, Lee, JW, Oh, ES and Yi, JY, 2009, 'Syndecan-2 overexpression regulates adhesion and migration through cooperation with integrin alpha2', Biochem Biophys Res Commun, vol. 384, no. 2, pp. 231-235.

Choi, WH, Yoo, IR, O, JH, Kim, SH and Chung, SK, 2011, 'The value of dual-time-point 18F-FDG PET/CT for identifying axillary lymph node metastasis in breast cancer patients', Br J Radiol, vol. 84, no. 1003, pp. 593-599.

Chung, SK, Lee, MG, Ryu, BK, Lee, JH, Han, J, Byun, DS, Chae, KS, Lee, KY, Jang, JY, Kim, HJ and Chi, SG, 2007, 'Frequent alteration of XAF1 in human colorectal cancers: implication for tumor cell resistance to apoptotic stresses', Gastroenterology, vol. 132, no. 7, pp. 2459-2477.

Clapp, AJ, Peller, PJ and Subramaniam, RM, 2011, 'AJR teaching file: incidental breast cancer detected with 18F-FDG PET/CT', AJR Am J Roentgenol, vol. 196, no. 6 Suppl, pp. WS83-WS85.

Clarke, DH, Lê, MG, Sarrazin, D, Lacombe, MJ, Fontaine, F, Travagli, JP, May-Levin, F, Contesso, G and Arriagada, R, 1985, 'Analysis of local-regional relapses in patients with early breast cancers treated by excision and radiotherapy: experience of the Institut Gustave-Roussy', Int J Radiat Oncol Biol Phys, vol. 11, no. 1, pp. 137-145.

Clarke, M, Collins, R, Darby, S, Davies, C, Elphinstone, P, Evans, E, Godwin, J, Gray, R, Hicks, C, James, S, MacKinnon, E, McGale, P, McHugh, T, Peto, R, Taylor, C, Wang, Y and Early Breast Cancer Trialists' Collaborative Group (EBCTCG), 2005, 'Effects of radiotherapy and of differences in the extent of surgery for early breast cancer on local recurrence and 15-year survival: an overview of the randomised trials', Lancet, vol. 366, no. 9503, pp. 2087-2106.

Colditz, GA, Sellers, TA and Trapido, E, 2006, 'Epidemiology - identifying the causes and preventability of cancer?', Nat Rev Cancer, vol. 6, no. 1, pp. 75-83.

Collaborative Group on Hormonal Factors in Breast Cancer, 2001, 'Familial breast cancer: collaborative reanalysis of individual data from 52 epidemiological studies including 58,209 women with breast cancer and 101,986 women without the disease', Lancet, vol. 358, no. 9291, pp. 1389-1399.

Collaborative Group on Hormonal Factors in Breast Cancer, 2002, 'Breast cancer and breastfeeding: collaborative reanalysis of individual data from 47 epidemiological studies in 30 countries, including 50302 women with breast cancer and 96973 women without the disease', Lancet, vol. 360, no. 9328, pp. 187-195.

Cöster, L,1991, 'Structure and properties of dermatan sulphate proteoglycans', Biochem Soc Trans, vol. 19, no. 4, pp. 866-868.

Cronin, KA, Ravdin, PM and Edwards, BK, 2009, 'Sustained lower rates of breast cancer in the United States', Breast Cancer Res Treat, vol. 117, no. 1, pp. 223-224.

Cullen, KJ, Yee, D, Sly, WS, Perdue, J, Hampton, B, Lippman, ME and Rosen, N, 1990, 'Insulin-like growth factor receptor expression and function in human breast cancer', Cancer Res, vol. 50, no. 1, pp. 48-53.

Dai, Y, Yang, Y, MacLeod, V, Yue, X, Rapraeger, AC, Shriver, Z, Venkataraman, G, Sasisekharan, R and Sanderson, RD, 2005, 'HSulf-1 and HSulf-2 are potent inhibitors of myeloma tumor growth *in vivo*', J Biol Chem, vol. 280, no. 48, pp. 40066-40073.

Dallas, NA, Xia, L, Fan, F, Gray, MJ, Gaur, P, van Buren, G, Samuel, S, Kim, MP, Lim, SJ and Ellis, LM, 2009, 'Chemoresistant colorectal cancer cells, the cancer stem cell phenotype, and increased sensitivity to insulin-like growth factor-I receptor inhibition', Cancer Res, vol. 69, no. 5, pp. 1951-1957.

D'cunja, J, Shalaby, T, Rivera, P, von Büren, A, Patti, R, Heppner, FL, Arcaro, A, Rorke-Adams, LB, Phillips, PC and Grotzer, MA, 2007, 'Antisense treatment of IGF-IR induces apoptosis and enhances chemosensitivity in central nervous system atypical teratoid/rhabdoid tumours cells', Eur J Cancer, vol. 43, no. 10, pp. 1581-1589.

De Haes, JC and Olschewski, M, 1998, 'Quality of life assessment in a cross-cultural context: use of the Rotterdam Symptom Checklist in a multinational randomised trial comparing CMF and Zoladex (Goserlin) treatment in early breast cancer', Ann Oncol, vol. 9, no. 7, pp. 745-750.

Denkert, C, Darb-Esfahani, S, Loibl, S, Anagnostopoulos, I and Jöhrens, K, 2011, 'Anti-cancer immune response mechanisms in neoadjuvant and targeted therapy', Semin Immunopathol, vol. 33, no. 4, pp. 341-351.

Dmitriev, OY, 2011, 'Mechanism of tumor resistance to cisplatin mediated by the copper transporter ATP7B', Biochem Cell Biol, vol. 89, no. 2, pp. 138-147.

Do, AT, Smeds, E, Spillmann, D and Kusche-Gullberg, M, 2006, 'Overexpression of heparan sulfate 6-O-sulfotransferases in human embryonic kidney 293 cells results in increased N-acetylglucosaminyl 6-O-sulfation', J Biol Chem, vol. 281, no. 9, pp. 5348-5356.

Dong, A, Kong, M, Ma, Z, Qian, J, Cheng, H and Xu, X, 2008, 'Knockdown of insulin-like growth factor 1 receptor enhances chemosensitivity to cisplatin in human lung adenocarcinoma A549 cells', Acta Biochim Biophys Sin (Shanghai), vol. 40, no. 6, pp. 497-504.

Dunn, SE, Ehrlich, M, Sharp, NJ, Reiss, K, Solomon, G, Hawkins, R, Baserga, R and Barrett, JC, 1998, 'A dominant negative mutant of the insulin-like growth factor-I receptor inhibits the adhesion, invasion, and metastasis of breast cancer', Cancer Res, vol. 58, no. 15, pp. 3353-3361.

Dupont, J and Le Roith, D, 2001, 'Insulin-like growth factor 1 and oestradiol promote cell proliferation of MCF-7 breast cancer cells: new insights into their synergistic effects', Mol Pathol, vol. 54, no. 3, pp. 149-154.

Early Breast Cancer Trialists' Collaborative Group (EBCTCG), Correa, C, McGale, P, Taylor, C, Wang, Y, Clarke, M, Davies, C, Peto, R, Bijker, N, Solin, L and Darby, S, 2010, 'Overview of the randomized trials of radiotherapy in ductal carcinoma in situ of the breast', J Natl Cancer Inst Monogr, vol. 2010, no. 41, pp. 162-177.

Eckstein, N, Servan, K, Hildebrandt, B, Pölitz, A, von Jonquières, G, Wolf-Kümmeth, S, Napierski, I, Hamacher, A, Kassack, MU, Budczies, J, Beier, M, Dietel, M, Royer-Pokora, B, Denkert, C and Royer, HD, 2009, 'Hyperactivation of the insulin-like growth factor receptor I signaling pathway is an essential event for cisplatin resistance of ovarian cancer cells', Cancer Res, vol. 69, no. 7, pp. 2996-3003.

Edge SB, Byrd DR, Compton CC, et al., 2010, Cancer Staging Manual. AJCC 7th ed. New York, NY: Springer, pp 347-76.

Edwards, BK, Ward, E, Kohler, BA, Eheman, C, Zauber, AG, Anderson, RN, Jemal, A, Schymura, MJ, Lansdorp-Vogelaar, I, Seeff, LC, van Ballegooijen, M, Goede, SL and Ries, LAG, 2010, 'Annual report to the nation on the status of cancer, 1975-2006, featuring colorectal cancer trends and impact of interventions (risk factors, screening, and treatment) to reduce future rates', Cancer, vol. 116, no. 3, pp. 544-573.

Edwards, DP, Kühnel, B, Estes, PA and Nordeen, SK 1989, 'Human progesterone receptor binding to mouse mammary tumor virus deoxyribonucleic acid: dependence on hormone and nonreceptor nuclear factor(s)', Mol Endocrinol, vol. 3, no. 2, pp. 381-391.
Egyed, Z, Járay, B and Péntek, Z, 2006, '[Invasive lobular breast cancer: pitfall for the radiologist?]', Orv Hetil, vol. 147, no. 5, pp. 219-226.

Eiermann, W, Paepke, S, Appfelstaedt, J, Llombart-Cussac, A, Eremin, J, Vinholes, J, Mauriac, L, Ellis, M, Lassus, M, Chaudri-Ross, HA, Dugan, M, Borgs, M and Letrozole Neo-Adjuvant Breast Cancer Study Group, 2001, 'Preoperative treatment of postmenopausal breast cancer patients with letrozole: A randomized double-blind multicenter study', Ann Oncol, vol. 12, no. 11, pp. 1527-1532.

Eliassen, AH, Colditz, GA, Rosner, B, Willett, WC and Hankinson, SE, 2006, 'Adult weight change and risk of postmenopausal breast cancer', JAMA, vol. 296, no. 2, pp. 193-201.

Escobar, PF, Patrick, RJ, Rybicki, LA, Weng, DE and Crowe, JP, 2007, 'The 2003 revised TNM staging system for breast cancer: results of stage re-classification on survival and future comparisons among stage groups', *Ann Surg Oncol*, vol. 14, no. 1, pp. 143-147.

Esko, JD and Lindahl, U, 2001, 'Molecular diversity of heparan sulfate', J Clin Invest, vol. 108, no. 2, pp. 169-173.

Esko, JD and Selleck, SB, 2002, 'Order out of chaos: assembly of ligand binding sites in heparan sulfate', Annu Rev Biochem, vol. 71, pp. 435-471.

Fakkert, IE, Jansen, L, Meijer, K, Kok, T, Oosterwijk, JC, Mourits, MJE and de Bock, GH, 2011, 'Breast cancer screening in BRCA1 and BRCA2 mutation carriers after risk reducing salpingo-oophorectomy', Breast Cancer Res Treat, vol. 129, no. 1, pp. 157-164.

Fang, L, Barekati, Z, Zhang, B, Liu, Z and Zhong, XY, 2011, 'Targeted therapy in breast cancer: what's new?', Swiss medical weekly, vol. 141, pp. w13231.

Farese, SA and Aebi, S, 2009, 'Infiltrating Lobular Carcinoma of the Breast: Systemic Treatment', Breast Dis, vol. 30, pp. 45-52.

Farooq, M, Hwang, SY, Park, MK, Kim, JC, Kim, MK and Sung, YK, 2003, 'Blocking endogenous glypican-3 expression releases Hep 3B cells from G1 arrest', Mol Cells, vol. 15, no. 3, pp. 356-360.

Feigelson, HS, Jonas, CR, Teras, LR, Thun, MJ and Calle, EE, 2004, 'Weight gain, body mass index, hormone replacement therapy, and postmenopausal breast cancer in a large prospective study', Cancer Epidemiol Biomarkers Prev, vol. 13, no. 2, pp. 220-224.

Ferreira, A, Vieira, C, Rodrigues, A, Pereira, D, Rodrigues, H, Dávila, C and Bento, S, 2011, 'Bevacizumab in the treatment of metastatic breast cancer: three case reports', Curr Opin Oncol, vol. 23 Suppl, pp. S11-S19.

Fitzal, F, Mittlboeck, M, Steger, G, Bartsch, R, Rudas, M, Dubsky, P, Riedl, O, Jakesz, R and Gnant, M, 2011, 'Neoadjuvant Chemotherapy Increases the Rate of Breast Conservation in Lobular-Type Breast Cancer Patients', Ann Surg Oncol, Vol. 19, no. 2, pp. 519-526.

Fong, WG, Liston, P, Rajcan-Separovic, E, St Jean, M, Craig, C and Korneluk, RG, 2000, 'Expression and genetic analysis of XIAP-associated factor 1 (XAF1) in cancer cell lines', Genomics, vol. 70, no. 1, pp. 113-122.

Ford, D, Easton, DF, Stratton, M, Narod, S, Goldgar, D, Devilee, P, Bishop, DT, Weber, B, Lenoir, G, Chang-Claude, J, Sobol, H, Teare, MD, Struewing, J, Arason, A, Scherneck, S, Peto, J, Rebbeck, TR, Tonin, P, Neuhausen, S, Barkardottir, R, Eyfjord, J, Lynch, H, Ponder, BA, Gayther, SA and Zelada-Hedman, M, 1998, 'Genetic heterogeneity and penetrance analysis of the BRCA1 and BRCA2 genes in breast cancer families. The Breast Cancer Linkage Consortium', Am J Hum Genet, vol. 62, no. 3, pp. 676-689.

Ford-Perriss, M, Guimond, SE, Greferath, U, Kita, M, Grobe, K, Habuchi, H, Kimata, K, Esko, JD, Murphy, M and Turnbull, JE, 2002, 'Variant heparan sulfates synthesized in developing mouse brain differentially regulate FGF signaling', Glycobiology, vol. 12, no. 11, pp. 721-727.

Frese, MA, Milz, F, Dick, M, Lamanna, WC and Dierks, T, 2009, 'Characterization of the human sulfatase Sulf1 and its high affinity heparin/heparan sulfate interaction domain', J Biol Chem, vol. 284, no. 41, pp. 28033-28044.

Friedenreich, CM and Cust, AE, 2008, 'Physical activity and breast cancer risk: impact of timing, type and dose of activity and population subgroup effects', Br J Sports Med, vol. 42, no. 8, pp. 636-647.

Fujishima, M, Inui, H, Hashimoto, Y, Azumi, T, Yamamoto, N, Kato, H, Hojo, T, Yamato, M, Matsunami, N, Shiozaki, H and Watatani, M, 2010, 'Relationship between thymidylate synthase (TYMS) gene polymorphism and TYMS protein levels in patients with high-risk breast cancer', Anticancer Res, vol. 30, no. 10, pp. 4373-4379.

Fujita, K, Takechi, E, Sakamoto, N, Sumiyoshi, N, Izumi, S, Miyamoto, T, Matsuura, S, Tsurugaya, T, Akasaka, K and Yamamoto, T, 2010, 'HpSulf, a heparan sulfate 6-O endosulfatase, is involved in the regulation of VEGF signaling during sea urchin development', Mech Dev, vol. 127, no. 3-4, pp. 235-245.

Funderburgh, JL, Caterson, B and Conrad, GW, 1986, 'Keratan sulfate proteoglycan during embryonic development of the chicken cornea', Dev Biol, vol. 116, no. 2, pp. 267-277.

Funderburgh, JL, Funderburgh, ML, Mann, MM and Conrad, GW, 1991, 'Physical and biological properties of keratan sulphate proteoglycan', Biochem Soc Trans, vol. 19, no. 4, pp. 871-876.

Funderburgh, JL, 2002, 'Keratan sulfate biosynthesis', IUBMB Life, vol. 54, no. 4, pp. 187-194.

Gama, CI, Tully, SE, Sotogaku, N, Clark, PM, Rawat, M, Vaidehi, N, Goddard, WA, Nishi, A and Hsieh-Wilson, LC, 2006, 'Sulfation patterns of glycosaminoglycans encode molecular recognition and activity', Nat Chem Biol, vol. 2, no. 9, pp. 467-473.

Gao, F, Liu, Y, He, Y, Yang, C, Wang, Y, Shi, X and Wei, G, 2010, 'Hyaluronan oligosaccharides promote excisional wound healing through enhanced angiogenesis', Matrix Biol, vol. 29, no. 2, pp. 107-116.

Gao, H, Shi, J, Ge, SF and DI, W, 2008, '[Suppression of insulin-like growth factor-1 receptor by RNA interference inhibits cell growth *in vitro* and induces chemosensitization of HO8910PM cell to cisplatin]', Zhonghua Fu Chan Ke Za Zhi, vol. 43, no. 1, pp. 45-49.

Gao, WX, Wang, X, Wei, XF, Chen, YX, Zhang, J and Zhu, LK, 2006, '[Expression and subcellular localization of XIAP and XAF1 in human normal oral keratinocytes and Tca8113 cells]', Zhonghua Kou Qiang Yi Xue Za Zhi, vol. 41, no. 11, pp. 682-683.

Garcia-Ortega, MJ, Benito, MA, Vahamonde, EF, Torres, PR, Velasco, AB and Paredes, MM, 2011, 'Pretreatment axillary ultrasonography and core biopsy in patients with suspected breast cancer: Diagnostic accuracy and impact on management', Eur J Radiol, vol. 79, no. 1, pp. 64-72.

Garg, HG, Yu, L, Hales, CA, Toida, T, Islam, T and Linhardt, RJ, 2003, 'Sulfation patterns in heparin and heparan sulfate: effects on the proliferation of bovine pulmonary artery smooth muscle cells', Biochim Biophys Acta, vol. 1639, no. 3, pp. 225-231.

Gibson, D, 2009, 'The mechanism of action of platinum anticancer agents--what do we really know about it?', Dalton Trans, no. 48, pp. 10681-10689.

Glasziou, P and Houssami, N, 2011, 'The evidence base for breast cancer screening', Prev Med, vol. 53, no. 3, pp.100-102.

Głowacki, A, Koźma, EM and Olczyk, K, 2004, '[Biosynthesis of keratan sulfate, chondroitin sulfate and dermatan sulfate proteoglycans]', Postepy Biochem, vol. 50, no. 2, pp. 170-181.

Golinger, RC, Gur, D, Fisher, B, Herbert, DL, Naugle, I, Reece, JG, Hayes, P and Grady, S, 1979, 'The significance of concordance in mammographic interpretations', Cancer, vol. 44, no. 4, pp. 1252-1255.

Goodwin, PJ, Ennis, M, Pritchard, KI, Trudeau, ME, Koo, J, Hartwick, W, Hoffma, B and Hood, N, 2002, 'Insulin-like growth factor binding proteins 1 and 3 and breast cancer outcomes', Breast Cancer Res Treat, vol. 74, no. 1, pp. 65-76.

Gorsi, B and Stringer, SE, 2007, 'Tinkering with heparan sulfate sulfation to steer development', Trends Cell Biol, vol. 17, no. 4, pp. 173-177.

Greiling, H, 1994, 'Structure and biological functions of keratan sulfate proteoglycans', EXS, vol. 70, pp. 101-122.

Groebner, AE, Schulke, K, Unterseer, S, Reichenbach, HD, Reichenbach, M, Büttner, M, Wolf, E, Meyer, HHD and Ulbrich, SE, 2010, 'Enhanced proapoptotic gene expression of XAF1, CASP8 and TNFSF10 in the bovine endometrium during early pregnancy is not correlated with augmented apoptosis', Placenta, vol. 31, no. 3, pp. 168-177.

Guarneri, V, Pecchi, A, Piacentini, F, Barbieri, E, Dieci, MV, Ficarra, G, Tazzioli, G, Frassoldati, A, Battista, R, Canossi, B, Mauri, C, D'Amico, R, Conte, P and Torricelli, P, 2011, 'Magnetic Resonance Imaging and Ultrasonography in Predicting Infiltrating

Residual Disease after Preoperative Chemotherapy in Stage II-III Breast Cancer', Ann Surg Oncol, vol. 18, no. 8, pp. 2150-2157.

Gusella, M, Frigo, AC, Bolzonella, C, Marinelli, R, Barile, C, Bononi, A, Crepaldi, G, Menon, D, Stievano, L, Toso, S, Pasini, F, Ferrazzi, E and Padrini, R, 2009, 'Predictors of survival and toxicity in patients on adjuvant therapy with 5-fluorouracil for colorectal cancer', Br J Cancer, vol. 100, no. 10, pp. 1549-1557.

Guvakova, MA and Surmacz, E, 1999, 'The activated insulin-like growth factor I receptor induces depolarization in breast epithelial cells characterized by actin filament disassembly and tyrosine dephosphorylation of FAK, Cas, and paxillin', Exp Cell Res, vol. 251, no. 1, pp. 244-255.

Habuchi, H, Tanaka, M, Habuchi, O, Yoshida, K, Suzuki, H, Ban, K and Kimata, K, 2000, 'The occurrence of three isoforms of heparan sulfate 6-O-sulfotransferase having different specificities for hexuronic acid adjacent to the targeted N-sulfoglucosamine', J Biol. Chem, vol. 275, no. 4, pp. 2859-2868.

Habuchi, H, Habuchi, O and Kimata, K, 2004, 'Sulfation pattern in glycosaminoglycan: does it have a code?', Glycoconj J, vol. 21, no. 1-2, pp. 47-52.

Habuchi, H and Kimata, K, 2010, 'Mice deficient in heparan sulfate 6-O-sulfotransferase-1', Progress in molecular biology and translational science, vol. 93, pp. 79-111.

Habuchi, H, Nagai, N, Sugaya, N, Atsumi, F, Stevens, RL and Kimata, K, 2007, 'Mice deficient in heparan sulfate 6-O-sulfotransferase-1 exhibit defective heparan sulfate biosynthesis, abnormal placentation, and late embryonic lethality', J Biol Chem, vol. 282, no. 21, pp. 15578-15588.

Hadsell, DL, Greenberg, NM, Fligger, JM, Baumrucker, CR and Rosen, JM, 1996, 'Targeted expression of des(1-3) human insulin-like growth factor I in transgenic mice influences mammary gland development and IGF-binding protein expression', Endocrinology, vol. 137, no. 1, pp. 321-330.

Hagner-McWhirter, A, Li, JP, Oscarson, S and Lindahl, U, 2004, 'Irreversible glucuronyl C5-epimerization in the biosynthesis of heparan sulfate', J Biol Chem, vol. 279, no. 15, pp. 14631-14638.

Hall, C, Krishnamurthy, S, Lodhi, A, Bhattacharyya, A, Anderson, A, Kuerer, H, Bedrosian, I, Singh, B and Lucci, A, 2011, 'Disseminated tumor cells predict survival after neoadjuvant therapy in primary breast cancer', Cancer, vol. 118, no. 2, pp. 342-348.

Harris, M, Howell, A, Chrissohou, M, Swindell, RI, Hudson, M and Sellwood, RA, 1984, 'A comparison of the metastatic pattern of infiltrating lobular carcinoma and infiltrating duct carcinoma of the breast', Br J Cancer, vol. 50, no. 1, pp. 23-30.

Heiss, G, Wallace, R, Anderson, GL, Aragaki, A, Beresford, SAA, Brzyski, R, Chlebowski, RT, Gass, M, LaCroix, A, Manson, JE, Prentice, RL, Rossouw, J, Stefanick, ML and WHI Investigators, 2008, 'Health risks and benefits 3 years after stopping randomized treatment with estrogen and progestin', JAMA, vol. 299, no. 9, pp. 1036-1045.

Hellawell, GO, Ferguson, DJP, Brewster, SF and Macaulay, VM, 2003, 'Chemosensitization of human prostate cancer using antisense agents targeting the type 1 insulin-like growth factor receptor', BJU Int, vol. 91, no. 3, pp. 271-277.

Holcik, M, Gibson, H and Korneluk, RG, 2001, 'XIAP: apoptotic brake and promising therapeutic target', Apoptosis, vol. 6, no. 4, pp. 253-261.

Holst, CR, Bou-Reslan, H, Gore, BB, Wong, K, Grant, D, Chalasani, S, Carano, RA, Frantz, GD, Tessier-Lavigne, M, Bolon, B, French, DM and Ashkenazi, A, 2007, 'Secreted sulfatases Sulf1 and Sulf2 have overlapping yet essential roles in mouse neonatal survival', PloS one, vol. 2, no. 6, pp. e575.

Hong, ZJ, Chu, CH, Fan, HL, Hsu, HM, Chen, CJ, Chan, DC and Yu, JC, 2011, 'Factors predictive of breast cancer in open biopsy in cases with atypical ductal hyperplasia diagnosed by ultrasound-guided core needle biopsy', Eur J Surg Oncol, vol. 37, no. 9, pp.758-64.

Horio, A, Fujita, T, Hayashi, H, Hattori, M, Kondou, N, Yamada, M, Adachi, E, Ushio, A, Gondou, N, Sueta, A, Yatabe, Y and Iwata, H, 2011, 'High recurrence risk and use of adjuvant trastuzumab in patients with small, HER2-positive, node-negative breast cancers', Int J Clin Oncol.

Horner MJ, Ries LAG, Krapcho M, et al., eds. SEER Cancer Statistics Review, 1975-2006.

Howard, BA and Gusterson, BA, 2000, 'Human breast development', J Mammary Gland Biol Neoplasia, vol. 5, no. 2, pp. 119-137.

Huang, J, Yao, WY, Zhu, Q, Tu, SP, Yuan, F, Wang, HF, Zhang, YP and Yuan, YZ, 2010, 'XAF1 as a prognostic biomarker and therapeutic target in pancreatic cancer', Cancer Sci, vol. 101, no. 2, pp. 559-567.

Huang, Y, Park, YC, Rich, RL, Segal, D, Myszka, DG and Wu, H, 2001, 'Structural basis of caspase inhibition by XIAP: differential roles of the linker versus the BIR domain', Cell, vol. 104, no. 5, pp. 781-790.

Hulka, BS and Moorman, PG, 2001, 'Breast cancer: hormones and other risk factors', Maturitas, vol. 38, no. 1, pp. 103-13; discussion 113.

Hulka, BS and Moorman, PG, 2008, 'Breast cancer: hormones and other risk factors', Maturitas, vol. 61, no. 1-2, pp. 203-13; discussion 213.

Ichikawa, W, Takahashi, T, Suto, K, Shirota, Y, Nihei, Z, Shimizu, M, Sasaki, Y and Hirayama, R, 2006, 'Simple combinations of 5-FU pathway genes predict the outcome of metastatic gastric cancer patients treated by S-1', Int J Cancer, vol. 119, no. 8, pp. 1927-1933.

Iozzo, RV, 1988, 'Cell surface heparan sulfate proteoglycan and the neoplastic phenotype', J Cell Biochem, vol. 37, no. 1, pp. 61-78.

Iozzo, RV, 1988, 'Proteoglycans and neoplasia', Cancer Metastasis Rev, vol. 7, no. 1, pp. 39-50.

Ito, Y, Ioka, A, Tanaka, M, Nakayama, T and Tsukuma, H, 2009, 'Trends in cancer incidence and mortality in Osaka, Japan: evaluation of cancer control activities', Cancer Sci, vol. 100, no. 12, pp. 2390-2395.

Izumikawa, T, Egusa, N, Taniguchi, F, Sugahara, K and Kitagawa, H, 2006, 'Heparan sulfate polymerization in Drosophila', J Biol Chem, vol. 281, no. 4, pp. 1929-1934.

Izvolsky, KI, Lu, J, Martin, G, Albrecht, KH and Cardoso, WV, 2008, 'Systemic inactivation of Hs6st1 in mice is associated with late postnatal mortality without major defects in organogenesis', Genesis, vol. 46, no. 1, pp. 8-18.

Jang, JY, Kim, HJ, Chi, SG, Lee, KY, Nam, KD, Kim, NH, Lee, SK, Joo, KR, Dong, SH, Kim, BH, Chang, YW, Lee, JI and Chang, R, 2005, '[Frequent epigenetic inactivation of XAF1 by promotor hypermethylation in human colon cancers]', Korean J Gastroenterol, vol. 45, no. 4, pp. 285-293.

Jansen, SA, 2011, 'Ductal carcinoma in situ: detection, diagnosis, and characterization with magnetic resonance imaging', Semin Ultrasound CT MR, vol. 32, no. 4, pp. 306-318.

Jastrebova, N, Vanwildemeersch, M, Lindahl, U and Spillmann, D, 2010, 'Heparan sulfate domain organization and sulfation modulate FGF-induced cell signaling', J Biol Chem, vol. 285, no. 35, pp. 26842-26851.

Jemal, A, Bray, F, Center, MM, Ferlay, J, Ward, E and Forman, D, 2011, 'Global cancer statistics', CA Cancer J Clin, vol. 61, no. 2, pp. 69-90.

Jemal, A, Center, MM, DeSantis, C and Ward, EM, 2010, 'Global patterns of cancer incidence and mortality rates and trends', Cancer Epidemiol Biomarkers Prev, vol. 19, no. 8, pp. 1893-1907.

Jensen, SA, Vainer, B, Witton, CJ, Jørgensen, JT and Sørensen, JB, 2008, 'Prognostic significance of numeric aberrations of genes for thymidylate synthase, thymidine phosphorylase and dihydrofolate reductase in colorectal cancer', Acta Oncol, vol. 47, no. 6, pp. 1054-1061.

Johnson, KH and Millard, PS, 1996, 'Oral contraceptives and breast cancer', J Fam Pract, vol. 43, no. 4, pp. 340-341.

Jones, RA, Petrik, JJ and Moorehead, RA, 2010, 'Preneoplastic changes persist after IGF-IR downregulation and tumor regression', Oncogene, vol. 29, no. 34, pp. 4779-4786.

Jones, RA, Campbell, CI, Petrik, JJ and Moorehead, RA, 2008, 'Characterization of a novel primary mammary tumor cell line reveals that cyclin D1 is regulated by the type I insulin-like growth factor receptor', Mol Cancer Res, vol. 6, no. 5, pp. 819-828.

Junnila, S, Kokkola, A, Mizuguchi, T, Hirata, K, Karjalainen-Lindsberg, ML, Puolakkainen, P and Monni, O, 2010, 'Gene expression analysis identifies over-expression of CXCL1, SPARC, SPP1, and SULF1 in gastric cancer', Genes Chromosomes Cancer, vol. 49, no. 1, pp. 28-39.

Kai, K, D'Costa, S, Sills, RC and Kim, Y, 2009, 'Inhibition of the insulin-like growth factor 1 receptor pathway enhances the antitumor effect of cisplatin in human malignant mesothelioma cell lines', Cancer Lett, vol. 278, no. 1, pp. 49-55.

Kamimura, K, Fujise, M, Villa, F, Izumi, S, Habuchi, H, Kimata, K and Nakato, H, 2001, 'Drosophila heparan sulfate 6-O-sulfotransferase (dHS6ST) gene. Structure, expression, and function in the formation of the tracheal system', J Biol Chem, vol. 276, no. 20, pp. 17014-17021.

Kang, HG, Jenabi, JM, Liu, XF, Reynolds, CP, Triche, TJ and Sorensen, PHB, 2010, 'Inhibition of the insulin-like growth factor I receptor by epigallocatechin gallate blocks proliferation and induces the death of Ewing tumor cells', Mol Cancer Ther, vol. 9, no. 5, pp. 1396-1407.

Kanoh, A, Seko, A, Ideo, H, Yoshida, M, Nomoto, M, Yonezawa, S, Sakamoto, M, Kannagi, R and Yamashita, K, 2006, 'Ectopic expression of N-acetylglucosamine 6-O-sulfotransferase 2 in chemotherapy-resistant ovarian adenocarcinomas', Glycoconj J, vol. 23, no. 5-6, pp. 453-460.

Karey, KP and Sirbasku, DA, 1988, 'Differential responsiveness of human breast cancer cell lines MCF-7 and T47D to growth factors and 17 beta-estradiol', Cancer Res, vol. 48, no. 14, pp. 4083-4092.

Kasim, K, Levallois, P, Abdous, B, Auger, P, Johnson, KC and Canadian Cancer Registries Epidemiology Research Group, 2005, 'Environmental tobacco smoke and risk of adult leukemia', Epidemiology, vol. 16, no. 5, pp. 672-680.

Kawai, Y, Kaidoh, M, Yokoyama, Y, Sano, K and Ohhashi, T, 2009, 'Chemokine CCL2 facilitates ICAM-1-mediated interactions of cancer cells and lymphatic endothelial cells in sentinel lymph nodes', Cancer Sci, vol. 100, no. 3, pp. 419-428.

Kempkensteffen, C, Hinz, S, Jäger, T, Weikert, S, Krause, H, Schostak, M, Christoph, F, Strenziok, R, Miller, K and Schrader, M, 2008, '[Expression levels of the IAP antagonists XAF1, Smac/DIABLO and HtrA2 in testicular germ cell tumours]', Aktuelle Urol, vol. 39, no. 6, pp. 436-441.

Kempkensteffen, C, Hinz, S, Schrader, M, Christoph, F, Magheli, A, Krause, H, Schostak, M, Miller, K and Weikert, S, 2007, 'Gene expression and promoter methylation of the XIAP-associated Factor 1 in renal cell carcinomas: correlations with pathology and outcome', Cancer Lett, vol. 254, no. 2, pp. 227-235.

Kerlikowske, K, 2010, 'Epidemiology of ductal carcinoma in situ', J Natl Cancer Inst Monogr, vol. 2010, no. 41, pp. 139-141.

Kimmick, G, 2011, 'Adjuvant Chemotherapy for Breast Cancer in Older Women: Emerging Evidence to Aid in Decision Making', Curr Treat Options Oncol, vol. 12, no. 3, pp. 286-301.

Kleinman, HK and Jacob, K, 2001, 'Invasion assays', Curr Protoc Cell Biol, vol. Chapter 12, pp. Unit 12.2.

Knight, CH and Sorensen, A, 2001, 'Windows in early mammary development: critical or not?', Reproduction, vol. 122, no. 3, pp. 337-345.

Kobayashi, T, Habuchi, H, Tamura, K, Ide, H and Kimata, K, 2007, 'Essential role of heparan sulfate 2-O-sulfotransferase in chick limb bud patterning and development', J Biol Chem, vol. 282, no. 27, pp. 19589-19597.

Kozlowski, EO and Pavao, MSG, 2011, 'Effect of sulfated glycosaminoglycans on tumor invasion and metastasis', Frontiers in bioscience (Scholar edition), vol. 3, pp. 1541-1551.

Kozma, EM, Olczyk, K and Głowacki, A, 2001, 'Dermatan sulfates of normal and scarred fascia', Comp Biochem Physiol B Biochem Mol Biol, vol. 128, no. 2, pp. 221-232.

Kramer, KL and Yost, HJ, 2003, 'Heparan sulfate core proteins in cell-cell signaling', Annu Rev Genet, vol. 37, pp. 461-484.

Kramer, RH, Bensch, KG and Wong, J, 1986, 'Invasion of reconstituted basement membrane matrix by metastatic human tumor cells', Cancer Res, vol. 46, no. 4 Pt 2, pp. 1980-1989.

Krause-Heuer, AM, Grünert, R, Kühne, S, Buczkowska, M, Wheate, NJ, Le Pevelen, DD, Boag, LR, Fisher, DM, Kasparkova, J, Malina, J, Bednarski, PJ, Brabec, V and

Aldrich-Wright, JR, 2009, 'Studies of the mechanism of action of platinum(II) complexes with potent cytotoxicity in human cancer cells', J Med Chem, vol. 52, no. 17, pp. 5474-5484.

Kumar, K, Vamsy, M and Jamil, K, 2010, 'Thymidylate synthase gene polymorphisms effecting 5-FU response in breast cancer patients', Cancer Biomark, vol. 6, no. 2, pp. 83-93.

Kümler, I and Nielsen, DL, 2011, 'Trials of bevacizumab in breast cancer - a safety review', Expert Opin Drug Saf, vol. 11, Suppl. 1, pp. S37-48.

Labbé, E, Lock, L, Letamendia, A, Gorska, AE, Gryfe, R, Gallinger, S, Moses, HL and Attisano, L, 2007, 'Transcriptional cooperation between the transforming growth factor-beta and Wnt pathways in mammary and intestinal tumorigenesis', Cancer Res, vol. 67, no. 1, pp. 75-84.

Lai, JP, Chien, JR, Moser, DR, Staub, JK, Aderca, I, Montoya, DP, Matthews, TA, Nagorney, DM, Cunningham, JM, Smith, DI, Greene, EL, Shridhar, V and Roberts, LR, 2004, 'hSulf1 Sulfatase promotes apoptosis of hepatocellular cancer cells by decreasing heparin-binding growth factor signaling', Gastroenterology, vol. 126, no. 1, pp. 231-248.

Lai, J, Chien, J, Staub, J, Avula, R, Greene, EL, Matthews, TA, Smith, DI, Kaufmann, SH, Roberts, LR and Shridhar, V, 2003, 'Loss of HSulf-1 up-regulates heparin-binding growth factor signaling in cancer', J Biol Chem, vol. 278, no. 25, pp. 23107-23117.

Lai, JP, Yu, C, Moser, CD, Aderca, I, Han, T, Garvey, TD, Murphy, LM, Garrity-Park, MM, Shridhar, V, Adjei, AA and Roberts, LR, 2006, 'SULF1 inhibits tumor growth and potentiates the effects of histone deacetylase inhibitors in hepatocellular carcinoma', Gastroenterology, vol. 130, no. 7, pp. 2130-2144.

Lamanna, WC, Kalus, I, Padva, M, Baldwin, RJ, Merry, CLR and Dierks, T, 2007, 'The heparanome--the enigma of encoding and decoding heparan sulfate sulfation', J Biotechnol, vol. 129, no. 2, pp. 290-307.

Lambe, M, Hsieh, C, Trichopoulos, D, Ekbom, A, Pavia, M and Adami, HO, 1994, 'Transient increase in the risk of breast cancer after giving birth', N Engl J Med, vol. 331, no. 1, pp. 5-9.

Langer, R, Specht, K, Becker, K, Ewald, P, Ott, K, Lordick, F, Siewert, JR and Höfler, H, 2007, 'Comparison of pretherapeutic and posttherapeutic expression levels of chemotherapy-associated genes in adenocarcinomas of the esophagus treated by 5-fluorouracil- and cisplatin-based neoadjuvant chemotherapy', Am J Clin Pathol, vol. 128, no. 2, pp. 191-197.

Leaman, DW, Chawla-Sarkar, M, Vyas, K, Reheman, M, Tamai, K, Toji, S and Borden, EC, 2002, 'Identification of X-linked inhibitor of apoptosis-associated factor-1 as an

interferon-stimulated gene that augments TRAIL Apo2L-induced apoptosis', J Biol Chem, vol. 277, no. 32, pp. 28504-28511.

Lecomte, T, Ferraz, JM, Zinzindohoué, F, Loriot, MA, Tregouet, DA, Landi, B, Berger, A, Cugnenc, PH, Jian, R, Beaune, P and Laurent-Puig, P, 2004, 'Thymidylate synthase gene polymorphism predicts toxicity in colorectal cancer patients receiving 5-fluorouracil-based chemotherapy', Clin Cancer Res, vol. 10, no. 17, pp. 5880-5888.

Lee, JH, Park, S, Park, HS and Park, BW, 2010, 'Clinicopathological features of infiltrating lobular carcinomas comparing with infiltrating ductal carcinomas: a case control study', World J Surg Oncol, vol. 8, pp. 34.

Lee, MG, Huh, JS, Chung, SK, Lee, JH, Byun, DS, Ryu, BK, Kang, MJ, Chae, KS, Lee, SJ, Lee, CH, Kim, JI, Chang, SG and Chi, SG, 2006, 'Promoter CpG hypermethylation and downregulation of XAF1 expression in human urogenital malignancies: implication for attenuated p53 response to apoptotic stresses', Oncogene, vol. 25, no. 42, pp. 5807-5822.

Lee, PN and Hamling, J, 2006, 'Environmental tobacco smoke exposure and risk of breast cancer in nonsmoking women: a review with meta-analyses', Inhal Toxicol, vol. 18, no. 14, pp. 1053-1070.

Lemjabbar-Alaoui, H, van Zante, A, Singer, MS, Xue, Q, Wang, YQ, Tsay, D, He, B, Jablons, DM and Rosen, SD, 2010, 'Sulf-2, a heparan sulfate endosulfatase, promotes human lung carcinogenesis', Oncogene, vol. 29, no. 5, pp. 635-646.

Leonard, GD and Swain, SM, 2004, 'Ductal carcinoma in situ, complexities and challenges', J Natl Cancer Inst, vol. 96, no. 12, pp. 906-920.

Leong, CO, Vidnovic, N, DeYoung, MP, Sgroi, D and Ellisen, LW, 2007, 'The p63/p73 network mediates chemosensitivity to cisplatin in a biologically defined subset of primary breast cancers', J Clin Invest, vol. 117, no. 5, pp. 1370-1380.

Le-Petross, HT and Shetty, MK, 2011, 'Magnetic resonance imaging and breast ultrasonography as an adjunct to mammographic screening in high-risk patients', Semin Ultrasound CT MR, vol. 32, no. 4, pp. 266-272.

Lester, GE, Toussiant, LG, Blackwood, AD and Bos, GD, 2001, 'Cartilaginous extracellular matrix of failed massive osteoarticular allografts', Clin Orthop Relat Res, no. 382, pp. 13-20.

Lew, JQ, Freedman, ND, Leitzmann, MF, Brinton, LA, Hoover, RN, Hollenbeck, AR, Schatzkin, A and Park, Y, 2009, 'Alcohol and risk of breast cancer by histologic type and hormone receptor status in postmenopausal women: the NIH-AARP Diet and Health Study', Am J Epidemiol, vol. 170, no. 3, pp. 308-317.

Li, J, Kleeff, J, Abiatari, I, Kayed, H, Giese, NA, Felix, K, Giese, T, Büchler, MW and Friess, H, 2005, 'Enhanced levels of Hsulf-1 interfere with heparin-binding growth factor signaling in pancreatic cancer', Mol Cancer, vol. 4, no. 1, pp. 14.

Li, T, Chen, CL, Wang, JD, Cui, SD, Cui, DY and Guo, W, 2007, '[Expression of HSF1 and XAF1 in gastro-intestinal cancer]', Nan Fang Yi Ke Da Xue Xue Bao, vol. 27, no. 9, pp. 1447-1450.

Li, T, Chen, CL, Wang, JD, Cui, SD, Cui, DY and Guo, W, 2008, '[Expression of heat-shock transcription factor 1 and X-linked inhibitor of apoptosis protein-associated factor-1 in gastrointestinal cancer]', Nan Fang Yi Ke Da Xue Xue Bao, vol. 28, no. 3, pp. 487-490.

Lianidou, ES and Markou, A, 2011, 'Circulating Tumor Cells in Breast Cancer: Detection Systems, Molecular Characterization, and Future Challenges', Clin Chem, vol. 57, no. 9, pp. 1242-1255.

Lichtenstein, P, Holm, NV, Verkasalo, PK, Iliadou, A, Kaprio, J, Koskenvuo, M, Pukkala, E, Skytthe, A and Hemminki, K, 2000, 'Environmental and heritable factors in the causation of cancer--analyses of cohorts of twins from Sweden, Denmark, and Finland', N Engl J Med, vol. 343, no. 2, pp. 78-85.

Lin, X, Wei, G, Shi, Z, Dryer, L, Esko, JD, Wells, DE and Matzuk, MM, 2000, 'Disruption of gastrulation and heparan sulfate biosynthesis in EXT1-deficient mice', Dev Biol, vol. 224, no. 2, pp. 299-311.

Lin, X, 2004, 'Functions of heparan sulfate proteoglycans in cell signaling during development', Development, vol. 131, no. 24, pp. 6009-6021.

Lindahl, B, Eriksson, L, Spillmann, D, Caterson, B and Lindahl, U, 1996, 'Selective loss of cerebral keratan sulfate in Alzheimer's disease', J Biol Chem, vol. 271, no. 29, pp. 16991-16994.

Linnerth, NM, Siwicky, MD, Campbell, CI, Watson, KLM, Petrik, JJ, Whitsett, JA and Moorehead, RA, 2009, 'Type I insulin-like growth factor receptor induces pulmonary tumorigenesis', Neoplasia, vol. 11, no. 7, pp. 672-682.

Liston, P, Fong, WG, Kelly, NL, Toji, S, Miyazaki, T, Conte, D, Tamai, K, Craig, CG, McBurney, MW and Korneluk, RG, 2001, 'Identification of XAF1 as an antagonist of XIAP anti-Caspase activity', Nat Cell Biol, vol. 3, no. 2, pp. 128-133.

Litwack, ED, Ivins, JK, Kumbasar, A, Paine-Saunders, S, Stipp, CS and Lander, AD, 1998, 'Expression of the heparan sulfate proteoglycan glypican-1 in the developing rodent', Dev Dyn, vol. 211, no. 1, pp. 72-87.

Liu, P, Khurana, A, Rattan, R, He, X, Kalloger, S, Dowdy, S, Gilks, B and Shridhar, V, 2009, 'Regulation of HSulf-1 expression by variant hepatic nuclear factor 1 in ovarian cancer', Cancer Res, vol. 69, no. 11, pp. 4843-4850.

Liu, S, Jin, F, Dai, W and Yu, Y, 2010, 'Antisense treatment of IGF-IR enhances chemosensitivity in squamous cell carcinomas of the head and neck', Eur J Cancer, vol. 46, no. 9, pp. 1744-1751.

Liu, YC, Leu, CM, Wong, FH, Fong, WS, Chen, SC, Chang, C and Hu, CP, 2002, 'Autocrine stimulation by insulin-like growth factor I is involved in the growth, tumorigenicity and chemoresistance of human esophageal carcinoma cells', J Biomed Sci, vol. 9, no. 6 Pt 2, pp. 665-674.

Lo, SL, Thike, AA, Tan, SY, Lim, TKH, Tan, IBH, Choo, SP, Tan, PH, Bay, BH and Yip, GWC, 2011, 'Expression of heparan sulfate in gastric carcinoma and its correlation with clinicopathological features and patient survival', J Clin Pathol, vol. 64, no. 2, pp. 153-158.

Longley, DB, Harkin, DP and Johnston, PG, 2003, '5-fluorouracil: mechanisms of action and clinical strategies', Nat Rev Cancer, vol. 3, no. 5, pp. 330-338.

Lu, Y, Levick, JR and Wang, W, 2005, 'The mechanism of synovial fluid retention in pressurized joint cavities', Microcirculation, vol. 12, no. 7, pp. 581-595.

Lv, H, Yu, G, Sun, L, Zhang, Z, Zhao, X and Chai, W, 2007, 'Elevate level of glycosaminoglycans and altered sulfation pattern of chondroitin sulfate are associated with differentiation status and histological type of human primary hepatic carcinoma', Oncology, vol. 72, no. 5-6, pp. 347-356.

Ma, H, Hill, CK, Bernstein, L and Ursin, G, 2008, 'Low-dose medical radiation exposure and breast cancer risk in women under age 50 years overall and by estrogen and progesterone receptor status: results from a case-control and a case-case comparison', Breast Cancer Res Treat, vol. 109, no. 1, pp. 77-90.

Ma, TL, Ni, PH, Zhong, J, Tan, JH, Qiao, MM and Jiang, SH, 2005, 'Low expression of XIAP-associated factor 1 in human colorectal cancers', Chin J Dig Dis, vol. 6, no. 1, pp. 10-14.

Maeda, N, Ishii, M, Nishimura, K and Kamimura, K, 2011, 'Functions of chondroitin sulfate and heparan sulfate in the developing brain', Neurochem Res, vol. 36, no. 7, pp. 1228-1240.

Maeda, T, Alexander, CM and Friedl, A, 2004, 'Induction of syndecan-1 expression in stromal fibroblasts promotes proliferation of human breast cancer cells', Cancer Res, vol. 64, no. 2, pp. 612-621.

Maeshima, N, Poon, GFT, Dosanjh, M, Felberg, J, Lee, SSM, Cross, JL, Birkenhead, D and Johnson, P, 2011, 'Hyaluronan binding identifies the most proliferative activated and memory T cells', Eur J Immunol, vol. 41, no. 4, pp. 1108-1119.

Maiani, E, Diederich, M and Gonfloni, S, 2011, 'DNA damage response: The emerging role of c-Abl as a regulatory switch?', Biochem Pharmacol, vol. 82, no.10, pp. 1269-1276.

Maimone, MM and Tollefsen, DM, 1990, 'Structure of a dermatan sulfate hexasaccharide that binds to heparin cofactor II with high affinity', J Biol Chem, vol. 265, no. 30, pp. 18263-18271.

Manevich, E, Grabovsky, V, Feigelson, SW and Alon, R, 2007, 'Talin 1 and paxillin facilitate distinct steps in rapid VLA-4-mediated adhesion strengthening to vascular cell adhesion molecule 1', J Biol Chem, vol. 282, no. 35, pp. 25338-25348.

Marsh, S, 2005, 'Thymidylate synthase pharmacogenetics', Invest New Drugs, vol. 23, no. 6, pp. 533-537.

Martinez-Balibrea, E, Abad, A, Martínez-Cardús, A, Ginés, A, Valladares, M, Navarro, M, Aranda, E, Marcuello, E, Benavides, M, Massutí, B, Carrato, A, Layos, L, Manzano, JL and Moreno, V, 2010, 'UGT1A and TYMS genetic variants predict toxicity and response of colorectal cancer patients treated with first-line irinotecan and fluorouracil combination therapy', Br J Cancer, vol. 103, no. 4, pp. 581-589.

Mauro, L, Bartucci, M, Morelli, C, Andò, S and Surmacz, E, 2001, 'IGF-I receptor-induced cell-cell adhesion of MCF-7 breast cancer cells requires the expression of junction protein ZO-1', J Biol Chem, vol. 276, no. 43, pp. 39892-39897.

Mauro, L, Salerno, M, Morelli, C, Boterberg, T, Bracke, ME and Surmacz, E, 2003, 'Role of the IGF-I receptor in the regulation of cell-cell adhesion: implications in cancer development and progression', J Cell Physiol, vol. 194, no. 2, pp. 108-116.

McCormick, C, Duncan, G, Goutsos, KT and Tufaro, F, 2000, 'The putative tumor suppressors EXT1 and EXT2 form a stable complex that accumulates in the Golgi apparatus and catalyzes the synthesis of heparan sulfate', Proc Natl Acad Sci U S A, vol. 97, no. 2, pp. 668-673.

McGee, M and Wagner, WD, 2003, 'Chondroitin sulfate anticoagulant activity is linked to water transfer: relevance to proteoglycan structure in atherosclerosis', Arterioscler Thromb Vasc Biol, vol. 23, no. 10, pp. 1921-1927.

McLaughlin, R and Hylton, N, 2011, 'MRI in breast cancer therapy monitoring', NMR Biomed, vol. 24, no. 6, pp. 712-720.

Meran, S, Luo, DD, Simpson, R, Martin, J, Wells, A, Steadman, R and Phillips, AO, 2011, 'Hyaluronan facilitates transforming growth factor-β1-dependent proliferation via

CD44 and epidermal growth factor receptor interaction', J Biol Chem, vol. 286, no. 20, pp. 17618-17630.

Micali, OC, Cheung, HH, Plenchette, S, Hurley, SL, Liston, P, LaCasse, EC and Korneluk, RG, 2007, 'Silencing of the XAF1 gene by promoter hypermethylation in cancer cells and reactivation to TRAIL-sensitization by IFN-beta', BMC Cancer, vol. 7, pp. 52.

Michelow, P, Dezube, BJ and Pantanowitz, L, 2010, 'Fine needle aspiration of breast masses in HIV-infected patients: results from a large series', Cancer cytopathology, vol. 118, no. 4, pp. 218-224.

Miller, BT, Abbott, AM and Tuttle, TM, 2011, 'The Influence of Preoperative MRI on Breast Cancer Treatment', Ann Surg Oncol, vol. 19, no. 2, pp. 536-540.

Miller, MD, Marty, MA, Broadwin, R, Johnson, KC, Salmon, AG, Winder, B, Steinmaus, C and California Environmental Protection Agency, 2007, 'The association between exposure to environmental tobacco smoke and breast cancer: a review by the California Environmental Protection Agency', Prev Med, vol. 44, no. 2, pp. 93-106.

Milosavljevic, N, Duranton, C, Djerbi, N, Puech, PH, Gounon, P, Lagadic-Gossmann, D, Dimanche-Boitrel, MT, Rauch, C, Tauc, M, Counillon, L and Poët, M, 2010, 'Nongenomic effects of cisplatin: acute inhibition of mechanosensitive transporters and channels without actin remodeling', Cancer Res, vol. 70, no. 19, pp. 7514-7522.

Miyake, T, Shimazu, K, Ohashi, H, Taguchi, T, Ueda, S, Nakayama, T, Kim, SJ, Aozasa, K, Tamaki, Y and Noguchi, S, 2011, 'Indication for sentinel lymph node biopsy for breast cancer when core biopsy shows ductal carcinoma in situ', Am J Surg, vol. 202, no. 1, pp. 59-65.

Monticciolo, DL, 2011, 'Magnetic resonance imaging of the breast for cancer diagnosis and staging', Semin Ultrasound CT MR, vol. 32, no. 4, pp. 319-330.

Mooney, LM, Al-Sakkaf, KA, Brown, BL and Dobson, PRM, 2002, 'Apoptotic mechanisms in T47D and MCF-7 human breast cancer cells', Br J Cancer, vol. 87, no. 8, pp. 909-917.

Morimoto, LM, White, E, Chen, Z, Chlebowski, RT, Hays, J, Kuller, L, Lopez, AM, Manson, J, Margolis, KL, Muti, PC, Stefanick, ML and McTiernan, A, 2002, 'Obesity, body size, and risk of postmenopausal breast cancer: the Women's Health Initiative (United States)', Cancer Causes Control, vol. 13, no. 8, pp. 741-751.

Morimoto-Tomita, M, Uchimura, K, Bistrup, A, Lum, DH, Egeblad, M, Boudreau, N, Werb, Z and Rosen, SD, 2005, 'Sulf-2, a proangiogenic heparan sulfate endosulfatase, is upregulated in breast cancer', Neoplasia, vol. 7, no. 11, pp. 1001-1010.

Morimoto-Tomita, M, Uchimura, K, Werb, Z, Hemmerich, S and Rosen, SD, 2002, 'Cloning and characterization of two extracellular heparin-degrading endosulfatases in mice and humans', J Biol Chem, vol. 277, no. 51, pp. 49175-49185.

Moriya, T and Silverberg, SG, 1994, 'Intraductal carcinoma (ductal carcinoma in situ) of the breast. A comparison of pure noninvasive tumors with those including different proportions of infiltrating carcinoma', Cancer, vol. 74, no. 11, pp. 2972-2978.

Mouna, B, Rhizlane, B, Amine, S, Hind, M, Fouad, T and Hassan, E, 2011, 'Male breast cancer: A report of 127 cases at a Moroccan institution', BMC research notes, vol. 4, no. 1, pp. 219.

Mouridsen, H, Gershanovich, M, Sun, Y, Perez-Carrion, R, Boni, C, Monnier, A, Apffelstaedt, J, Smith, R, Sleeboom, HP, Jaenicke, F, Pluzanska, A, Dank, M, Becquart, D, Bapsy, PP, Salminen, E, Snyder, R, Chaudri-Ross, H, Lang, R, Wyld, P and Bhatnagar, A, 2003, 'Phase III study of letrozole versus tamoxifen as first-line therapy of advanced breast cancer in postmenopausal women: analysis of survival and update of efficacy from the International Letrozole Breast Cancer Group', J Clin Oncol, vol. 21, no. 11, pp. 2101-2109.

Moutasim, KA, Nystrom, ML and Thomas, GJ, 2011, 'Cell migration and invasion assays', Methods Mol Biol, vol. 731, pp. 333-343.

Müller, AMS, Kohrt, HEK, Cha, S, Laport, G, Klein, J, Guardino, AE, Johnston, LJ, Stockerl-Goldstein, KE, Hanania, E, Juttner, C, Blume, KG, Negrin, RS, Weissman, IL and Shizuru, JA, 2011, 'Long-term Outcome of Patients with Metastatic Breast Cancer Treated with High-Dose Chemotherapy and Transplantation of Purified Autologous Hematopoietic Stem Cells', Biol Blood Marrow Transplant, vol. 18, no. 1, pp. 125-133.

Mulligan, AM, O'Malley, FP, Ennis, M, Fantus, IG and Goodwin, PJ, 2007, 'Insulin receptor is an independent predictor of a favorable outcome in early stage breast cancer', Breast Cancer Res Treat, vol. 106, no. 1, pp. 39-47.

Munagala, R, Aqil, F and Gupta, RC, 2011, 'Promising molecular targeted therapies in breast cancer', Indian journal of pharmacology, vol. 43, no. 3, pp. 236-245.

Murphy, TM, Perry, AS and Lawler, M, 2008, 'The emergence of DNA methylation as a key modulator of aberrant cell death in prostate cancer', Endocr Relat Cancer, vol. 15, no. 1, pp. 11-25.

Nadir, Y, Vlodavsky, I and Brenner, B, 2008, 'Heparanase, tissue factor, and cancer', Semin Thromb Hemost, vol. 34, no. 2, pp. 187-194.

Naor, D, Sionov, RV and Ish-Shalom, D, 1997, 'CD44: structure, function, and association with the malignant process', Adv Cancer Res, vol. 71, pp. 241-319.

Narita, K, Chien, J, Mullany, SA, Staub, J, Qian, X, Lingle, WL and Shridhar, V, 2007, 'Loss of HSulf-1 expression enhances autocrine signaling mediated by amphiregulin in breast cancer', J Biol Chem, vol. 282, no. 19, pp. 14413-14420.

Narita, K, Staub, J, Chien, J, Meyer, K, Bauer, M, Friedl, A, Ramakrishnan, S and Shridhar, V, 2006, 'HSulf-1 inhibits angiogenesis and tumorigenesis *in vivo*', Cancer Res, vol. 66, no. 12, pp. 6025-6032.

National Cancer Institute. SEER Cancer Statistics Review, 1975-2006, http://seer.cancer.gov/csr/1975_2006/, access date: 08/01/2011.

National Cancer Institute. Genetics of Breast and Ovarian Cancer, Last updated 05/14/2009, http://www.cancer.gov/cancertopics/pdq/genetics/breast-and-ovarian/HealthProfessional/page1, access date: 08/01/2011.

National Registry of Diseases Office. Trends In Cancer Incidences In Singapore during 2005-2009, 2011, http://www.nrdo.gov.sg/uploadedFiles/NRDO/Cancer_Trends_Report%20_05-09.pdf, access date: 08/01/2011.

Neilson, HK, Friedenreich, CM, Brockton, NT and Millikan, RC, 2009, 'Physical activity and postmenopausal breast cancer: proposed biologic mechanisms and areas for future research', Cancer Epidemiol Biomarkers Prev, vol. 18, no. 1, pp. 11-27.

Nekolla, EA, Griebel, J and Brix, G, 2008, '[Radiation risk associated with mammography screening examinations for women younger than 50 years of age, Z Med Phys, vol. 18, no. 3, pp. 170-179.

Ng, A, Wong, M, Viviano, B, Erlich, JM, Alba, G, Pflederer, C, Jay, PY and Saunders, S, 2009, 'Loss of glypican-3 function causes growth factor-dependent defects in cardiac and coronary vascular development', Dev Biol, vol. 335, no. 1, pp. 208-215.

Ng, KCP, Campos, EI, Martinka, M and Li, G, 2004, 'XAF1 expression is significantly reduced in human melanoma', J Invest Dermatol, vol. 123, no. 6, pp. 1127-1134.

Niikura, N, Costelloe, CM, Madewell, JE, Hayashi, N, Yu, TK, Liu, J, Palla, SL, Tokuda, Y, Theriault, RL, Hortobagyi, GN, Ueno, NT, 2011, 'FDG-PET/CT Compared with Conventional Imaging in the Detection of Distant Metastases of Primary Breast Cancer', Oncologist, vol. 16, no. 8, pp. 1111-1119.

Nikolova, V, Koo, CY, Ibrahim, SA, Wang, Z, Spillmann, D, Dreier, R, Kelsch, R, Fischgräbe, J, Smollich, M, Rossi, LH, Sibrowski, W, Wülfing, P, Kiesel, L, Yip, GW and Götte, M, 2009, 'Differential roles for membrane-bound and soluble syndecan-1 (CD138) in breast cancer progression', Carcinogenesis, vol. 30, no. 3, pp. 397-407.

Osborne, C, Wilson, P and Tripathy, D, 2004, 'Oncogenes and tumor suppressor genes in breast cancer: potential diagnostic and therapeutic applications', Oncologist, vol. 9, no. 4, pp. 361-377.

Ostapenko, V, Mikalauskas, T, Bruzas, S, Mudenas, A, Sabonis, J, Tutkus, J, Meskauskas, R, Miliauskas, P, Jackevicius, A and Grinyte, L, 2004, '[Mamography and core biopsy value in diagnosis of nonpalpable breast tumors]', Medicina (Kaunas), vol. 40, no. 12, pp. 1165-1169.

Park, H, Han, I, Kwon, HJ and Oh, ES, 2005, 'Focal adhesion kinase regulates syndecan-2-mediated tumorigenic activity of HT1080 fibrosarcoma cells', Cancer Res, vol. 65, no. 21, pp. 9899-9905.

Park, JS, Moon, WK, Lyou, CY, Cho, N, Kang, KW and Chung, JK, 2011, 'The assessment of breast cancer response to neoadjuvant chemotherapy: comparison of magnetic resonance imaging and 18F-fluorodeoxyglucose positron emission tomography', Acta Radiol, vol. 52, no. 1, pp. 21-28.

Parker, JB and Stivers, JT, 2011, 'Dynamics of uracil and 5-fluorouracil in DNA', Biochemistry, vol. 50, no. 5, pp. 612-617.

Parkin, DM, 2009, 'Is the recent fall in incidence of post-menopausal breast cancer in UK related to changes in use of hormone replacement therapy?', Eur J Cancer, vol. 45, no. 9, pp. 1649-1653.

Parkin, DM, Nambooze, S, Wabwire-Mangen, F and Wabinga, HR, 2010, 'Changing cancer incidence in Kampala, Uganda, 1991-2006', Int J Cancer, vol. 126, no. 5, pp. 1187-1195.

Párrizas, M, Saltiel, AR and LeRoith, D, 1997, 'Insulin-like growth factor 1 inhibits apoptosis using the phosphatidylinositol 3'-kinase and mitogen-activated protein kinase pathways', J Biol Chem, vol. 272, no. 1, pp. 154-161.

Pauli, BU, Schwartz, DE, Thonar, EJ and Kuettner, KE, 1983, 'Tumor invasion and host extracellular matrix', Cancer Metastasis Rev, vol. 2, no. 2, pp. 129-152.

Peters, EJ, Kraja, AT, Lin, SJ, Yen-Revollo, JL, Marsh, S, Province, MA and McLeod, HL, 2009, 'Association of thymidylate synthase variants with 5-fluorouracil cytotoxicity', Pharmacogenet Genomics, vol. 19, no. 5, pp. 399-401.

Peters, TM, Schatzkin, A, Gierach, GL, Moore, SC, Lacey, JV, Wareham, NJ, Ekelund, U, Hollenbeck, AR and Leitzmann, MF, 2009, 'Physical activity and postmenopausal breast cancer risk in the NIH-AARP diet and health study', Cancer Epidemiol Biomarkers Prev, vol. 18, no. 1, pp. 289-296.

Petrelli, F, Cabiddu, M, Barbara, C and Barni, S, 2011, 'A patient presenting nasal

septum perforation during bevacizumab-containing chemotherapy for advanced breast cancer', Breast Cancer, vol. 18, no. 3, pp. 226-230.

Pilkington, GJ, Bjerkvig, R, De Ridder, L and Kaaijk, P, 1997, '*In vitro* and *in vivo* models for the study of brain tumour invasion', Anticancer Res, vol. 17, no. 6B, pp. 4107-4109.

Piñero-Madrona, A, Polo-García, L, Alonso-Romero, JL, Salinas-Ramos, J, Canteras-Jordana, M, Sola-Pérez, J, Galindo-Fernández, PJ, Illana-Moreno, J, Bermejo-López, J, Navarrete-Montoya, A and Parrilla-Paricio, P, 2008, '[Immunohistochemical characterisation of breast cancer: towards a new clasification?]', Cir Esp, vol. 84, no. 3, pp. 138-145.

Pinho, MB, Costas, F, Sellos, J, Dienstmann, R, Andrade, PB, Herchenhorn, D, Peixoto, FA, Santos, VO, Small, IA, Guimarães, DP and Ferreira, CG, 2009, 'XAF1 mRNA expression improves progression-free and overall survival for patients with advanced bladder cancer treated with neoadjuvant chemotherapy', Urol Oncol, vol. 27, no. 4, pp. 382-390.

Pivot, X, Schneeweiss, A, Verma, S, Thomssen, C, Passos-Coelho, JL, Benedetti, G, Ciruelos, E, von Moos, R, Chang, HT, Duenne, AA and Miles, DW, 2011, 'Efficacy and safety of bevacizumab in combination with docetaxel for the first-line treatment of elderly patients with locally recurrent or metastatic breast cancer: Results from AVADO', Eur J Cancer, vol. 47, no. 16, pp. 2387-2395.

Pogrel, MA, Lowe, MA and Stern, R, 1996, 'Hyaluronan (hyaluronic acid) in human saliva', Arch Oral Biol, vol. 41, no. 7, pp. 667-671.

Polyzos, A, Kalbakis, K, Kentepozidis, N, Giassas, S, Kalykaki, A, Vardakis, N, Bozionelou, V, Saloustros, E, Kontopodis, E, Georgoulias, V and Mavroudis, D, 2011, 'Salvage treatment in metastatic breast cancer with weekly paclitaxel and bevacizumab', Cancer Chemother Pharmacol, vol. 68, no. 1, pp. 217-223.

Poole, R and Paridaens, R, 2007, 'The use of third-generation aromatase inhibitors and tamoxifen in the adjuvant treatment of postmenopausal patients with hormone-dependent breast cancer: evidence based review', Curr Opin Oncol, vol. 19, no. 6, pp. 564-572.

Postma, EL, van Hillegersberg, R, Daniel, BL, Merckel, LG, Verkooijen, HM and van den Bosch, MAAJ, 2011, 'MRI-guided ablation of breast cancer: Where do we stand today?', J Magn Reson Imaging, vol. 34, no. 2, pp. 254-261.

Pratt, T, Conway, CD, Tian, NMML, Price, DJ and Mason, JO, 2006, 'Heparan sulphation patterns generated by specific heparan sulfotransferase enzymes direct distinct aspects of retinal axon guidance at the optic chiasm', J Neurosci, vol. 26, no. 26, pp. 6911-6923.

Qiao, L, Gu, Q, Dai, Y, Shen, Z, Liu, X, Qi, R, Ma, J, Zou, B, Li, Z, Lan, HY and Wong, BCY, 2008, 'XIAP-associated factor 1 (XAF1) suppresses angiogenesis in mouse endothelial cells', Tumour Biol, vol. 29, no. 2, pp. 122-129.

Rabenstein, DL, 2002, 'Heparin and heparan sulfate: structure and function', Nat Prod Rep, vol. 19, no. 3, pp. 312-331.

Rack, B, Jückstock, J, Günthner-Biller, M, Andergassen, U, Neugebauer, J, Hepp, P, Schoberth, A, Mayr, D, Zwingers, T, Schindlbeck, C, Friese, K and Janni, W, 2011, 'Trastuzumab clears HER2/neu-positive isolated tumor cells from bone marrow in primary breast cancer patients', Arch Gynecol Obstet, vol. 285, no. 2, pp. 485-492.

Ragaz, J, 1990, 'Biologic aspects, classification, surgery, and radiotherapy of stage III breast cancer', Curr Opin Oncol, vol. 2, no. 6, pp. 1053-1067.

Ragaz, J, Spinelli, JJ and Coldman, AJ, 2000, 'Breast cancer survival advantage with radiotherapy', Lancet, vol. 356, no. 9237, pp. 1270; author reply 1271.

Raman, K and Kuberan, B, 2010, 'Chemical Tumor Biology of Heparan Sulfate Proteoglycans', Current chemical biology, vol. 4, no. 1, pp. 20-31.

Ravdin, PM, Cronin, KA, Howlader, N, Berg, CD, Chlebowski, RT, Feuer, EJ, Edwards, BK and Berry, DA, 2007, 'The decrease in breast-cancer incidence in 2003 in the United States', N Engl J Med, vol. 356, no. 16, pp. 1670-1674.

Richards, RG, Klotz, DM, Walker, MP and Diaugustine, RP, 2004, 'Mammary gland branching morphogenesis is diminished in mice with a deficiency of insulin-like growth factor-I (IGF-I), but not in mice with a liver-specific deletion of IGF-I', Endocrinology, vol. 145, no. 7, pp. 3106-3110.

Riedl, SJ, Renatus, M, Schwarzenbacher, R, Zhou, Q, Sun, C, Fesik, SW, Liddington, RC and Salvesen, GS, 2001, 'Structural basis for the inhibition of caspase-3 by XIAP', Cell, vol. 104, no. 5, pp. 791-800.

Rochester, MA, Riedemann, J, Hellawell, GO, Brewster, SF and Macaulay, VM, 2005, 'Silencing of the IGF1R gene enhances sensitivity to DNA-damaging agents in both PTEN wild-type and mutant human prostate cancer', Cancer Gene Ther, vol. 12, no. 1, pp. 90-100.

Rouette, A, Parent, S, Girouard, J, Leblanc, V and Asselin, E, 2011, 'Cisplatin increases B-cell-lymphoma-2 expression via activation of protein kinase C and Akt2 in endometrial cancer cells', Int J Cancer, vol.130, no. 8, pp. 1755-1767.

Ruoslahti, E, 1984, 'Fibronectin in cell adhesion and invasion', Cancer Metastasis Rev, vol. 3, no. 1, pp. 43-51.

Russo, J and Russo, IH, 2004, 'Development of the human breast', Maturitas, vol. 49, no. 1, pp. 2-15.

Russo, J and Russo, IH, 2008, 'Breast development, hormones and cancer', Adv Exp Med Biol, vol. 630, pp. 52-56.

Ryde, CM, Nicholls, JE and Dowsett, M, 1992, 'Steroid and growth factor modulation of aromatase activity in MCF7 and T47D breast carcinoma cell lines', Cancer Res, vol. 52, no. 6, pp. 1411-1415.

Sachdev, D, Zhang, X, Matise, I, Gaillard-Kelly, M and Yee, D, 2010, 'The type I insulin-like growth factor receptor regulates cancer metastasis independently of primary tumor growth by promoting invasion and survival', Oncogene, vol. 29, no. 2, pp. 251-262.

Sachdev, D, Hartell, JS, Lee, AV, Zhang, X and Yee, D, 2004, 'A dominant negative type I insulin-like growth factor receptor inhibits metastasis of human cancer cells', J Biol Chem, vol. 279, no. 6, pp. 5017-5024.

Safaiyan, F, Lindahl, U and Salmivirta, M, 1998, 'Selective reduction of 6-O-sulfation in heparan sulfate from transformed mammary epithelial cells', Eur J Biochem, vol. 252, no. 3, pp. 576-582.

Sakemi, R, Yano, H, Ogasawara, S, Akiba, J, Nakashima, O, Fukahori, S, Sata, M and Kojiro, M, 2007, 'X-linked inhibitor of apoptosis (XIAP) and XIAP-associated factor-1 expressions and their relationship to apoptosis in human hepatocellular carcinoma and non-cancerous liver tissues', Oncol Rep, vol. 18, no. 1, pp. 65-70.

Sakr, BJ and Dizon, DS, 2011, 'Breast cancer: adjuvant modalities', Clin Obstet Gynecol, vol. 54, no. 1, pp. 150-156.

Salk, RS, Grogan, KA and Chang, TJ, 2006, 'Topical 5% 5-fluorouracil cream in the treatment of plantar warts: a prospective, randomized, and controlled clinical study', J Drugs Dermatol, vol. 5, no. 5, pp. 418-424.

Samani, AA, Chevet, E, Fallavollita, L, Galipeau, J and Brodt, P, 2004, 'Loss of tumorigenicity and metastatic potential in carcinoma cells expressing the extracellular domain of the type 1 insulin-like growth factor receptor', Cancer Res, vol. 64, no. 10, pp. 3380-3385.

Sanderson, RD, Yang, Y, Kelly, T, MacLeod, V, Dai, Y and Theus, A, 2005, 'Enzymatic remodeling of heparan sulfate proteoglycans within the tumor microenvironment: growth regulation and the prospect of new cancer therapies', J Cell Biochem, vol. 96, no. 5, pp.

897-905.

Schmidt, ME, Chang-Claude, J, Slanger, T, Obi, N, Flesch-Janys, D and Steindorf, K, 2009, 'Physical activity and postmenopausal breast cancer: effect modification by other breast cancer risk factors', Methods Inf Med, vol. 48, no. 5, pp. 444-450.

Schröder, C, Witzel, I, Müller, V, Krenkel, S, Wirtz, RM, Jänicke, F, Schumacher, U and Milde-Langosch, K, 2011, 'Prognostic value of intercellular adhesion molecule (ICAM)-1 expression in breast cancer', J Cancer Res Clin Oncol, vol. 137, no. 8, pp. 1193-1201.

Sebestyén, A, Tótth, A, Mihalik, R, Szakács, O, Paku, S and Kopper, L, 2000, 'Syndecan-1-dependent homotypic cell adhesion in HT58 lymphoma cells', Tumour Biol, vol. 21, no. 6, pp. 349-357.

Sedita, J, Izvolsky, K and Cardoso, WV, 2004, 'Differential expression of heparan sulfate 6-O-sulfotransferase isoforms in the mouse embryo suggests distinctive roles during organogenesis', Dev Dyn, vol. 231, no. 4, pp. 782-794.

Seko, A, Kataoka, F, Aoki, D, Sakamoto, M, Nakamura, T, Hatae, M, Yonezawa, S and Yamashita, K, 2009, 'N-Acetylglucosamine 6-O-sulfotransferase-2 as a tumor marker for uterine cervical and corpus cancer', Glycoconj J, vol. 26, no. 8, pp.1065-73.

Seko, A, Nagata, K, Yonezawa, S and Yamashita, K, 2002, 'Ectopic expression of a GlcNAc 6-O-sulfotransferase, GlcNAc6ST-2, in colonic mucinous adenocarcinoma', Glycobiology, vol. 12, no. 6, pp. 379-388.

Séradour, B, Allemand, H, Weill, A and Ricordeau, P, 2009, 'Changes by age in breast cancer incidence, mammography screening and hormone therapy use in France from 2000 to 2006', Bull Cancer, vol. 96, no. 4, pp. E1-E6.

Shahrokni, A, Rajebi, MR and Saif, MW, 2009, 'Toxicity and efficacy of 5-fluorouracil and capecitabine in a patient with TYMS gene polymorphism: A challenge or a dilemma?', Clin Colorectal Cancer, vol. 8, no. 4, pp. 231-234.

Shao, H, Cai, L, Grichnik, JM, Livingstone, AS, Velazquez, OC and Liu, ZJ, 2011, 'Activation of Notch1 signaling in stromal fibroblasts inhibits melanoma growth by upregulating WISP-1', Oncogene, vol. 30, no. 42, pp. 4316-4326.

Shebzukhov, YV, Koroleva, EP, Khlgatian, SV, Lagarkova, MA, Meshcheryakov, AA, Lichinitser, MR, Karbach, J, Jager, E, Kuprash, DV and Nedospasov, SA, 2005, 'Humoral immune response to thymidylate synthase in colon cancer patients after 5-FU chemotherapy', Immunol Lett, vol. 100, no. 1, pp. 88-93.

Sheridan, PL, Francis, MD and Horwitz, KB, 1989, 'Synthesis of human progesterone receptors in T47D cells. Nascent A- and B-receptors are active without a phosphorylation-dependent post-translational maturation step', J Biol Chem, vol. 264, no.

12, pp. 7054-7058.

Shetty, MK, 2011, 'Screening and diagnosis of breast cancer in low-resource countries: what is state of the art?', Semin Ultrasound CT MR, vol. 32, no. 4, pp. 300-305.

Shibata, T, Mahotka, C, Wethkamp, N, Heikaus, S, Gabbert, HE and Ramp, U, 2007, 'Disturbed expression of the apoptosis regulators XIAP, XAF1, and Smac/DIABLO in gastric adenocarcinomas', Diagn Mol Pathol, vol. 16, no. 1, pp. 1-8.

Shibata, T, Noguchi, T, Takeno, S, Gabbert, HE, Ramp, U and Kawahara, K, 2008, 'Disturbed XIAP and XAF1 expression balance is an independent prognostic factor in gastric adenocarcinomas', Ann Surg Oncol, vol. 15, no. 12, pp. 3579-3587.

Shin, HJ, Kim, HH, Ahn, JH, Kim, SB, Jung, KH, Gong, G, Son, BH and Ahn, SH, 2011, 'Comparison of mammography, sonography, MRI and clinical examination in patients with locally advanced or inflammatory breast cancer who underwent neoadjuvant chemotherapy', Br J Radiol, vol. 84, no. 1003, pp. 612-620.

Shirk, RA, Parthasarathy, N, San Antonio, JD, Church, FC and Wagner, WD, 2000, 'Altered dermatan sulfate structure and reduced heparin cofactor II-stimulating activity of biglycan and decorin from human atherosclerotic plaque', J Biol Chem, vol. 275, no. 24, pp. 18085-18092.

Silveri, CP, Kaplan, FS, Fallon, MD, Bayever, E and August, CS, 1991, 'Hurler syndrome with special reference to histologic abnormalities of the growth plate', Clin Orthop Relat Res, no. 269, pp. 305-311.

Simpson, MJ, Towne, C, McElwain, DLS and Upton, Z, 2010, 'Migration of breast cancer cells: understanding the roles of volume exclusion and cell-to-cell adhesion', Phys Rev E Stat Nonlin Soft Matter Phys, vol. 82, no. 4 Pt 1, pp. 041901.

Simsir, A, Rapkiewicz, A and Cangiarella, J, 2009, 'Current utilization of breast FNA in a cytology practice', Diagn Cytopathol, vol. 37, no. 2, pp. 140-142.

Singletary, KW and Gapstur, SM, 2001, 'Alcohol and breast cancer: review of epidemiologic and experimental evidence and potential mechanisms', JAMA, vol. 286, no. 17, pp. 2143-2151.

Slavkovsky, R, Kohlerova, R, Jiroutova, A, Hajzlerova, M, Sobotka, L, Cermakova, E and Kanta, J, 2010, 'Effects of hyaluronan and iodine on wound contraction and granulation tissue formation in rat skin wounds', Clin Exp Dermatol, vol. 35, no. 4, pp. 373-379.

Song, K, Li, Q, Peng, YB, Li, J, Ding, K, Chen, LJ, Shao, CH, Zhang, LJ and Li, P, 2011, 'Silencing of hHS6ST2 inhibits progression of pancreatic cancer through inhibition of

Notch signalling', Biochem J, vol. 436, no. 2, pp. 271-282.

Sousa, SB, Pina, R, Ramos, L, Pereira, N, Krahn, M, Borozdin, W, Kohlhase, J, Amorim, M, Gonnet, K, Lévy, N, Carreira, IM, Couceiro, AB and Saraiva, JM, 2008, 'Tetra-amelia and lung hypo/aplasia syndrome: new case report and review', Am J Med Genet A, vol. 146A, no. 21, pp. 2799-2803.

Spano, JP, Falandry, C, Chaibi, P and Freyer, G, 2011, 'Current Targeted Therapies in Breast Cancer: Clinical Applications in the Elderly Woman', Oncologist, vol. 16, no. 8, pp. 1144-1153.

Spinelli, GP, Tomao, F, Miele, E, Pasciuti, G, Russillo, M and Tomao, S, 2008, '[Aromatase inhibitors in advanced breast cancer]', Recenti Prog Med, vol. 99, no. 1, pp. 34-38.

Staub, J, Chien, J, Pan, Y, Qian, X, Narita, K, Aletti, G, Scheerer, M, Roberts, LR, Molina, J and Shridhar, V, 2007, 'Epigenetic silencing of HSulf-1 in ovarian cancer:implications in chemoresistance', *Oncogene*, vol. 26, no. 34, pp. 4969-4978.

Stickens, D, Zak, BM, Rougier, N, Esko, JD and Werb, Z, 2005, 'Mice deficient in Ext2 lack heparan sulfate and develop exostoses', Development, vol. 132, no. 22, pp. 5055-5068.

Su, G, Blaine, SA, Qiao, D and Friedl, A, 2007, 'Shedding of syndecan-1 by stromal fibroblasts stimulates human breast cancer cell proliferation via FGF2 activation', J Biol Chem, vol. 282, no. 20, pp. 14906-14915.

Sugaya, N, Habuchi, H, Nagai, N, Ashikari-Hada, S and Kimata, K, 2008, '6-O-sulfation of heparan sulfate differentially regulates various fibroblast growth factor-dependent signalings in culture', J Biol Chem, vol. 283, no. 16, pp. 10366-10376.

Sun, PH, Zhu, LM, Qiao, MM, Zhang, YP, Jiang, SH, Wu, YL and Tu, SP, 2011, 'The XAF1 tumor suppressor induces autophagic cell death via upregulation of Beclin-1 and inhibition of Akt pathway', Cancer Lett, vol. 310, no. 2, pp. 170-180.

Sun, Y, Qiao, L, Xia, HHX, Lin, MCM, Zou, B, Yuan, Y, Zhu, S, Gu, Q, Cheung, TK, Kung, HF, Yuen, MF, Chan, AO and Wong, BCY, 2008, 'Regulation of XAF1 expression in human colon cancer cell by interferon beta: activation by the transcription regulator STAT1', Cancer Lett, vol. 260, no. 1-2, pp. 62-71.

Sutherland, AE, Sanderson, RD, Mayes, M, Seibert, M, Calarco, PG, Bernfield, M and Damsky, CH, 1991, 'Expression of syndecan, a putative low affinity fibroblast growth factor receptor, in the early mouse embryo', Development, vol. 113, no. 1, pp. 339-351.

Suzuki, A, Horiuchi, A, Ashida, T, Miyamoto, T, Kashima, H, Nikaido, T, Konishi, I and Shiozawa, T, 2010, 'Cyclin A2 confers cisplatin resistance to endometrial carcinoma cells

via up-regulation of an Akt-binding protein, periplakin', J Cell Mol Med, vol. 14, no. 9, pp. 2305-2317.

Suzuki, M, Sugimoto, K, Tanaka, J, Tameda, M, Inagaki, Y, Kusagawa, S, Nojiri, K, Beppu, T, Yoneda, K, Yamamoto, N, Ito, M, Yoneda, M, Uchida, K, Takase, K and Shiraki, K, 2010, 'Up-regulation of glypican-3 in human hepatocellular carcinoma', Anticancer Res, vol. 30, no. 12, pp. 5055-5061.

Swann, DA, Bloch, KJ, Swindell, D and Shore, E, 1984, 'The lubricating activity of human synovial fluids', Arthritis Rheum, vol. 27, no. 5, pp. 552-556.

Syrigos, KN, Karapanagiotou, E, Boura, P, Manegold, C and Harrington, K, 2011, 'Bevacizumab-induced hypertension: pathogenesis and management', BioDrugs, vol. 25, no. 3, pp. 159-169.

Tabata, K, Sakai, H, Nakajima, R, Saya-Nishimura, R, Motani, K, Okano, S, Shibata, Y, Abiko, Y and Suzuki, T, 2011, 'Acute application of cisplatin affects methylation status in neuroblastoma cells', Oncol Rep, vol. 25, no. 6, pp. 1655-1660.

Takagi, K, Sowa, Y, Cevik, OM, Nakanishi, R and Sakai, T, 2008, 'CDK inhibitor enhances the sensitivity to 5-fluorouracil in colorectal cancer cells', Int J Oncol, vol. 32, no. 5, pp. 1105-1110.

Takezaki, T, Hirose, K, Inoue, M, Hamajima, N, Kuroishi, T, Nakamura, S, Koshikawa, T, Matsuura, H and Tajima, K, 1996, 'Tobacco, alcohol and dietary factors associated with the risk of oral cancer among Japanese', Jpn J Cancer Res, vol. 87, no. 6, pp. 555-562.

Tan, BR, Thomas, F, Myerson, RJ, Zehnbauer, B, Trinkaus, K, Malyapa, RS, Mutch, MG, Abbey, EE, Alyasiry, A, Fleshman, JW and McLeod, HL, 2011, 'Thymidylate synthase genotype-directed neoadjuvant chemoradiation for patients with rectal adenocarcinoma', J Clin Oncol, vol. 29, no. 7, pp. 875-883.

Tang, HB, Ren, YP, Zhang, J, Ma, SH, Gao, F and Wu, YP, 2007, '[Correlation of insulin-like growth factor-1 (IGF-1) to angiogenesis of breast cancer in IGF-1-deficient mice]', Ai Zheng, vol. 26, no. 11, pp. 1215-1220.

Tátrai, P, Egedi, K, Somorácz, A, van Kuppevelt, TH, Ten Dam, G, Lyon, M, Deakin, JA, Kiss, A, Schaff, Z and Kovalszky, I, 2010, 'Quantitative and qualitative alterations of heparan sulfate in fibrogenic liver diseases and hepatocellular cancer', J Histochem Cytochem, vol. 58, no. 5, pp. 429-441.

Theodoro, TR, de Matos, LL, Sant Anna, AVL, Fonseca, FLA, Semedo, P, Martins, LC, Nader, HB, Del Giglio, A and da Silva Pinhal, MA, 2007, 'Heparanase expression in circulating lymphocytes of breast cancer patients depends on the presence of the primary

tumor and/or systemic metastasis', Neoplasia, vol. 9, no. 6, pp. 504-510.

Timson, G, Banavali, S, Gutierrez, MI, Magrath, I, Bhatia, KG and Goyns, MH, 2006, 'High level expression of N-acetylgluosamine-6-O-sulfotransferase is characteristic of a subgroup of paediatric precursor-B acute lymphoblastic leukaemia', Cancer Lett, vol. 242, no. 2, pp. 239-244.

Toniolo, P, Bruning, PF, Akhmedkhanov, A, Bonfrer, JM, Koenig, KL, Lukanova, A, Shore, RE and Zeleniuch-Jacquotte, A, 2000, 'Serum insulin-like growth factor-I and breast cancer', Int J Cancer, vol. 88, no. 5, pp. 828-832.

Trowbridge, JM and Gallo, RL, 2002, 'Dermatan sulfate: new functions from an old glycosaminoglycan', Glycobiology, vol. 12, no. 9, pp. 117R-125R.

Tu, SP, Liston, P, Cui, JT, Lin, MCM, Jiang, XH, Yang, Y, Gu, Q, Jiang, SH, Lum, CT, Kung, HF, Korneluk, RG and Wong, BCY, 2009, 'Restoration of XAF1 expression induces apoptosis and inhibits tumor growth in gastric cancer', Int J Cancer, vol. 125, no. 3, pp. 688-697.

Tumova, S, Woods, A and Couchman, JR, 2000, 'Heparan sulfate proteoglycans on the cell surface: versatile coordinators of cellular functions', Int J Biochem Cell Biol, vol. 32, no. 3, pp. 269-288.

Umezu, T, Shibata, K, Kajiyama, H, Yamamoto, E, Nawa, A and Kikkawa, F, 2010, 'Glypican-3 expression predicts poor clinical outcome of patients with early-stage clear cell carcinoma of the ovary', J Clin Pathol, vol. 63, no. 11, pp. 962-966.

van den Born, J, Salmivirta, K, Henttinen, T, Ostman, N, Ishimaru, T, Miyaura, S, Yoshida, K and Salmivirta, M, 2005, 'Novel heparan sulfate structures revealed by monoclonal antibodies', J Biol Chem, vol. 280, no. 21, pp. 20516-20523.

Van Slambrouck, S, Jenkins, AR, Romero, AE and Steelant, WFA, 2009, 'Reorganization of the integrin alpha2 subunit controls cell adhesion and cancer cell invasion in prostate cancer', Int J Oncol, vol. 34, no. 6, pp. 1717-1726.

Vera-Ramirez, L, Sanchez-Rovira, P, Ramirez-Tortosa, MC, Ramirez-Tortosa, CL, Granados-Principal, S, Fernandez-Navarro, M, Lorente, JA and Quiles, JL, 2011, 'Does chemotherapy-induced oxidative stress improve the survival rates of breast cancer patients?', Antioxid Redox Signal, vol. 15, no. 4, pp. 903-909.

Vidal, B and Cozzi, PA, 1970, '[Role of mamography in the diagnosis of breast diseases]', Friuli Med, vol. 25, no. 3, pp. 173-204.

Vlodavsky, I, Eldor, A, Bar-Ner, M, Fridman, R, Cohen, IR and Klagsbrun, M, 1988, 'Heparan sulfate degradation in tumor cell invasion and angiogenesis', Adv Exp Med

Biol, vol. 233, pp. 201-210.

Von Minckwitz, G, Costa, SD, Raab, G, Blohmer, JU, Eidtmann, H, Hilfrich, J, Merkle, E, Jackisch, C, Gademann, G, Tulusan, AH, Eiermann, W, Graf, E, Kaufmann, M and German Preoperative Adriamycin-Docetaxel and German Adjuvant Breast Cancer Study Groups, 2001, 'Dose-dense doxorubicin, docetaxel, and granulocyte colony-stimulating factor support with or without tamoxifen as preoperative therapy in patients with operable carcinoma of the breast: a randomized, controlled, open phase IIb study', J Clin Oncol, vol. 19, no. 15, pp. 3506-3515.

Vrbanec, D, Belev, B, Pavlinić-Diminić, V, Pezerović, D, Dusper, B, Plestina, S and Unusić, J, 1998, '[Hormonal therapy with aromatase inhibitor in advanced breast cancer]', Lijecnicki vjesnik, vol. 120, no. 10-11, pp. 315-318.

Waddington, RJ and Embery, G, 2001, 'Proteoglycans and orthodontic tooth movement', J Orthod, vol. 28, no. 4, pp. 281-290.

Wang, J, Gu, Q, Li, M, Zhang, W, Yang, M, Zou, B, Chan, S, Qiao, L, Jiang, B, Tu, S, Ma, J, Hung, IF, Lan, HY and Wong, BCY, 2009, 'Identification of XAF1 as a novel cell cycle regulator through modulating G(2)/M checkpoint and interaction with checkpoint kinase 1 in gastrointestinal cancer', Carcinogenesis, vol. 30, no. 9, pp. 1507-1516.

Wang, J, Peng, Y, Sun, YW, He, H, Zhu, S, An, X, Li, M, Lin, MCM, Zou, B, Xia, HHX, Jiang, B, Chan, AOO, Yuen, MF, Kung, HF and Wong, BCY, 2006, 'All-trans retinoic acid induces XAF1 expression through an interferon regulatory factor-1 element in colon cancer', Gastroenterology, vol. 130, no. 3, pp. 747-758.

Wang, Y, Thakur, A, Sun, Y, Wu, J, Biliran, H, Bollig, A and Liao, DJ, 2007, 'Synergistic effect of cyclin D1 and c-Myc leads to more aggressive and invasive mammary tumors in severe combined immunodeficient mice', Cancer Res, vol. 67, no. 8, pp. 3698-3707.

Warning, K, Hildebrandt, MG, Kristensen, B and Ewertz, M, 2011, 'Utility of 18FDG-PET/CT in breast cancer diagnostics - a systematic review', Dan Med Bull, vol. 58, no. 7, pp. A4289.

Wasif, N, Maggard, MA, Ko, CY and Giuliano, AE, 2010, 'Invasive lobular vs. ductal breast cancer: a stage-matched comparison of outcomes', Ann Surg Oncol, vol. 17, no. 7, pp. 1862-1869.

Watanabe, H, Yamada, Y and Kimata, K, 1998, 'Roles of aggrecan, a large chondroitin sulfate proteoglycan, in cartilage structure and function', J Biochem, vol. 124, no. 4, pp. 687-693.

Watson, RG, Muhale, F, Thorne, LB, Yu, J, O'Neil, BH, Hoskins, JM, Meyers, MO, Deal, AM, Ibrahim, JG, Hudson, ML, Walko, CM, McLeod, HL and Auman, JT, 2010,

'Amplification of thymidylate synthetase in metastatic colorectal cancer patients pretreated with 5-fluorouracil-based chemotherapy', Eur J Cancer, vol. 46, no. 18, pp. 3358-3364.

Wei, M, Zhu, L, Li, Y, Chen, W, Han, B, Wang, Z, He, J, Yao, H, Yang, Z, Zhang, Q, Liu, B, Gu, Q, Zhu, Z and Shen, K, 2011, 'Knocking down cyclin D1b inhibits breast cancer cell growth and suppresses tumor development in a breast cancer model', Cancer Sci, vol. 102, no. 8, pp. 1537-1544.

Werner, H and Le Roith, D, 1997, 'The insulin-like growth factor-I receptor signaling pathways are important for tumorigenesis and inhibition of apoptosis', Crit Rev Oncog, vol. 8, no. 1, pp. 71-92.

Whitelock, JM and Iozzo, RV, 2005, 'Heparan sulfate: a complex polymer charged with biological activity', Chem Rev, vol. 105, no. 7, pp. 2745-2764.

Whitelock, J and Melrose, J, 2011, 'Heparan sulfate proteoglycans in healthy and diseased systems', Wiley interdisciplinary reviews. Systems biology and medicine, vol.3, no. 6, pp. 739-751.

Woodward, WA, Truong, PT, Yu, TK, Tereffe, W, Oh, J, Perkins, G, Strom, E, Meric-Bernstam, F, Gonzalez-Angulo, AM, Speers, C, Ragaz, J and Buchholz, TA, 2010, 'Among women who experience a recurrence after postmastectomy radiation therapy irradiation is not associated with more aggressive local recurrence or reduced survival', Breast Cancer Res Treat, vol. 123, no. 2, pp. 597-605.

Xing, Z, Zhou, Z, Yu, R, Li, S, Li, C, Nilsson, S and Liu, Z, 2010, 'XAF1 expression and regulatory effects of somatostatin on XAF1 in prostate cancer cells', J Exp Clin Cancer Res, vol. 29, pp. 162.

Yagata, H, Kajiura, Y and Yamauchi, H, 2011, 'Current strategy for triple-negative breast cancer: appropriate combination of surgery, radiation, and chemotherapy', Breast Cancer, vol. 18, no. 3, pp. 165-173.

Yang, DC, Elliott, RL and Head, JF, 2002, 'Gene targets of antisense therapies in breast cancer', Expert Opin Ther Targets, vol. 6, no. 3, pp. 375-385.

Yang, L, Cao, Z, Yan, H and Wood, WC, 2003, 'Coexistence of high levels of apoptotic signaling and inhibitor of apoptosis proteins in human tumor cells: implication for cancer specific therapy', Cancer Res, vol. 63, no. 20, pp. 6815-6824.

Yang, Y, Macleod, V, Miao, HQ, Theus, A, Zhan, F, Shaughnessy, JD, Sawyer, J, Li, JP, Zcharia, E, Vlodavsky, I and Sanderson, RD, 2007, 'Heparanase enhances syndecan-1 shedding: a novel mechanism for stimulation of tumor growth and metastasis', J Biol Chem, vol. 282, no. 18, pp. 13326-13333.

Yanochko, GM and Eckhart, W, 2006, 'Type I insulin-like growth factor receptor over-expression induces proliferation and anti-apoptotic signaling in a three-dimensional culture model of breast epithelial cells', Breast Cancer Res, vol. 8, no. 2, pp. R18.

Yavari, K, Taghikhani, M, Ghannadi Maragheh, M, Mesbah-Namin, SA and Babaei, MH, 2010, 'Downregulation of IGF-IR expression by RNAi inhibits proliferation and enhances chemosensitization of human colon cancer cells', Int J Colorectal Dis, vol. 25, no. 1, pp. 9-16.

Yeatman, TJ, Cantor, AB, Smith, TJ, Smith, SK, Reintgen, DS, Miller, MS, Ku, NN, Baekey, PA and Cox, CE, 1995, 'Tumor biology of infiltrating lobular carcinoma. Implications for management', Ann Surg, vol. 222, no. 4, pp. 549-59; discussion 559.

Yeh, AH, Bohula, EA and Macaulay, VM, 2006, 'Human melanoma cells expressing V600E B-RAF are susceptible to IGF1R targeting by small interfering RNAs', Oncogene, vol. 25, no. 50, pp. 6574-6581.

Yin, S, Xu, L, Bandyopadhyay, S, Sethi, S and Reddy, KB, 2011, 'Cisplatin and TRAIL enhance breast cancer stem cell death', Int J Oncol, vol. 39, no. 4, pp. 891-898.

Yin, W, Cheepala, S and Clifford, JL, 2006, 'Identification of a novel splice variant of X-linked inhibitor of apoptosis-associated factor 1', Biochem Biophys Res Commun, vol. 339, no. 4, pp. 1148-1154.

Yu, LF, Wang, J, Zou, B, Lin, MCM, Wu, YL, Xia, HHX, Sun, YW, Gu, Q, He, H, Lam, SK, Kung, HF and Wong, BCY, 2007, 'XAF1 mediates apoptosis through an extracellular signal-regulated kinase pathway in colon cancer', Cancer, vol. 109, no. 10, pp. 1996-2003.

Yuen, JSP, Akkaya, E, Wang, Y, Takiguchi, M, Peak, S, Sullivan, M, Protheroe, AS and Macaulay, VM, 2009, 'Validation of the type 1 insulin-like growth factor receptor as a therapeutic target in renal cancer', Mol Cancer Ther, vol. 8, no. 6, pp. 1448-1459.

Zeng, X, Sachdev, D, Zhang, H, Gaillard-Kelly, M and Yee, D, 2009, 'Sequencing of type I insulin-like growth factor receptor inhibition affects chemotherapy response *in vitro* and *in vivo*', Clin Cancer Res, vol. 15, no. 8, pp. 2840-2849.

Zhang, C, Hao, L, Wang, L, Xiao, Y, Ge, H, Zhu, Z, Luo, Y, Zhang, Y and Zhang, Y, 2010, 'Elevated IGF1R expression regulating VEGF and VEGF-C predicts lymph node metastasis in human colorectal cancer', BMC Cancer, vol. 10, pp. 184.

Zhang, L, Beeler, DL, Lawrence, R, Lech, M, Liu, J, Davis, JC, Shriver, Z, Sasisekharan, R and Rosenberg, RD, 2001, '6-O-sulfotransferase-1 represents a critical enzyme in the anticoagulant heparan sulfate biosynthetic pathway', J Biol Chem, vol. 276, no. 45, pp. 42311-42321.

Zhang, W, Guo, Z, Jiang, B, Niu, L, Xia, G, Wang, X, Cheng, T, Zhang, Y and Wang, J ,2010, 'Identification of a functional p53 responsive element within the promoter of XAF1 gene in gastrointestinal cancer cells', Int J Oncol, vol. 36, no. 4, pp. 1031-1037.

Zhao, C, Raza, A, Martin, SE, Pan, J, Greaves, TS and Cobb, CJ, 2009, 'Breast fine-needle aspiration samples reported as "proliferative breast lesion": clinical utility of the subcategory "proliferative breast lesion with atypia"', Cancer, vol. 117, no. 2, pp. 137-147.

Zou, B, Chim, CS, Pang, R, Zeng, H, Dai, Y, Zhang, R, Lam, CSC, Tan, VPY, Hung, IFN, Lan, HY and Wong, BCY, 2011, 'XIAP-associated factor 1 (XAF1), a novel target of p53, enhances p53-mediated apoptosis via post-translational modification', Mol Carcinog, vol. 51, no. 5, pp. 422-432.

Zou, B, Chim, CS, Zeng, H, Leung, SY, Yang, Y, Tu, SP, Lin, MCM, Wang, J, He, H, Jiang, SH, Sun, YW, Yu, LF, Yuen, ST, Kung, HF and Wong, BCY, 2006, 'Correlation between the single-site CpG methylation and expression silencing of the XAF1 gene in human gastric and colon cancers', Gastroenterology, vol. 131, no. 6, pp. 1835-1843.

Zuo, Q and Luo, RC, 2010, '[Relationship between the insulin-like growth factor 1 receptor signaling pathway and the resistance of nasopharyngeal carcinoma to cetuximab]', Zhonghua Zhong Liu Za Zhi, vol. 32, no. 8, pp. 575-579.

APPENDIX

The illustrated figures of this section are related to the discussion chapter of the current study.

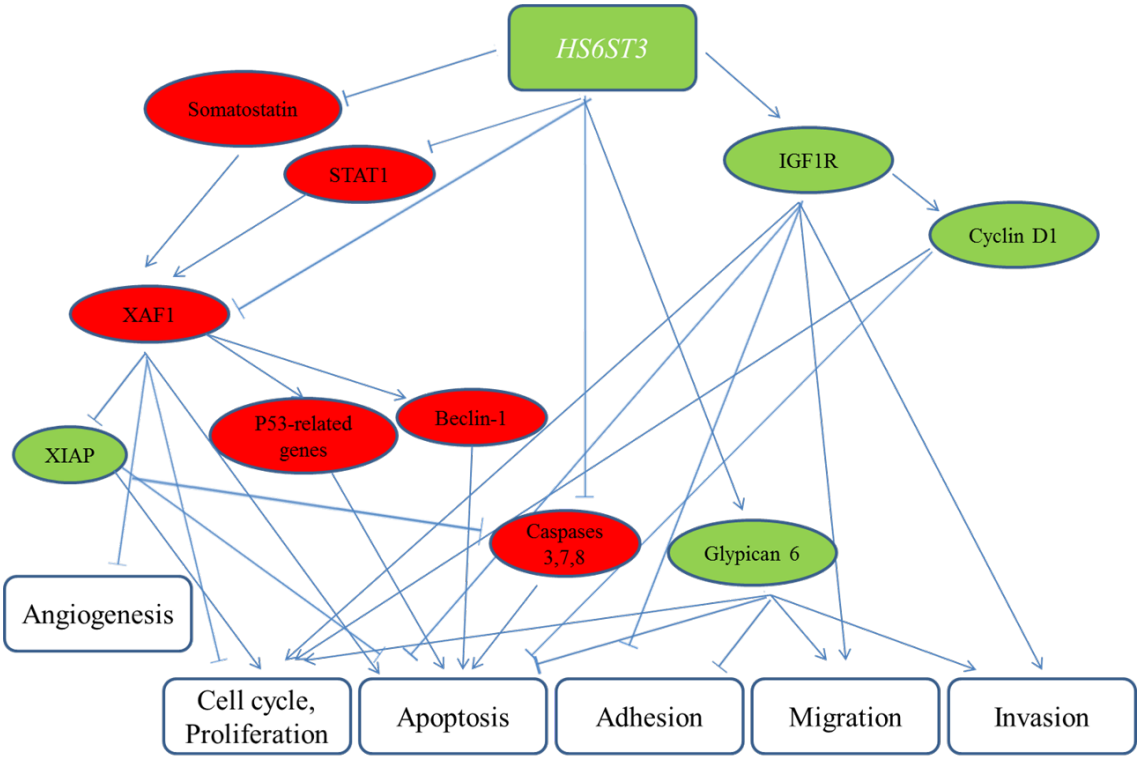

Figure 4.1. Proposed schematic pathway analysis for the genomic functions of HS6ST3 in the breast cancer. Silencing HS6ST3 significantly diminished the tumoral growth and progression in the breast cancer. Green color reveals the down-regulation and red color reveals the up-regulation of the gene(s). Arrow indicates the positive regulation and the blunt-end line indicates the negative regulation.

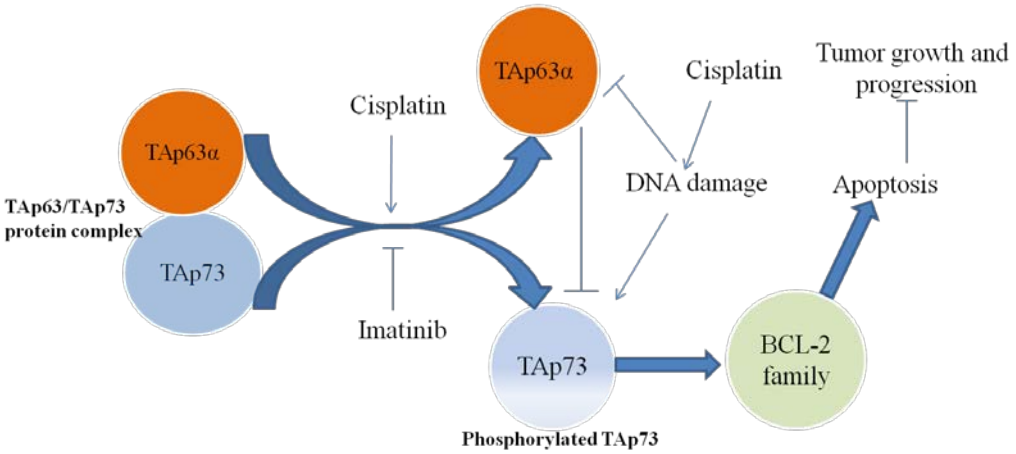

Figure 4.2. Schematic diagram for p63/ p73 pathway. Dissociation of the Tap73 activates the BCL-2 family which results in apoptosis. Arrow reveals the positive regulation and the blunt-end line reveals the negative regulation.

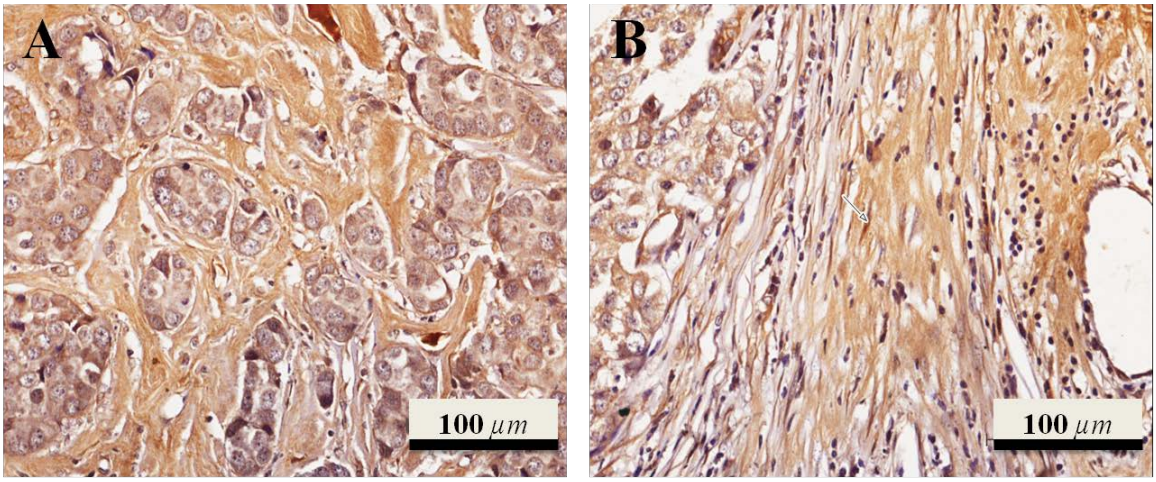

Figure 4.3. Expression of SULF1 in stromal cells of the breast cancer tissue. Expression of SULF1 in reactive stromal cells (arrow) enhanced in response to the cancer microenvironment, while this expression in epithelial cells reduced. (A) Breast ductal carcinoma histograde 2 (B) Breast ductal carcinoma histograde 3. SULF1 expression of reactive stromal cells increase when grade 2 shift to grade 3; however, due to the high turnover of stromal cells around malignant epithelial cells, SULF1 expression may increase in stroma matrix.